

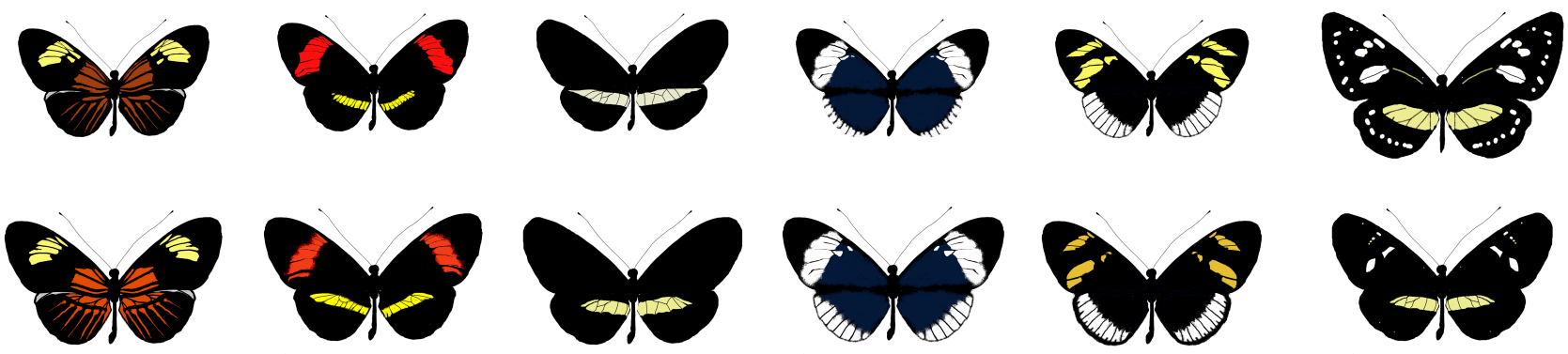
INTRA AND INTER-SPECIFIC
COMMUNICATION IN *Heliconius*

MARÍA FERNANDA GONZÁLEZ ROJAS

DOCTORATE PROGRAM IN BIOMEDICAL AND BIOLOGICAL SCIENCES

UNIVERSIDAD DEL ROSARIO

This dissertation is submitted for the Degree of Doctor of Philosophy



DECLARATION

This dissertation is the result of my own work and includes nothing which is the outcome of work done in collaboration except where specifically indicated in the text or the acknowledgments below. None of the work has been submitted for a degree, diploma, or dissertation at any other university.

María Fernanda González-Rojas

SUMMARY

Heliconius butterflies are an excellent example of Müllerian mimicry, where phylogenetically distant species converge to nearly identical wing phenotype when occurring in sympatry. However, few studies have comprehensively addressed mimicry accuracy and variation in mimicry signals across the fitness landscape (which may comprise multiple fitness peaks). In this study, using analysis of colour quantification, wing size and shape, I investigate the extent of phenotypic resemblance between co-mimic species in multiple *Heliconius* mimicry rings. I found that wing size and shape do not contribute to mimicry. In contrast, colour phenotype is the main contributor, but some phenotypes are more accurate between co-mimics than others. This suggests the presence of multiple adaptive peaks within the same mimetic ring.

In these butterflies, colour pattern is recognised as the main cue for mate recognition between species that are phylogenetically close, but when this cue is compromised alternative mating signals must evolve to ensure reproductive isolation and species integrity. The closely related species *H. melpomene malleti* and *H. timareta florencia* occur in the same geographical region, and despite being co-mimics, they display strong reproductive isolation. Here, I tested which cues differ between species, and potentially contribute to reproductive isolation. Wing colour pattern was indistinguishable between the two species, while the chemical profile of the males' androconia and genitalia showed marked differences. Finally, I conducted behavioural experiments to study the importance of colour and chemical signals in mate recognition by females. I found that chemical blends and not wing colour pattern drive the preference of females for conspecific males. Also, experiments with hybrid males and females suggested an important genetic compound for both chemical production and preference suggesting that chemicals are

the major reproductive barrier opposing gene flow between these two sister and co-mimic species.

Altogether, these results agree with the idea that mimicry adaptation is a complex and dynamic process affected by more than one factor and that an effective combination of these signals (visual and chemical) is essential for intra- and interspecific communication processes in butterflies.

ACKNOWLEDGEMENTS

Quisiera agradecer a mi director de tesis Dr. Camilo Salazar, y codirectora Dr. Carolina Pardo por guiarme durante estos años e introducirme al maravilloso mundo de las mariposas. Agradezco también a mis compañeros miembros del Grupo de Genética Evolutiva, Filogeografía y Ecología de Biodiversidad Neotropical de la Universidad del Rosario.

I would also like to thank Dr. Chris Jiggins, who supervised my work during the internship I did at the University of Cambridge. Dr. Stefan Schulz from the Technische Universität Braunschweig, Institute of Organic Chemistry, allowed me to use the reference library to identify the chemical compounds. During the internship I did at the Smithsonian Tropical Research Institute (STRI), I was under the supervision of Dr. Owen McMillan. I would like to thank him and the amazing teamwork at STRI where I analysed the GC/MS data.

My gratitude to the people who participated and collaborated in the culmination of this work: Dr. Kathy Darragh, Dr. Mauricio Linares, Jean Francois Le Crom, Dr. Melissa Sanchez-Herrera, Dr. William Kuhn, Dr. Steven Van Belleghem, Juan Enciso, Dr. Jorge Robles, Dr. Kelsey Bryers, and the teamwork at the insectaries (Oscar Penagos, Sebastian Sanchez and Isabel).

Agradezco el financiamiento recibido por parte de COLCIENCIAS y COLFUTURO (Convocatoria 727 y FP44842-5-2017) y Universidad del Rosario (QFN-DG001 y Apoyo para Estudiantes Doctorales).

Adicionalmente, los ingenieros David Oviedo y Francisco Gallón ofrecieron ayuda bioinformática importante. Francisco José Gallón realizó las ilustraciones de mariposas que usé en congresos y seminarios. A mis amigos, especialmente Adrián Martínez Molina, quien ha estado ahí para mí todos los días compartiendo risas y memes. A Elvira que llegó un día a nuestro almuerzo y nunca nos abandonó. A Osvaldo Gil, por compartir almuerzos y descansos agradables durante las jornadas en el hueco y por hacerme reír en medio de tanta desgracia junta.

Principalmente quisiera agradecer a mi familia que a lo largo de todos estos años me han acompañado y apoyado incondicionalmente. Sin su apoyo moral y económico, este largo camino no habría sido posible (Familias González-Rojas, Rojas-Hoyos, Gallón-Soto, Bahamón-Soto). A mis papás y mi hermana que me inculcaron el amor y respeto por la naturaleza y la determinación para cumplir mis sueños. A mi esposo, Francisco José Gallón, quién me ha apoyado, acompañado y me ha mantenido sana y cuerda durante estos años. Gracias por ser mi roca, confiar en mi y tenerme toda la paciencia. Finalmente, a mis sobrinitos Juan Martín, Ignacio y María por ser mi mayor inspiración.

CONTENTS

DECLARATION	ii
SUMMARY	iii
ACKNOWLEDGEMENTS	v
CONTENTS	vii
INTRODUCTION	1
INTRA AND INTER-SPECIFIC COMMUNICATION IN ANIMALS	1
<i>Heliconius</i> : AS A STUDY SYSTEM, COLOUR AND MIMICRY	3
CHEMICAL COMMUNICATION	8
PHEROMONE PRODUCTION, PERCEPTION AND GENETICS	9
THESIS OUTLINE	12
COLLABORATIONS AND PUBLICATIONS	13
CHAPTER 1. PHENOTYPIC RESEMBLANCE ACROSS MULTIPLE MIMICRY RINGS IN <i>Heliconius</i>	15
INTRODUCTION	15
MATERIALS AND METHODS	17
WING SHAPE AND SIZE	18
WING PATTERN	25
RESULTS	26
WING SIZE AND SHAPE	26
WING PATTERN	44
DISCUSSION	52
CHAPTER 2. REPRODUCTIVE ISOLATION DRIVEN BY PHEROMONES IN MIMETIC AND CLOSELY RELATED BUTTERFLIES	60
INTRODUCTION	60
MATERIALS AND METHODS	62
QUANTIFICATION OF WING PHENOTYPE	62
WILD SAMPLING	63
BEHAVIOURAL EXPERIMENTS	64
RESULTS	67
QUANTIFICATION OF WING PHENOTYPE	67
BEHAVIOURAL EXPERIMENTS	71
DISCUSSION	78

CHAPTER 3. MATE PREFERENCE AND PHEROMONE COMPOSITION IN A PAIR OF CLOSELY RELATED AND MIMETIC SPECIES OF THE GENUS <i>Heliconius</i>	81
INTRODUCTION	81
MATERIALS AND METHODS	83
WILD SAMPLING AND INTERSPECIFIC CROSSES	83
BEHAVIOURAL EXPERIMENTS	84
CHARACTERIZATION OF CHEMICAL PROFILES	85
RESULTS	86
WILD SAMPLING AND INTERSPECIFIC CROSSES	86
BEHAVIOURAL EXPERIMENTS	87
CHARACTERISATION OF CHEMICAL PROFILES	90
DISCUSSION	92
CONCLUSIONS	97
REFERENCES	99
SUPPLEMENTARY INFORMATION	113
CHAPTER 1. PHENOTYPIC RESEMBLANCE ACROSS MULTIPLE MIMICRY RINGS IN <i>Heliconius</i>	113
CHAPTER 2. REPRODUCTIVE ISOLATION DRIVEN BY PHEROMONES IN MIMETIC AND CLOSELY RELATED BUTTERFLIES	199
CHAPTER 3. MATE PREFERENCE AND PHEROMONE COMPOSITION IN A PAIR OF CLOSELY RELATED AND MIMETIC SPECIES OF THE GENUS <i>Heliconius</i>	206

LIST OF FIGURES

Figure 1.1. Geographic distribution of the co-mimics <i>H. erato</i> and <i>H. melpomene</i> .	6
Figure 1.2. Geographic distribution of the clade <i>H. sara/sapho</i> and its co-mimics <i>H. cydno</i> .	7
Figure 1.3. Proposed biosynthesis and degradation pathways of sex pheromones in moths.	10
Figure 2.1. Position of the landmark coordinates (LM) used in the analysis of shape and size and colour pattern.	24
Figure 2.2. Wing size variation between subspecies with the red-band phenotype.	30
Figure 2.3. Wing size variation between species and subspecies with the dennis-ray mimetic ring in the Amazon.	31
Figure 2.4. Wing size variation between subspecies with the yellow/white phenotype.	32
Figure 2.5. Wing size variation between subspecies of <i>H. melpomene</i> .	33
Figure 2.6. Wing size variation between subspecies of <i>H. erato</i> .	34
Figure 2.7. Wing size variation between subspecies of <i>H. cydno</i> .	35
Figure 2.8. Wing size variation between subspecies of <i>H. timareta</i> .	36
Figure 2.9. Comparison of wing shape between subspecies with the red-band phenotype.	37
Figure 2.10. Comparison of wing shape between species and subspecies that participate in the dennis-ray mimicry ring in the Amazon.	38
Figure 2.11. Comparison of wing shape between subspecies with the yellow/white phenotype.	39
Figure 2.12. Comparison of wing shape between subspecies of <i>H. melpomene</i> .	40
Figure 2.13. Comparison of wing shape between subspecies of <i>H. erato</i> .	41
Figure 2.14. Comparison of wing shape between subspecies of <i>H. cydno</i> .	42
Figure 2.15. Comparison of wing shape between subspecies of <i>H. timareta</i> .	43
Figure 2.16. Comparison of colour pattern between subspecies exhibiting the red-banded phenotype.	48
Figure 2.17. Comparison of colour pattern between species and subspecies exhibiting the dennis-ray phenotype in the Amazon.	49
Figure 2.18. Comparison of colour pattern between subspecies exhibiting the dennis-ray phenotype in the southeast Andean foothills.	50
Figure 2.19. Comparison of colour pattern between subspecies exhibiting the yellow/white phenotype.	51
Figure 3.1. Map showing the geographic distribution and wing phenotype of <i>H. timareta florenci</i> and <i>H. melpomene malleti</i> in the South Eastern Andes of Colombia.	62
Figure 3.2. Species wing size and shape.	68
Figure 3.3. Shape variation of forewings of <i>H. melpomene malleti</i> and <i>H. timareta florenci</i> .	69
Figure 3.4. Colour pattern comparison between the two species.	70
Figure 3.5. Mate choice triads testing the importance of wing colour pattern in mate preference.	71
Figure 3.6. Proportion of courtships that resulted in female behavioural responses towards control and treatment males.	72
Figure 3.7. Mate choice triads in where male chemical blend was blocked.	74
Figure 3.8. Female behavioural responses towards males with an altered capacity to emit sexual pheromones.	75
Figure 3.9. Female behavioural responses towards males “perfumed” with a hexane extract from five males either of <i>H. m. malleti</i> or <i>H. t. florenci</i> .	77
Figure 4.1. Mate choice triads testing behavioural responses in F_1 and backcross (BC) females.	88
Figure 4.2. Proportion of courtships that resulted in behavioural responses in F_1 and BC females.	89
Figure 4.3. Discriminant analysis based on individual composition of wing androconia and abdominal gland extracts of males of <i>H. m. malleti</i> , <i>H. t. florenci</i> , F_1 and BC.	91
Figure S1.1. Shapes deformation and PC loadings representing the shape variation in the forewing between subspecies with the red-band phenotype.	156
Figure S1.2. Shapes deformation and PC loadings representing the shape variation in the hindwing between subspecies with the red-band phenotype.	157
Figure S1.3. Shapes deformation and PC loadings representing the shape variation in the forewing between species and subspecies with the dennis-ray mimetic ring in the Amazon.	159

Figure S1.4. Shapes deformation and PC loadings representing the shape variation in the hindwing between species and subspecies with the dennis-ray mimetic ring in the Amazon.	160
Figure S1.5. Comparison of wing shape between species and subspecies that participate in the dennis-ray mimicry ring in the Amazon including non-Heliconius species.	161
Figure S1.6. Shapes deformation and PC loadings representing the shape variation in the forewing between subspecies with the yellow/white phenotype.	163
Figure S1.7. Shapes deformation and PC loadings representing the shape variation in the hindwing between subspecies with the yellow/white phenotype.	164
Figure S1.8. Comparison of forewing shape between subspecies with the yellow/white phenotype.	165
Figure S1.9. Comparison of hindwing shape between subspecies with the yellow/white phenotype.	166
Figure S1.10. Comparison of colour pattern between <i>H. erato venus</i> and <i>H. melpomene vulcanus</i> , subspecies exhibiting the red-banded phenotype.	186
Figure S1.11. Comparison of colour pattern between <i>H. erato guarica</i> and <i>H. melpomene martinae</i> , subspecies exhibiting the red-banded phenotype.	187
Figure S1.12. Comparison of colour pattern between <i>H. erato hydara</i> and <i>H. melpomene melpomene</i> , subspecies exhibiting the red-banded phenotype.	188
Figure S1.13. Comparison of colour pattern between <i>H. erato dignus</i> , <i>H. melpomene bellula</i> and <i>H. tristero</i> , subspecies exhibiting the red-banded phenotype.	189
Figure S1.14. Comparison of colour pattern between subspecies of <i>H. melpomene</i> with the red-banded phenotype	190
Figure S1.15. Comparison of colour pattern between subspecies of <i>H. erato</i> with the red-banded phenotype.	191
Figure S1.16. Comparison of colour pattern between <i>H. cydno zelinde</i> , <i>H. eleuchia eleusinus</i> and <i>H. sapho chochoensis</i> , subspecies exhibiting the yellow/white phenotype.	192
Figure S1.17. Comparison of colour pattern between <i>H. cydno wanningeri</i> and <i>H. sapho sapho</i> , subspecies exhibiting the yellow/white phenotype.	193
Figure S1.18. Comparisons of colour pattern between <i>H. cydno chioneus</i> , <i>H. cydno cydno</i> , <i>H. eleuchia eleuchia</i> and <i>H. sapho sapho</i> .	194
Figure S1.19. Comparison of colour pattern between <i>H. sara magdalena</i> , <i>H. sapho sapho</i> , <i>H. eleuchia eleuchia</i> and <i>H. cydno lisethae</i> , subspecies exhibiting the yellow/white phenotype.	195
Figure S1.20. Comparison of colour pattern between <i>H. cydno cydnides</i> and <i>H. eleuchia eleuchia</i> , subspecies exhibiting the yellow/white phenotype .	196
Figure S1.21. Comparison of colour pattern between <i>Elzunia humboldt tamasea</i> , <i>H. hecuba tolima</i> and <i>H. cydno hermogenes</i> , subspecies exhibiting the yellow/white phenotype.	197
Figure S1.22. Comparison of colour pattern between <i>Elzunia humboldt regalis</i> and two races of <i>H. cydno weymeri</i> , exhibiting the yellow/white phenotype.	198
Figure S2.1. Amount (ng) of compounds that remained in the wings of perfumed males before evaporation.	205
Figure S3.1. Species differences in male androconial extracts.	213
Figure S3.2. Cluster analysis based on Euclidian distance of compound composition in the wing androconia of males of <i>H. m. malleti</i> , <i>H. t. florencia</i> , F_1 and BC..	214
Figure S3.3. Chromatogram patterns obtained from androconial extracts of hybrid F_1 and backcross males.	215
Figure S3.4. Chromatogram pattern of the abdominal gland bouquet of males.	216
Figure S3.5. Cluster analysis based on Euclidian distance of the compound composition of the wing androconia of males of <i>H. m. malleti</i> , <i>H. t. florencia</i> , F_1 and BC.	217
Figure S3.6. Chromatogram patterns obtained from abdominal gland bouquet of F_1 and backcross males.	218

LIST OF TABLES

Table 2.1. Samples included in the morphometric analysis. _____	19
Table 3.1. Female behavioural response towards males with normal and altered wing phenotype. _____	73
Table 3.2. Female behavioural responses in triads that tested the female's preference for the male's sex pheromones. _____	76
Table 3.3. Female behavioural responses in triads that tested female preference for males "perfumed" with a hexanic extract from five either of conspecific or heterospecific male. _____	78
Table 4.1. Probability of mating in no-choice experiments. _____	87
Table 4.2. Behavioural response of F_1 and BC females towards pure males of <i>H. m. malleti</i> and <i>H. t. florencia</i> . ____	88
Table S1.1. Samples included in the morphometric analyses. _____	113
Table S1.2. Statistical analyses. _____	167
Table S2.1. Samples included in the quantification of wing phenotype.. _____	199
Table S2.2. Amount (ng) of compounds that remained in the wings of perfumed males before evaporation. ____	202
Table S3.1. Compounds identified in wing androconia's extracts of <i>H. melpomene malleti</i> , <i>H. timareta florencia</i> , F_1 and backcross. _____	206
Table S3.2. Compounds identified in extracts of abdominal glands' extracts of males of <i>H. melpomene malleti</i> , <i>H. timareta florencia</i> , F_1 and backcross.. _____	209

INTRODUCTION

INTRA AND INTER-SPECIFIC COMMUNICATION IN ANIMALS

Communication is the production and transmission of a message through a signal by a sender, which generates a response from a receiver (1). This process usually involves complex signals that convey information simultaneously in multiple sensory modalities (2). In particular, animal communication, both intra and inter-specific, involves visual cues (nuptial colouration or body size), acoustic signals (bird songs or vibration), and chemical signals (cuticular hydrocarbons or pheromones), among others (3,4). These signals are usually combined to effectively communicate (5,6). For example, male birds exhibit brightly ornamentals as well as perform elaborated songs to attract their partners (3), while in *Drosophila* the courtship behaviour combines visual and chemical stimuli (7). Also, tiger moths (Arctiidae) use ultrasound to avoid predation by bats and mate choice (8,9). In other cases, a single signal can serve multiple communication purposes. For instance, butterflies and moths use pyrrolizidine alkaloids as a defence against predators and as a sex pheromone precursor (10–14).

The role of visual cues in animal communication has been extensively studied (15). As such, there is plenty of evidence showing their importance in reproduction and predation avoidance (16–19). For example, some butterfly wing patterns act as aposematic warning signals (20,21) and also as an intraspecific signal for partner recognition (22,23). However, when the same signal is used by multiple species to avoid predation (mimicry) and to recognise conspecific sex partners, conflicts may arise (14,24). This is particularly important in the case of closely related, sympatric and mimetic species because there is a higher chance of heterospecific attraction due to mimicry, which could

lead to heterospecific mating thus affecting fitness (10,14,15). To mitigate this effect, other types of signals (i.e. acoustic or chemical) should mediate species recognition (10).

Although studies on sexual communication have focused on visual signals, chemical communication is of great importance in animals, predominantly in insects (25–27). Olfactory signals, which are highly specific (1), convey individual information such as reproductive status (28–31), territoriality and competitive ability (32,33), trail recruitment (34), mating status of females (35,36), quality and age of males (37,38), quality and quantity of nuptial gifts (39), body size (40), dominance status (41), and degree of relatedness (42). However, olfactory signals also mediate species-specific recognition (5) in insects including *Drosophila* (43,44), *Rhagoletis* (45,46), grasshoppers (47), stick insects (48), moths and butterflies (49–53), and other taxa such as salamanders (54), lizards (55), garter snakes (40) and mice (5,56).

Pheromones are one of the best studied olfactory signals in the animal kingdom, and are species-specific chemical compounds used for intra and inter-specific communication (6,57–60). Their variation has important implications for reproductive isolation and speciation (37,61). Several closely related and sympatric insects have marked differences in their pheromones, both in terms of composition or concentration, these differences affect mate choice thus being crucial for the recognition of conspecific sex partners (45,46,53,62–64). Moreover, cuticular hydrocarbons mediate mating preferences in closely related species of the Coleopteran families Cerambycidae (65), Chrysomelidae (66–68), Lampyridae (69), as well as in many Lepidoptera such as *Danaus* (70). Species recognition and sexual signalling have also been identified in the Hymenopteran wasp families Braconidae (71), Bethyridae (72), and Pteromalidae (15).

***Heliconius*: AS A STUDY SYSTEM, COLOUR AND MIMICRY**

Heliconius is a genus of butterflies extensively used as a model to understand the mechanisms behind the processes of speciation and adaptation (73–75). These butterflies constitute an adaptive radiation with about 40 species and more than 400 subspecies (or geographic races) across the Neotropics (75). They are an excellent study system because of: (i) their relative abundance in the field and natural collections, (ii) their feasibility to be reared in insectaries, (iii) their moderately small genomes, and (iv) their bright and diverse colour patterns, which are involved in complex mimicry across the Neotropics. As such, *Heliconius* constitute a textbook example of Müllerian mimicry in which distantly related but sympatric species converge on the same wing colour phenotype to efficiently advertise their unpalatability to predators (76–78). These so-called mimicry ‘rings’ (multiple species sharing a similar appearance (79)), comprise species of *Heliconius* but also other genera like *Melipotis* (Danainae: Ithomiini) or *Chetone* (day-flying Arctiidae) (75). Nevertheless, co-mimics in a given locality are usually phylogenetically distant while closely related species often differ in their wing phenotype (12,80,81). This is due to frequency dependent mimicry selection coupled with species recognition mediated by visual cues (12,14,82–85), although chemical, behavioural and even acoustic signals are also involved (60,86). In consequence, hybrid colour patterns are penalized by natural selection and males are more likely to approach and court females exhibiting their own phenotype (12).

The unpalatability of *Heliconius* is the result of their adults having cyanogenic compounds in their bodies. These compounds are captured by larvae when feeding on *Passiflora* plants, although some *Heliconius* are able to *de novo* synthesise cyanogenic compounds (87–90). Although the interplay between host plant use by larvae, toxicity levels in adults and mimicry still is not completely understood (88), field and insectary experiments demonstrated that wing colouration is indeed a good signal advertising toxicity to local predators (21,77,87,88,91). Even so, there is considerable variation in toxicity levels between populations that bear a similar phenotype in different locations and

between species with different phenotypes occurring in the same place (21,77,87,88,91). The importance of wing elements and colour (or their combination) in predator deterrence is still an open question. Only one experiment suggests that birds (the most common predator of these butterflies) perceive a generalized wing pattern, and that red colour is a more effective warning signal (16,79,92). Interestingly, wing colours seem to contain information that can selectively signal both predators and potential mates (16). For example, yellow patches in *H. erato* are apparently better distinguishable by conspecifics than birds, but the generality of this result across the genus has not been shown.

Mimicry in *Heliconius* is very diverse. Usually, there is local convergence to few wing phenotypes, and in some cases, this convergence extends to a regional scale. Also, polymorphic colour patterns involving multiple rings can coexist in the same locality (Figure 1.1 and 1.2). A striking example of the *Heliconius* mimicry tapestry occurs between *H. melpomene* and *H. erato*. These species converge to the same wing phenotype in all localities where they co-occur (93), but at the same time, their phenotype varies across Central and South America (Figure 1.1) (94). In general terms, the wing phenotypic variation of *H. melpomene* and *H. erato* variation can be grouped into two patterns: red-band and dennis-ray (95). The red-band phenotype consists of a broad medial red mid-forewing band (*H. e. guarica* in Figure 1.1). The dennis-ray pattern refers to an orange/red basal patch on the forewing combined with orange rays on the hindwing (rays), and a yellow anteromedial band in the forewing (for example *H. m. malleti* in Figure 1.1). A second great example of mimicry in the genus is *H. cydno*, a species that usually mimics species of the *H. sara/sapho* clade (Figure 1.2) (94,95). However, in the south of the Cauca valley, *H. cydno* mimics *H. erato* and the Ithomiine butterfly *Elzunia humboldt regalis* thus constituting very unusual mimicry pairs (96). Similarly, *H. cydno* participates in a mimetic ring with *H. hecuba* and *Elzunia humboldt tamasea* in the Colombian Magdalena valley (Figure 1.2).

The geographical diversification in mimicry signals in these butterflies has been explained by the classical Wright's shifting balance theory, where alleles'

frequencies randomly vary due to genetic drift, and then local positive frequency-dependent selection acts on colour loci allowing the morphs to colonize new adaptive peaks (97). This theory is an alternative to the classical Fisher's model, where selection acts on the mutations that generate diversity (97,98). In contrast with the widely supported Fisher's model, the evidence supporting the Wright's shifting balance theory is rather scarce (except for *Heliconius* and dendrobatid frogs (99,100)). On the other hand, recent evidence has shown that polymorphic mimetic rings in *Heliconius* (at least those controlled by supergenes), are maintained by antagonistic natural and sexual frequency-dependent selection acting on the colour pattern (101,102).

Heliconius has a 'tool kit' of about five unlinked autosomal genes that control most of the colour pattern variation in the genus (103). Such genes are turned on or off in different species or wing regions thanks to the presence/absence of cis-regulatory modules around them (104–106). This modular architecture in the regulatory regions of the colour pattern genes facilitates both phenotypic convergence and divergence because they function as lego parts that can be combined in multiple arrangements thus permitting the formation of a great diversity of wing phenotypes (106). This is particularly important in *Heliconius* because wing pattern is recognized as a "magic trait" (12,75,107) that acts as an aposematic signal (21,107) and is also implicated in sexual recognition (75,108). Interestingly, the loci controlling the formation of wing colours are closely linked to the loci underlying mate preference (85,109), so divergence in colour pattern loci is expected to also affect preference loci, thus leading to the evolution of reproductive isolation.

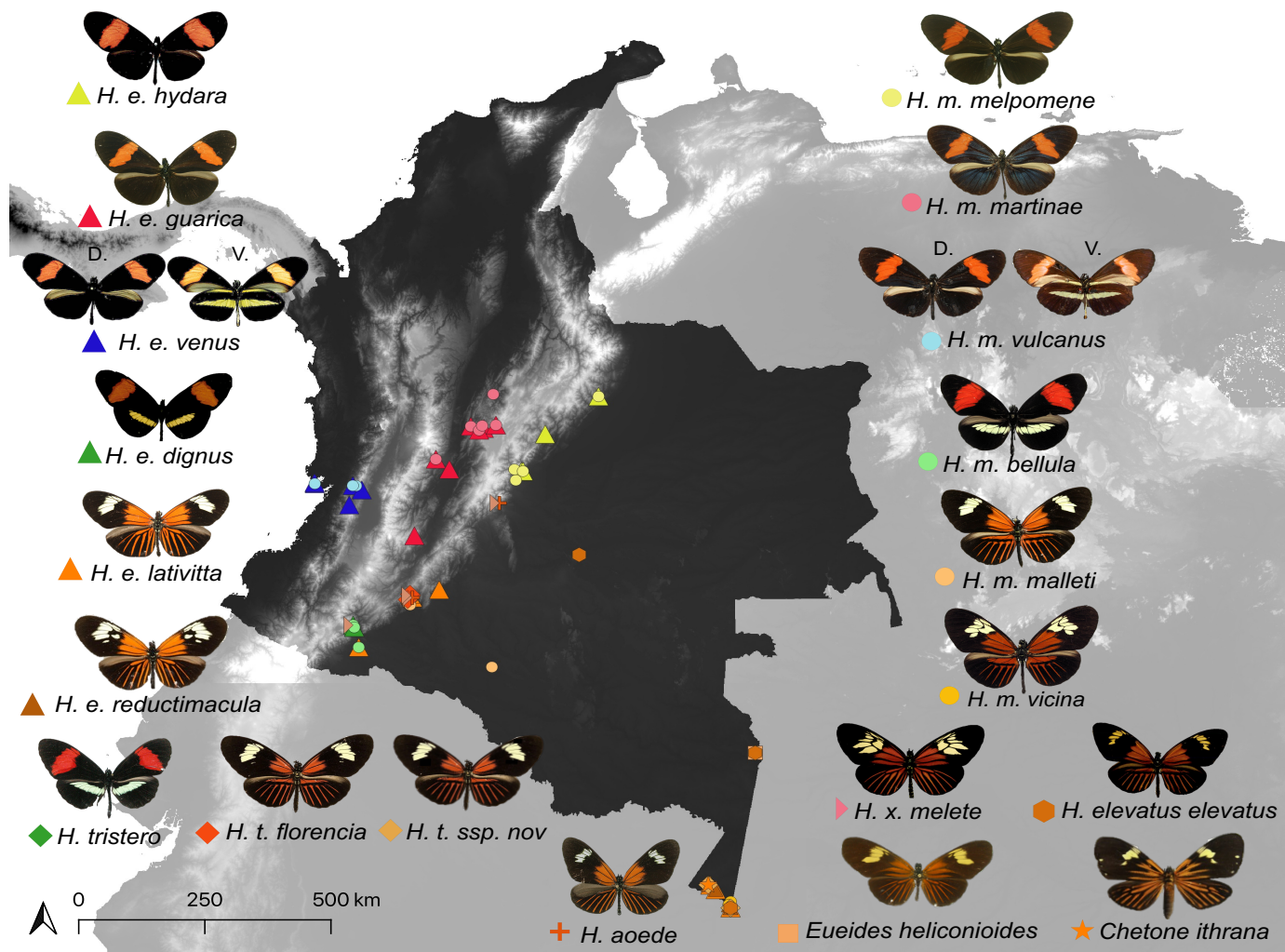


Figure 1.1. Geographic distribution of the co-mimics *H. erato* and *H. melpomene*. This map includes members of the genus *Heliconius*, *Eueides heliconioides* and a moth *Chetone ithrana*.

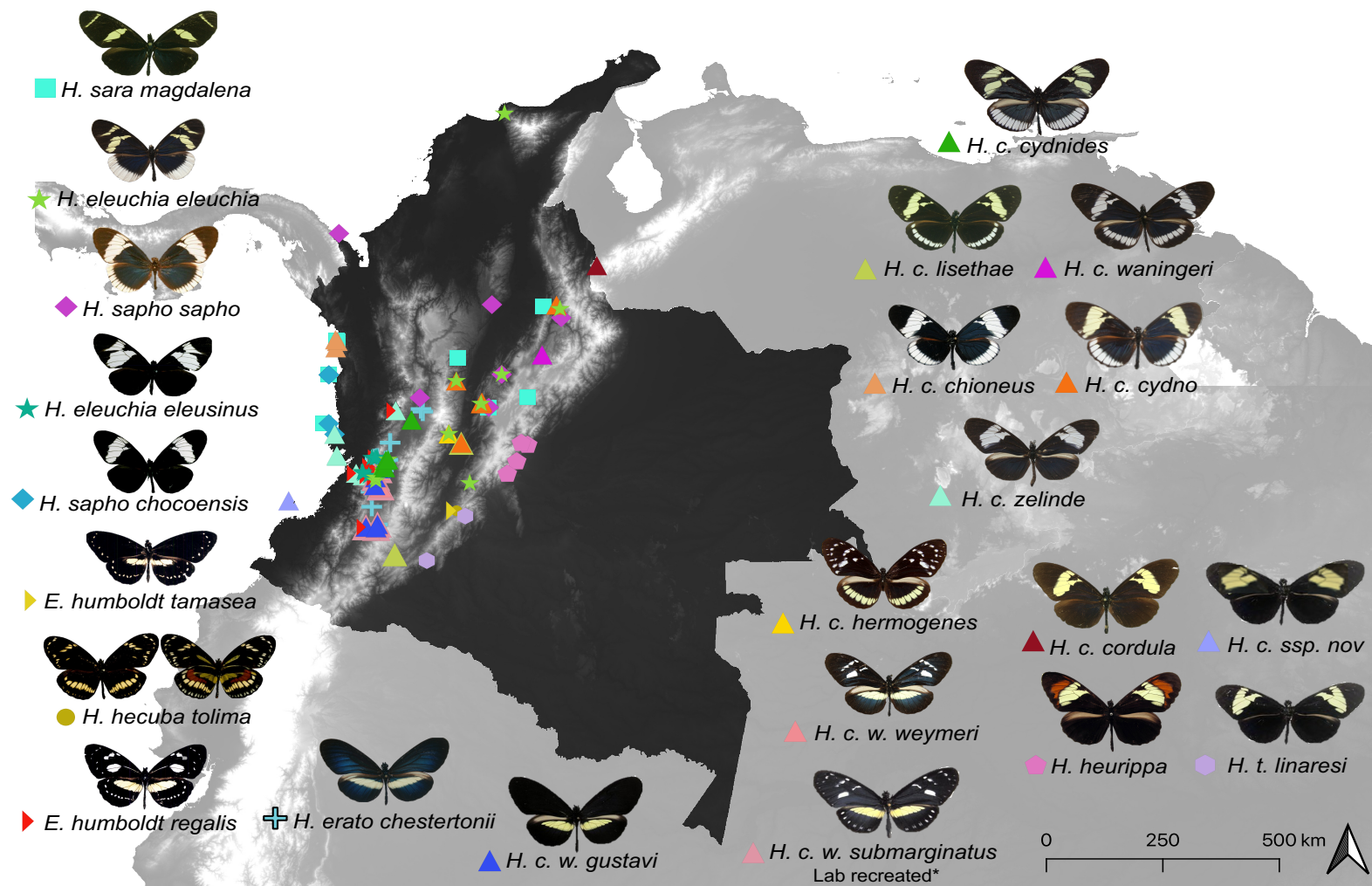


Figure 1.2. Geographic distribution of the clade *H. sara/sapho* and its co-mimics *H. cydno*. This map includes members of the genus *Heliconius* and the ithomiinae butterfly *Elzunia humboldt*.

CHEMICAL COMMUNICATION

Organisms interact both with their environment and with others through chemical cues (54,55,117,60,110–116), in consequence, chemical signalling has been recognised as an important cue in insects for aggregation (118), trail recruitment (34), interaction with plants (119) and sex (57,120).

In particular, sex pheromones are species-specific mixtures involved in intra and inter-specific communication (57), and are intensively studied in moth pests. In fact, the first chemical characterisation of sex pheromone was carried out in the moth *Bombyx mori* (121). These volatile compounds can be short-range cues (like cuticular hydrocarbons) or long-range cues released to attract mates over long distances (43,122–125). Pheromones play an important role in mate recognition and their divergence can lead to reproductive isolation and speciation (24,52,59,123,124).

Butterflies are usually regarded as highly visual organisms that rely on visual cues due to their diurnal habits (81,126,127). In consequence, few studies have focused on chemical signalling in butterflies. Even so, some male aphrodisiac pheromones that are used during courtship in Danaini (Nymphalidae: Danainae) have been identified, and they are known to be released by abdominal hair-pencil structures (86,126). Also, some Ithomiini (Nymphalidae: Danainae) sequester pyrrolizine alkaloids from plants and use them as precursors of pheromones (128). *Heliconius* do not have complex scent organs like those in Danainae (14), but have brush-like structures in the silvery overlapping region of the male hindwing, known as androconia (81,129–132). Behavioural experiments in *H. erato* revealed that males expose their androconia during courtship, thus suggesting a role for chemical signalling in courtship and mating in these butterflies (133,134). Likewise, males of *H. charitonia* use chemical cues to locate mates and are able to identify the sex of the pupae based on chemical cues (135). Moreover, anti-aphrodisiac compounds are transferred from males to females during mating to prevent re-mating by making the female unattractive to potential mates (136,137). Despite the importance of chemical signalling in *Heliconius*, the study of chemical cues in the genus has been poorly explored

compared to visual cues. In an attempt to address this gap, recent studies have characterised the compounds present in the male androconia of multiple species (108,138) and suggest a role for pheromones in conspecific mate recognition (108,138) so, these differences evolved by natural selection to avoid interspecific hybridisation (64,123).

PHEROMONE PRODUCTION, PERCEPTION AND GENETICS

Lepidoptera display tremendous chemical diversity in volatile pheromone components (139). The chemical bouquets often included a combination of multiple types of compounds such as macrolides, alkanes, alkenes, alcohols, ketones, aldehydes and terpenoids; in many cases inferred or proved to be plant-derived (89,117,140–142). Currently, sex pheromones of various Lepidoptera have been characterized, specifically in moths the synthesis pathway of these compounds and the participating enzymes, have been deeply studied. (140–143; Figure 1.3). Lepidopteran sex pheromones are classified as type-I (most common) or type-II based on the presence of terminal functional group: type I pheromones are C10-C18 fatty acid derivatives with an oxygenated functional group that can be an aldehyde, alcohol or an acetate ester, while type-II pheromones are hydrocarbons or epoxides (143,144,146). In female moths, type I sex pheromones are synthesized by specialized pheromone glands (PG) through a fatty-acid biosynthesis pathway where palmitic or stearic acids are converted to the final pheromone components by multiple steps of acetylation, desaturation, chain shortening, reduction, and oxidation (143,144,146; Figure 1.3).

The detection of these pheromones relies on hair-like sensilla on the antenna. Specifically, pheromones bind to odorant-binding proteins and are transported to olfactory sensory dendrites, where pheromone receptors induce the opening of ion channels, depolarise membranes and generate action potentials (147). Pheromone receptors bind with high specificity, and evidence from *Ostrinia furnacalis* shows that pheromone receptors are a crucial component in qualitative pheromone preference shifts (148,149).

In moths, the perception and degradation of female pheromones relies on three major classes of proteins: pheromone binding proteins (PBPs), odorant receptors (ORs), and pheromone degrading enzymes (PDEs) (143,150). Although few PDEs have been functionally characterized, it is known that these enzymes include aldehyde oxidases (AOX), aldehyde dehydrogenases (ALDH), aldehyde reductases (AR), carboxylesterases (CCE), UDP-glycosyltransferases (UGT), glutathione S-transferase (GSTs) and cytochrome p450s (CYPs) (143,151; Figure 1.3). Also, the recent sequencing of the transcriptome of pheromone glands and antennae in multiple moths has pinpointed some of the genes that code for the enzymes likely implicated in the production, detection and degradation of sex pheromones in these organisms (143,144,159–162,151–158).

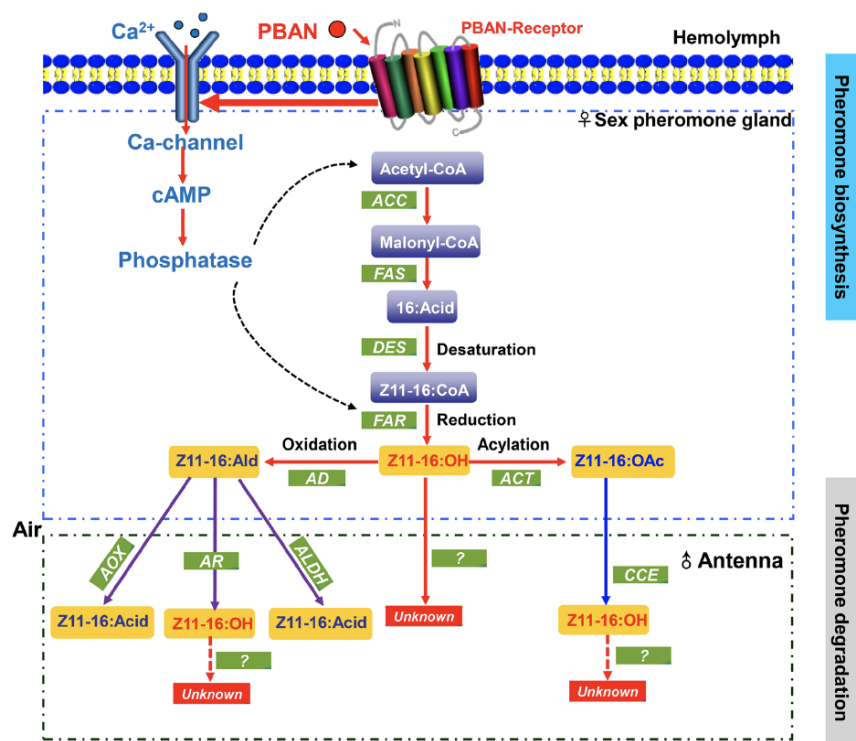


Figure 1.3. Proposed biosynthesis (top, occurs in the PG) and degradation (bottom, occurs in the antennae) pathways of sex pheromones in moths. Enzymes are shown in green, precursor compounds are shown in blue, while pheromone compounds are shown in yellow. Figure from He, 2017 (144). Biosynthesis of sex pheromones is initiated when the pheromone biosynthesis activating neuropeptide (PBAN) is released from the subesophageal ganglion in the brain and binds to its receptor (PBANr) in the PG. This induces a calcium channel to open causing an influx of extracellular calcium. This calcium binds to calmodulin, and together, they will activate adenylate cyclase to produce cAMP that will then act through kinases to stimulate the acetyl-CoA carboxylase (ACC), thus initiating the pheromone

biosynthesis. ACC carboxylates acetyl-CoA to malonyl-CoA. Then, a fatty acid synthase (FAS) produces a saturated fatty acid from malonyl-CoA and NADPH (the resulting products are palmitic (16C) or and stearic acids (18C)). A desaturase (DES) modifies these even numbered carbon chains introducing double bonds into specific locations. Subsequently, a fatty acid reductase (FAR) reduces such fatty acids to alcohols, that are either oxidized by an alcohol oxidase or alcohol dehydrogenase (AO or AD) into the corresponding aldehyde components or converted into acetate esters by an acetyltransferase (ACT). The perception of such pheromone compounds relies on three major classes of proteins: pheromone binding proteins (PBPs), odorant receptors (ORs), and pheromone degrading enzymes (PDEs). The PDEs are far less characterized, although some are known. For example, the aldehyde oxidase (AOX) is a sensillum enzyme that degrades aldehyde sex pheromone components) to corresponding acids, while the aldehyde dehydrogenase (ALDH) and aldehyde reductase (AR) are NAD(P)⁻ dependent enzymes that catalyse the oxidation and reduction of aldehyde substrates to their corresponding acids and alcohols, respectively. On the other hand, the carboxyl/cholinesterase (CCE) are secretory enzymes that degrade acetate ester pheromones. Finally, some UDP-glycosyltransferases (UGT) and glutathione S-transferase (GSTs) have been suggested as odorant degrading enzymes in moths.

Conversely, little is known about olfactory sexual communication in butterflies, where not only females but also males (in some species) produce sexual pheromones (38,51,138,141,163,164). Notwithstanding this, the composition and biosynthetic pathways of sex pheromones between butterflies and moths are considered to be highly conserved (138,139,145,147,156,164–166). In fact, genomic comparisons between moths and butterflies of the genera *Heliconius*, *Papilio* and *Danaus* have suggested high similarity between their sex pheromone biosynthetic gene clade (139,167).

A recent study in the species pair *H. melpomene* and *H. cydno* (divergence time ~1Mya) suggests a polygenic basis for both pheromone production and perception in *Heliconius*. There are 40 significant quantitative trait loci (QTL; 33 potential pheromone compounds) and chromosome 20 seems to be enriched for potential pheromone biosynthesis genes (168). Similarly, multiple loci involved in chemoperception including OBPs, were identified (168). Both sets of genes are unlinked to colour pattern loci or visual mate preference loci, thus suggesting that, assuming a role of pheromones in mate recognition, speciation in the face of gene flow involves multiple barrier loci.

THESIS OUTLINE

This thesis comprises three data chapters:

First, mimicry in butterflies has been suggested to be a multifactorial signal where, besides colour pattern, other traits such as wing shape and size may potentially play a role. However, few studies have addressed mimicry accuracy in terms of wing shape, size and pattern. In chapter 1, I evaluated fine-scale morphological differences in size, shape and wing colour pattern to investigate the extent of phenotypic resemblance among co-mimic species in multiple *Heliconius* mimicry rings in Colombia.

Second, because some closely related and sympatric *Heliconius* species converge in colour pattern and this signal is used for partner recognition, conflicts may arise, and other signals should mediate such recognition. In chapter 2, I quantified wing colour pattern in order to investigate how accurate is the resemblance between the closely related species *H. melpomene malleti* and *H. timareta florencia*, which belong to the same mimicry ring in Caquetá (Colombia). I also conducted experiments to test female preferences for male wing phenotype and male sex pheromones to test whether sex pheromones mediate reproductive isolation between closely related and mimetic species.

Based on the results from chapter 2, in chapter 3, I characterised the chemical bouquets of males of *H. m. malleti* and *H. t. florencia*, their F₁ and backcrosses (BC). This characterisation coupled with further behavioural experiments allowed me to understand how chemical cues mediate reproductive isolation in this mimetic pair.

COLLABORATIONS AND PUBLICATIONS

This thesis presented here is the result of my work in collaboration with other colleagues.

The wings used in chapter 1 were obtained from: (i) the “Colección de Artropodos – Universidad del Rosario- CAUR229”, (ii) the butterfly collection of Dr. Chris Jiggins and the University of Cambridge, (iii) Instituto de Ciencias Naturales at Universidad Nacional de Colombia, (iv) personal collection of Jean Francois Le Crom in Bogota. I scanned the wings, conducted the analysis and wrote the manuscript supervised by Dr. Camilo Salazar and Dr. Carolina Pardo. Dr. Melissa Sanchez-Herrera and Dr. William Kuhn made suggestions on the morphometrics analysis. Dr. Steven Van Belleghem trained me in the use of the package Patternize. This chapter was written in view of eventual publication and is under preparation.

In chapter 2 I carried out the experiments at the insectaries of Universidad del Rosario in La Vega (Cundinamarca). I collected the behavioural data, conducted the analyses and wrote the manuscript supervised by Dr. Camilo Salazar and Dr. Carolina Pardo. Part of this chapter was published in the journal *PeerJ* (Q1) in 2017, where I participate as joint first author:

Darragh K.*, Vanjari S.*, Mann F.*, **Gonzalez-Rojas M. F.***, Morrison C. R., Salazar C., Pardo-Diaz G. C., Merrill R. M., McMillan W. O., Schulz S., and C. D. Jiggins (2017). Male sex pheromone components in *Heliconius* butterflies released by the androconia affect female choice. *PeerJ* 5:e3953. doi: 10.7717/peerj.3953 (*Equal contribution).

In chapter 3, I generated inter-specific crosses using the individuals from chapter 2. Pheromone collection and behavioural experiments were done following recommendations of Dr. Kathy Darragh and Dr. Chris Jiggins from the University of

Cambridge, which also contributed with reagents and materials. Dr. Owen McMillan acted as my supervisor at the Smithsonian Tropical Research Institute (STRI) where I analysed the GC/MS data. Dr. Stefan Schulz at the Technische Universität Braunschweig, Institute of Organic Chemistry, helped with the identification of chemical compounds facilitating the reference library and depurating the identification. Dr. Jorge Robles from Universidad Javeriana also reviewed the chemical identification. Dr. Kelsey Bryers gave useful feedback on the data analysis. I collected the data, analysed it and wrote the manuscript supervised by Dr. Camilo Salazar and Dr. Carolina Pardo. The result of this work and part of chapter 2 was published in *Proceedings of the Royal Society* (Q1) where I am first author:

Gonzalez-Rojas M. F., Darragh K., Robles J., Linares M, Schulz S., McMillan O. W., Jiggings C. D., Pardo-Diaz G. C., C. Salazar (2020). Chemical signals act as the main reproductive barrier between sister and mimetic *Heliconius* butterflies. *Proc. R. Soc. B.* 287(1926): 20200587. doi: 10.1098/rspb.2020.0587.

CHAPTER 1. PHENOTYPIC RESEMBLANCE ACROSS MULTIPLE MIMICRY RINGS IN *Heliconius*

INTRODUCTION

Müllerian mimicry is a process where natural selection favours the convergence on warning signals among co-occurring and defended prey species to share the cost of predator learning (169–173). This phenomenon is the result of positive frequency-dependent selection because as the warning signal becomes more common, the higher the probability that a predator has already learned to avoid it, thus reducing the chance of a prey having that signal to be attacked (20,174–177). The ability of a predator to learn and generalize a warning signal is crucial for Müllerian mimicry to work, and in fact, many examples support such learning (170–173). For instance, experienced birds avoid aposematic patterns when they are associated with an unpalatable prey (178,179), and naive birds learn rapidly to avoid those patterns (180). Similarly, great tits can recognize simulated preys with varying levels of perfection (178), while jacamars attack more frequently butterflies with altered wing phenotypes compared to non-altered phenotypes (91). Also, field transplant experiments show that preys with a different or manipulated pattern are more attacked than those matching the local mimetic pattern (21,93,107,127,181,182).

Under the Müllerian mimicry theory, it is not expected to find polymorphisms in a single mimicry ring, as this would lead to mimicry imperfection and thus higher rates of an attack on rare variants (177). However, there are exceptions even in the best known Müllerian mimicry examples, such *Danaus chrysippus* and its co-mimic *Acraea encedon*, *A. encedana* and *Hypolimnas misippus* (177) where polymorphism probably involves allopatric monomorphic subspecies in

secondary contact as a recent expansion of their geographical range resulting from forest clearance and the subsequent establishment of savanna-like conditions in earlier forested areas (183,184). Similarly, the Amazonian butterfly *Heliconius numata* displays mimetic polymorphism throughout its entire range and exhibits up to seven morphs, each one mimicking local *Melinaea* or *Mechanitis* butterflies (Ithomiinae) (101). The causes behind this polymorphism have been recently described, while positive frequency-dependent selection imposed by predators favours the fixation of the locally most abundant morph (*H. n. bicoloratus*), there are disassortative mate preferences that result in a negative frequency-dependent selection (101). The combined effect of these antagonistic selection pressures is sufficient to maintain polymorphism in this species (101,185).

The *Heliconius* butterflies are an excellent example of Müllerian mimicry, where phylogenetically distant species converge to a similar wing phenotype when occurring in sympatry (186). For example, the closely related species *Heliconius melpomene* and *H. cydno* -the former exhibiting red/orange wing colouration and the latter with typical white/yellow wing phenotypes- converge phenotypically with members of the phylogenetically distant species *H. erato* and *H. sarah*/*H. sapho* respectively (12). The only exception to this general rule is the closely related pair *H. timareta* and *H. melpomene*, which mimic each other when in sympatry (187–190). Such interspecific convergence in *Heliconius* is coupled to intraspecific phenotypic divergence, thus there are extreme differences in the wing colour patterns displayed by subspecies that occur in different geographic locations (186). This leads to a spectacular diversity in wing colour patterns, that can be summarised into four major categories: (i) red-banded, (ii) dennis-ray, (iii) yellow/white, and (iv) tiger.

In this butterfly genus, the study of colouration has received a great deal of attention, while fewer studies have comprehensively addressed mimicry accuracy in terms of wing shape, wing size and wing pattern (i.e., the spatial arrangement of markings elements such as bars, bands, spots, patches, etc) within a given mimicry ring. Mérot et al. (172), revealed subtle but consistent variation between populations of *H. timareta thelxinoe* and its co-mimics *H.*

erato favorinus and *H. melpomene amaryllis*, a red-banded mimicry ring in Northern Peru. Likewise, Rossato et al. (191), showed subtle variation in shape and size of the forewing and the red band in a *Heliconius* red-banded mimicry ring in Brazil (*H. erato phyllis* and its co-mimics *H. besckei*, *H. melpomene burchelli*, and *H. melpomene nanna*). Both studies found different mimetic optima shaped by changes in the composition of the local mimetic communities (172,191). Also, a recent study quantified wing colour pattern differences in the mid-forewing region of 14 co-mimic races of *H. erato* and *H. melpomene* and found that, while the relative size of the mid-forewing pattern is nearly similar, there are still developmental constraints that prevent the species from being identical (192). These studies have either focused on red-banded phenotypes or single wing elements. Moreover, additional effects on mimicry that also could shape the colour pattern variation such as geography, number of involved species, and the presence of other genera in the mimetic ring are less studied. Therefore, it is necessary to investigate the generality of such findings.

Colombia has 34 species and 110 subspecies of *Heliconius* (193,194), and in fact, the four major phenotypes of the genus can be found across a wide geographic range in this country. This offers a unique opportunity to (i) test how accurate is the resemblance among co-mimics, (ii) investigate whether quantitative changes in phenotype (if any) are affected by the distribution of the mimicry ring (geography); (iii) test the existence of differences in the phenotypic accuracy between mimetic rings composed with several species versus those with few ones. To address these questions, in this chapter, I evaluated fine-scale morphological differences in size, shape and wing colour pattern of both forewings and hindwings among a comprehensive sampling of mimetic rings in Colombia that bear any of the following colour phenotypes: red-band, dennis-ray, white/yellow.

MATERIALS AND METHODS




















I scanned forewings (FW, hereafter) and hindwings (HW, hereafter) in ventral and dorsal view of 1,102 males from the genera *Chetone*, *Elzunia*, *Euedes* and *Heliconius* (Table 2.1 and Table S1.1). We used a high-resolution flatbed scanner Epson Perfection V550, in RGB colour format with a resolution of 2400 dpi. This was done on specimens with undamaged wings. Right side wings were always used. These images were used to compare wing size, shape and colour pattern in the comparisons listed in Table 2.1.





































WING SHAPE AND SIZE
























The overall shape and size of wings were measured only on the dorsal side using landmark coordinates (LMs, hereafter) placed at vein intersections and vein termini: 17 LMs for the FW and 15 LMs for the HW (Figure 2.1A). LMs were scored by the same person using tpsDig2 (195) and later superimposed using a General Procrustes Analysis (GPA) in the R package “*geomorph*” (196–198). GPA aligns, scales and rotates the configurations to line up the corresponding LMs as carefully as possible, minimizing differences. The resulting coordinates in the tangent space were used as shape data, while the log-transformed centroid size was used as a size estimate (197). Differences in wing size were investigated with a one-way ANOVA with size as dependent variable and subspecies as a factor (as in Table 2.1), followed by a Tukey’s post-hoc test. I calculated the minimum geographic distance between mimicry rings using the function “*distHaversine*” in the Geosphere package (199). Differences in wing shape due to subspecies and geography were assessed using Procrustes MANOVA with the *procD.lm* function in the “*geomorph*” R package (196). I also conducted a principal component analysis (PCA) followed by a linear discriminant analysis (LDA) based on those PCs that explain >95% of the wing shape variation in the “*candisc*” package in R (200). Likewise, I performed a multivariate analysis of covariance (MANCOVA) in R based on those PCs to test for differences in wing shape. The MANCOVA was done with subspecies as an explanatory variable, geographic distance was included as a covariable, and the formula included an interaction term between these two variables.


















Table 2.1. Samples included in the morphometric analysis. A total of 22 comparisons, each one corresponding to a particular mimicry ring (sympatric) and geographic (allopatric) comparisons. Numbers on parentheses indicate the number of individuals scanned. Comparison (C). Simpatry (S), Allopatry (A). **Lab recreated. Dash lines indicate a different geographic mimetic ring.

C	Phenotype	Location/ Occurrence		Mimicry ring
1	Red-banded	Magdalena Valley/ North-East Andean foothills/ Pacific/ Putumayo	A	 <i>H. erato guarica</i> (44) <i>H. melpomene martinae</i> (27) <i>H. erato hydara</i> (50) <i>H. melpomene melpomene</i> (46) <hr style="border-top: 1px dashed black;"/> <i>H. erato venus</i> (19) <i>H. melpomene vulcanus</i> (16) <i>H. erato dignus</i> (25) <i>H. melpomene bellula</i> (41) <i>H. tristero</i> (16)
2		Pacific	S	 <i>H. erato venus</i> (19) <i>H. melpomene vulcanus</i> (16)
3		Magdalena Valley	S	 <i>H. erato guarica</i> (44) <i>H. melpomene martinae</i> (27)
4		North-East Andean foothills	S	 <i>H. erato hydara</i> (50) <i>H. melpomene melpomene</i> (46)
5		Putumayo	S	 <i>H. erato dignus</i> (25) <i>H. melpomene bellula</i> (41) <i>H. tristero</i> (16)
6		Magdalena Valley/	A	 <i>H. melpomene bellula</i> (41) <i>H. melpomene martinae</i> (27) <i>H. melpomene melpomene</i> (46) <i>H. melpomene vulcanus</i> (16)

		North-East Andean foothills/ Pacific/ Putumayo		
7		Magdalena Valley/ North-East Andean foothills/ Pacific/ Putumayo	A	 <i>H. erato dignus</i> (25)  <i>H. erato guarica</i> (44)  <i>H. erato hydara</i> (50)  <i>H. erato venus</i> (19)
8	Dennis-ray	Amazon	S	 <i>Chetone ithrana</i> (4)  <i>Eueides heliconioides eanes</i> (8)  <i>H. aoede</i> (3)  <i>H. elevatus elevatus</i> (11)
				 <i>H. erato lativitta</i> (50)  <i>H. erato reductimacula</i> (28)  <i>H. melpomene malleti</i> (41)  <i>H. melpomene vicina</i> (16)
				 <i>H. timareta subsp. nov.</i> (4)  <i>H. timareta florencia</i> (44)  <i>H. xanthocles melete</i> (12)
9		South-East Andean foothills	S	 <i>H. erato lativitta</i> (50)  <i>H. melpomene malleti</i> (41)  <i>H. timareta florencia</i> (44)  <i>H. xanthocles melete</i> (12)

10	Yellow/White	Cauca Valley/ Magdalena Valley/ Pacific/ North-East Andean foothills	A	 <i>Elzunia humboldt regalis</i> (34)	 <i>Elzunia humboldt tamasea</i> (9)	 <i>H. hecuba tolima</i> (1)	 <i>H. eleuchia eleuchia</i> (49)	 <i>H. eleuchia eleusinus</i> (18)
				 <i>H. erato chestertonii</i> (71)	 <i>H. sapho sapho</i> (8)	 <i>H. sapho chocoensis</i> (13)	 <i>H. sara magdalena</i> (13)	 <i>H. cydno cydno</i> (43)
				 <i>H. cydno cydnides</i> (50)	 <i>H. cydno weymeri f. gustavi</i> (49)	 <i>H. cydno weymeri f. weymeri</i> (51)	 <i>H. cydno weymeri f. submarginatus</i> (50)**	 <i>H. cydno zelinde</i> (51)
				 <i>H. cydno chioneus</i> (4)	 <i>H. cydno wanningeri</i> (15)	 <i>H. cydno lisethae</i> (13)	 <i>H. cydno hermogenes</i> (7)	 <i>H. heurippa</i> (26)
					 <i>H. cydno cordula</i> (17)	 <i>H. cydno subsp. nov.</i> (2)	 <i>H. timareta linaresi</i> (7)	
11		Pacific	S	 <i>H. cydno zelinde</i> (51)	 <i>H. eleuchia eleusinus</i> (18)	 <i>H. sapho chocoensis</i> (13)		
12		Magdalena Valley	S	 <i>H. cydno wanningeri</i> (15)	 <i>H. sapho sapho</i> (8)			
13		Magdalena Valley	S	 <i>H. eleuchia eleuchia</i> (49)	 <i>H. cydno cydno</i> (43)	 <i>H. cydno chioneus</i> (4)	 <i>H. sapho sapho</i> (8)	
14		Magdalena Valley	S	 <i>H. sara magdalena</i> (13)	 <i>H. eleuchia eleuchia</i> (49)	 <i>H. cydno lisethae</i> (13)	 <i>H. sapho sapho</i> (8)	

15		Cauca Valley	S	  <i>H. cydno cydnides</i> (50) <i>H. eleuchia eleuchia</i> (49)
16		Magdalena Valley	S	   <i>Elzunia humboldt tamasea</i> (9) <i>H. cydno hermogenes</i> (7) <i>H. hecuba tolima</i> (1)
17		Cauca Valley	S	   <i>Elzunia humboldt regalis</i> (34) <i>H. cydno weymeri submarginatus</i> (50)** <i>H. cydno weymeri weymeri</i> (51)
18		Cauca Valley	S	  <i>H. cydno weymeri f. gustavi</i> (49) <i>H. erato chestertonii</i> (71)
19	<i>H. melpomene</i> subspecies Red-banded/ Dennis-ray	Magdalena Valley/ North-East Andean foothills/ Pacific/ Putumayo/ Amazon	A	    <i>H. melpomene melpomene</i> (46) <i>H. melpomene bellula</i> (41) <i>H. melpomene martinae</i> (27) <i>H. melpomene vulcanus</i> (16) <hr style="border-top: 1px dashed black;"/>   <i>H. melpomene malleti</i> (41) <i>H. melpomene vicina</i> (16)
20	<i>H. erato</i> subspecies Red-banded/ Dennis-ray/ White/Yellow	Magdalena Valley/ North-East Andean foothills/ Pacific/ Putumayo/ Amazon/ Cauca Valley	A	    <i>H. erato hydara</i> (50) <i>H. erato dignus</i> (25) <i>H. erato guarica</i> (44) <i>H. erato venus</i> (19) <hr style="border-top: 1px dashed black;"/>    <i>H. erato lativitta</i> (50) <i>H. erato reductimacula</i> (28) <i>H. erato chestertonii</i> (71)

21	<i>H. cydno</i> subspecies Yellow/White	South-East Andean foothills/ Cauca Valley/ Magdalena Valley/ Pacific/ North-East Andean foothills	A	 <i>H. cydno cydnides</i> (50)  <i>H. cydno chioneus</i> (4)  <i>H. cydno cydno</i> (43)  <i>H. cydno waningeri</i> (15)  <i>H. cydno lisethae</i> (13)  <i>H. cydno hermogenes</i> (7)  <i>H. cydno cordula</i> (17)  <i>H. cydno subsp. nov.</i> (2)  <i>H_c_weymeri</i> f. <i>weymeri</i> (51)  <i>H. cydno zelinde</i> (51)  <i>H. cydno weymeri</i> f. <i>submarginatus</i> (50)**  <i>H. cydno weymeri</i> f. <i>gustavi</i> (49)
22	<i>H. timareta</i> subspecies Red-banded/ Dennis-ray/ White/Yellow	Putumayo/ Amazon/ Eastern slopes of the Andes	A	 <i>H. tristero</i> (16)  <i>H. timareta florencia</i> (44)  <i>H. timareta subsp. nov.</i> (4)  <i>H. timareta linaresi</i> (7)  <i>H. heurippa</i> (26)

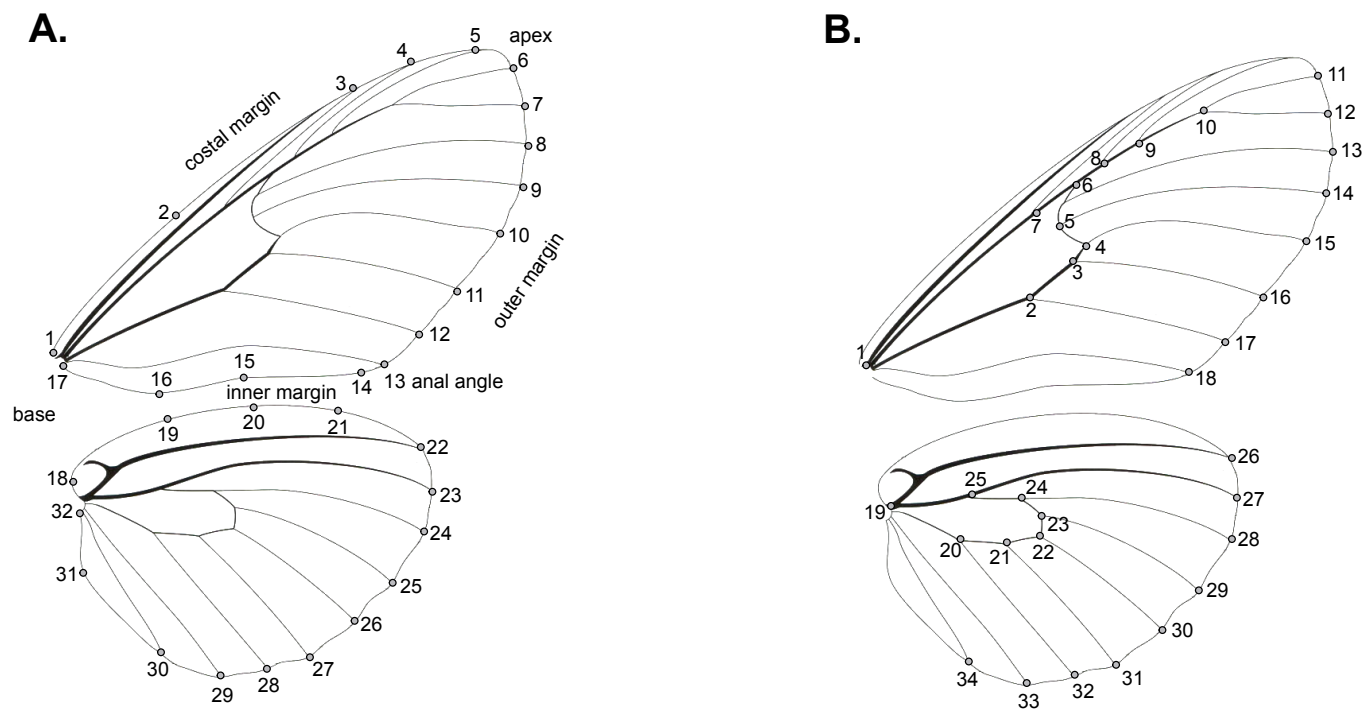


Figure 2.1. Position of the landmark coordinates (LM) used in the analysis of (A) shape and size and (B) colour pattern.

WING PATTERN

To quantify variation in wing colour patterns (i.e. the spatial arrangement of wing elements such as bars, bands, spots, patches, etc), I used the R package *Patternize* which extracts, transforms and superimposes colour patterns to finely quantify their variation among populations (201). I used the program Image J (202) to place a set of 34 LMs per individual (18 on the FW and 16 on the HW, dorsally and ventrally, Figure 2.1B). To ensure that LMs were homologous among individuals, I used vein intersections and vein termini as reference for their position (Figure 2.1B). With this information, *Patternize* defines homology between wing elements' position across specimens and then, the software transforms these LMs by translating, rotating, scaling and skewing them (201). A RGB (Red, Green and Blue) value was specified for the wing colour pattern of interest (red-banded, dennis-ray, yellow/white phenotype), to fully extract it. *Patternize* uses a basic image segmentation approach to identify the correct colour boundaries by specifying a RGB value and selecting pixels within the specified colour. Therefore, each pixel coordinates with the colour of interest in a sample get a value of one, and pixel coordinates without the colour of interest have a value of zero (201). Next, a tps (thin-plate spline) transformation was obtained using a random reference sample and these tps transformations were used to align and compare the extracted pattern from each subspecies. The differences in the pattern of interest were obtained using the function *SumRaster* to compare between co-mimics. Later, using the *patArea* function, I estimated the relative size as the proportion of the total wing area in which the pattern is identified.

A principal component analysis (PCA) is performed to characterize variation in colour pattern elements between subspecies; this is done using the variance-covariance matrix obtained from the binary matrix. When visualizing the predicted colour pattern changes across the PC axis, positive values mean a higher predicted expression of the colour pattern element of interest (red) where negative values indicate an absence of the element (blue) (201).

Differences in wing pattern were tested using a multivariate analysis of covariance (MANCOVA) in R based on a subset of PCs (those that explain >95% of the variation). The MANCOVA was done with subspecies as an explanatory variable, geographic distance was included as co-variable, and the formula included an interaction term between these two variables as mentioned before.

RESULTS

WING SIZE AND SHAPE

Overall, I observed that wing size is not a component of mimicry in the rings I evaluated. For example, in rings where *H. erato* and *H. melpomene* participate, the wings of latter are consistently larger (except for *H. m. vulcanus*; Figure 2.2 and 2.3; Table S1.2 - Comparisons 1-5, 8-9). Similarly, *H. cydno* also showed larger wings than all of its co-mimics (except for *Elzunia* or *H. hecuba*; Figure 2.4, Table S1.2 – Comparisons 10-18). When I compared wing size within a single species, I recovered associations with geography (Figures 2.5-2.8; Table S1.2 – Comparisons 19-21). For instance, all Amazonian (dennis-ray) subspecies of *H. melpomene* were similar in wing size, but they were slightly larger than subspecies of *H. melpomene* from the Andes or the Pacific coast (Figure 2.5; Table S1.2 – Comparison 19). I observed the same pattern in *H. erato* (Figure 2.6; Table S1.2 – Comparison 20), except for the subspecies *H. e. venus* which varies greatly in wing size across its distribution. In agreement with this observation, the Andean/Pacific subspecies *H. e. chestertonii* stood out as the smaller *H. erato*. In contrast, I detected the opposite pattern in *H. cydno* (although this species shows considerable variation in wing size across its distribution). Overall, subspecies of *H. cydno* from the Pacific (such as *H. c. zelinde*) and the north of the Magdalena Valley (such as *H. c. cydno* and *H. c. waningeri*) are those with larger wings (Figure 2.4 and 2.7; Table S1.2 –

Comparison 21). *H. timareta*, on the other hand, was the species with the largest wings compared to other *Heliconius* (Figure 2.2, 2.3 and 2.4; Table 2.2 – Comparisons 1, 5, 8-10). There is some variation in FW size among subspecies that are associated with geography, where the Andean *H. t. linaresi* and *H. heurippa* are similar and both have larger FW than the Amazonian *H. t. spp. nov.* (although the sample size of the latter subspecies is reduced; n=4, Figure 2.8; Table S1.2 – Comparison 22).

I also found that wing shape seems not to contribute to mimicry (Table S1.2). Overall, species that are considered as the ‘model’ (i.e., *H. erato* and members of the *H. sara/sapho* clade) exhibit more elongated wings with a steep angle in the inner border. In contrast, their mimics (i.e., *H. melpomene* and *H. cydno*) show rounder wings (Figure 2.9-2.11; Figure S1.1-S1.9). As such, in the case of red-banded *H. melpomene* and *H. erato*, the PC1 recovers two clusters that group by species rather than by mimicry ring (Figure 2.9). Interestingly *H. tristero* appears right in the middle of these two clusters. In addition, in the dennis-ray ring (Amazonian), I could not differentiate species based on their wing shape except for *H. t. florencía* and *H. aoede* (Figure 2.10). The FW of these two species is more elongated towards the apex and their HW is less rounded than in other dennis-ray species (Figure 2.10A-C; Figure S1.3, S1.5; Table S1.2 – Comparison 8). Also, the inner border of the HW in *H. t. florencía* has a steeper angle (Figure S1.5). Similarly, in the yellow/white mimicry rings we also found that wing shape variation is mainly explained by phylogenetic distance. In the analyses of both the FW and HW, I observed two clusters (Figure 2.11): one that groups all subspecies of *H. sara*, *H. sapho* and *H. eleuchia*, and the second that groups all subspecies of *H. cydno* as well as *H. t. linaresi* and *H. heurippa* (these two and *H. c. cordula* have no co-mimic). The only exception was *H. e. chestertonii*, which grouped with *H. cydno* but separated from its co-mimic *H. c. gustavi* at least in the FW (Figure 2.11A-C). In general, *H. cydno* has rounder wings than those of *H. eleuchia*, *H. sapho* and *H. sara*, which all have HWs with a steeper edge towards the anal margin (Figure 2.11, S1.7, S1.9) and their FWs are more elongated towards the apex of the wing (Figure S1.6, S1.8). These differences in wing shape in all phenotypes analysed held true when we compared co-mimic species in each

local mimicry ring (Table S1.2 – Comparisons 11-18). We only detected a geographic effect on this trait in the red-banded mimicry ring of *H. e. guarica* and *H. m. martinae* (which occurs in the Magdalena Valley), but there was no interaction between subspecies and geographic distance (Table S1.2 – Comparison 3).

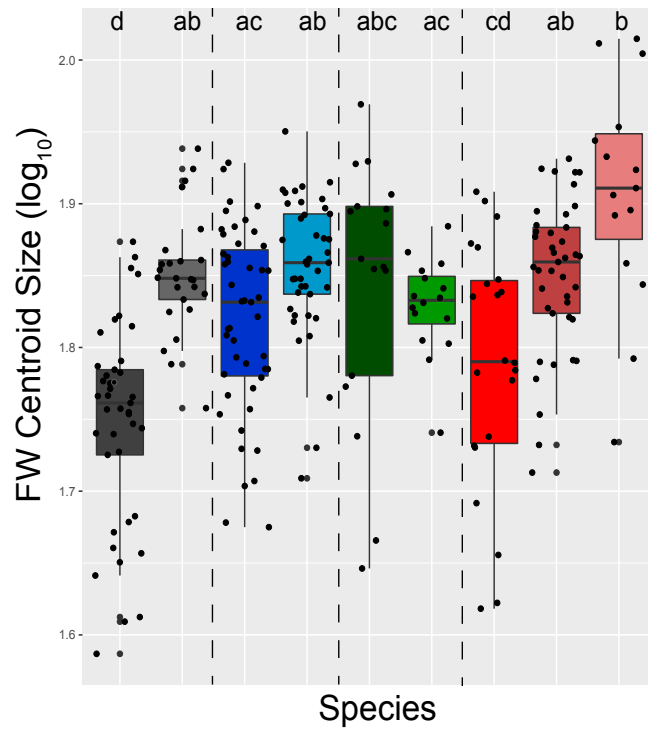
I also examined intraspecies variation in wing shape. In the red coloured *Heliconius*, specifically *H. melpomene* and *H. erato*, we found that this trait does not vary among subspecies (Table S1.2 – Comparison 19; Figure 2.12). In *H. erato*, however, individuals of *H. e. chestertonii* form a separate cluster in the PC1 of the FW analysis (Table S1.2 – Comparison 20, Figure 2.13A-C), which agrees with the fact that the FW of this subspecies is more elongated (Figure S1.6, S1.8). It is worth noting that all individuals of *H. e. chestertonii* cluster together regardless of how far they were collected (Table S1.2 – Comparison 20; Figure 2.13). In the yellow/white phenotype, the results were more variable. For example, in *H. cydno* there was a considerable variation in wing shape between subspecies. Shape variation in PC1 of the FW analysis separates forms of *H. c. weymeri* (i.e., *H. c. weymeri f. weymeri*, *H. c. weymeri f. gustavi*, and *H. c. weymeri f. submarginatus*; Figure 2.14A-C; Table S1.2 – Comparison 21), while the PC1 of the HW analysis separates the subspecies *H. c. cydno* (Figure 2.14D-F; Table S1.2 – Comparison 21). This agrees with the fact that *H. c. weymeri* has FW that are rounder towards the apex while the HW of *H. c. cydno* is the least rounder (Figure S1.6-S1.9). The comparisons that involved taxa sister to *H. cydno* (i.e., *H. heurippa* and *H. timareta*) revealed that *H. heurippa* has less elongated wings than *H. timareta*, which likely causes them to separate in the PC1 of the FW analysis (Figure 2.15A-C; Table S1.2 – Comparison 22). The PC1 of the HW analysis separated *H. t. florenciana* as it has an inner border with a steeper angle (less rounded than the other subspecies) (Figure 2.15; Table S1.2 – Comparison 22).

When I included in the analysis taxa from other genera that are known to participate in mimicry rings with *Heliconius*, they were recovered as a different group in both PC1 and PC2. For example, in the dennis/ray analysis, I recovered *Chetone ithrana* as a different group in PC2 of the FW and HW

(Figure S1.5). The FW of *C. ithrana* has an inner edge with a steeper angle, and it is less rounded than the FW and HW of other species in the dennis-ray ring (Figure 2.10, Figure S1.4, S1.5). Also, the PC1 of the FW analysis showed *E. heliconioides* slightly separated from *Heliconius* with the FW being more elongated towards the apex (Figure S1.3, S1.5). In the yellow/white phenotypes, *Elzunia* formed a separate cluster (Figure S1.8, S1.9). The FW of this species is more triangular and is wider towards the apex and apical margin (Figure 2.11A-C; Figure S1.6; S1.8; Table S1.2), while its HW is also wider than that of *Heliconius*, and the coastal margin is not straight but has a curve (Figure S1.7; S1.9). The only species of *Heliconius* with a wing shape similar to *Elzunia* is *H. hecuba*, but the sample size of this species is very limited (n=1).



A.



B.

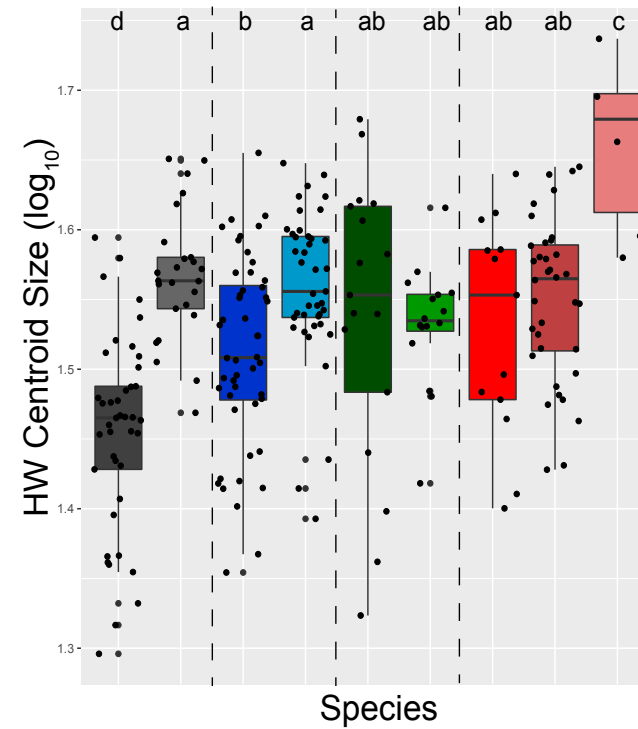


Figure 2.2. Wing size variation between subspecies with the red-band phenotype. (A) FW ($F_{(8,256)}=14.37$, $p<2e-16^*$) and (B) HW ($F_{(8,234)}=12.72$, $p=3.74e-15^*$) variation among geographic red-banded phenotype. Letters above each box indicate Tukey post-hoc statistically significant groups. Dash lines separate different local mimicry rings. Asterisk (*) is indicative of statistical significance ($\alpha=0.01$).

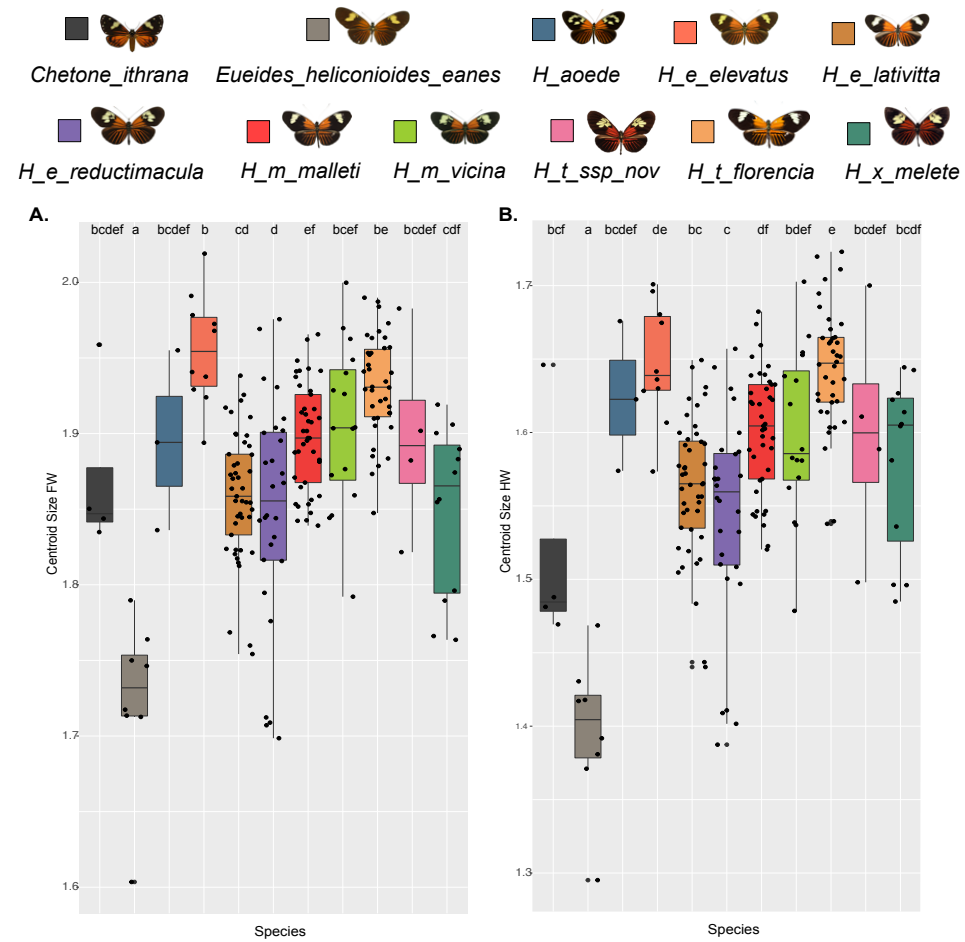


Figure 2.3. Wing size variation between species and subspecies with the dennis-ray mimetic ring in the Amazon. The analysis included members of Heliconius, Eueides heliconioides and the moth Chetone ithrana. **(A)** FW ($F_{(10,198)}=18.26$, $p<2e-16^*$) and **(B)** HW ($F_{(10,160)}=14.99$, $p<2e-16^*$). Letters above each box indicate Tukey post-hoc statistically significant groups. Asterisk (*) is indicative of statistical significance ($\alpha=0.01$).

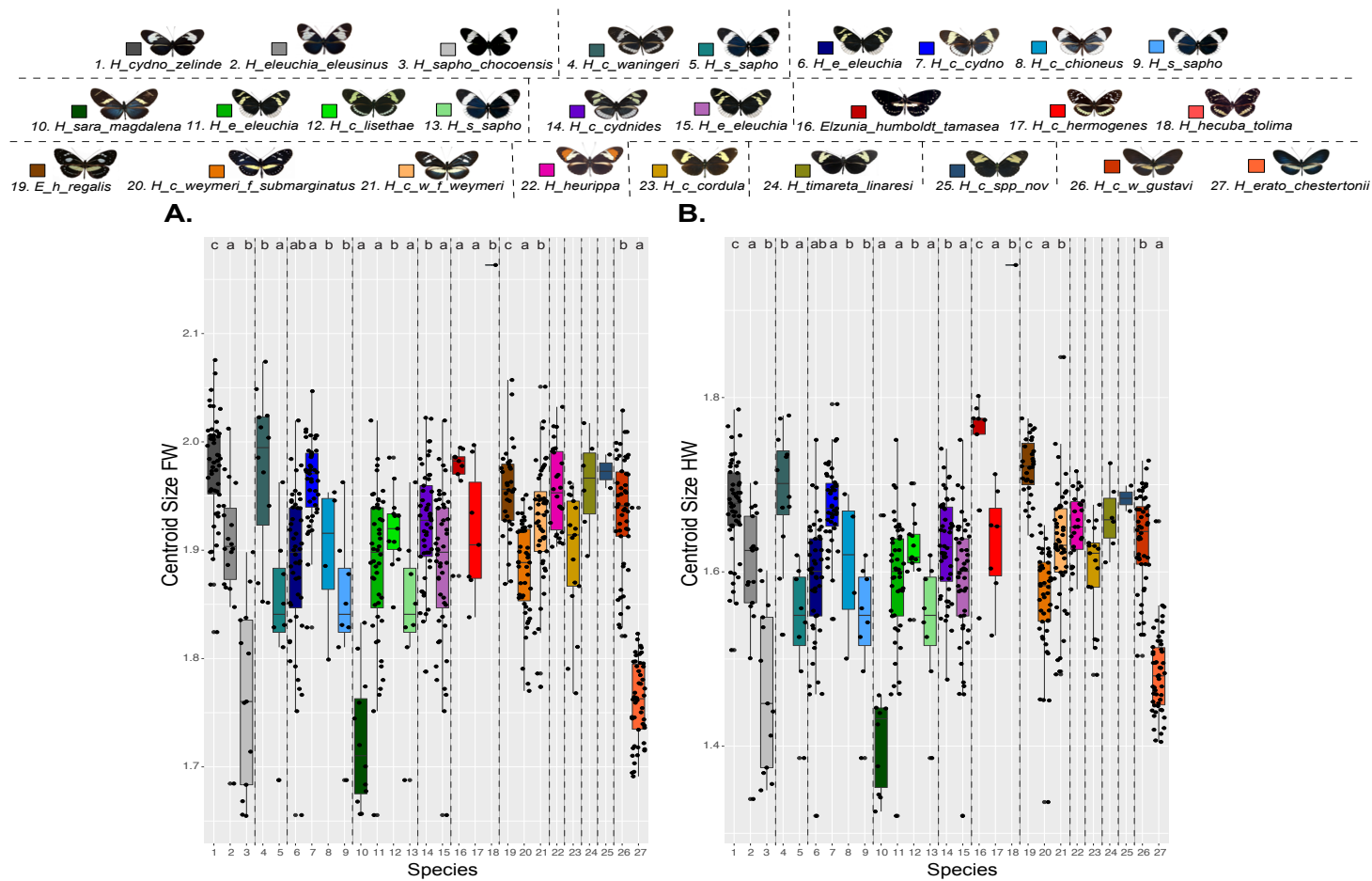
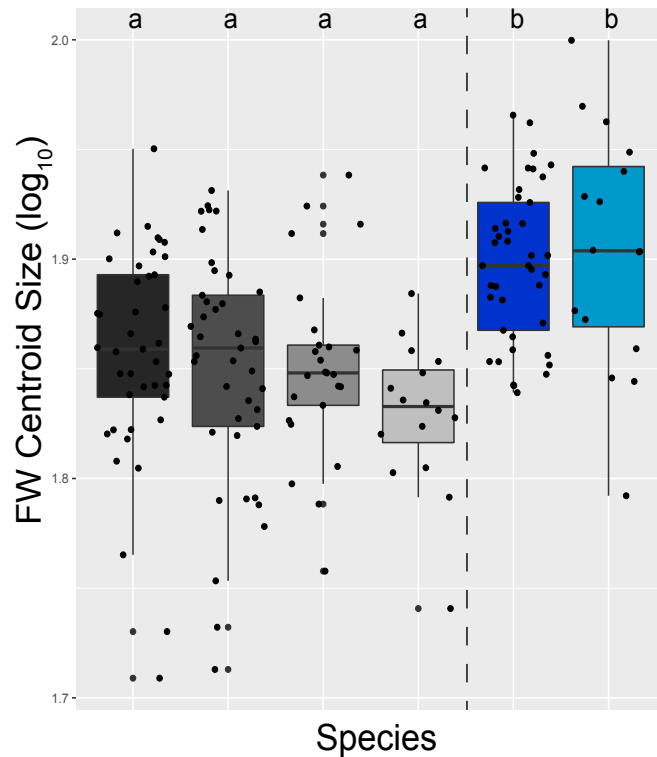


Figure 2.4. Wing size variation between subspecies with the yellow/white phenotype. (A) FW ($F_{(22,655)}=36.63$, $p<2e-16^*$) and **(B)** HW ($F_{(22,642)}=33.17$, $p<2e-16^*$). Letters above each box indicate Tukey post-hoc statistically significant groups. Dashed lines separate different local mimicry ring. *H. sapho sapho* and *H. eleuchia eleuchia* are included more than once to facilitate the comparison since they participate in more than one mimicry ring. Asterisk (*) is indicative of statistical significance ($\alpha=0.01$).



A.



B.

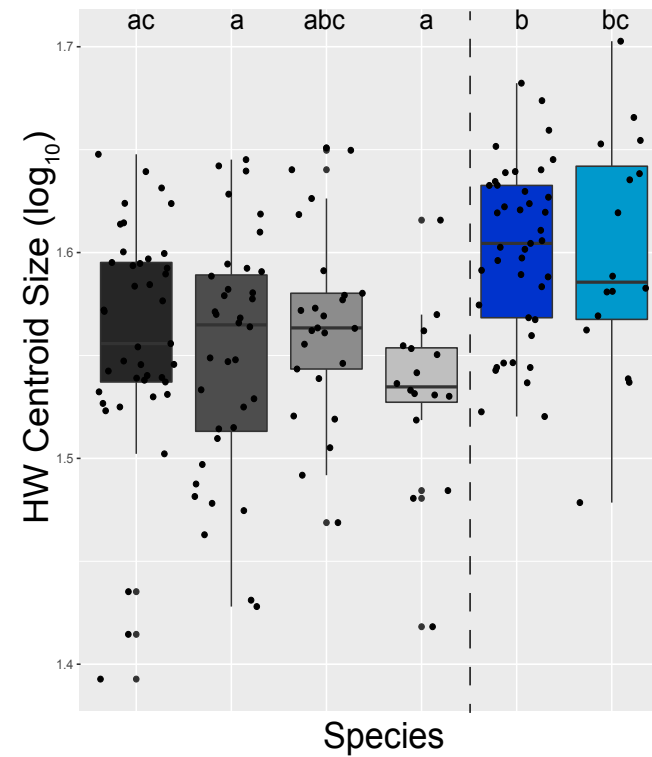
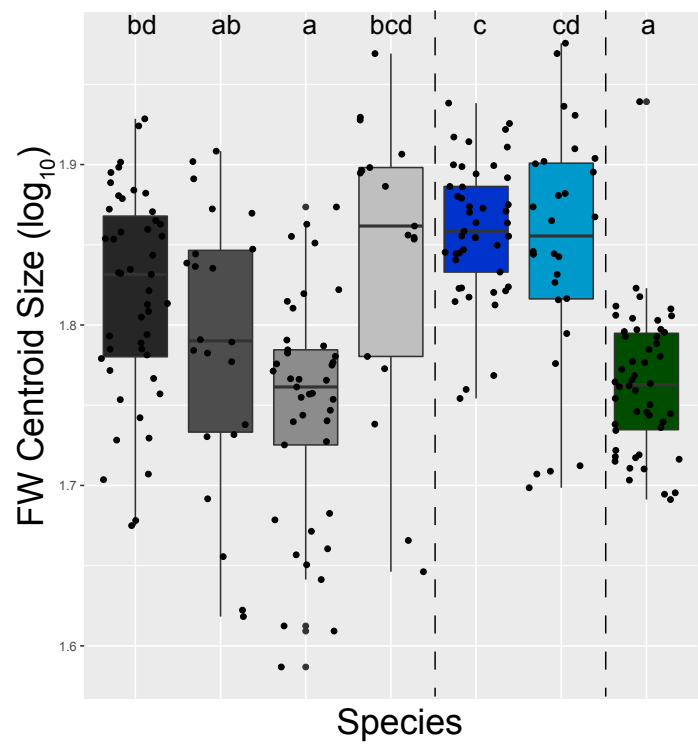


Figure 2.5. Wing size variation between subspecies of *H. melpomene*. (A) FW ($F_{(5,174)}=10.34$, $p=1.08e-08^*$) and (B) HW ($F_{(5,169)}=7.27$, $p=3.39e-06^*$). Letters above each box indicate Tukey post-hoc statistically significant groups. Dash lines separate local mimicy rings. Asterisk (*) is indicative of statistical significance ($\alpha=0.01$).



A.



B.

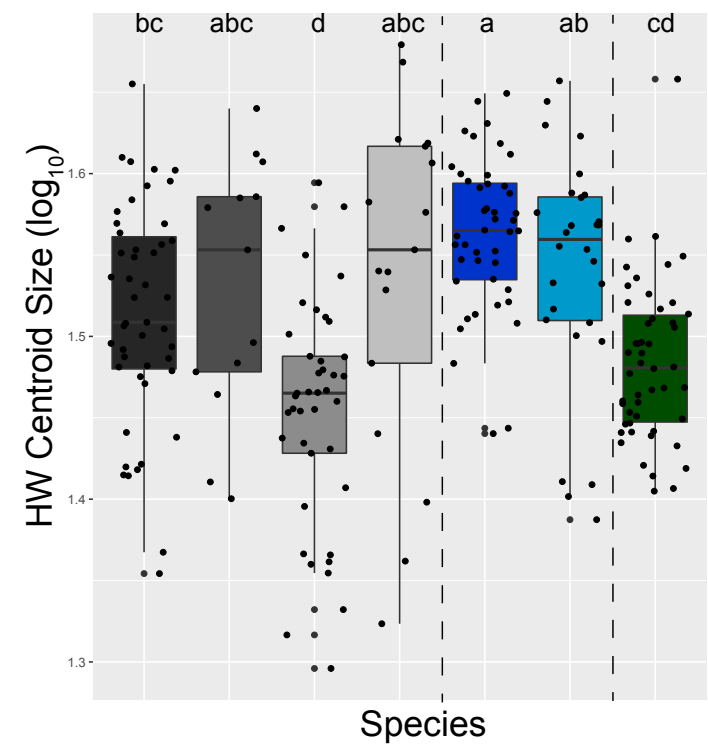


Figure 2.6. Wing size variation between subspecies of *H. erato*. (A) FW ($F_{(6,243)}=16.67$, $p<2e-16^*$) and (B) HW ($F_{(6,233)}=12.8$, $p=1.75e-12^*$). Letters above each box indicate Tukey post-hoc statistically significant groups. Dash lines separate local mimicry rings. Asterisk (*) is indicative of statistical significance ($\alpha=0.01$).

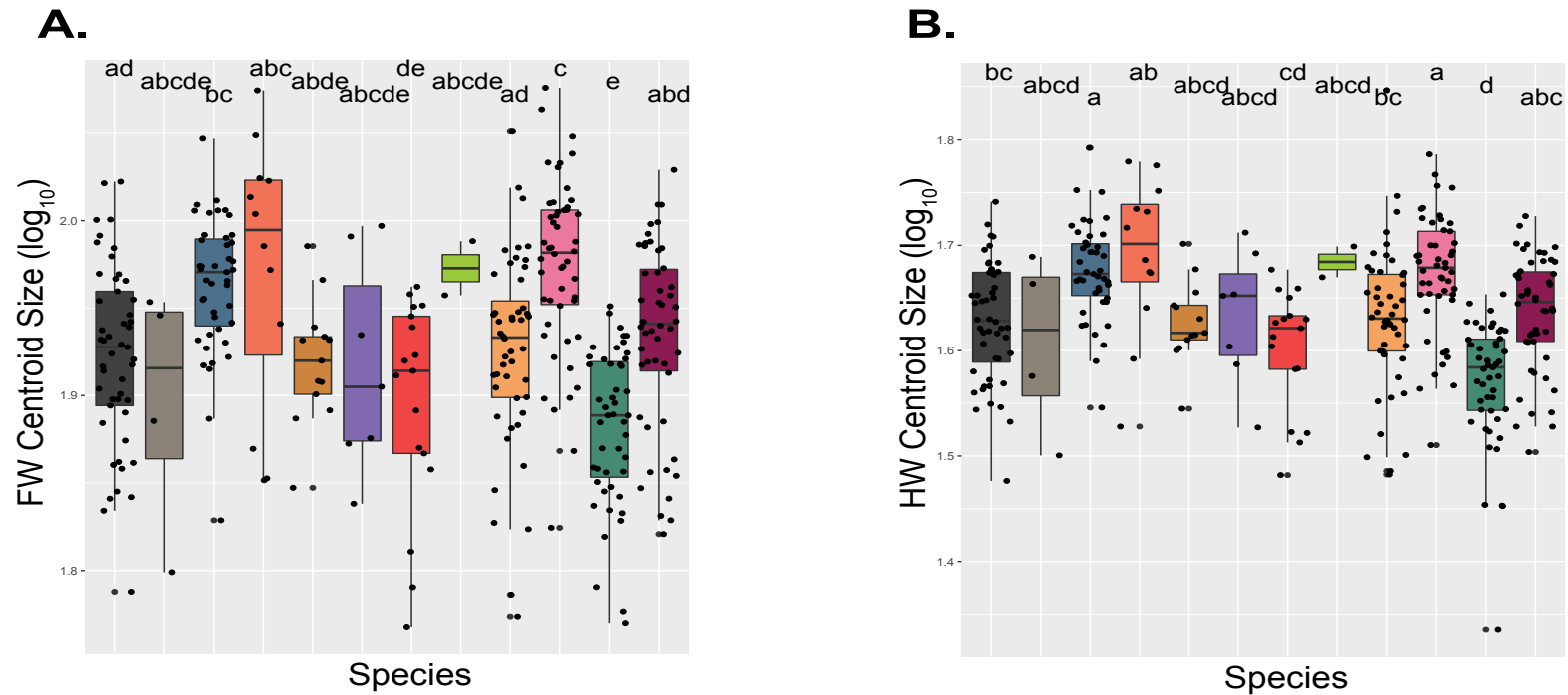
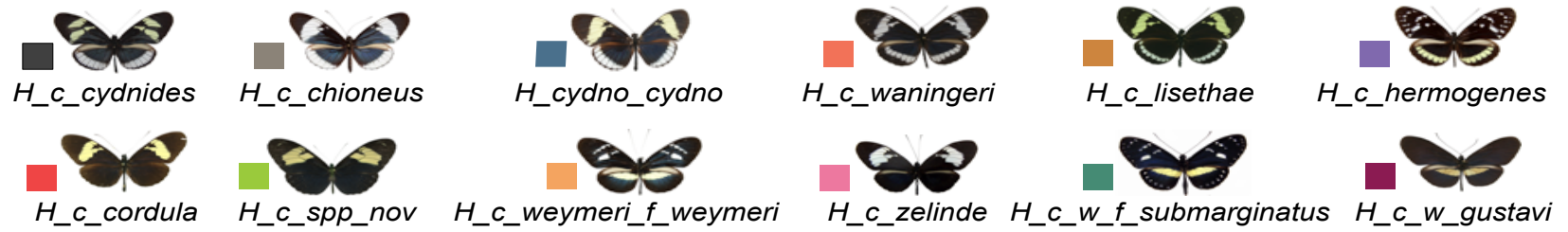


Figure 2.7. Wing size variation between subspecies of *H. cydno*. (A) FW ($F_{(11,330)}=10.71$, $p<2e-16^*$) and (B) HW ($F_{(11,328)}=11.07$, $p<2e-16^*$). Letters above each box indicate Tukey post-hoc statistically significant groups. Asterisk (*) is indicative of statistical significance ($\alpha=0.01$).

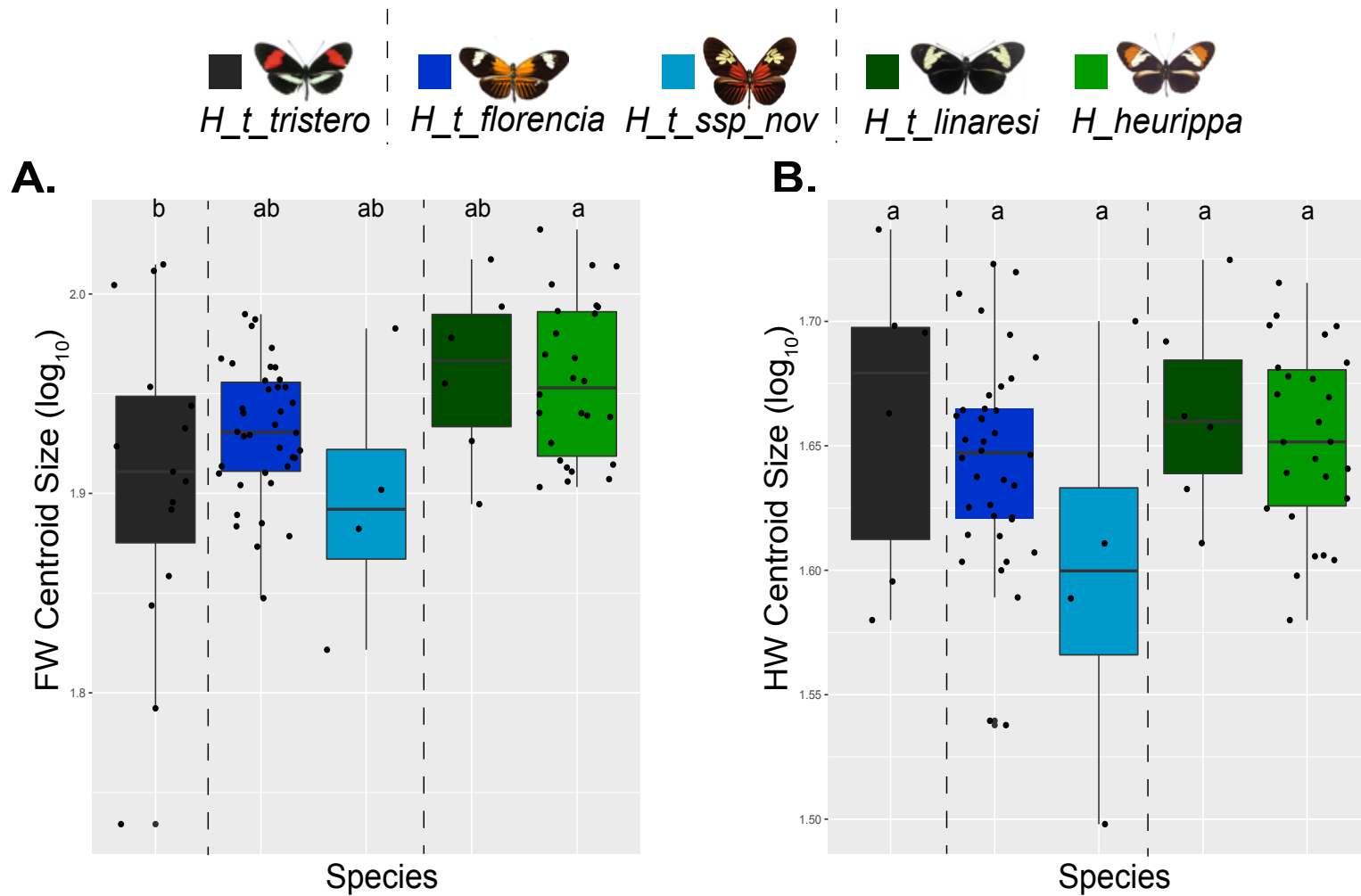


Figure 2.8. Wing size variation between subspecies of *H. timareta*. (A) FW ($F_{(4,84)}=3.70$, $p=0.007^*$) and (B) HW ($F_{(4,75)}=1.65$, $p=0.16$) Letters above each box indicate Tukey post-hoc statistically significant groups. Dash lines separate local mimicry rings. Asterisk (*) is indicative of statistical significance ($\alpha=0.01$).

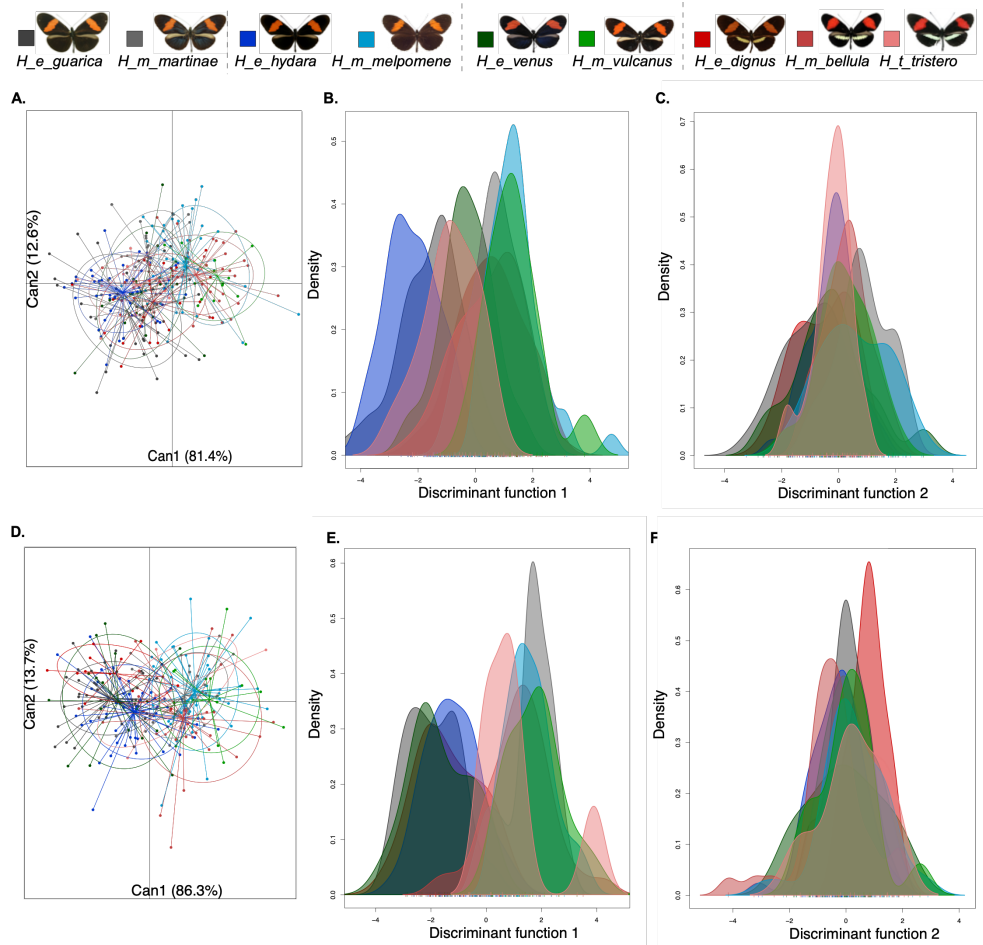


Figure 2.9. Comparison of wing shape between subspecies with the red-band phenotype. Discriminant analysis (**A, D**) and density plots (**B-C, E-F**) showing the variation in the shape of the FW (top row) and HW (bottom row). Dash lines separate different local mimicry rings. The MANCOVA test showed a significant main effect of subspecies (FW: $F_{(8,247)}=6.81$, $p=3.65e-14^*$; HW: $F_{(8,225)}=10.03$, $p=2.2e-16^*$), a non-significant effect of geographic distance (FW: $F_{(1,247)}=1.74$, $p=0.17$; HW: $F_{(1,225)}=0.89$, $p=4.11$) and a non-significant interaction between factors (FW: $F_{(8,247)}=0.91$, $p=0.54$; HW: $F_{(8,225)}=0.84$, $p=0.63$).

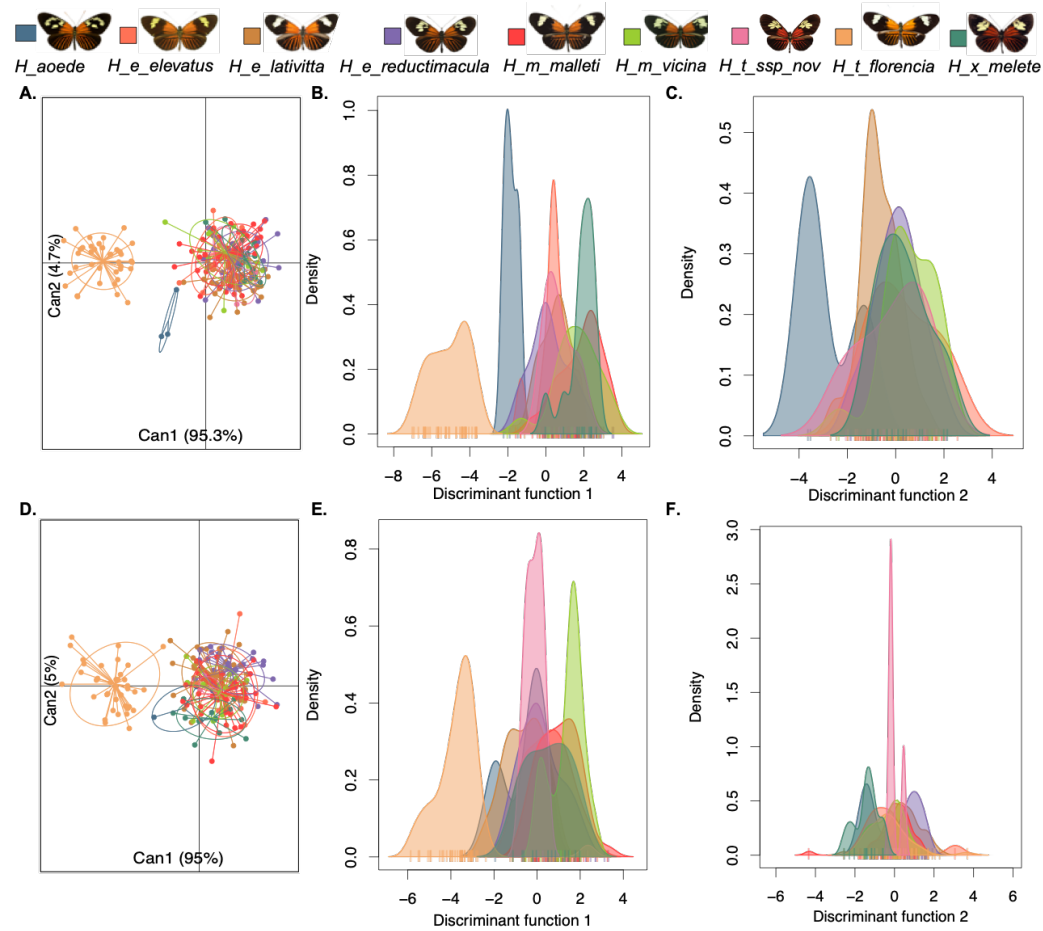


Figure 2.10. Comparison of wing shape between species and subspecies that participate in the dennis-ray mimicry ring in the Amazon. Discriminant analysis (A, D) and density plots (B-C, E-F) showing the variation in the shape of the FW (top row) and HW (bottom row). The MANCOVA test showed a significant main effect of subspecies (FW: $F_{(8,183)}=47.29$, $p=2.2e-16^*$; HW: $F_{(8,181)}=24.70$, $p=2.2e-16^*$), a non-significant effect of geographic distance (FW: $F_{(1,183)}=1.10$, $p=0.33$; HW: $F_{(1,181)}=0.28$, $p=0.75$), and a non-significant interaction between factors (FW: $F_{(4,183)}=0.97$, $p=0.45$; HW: $F_{(5,181)}=0.90$, $p=0.52$).

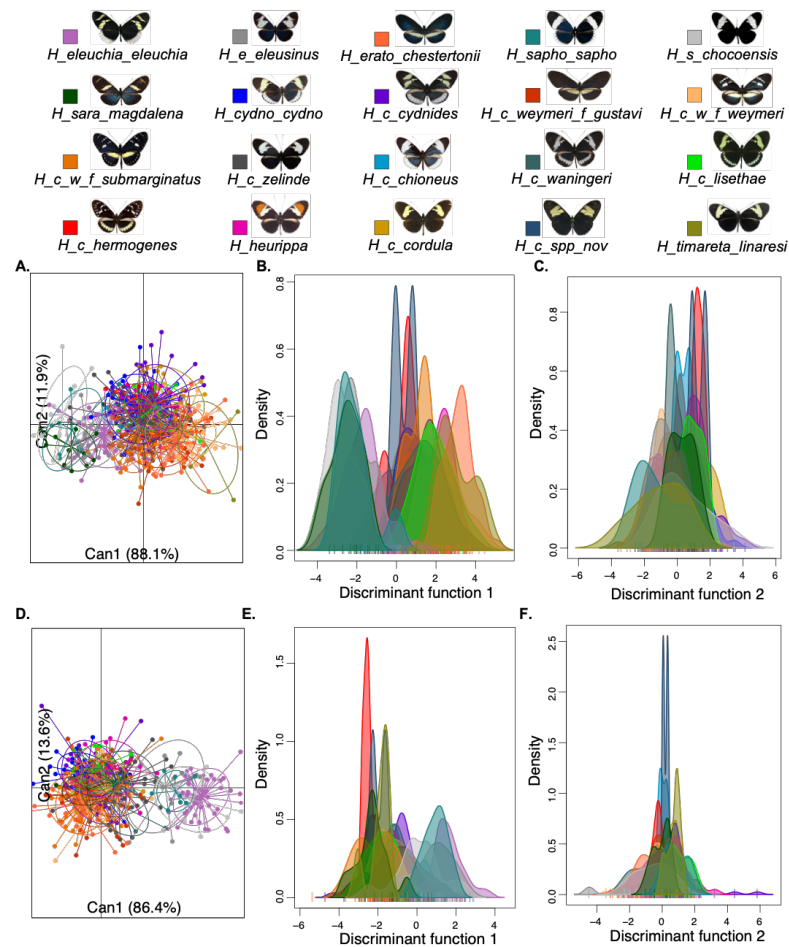


Figure 2.11. Comparison of wing shape between subspecies with the yellow/white phenotype. Discriminant analysis (A, D) and density plots (B-C, E-F) showing the variation in the shape of the FW (top row) and HW (bottom row). The MANCOVA test showed a significant main effect of subspecies (FW: $F_{(17,392)}=13.17$, $p<2.2e-16^*$; HW: $F_{(17,392)}=24.71$, $p<2.2e-16^*$), a non-significant effect of geographic distance (FW: $F_{(1,392)}=0.23$, $p=0.78$; HW: $F_{(1,392)}=2.05$, $p=0.12$), and a non-significant interaction between factors (FW: $F_{(12,392)}=0.91$, $p=0.58$; HW: $F_{(12,392)}=1.02$, $p=0.43$).

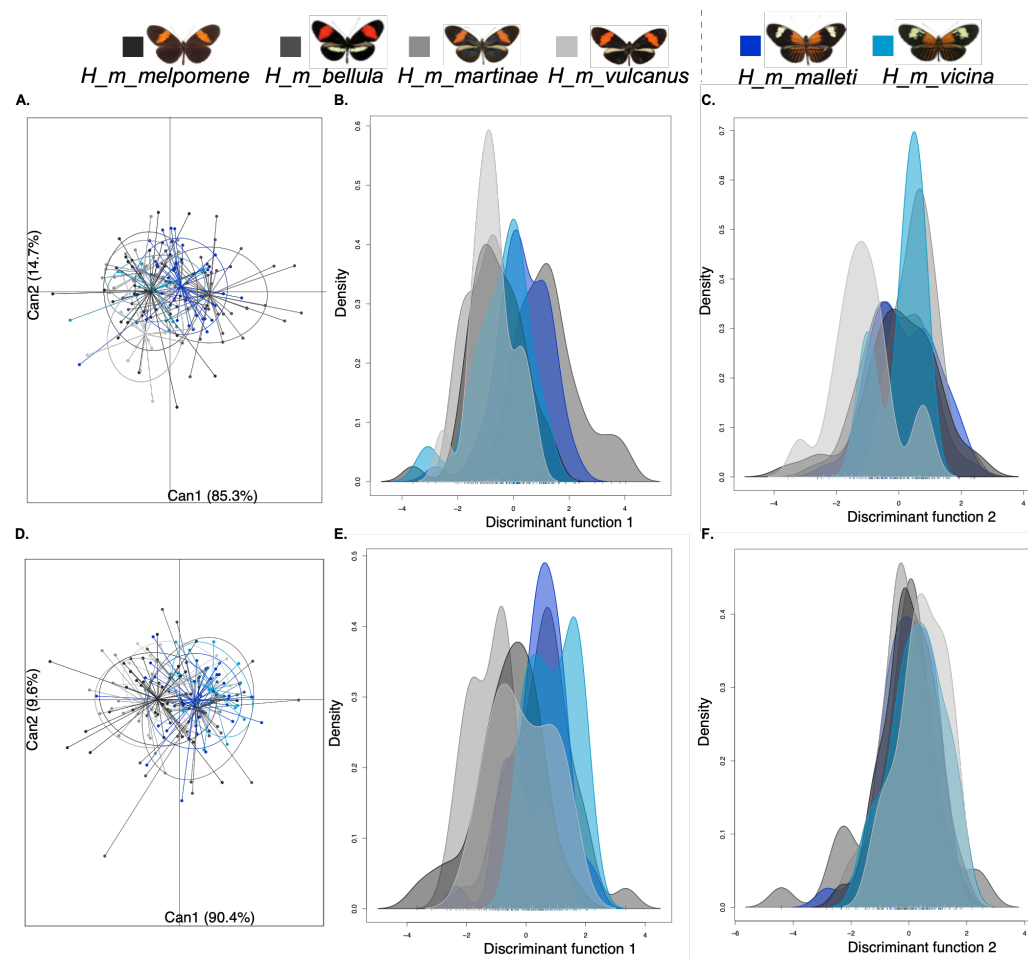


Figure 2.12. Comparison of wing shape between subspecies of *H. melpomene*. Discriminant analysis (A, D) and density plots (B-C, E-F) showing the variation in the shape of the FW (top row) and HW (bottom row). The MANCOVA test showed a non-significant main effect of subspecies (FW: $F_{(5,168)}=6.19$, $p=0.10$; HW: $F_{(5,163)}=2.16$, $p=0.06$), a non-significant effect of geographic distance (FW: $F_{(1,168)}=2.34$, $p=0.09$; HW: $F_{(1,163)}=1.02$, $p=0.36$), and a non-significant interaction between factors (FW: $F_{(5,168)}=0.41$, $p=0.10$; HW: $F_{(5,163)}=1.19$, $p=0.29$). Dash lines indicate different mimicry rings.

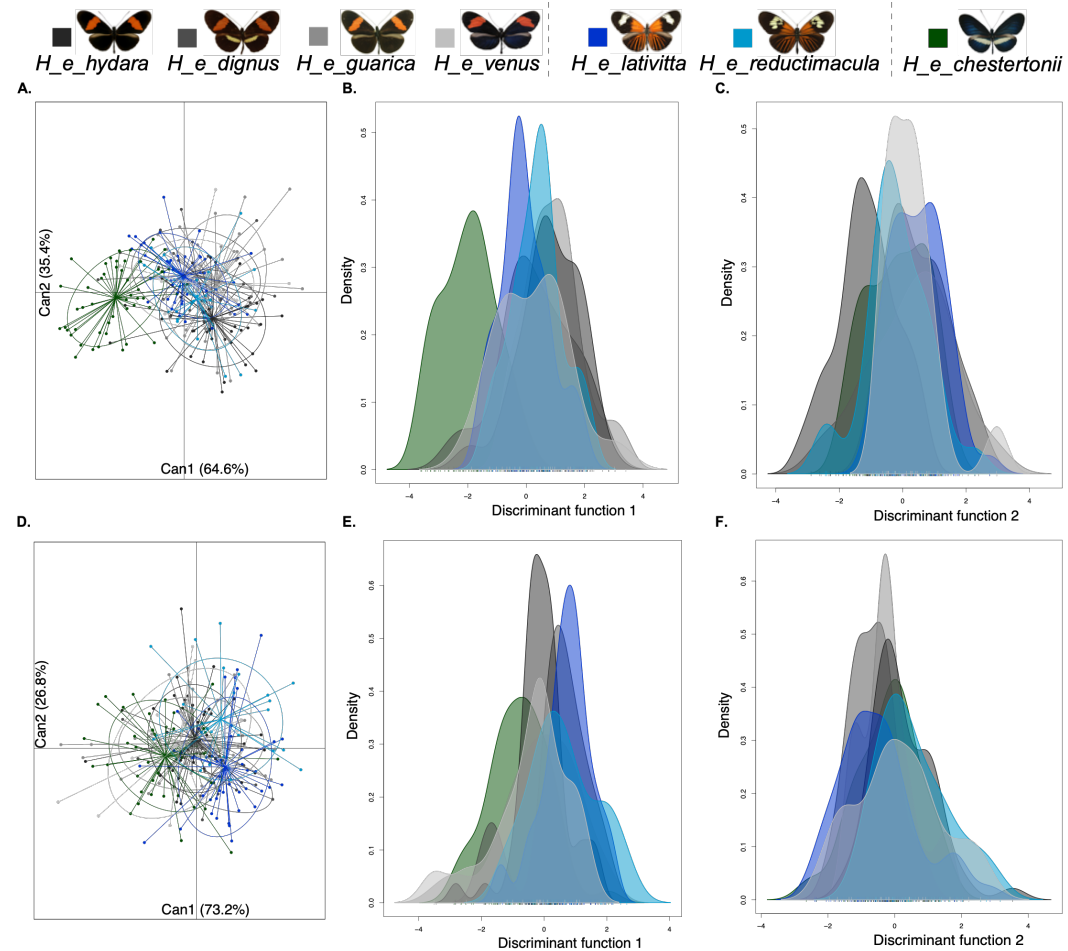


Figure 2.13. Comparison of wing shape between subspecies of *H. erato*. Discriminant analysis (A, D) and density plots (B-C, E-F) showing the variation in the shape of the FW (top row) and HW (bottom row). The MANCOVA test showed a significant main effect of subspecies in the FW ($F_{(6,235)}=6.37$, $p=1.62e-10^*$) but not in the HW ($F_{(6,226)}=7.30$, $p=0.26$). The MANCOVA test did not detect a significant effect of geographic distance (FW: $F_{(1,235)}=0.19$, $p=0.82$; HW: $F_{(1,226)}=0.82$, $p=0.43$), or interaction between factors (FW: $F_{(6,235)}=1.25$, $p=0.24$; HW: $F_{(6,226)}=0.92$, $p=0.52$). Dash lines indicate different mimicry rings.

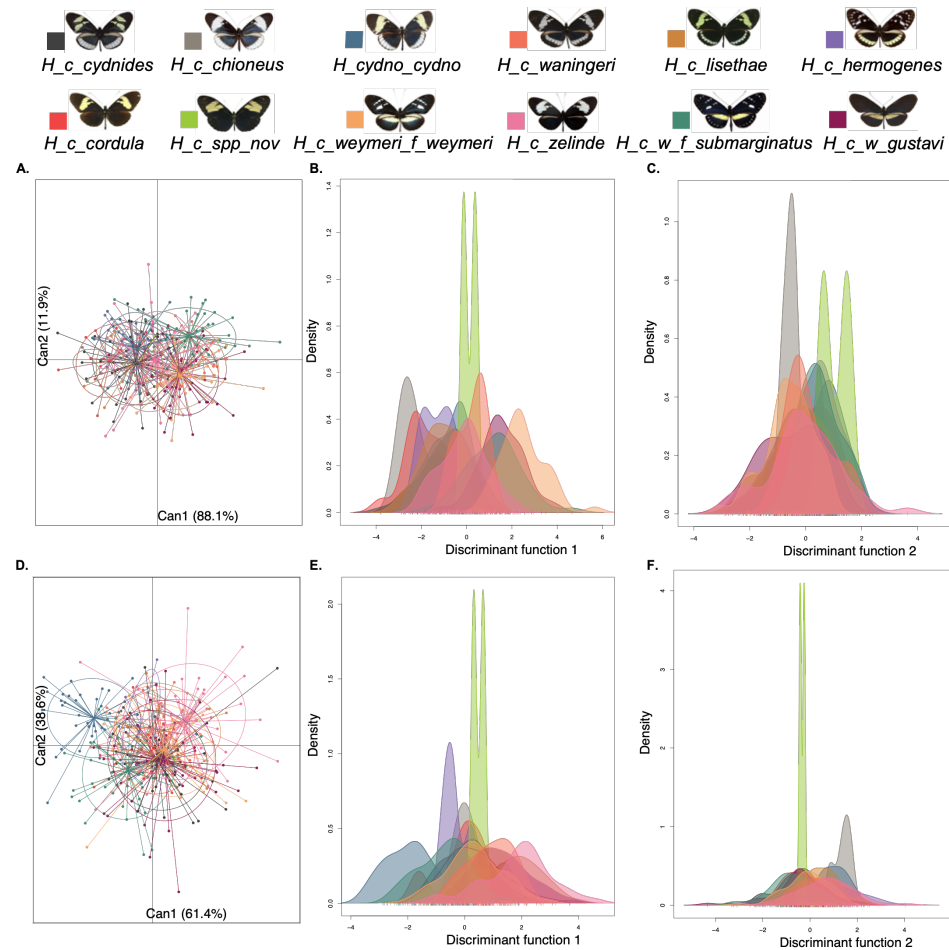


Figure 2.14. Comparison of wing shape between subspecies of *H. cydno*. Discriminant analysis (A, D) and density plots (B-C, E-F) showing the variation in the shape of the FW (top row) and HW (bottom row). The MANCOVA test showed a significant main effect of subspecies (FW: $F_{(11,323)}=13.87$, $p<2.2e-16^*$; HW: $F_{(11,226)}=8.46$, $p<2.2e-16^*$), a non-significant effect of geographic distance (FW: $F_{(1,323)}=0.35$, $p=0.70$; HW: $F_{(1,226)}=1.09$, $p=0.33$), and a non-significant interaction between factors (FW: $F_{(6,323)}=1.05$, $p=0.39$; HW: $F_{(6,226)}=1.03$, $p=0.41$).

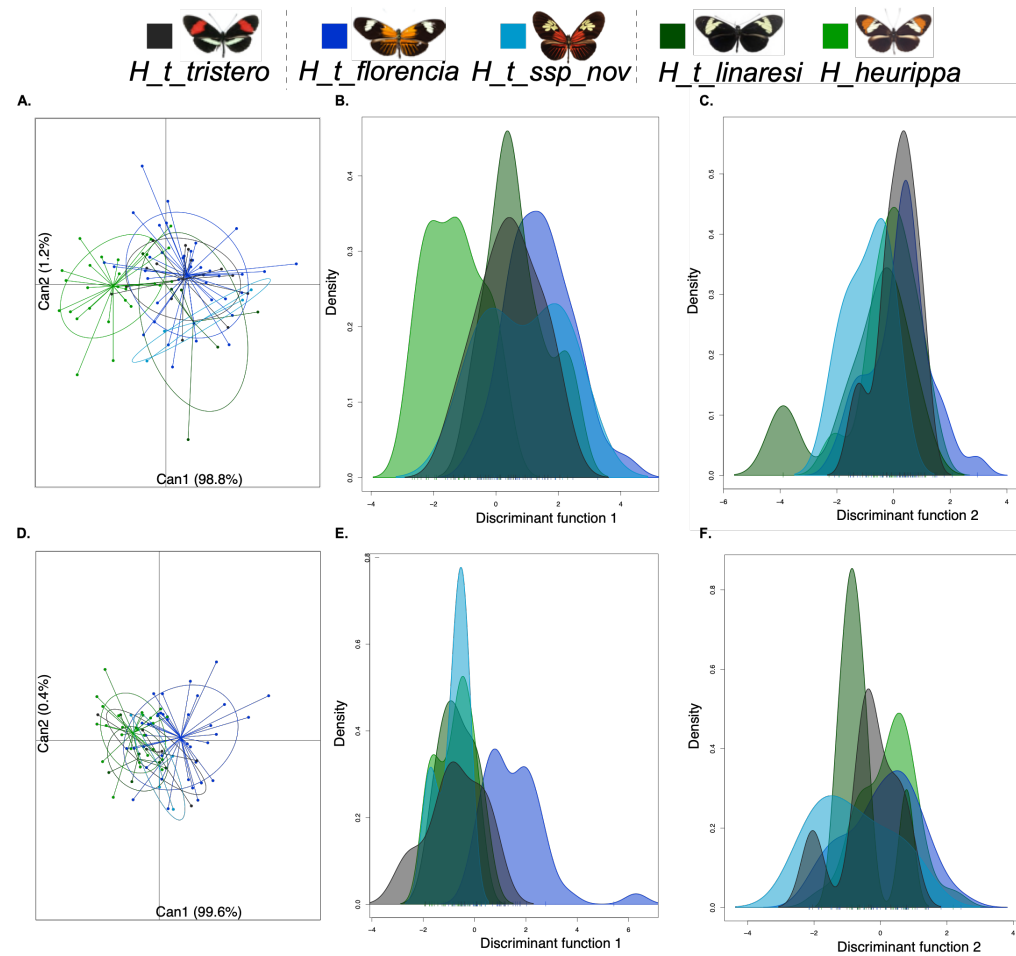


Figure 2.15. Comparison of wing shape between subspecies of *H. timareta*. Discriminant analysis (A, D) and density plots (B-C, E-F) showing the variation in the shape of the FW (top row) and HW (bottom row). The MANCOVA test showed a significant main effect of subspecies (FW: $F_{(4,81)}=41.42$, $p<2.2e-16^*$; HW: $F_{(4,72)}=24.49$, $p<2.2e-16^*$), a non-significant effect of geographic distance (FW: $F_{(1,81)}=3.12$, $p=0.05$; HW: $F_{(1,72)}=0.25$, $p=0.77$), and a significant interaction between factors for the FW ($F_{(4,72)}=24.49$, $p<2.2e-16^*$), but not the HW ($F_{(2,72)}=11.30$, $p=5.08e-8^*$). Dash lines indicate different mimicry rings.

WING PATTERN

For the red-band phenotype, I analysed two colour elements: FW red-band, and yellow HW bar (when present). The co-mimics were highly similar in these components of their colour phenotype at the local level, both ventrally and dorsally (Table S1.2 – Comparisons 2-6; Figure S1.10-S1.13). However, a global comparison (i.e., including all subspecies across the distribution of the red-banded phenotype) revealed subtle differences (Figure 2.16, Table S1.2 – Comparison 1). The red band of the species in Putumayo (south-west of Colombia) and the Pacific coast (also west of Colombia) was slightly wider compared to that of the species that occur in the Magdalena Valley and the northeast of the Andean foothills (Figure 2.16A, B). Also, the dorsal and ventral yellow HW bar of co-mimics in Putumayo (i.e., *H. e. dignus*, *H. m. bellula* and *H. tristero*) is different from the ventral bar of co-mimics in the Pacific coast (i.e., *H. e. venus* and *H. m. vulcanus*) not only because of the dorsal absence of this element in *H. e. venus*/*H. m. vulcanus* (PC1; Figure 2.16) but also because of variation in shape (Figure 2.16C, D; Table S1.2 – Comparison 1). Specifically, in the dorsal surface, *H. e. dignus* appears as separated in two clusters in PC2 due to slight variation in the position of the yellow bar, while its co-mimic *H. m. bellula* is the species that shows the most variation in this trait along PC1 (Figure 2.16B). Ventrally, differences are due to the orientation of the anterior and posterior edges (concave and convex), which differentiate subspecies from the Pacific from those of Putumayo (PC2; Figure 2.16D).

In the dennis-ray phenotype (Amazon), I examined the variation of three wing colour elements, namely FW yellow band, dennis (an orange proximal patch in the FW), and rays (orange rays in the HW). The FW yellow band, revealed the existence of multiple clusters based on the position of this trait both dorsally and ventrally (Table S1.2 – Comparison 8; Figure 2.17A, D). PC1 separates the only moth included in the analysis *Chetone ithrana* from all other butterflies; in the moth, the band has a proximal position, while in the butterflies this trait is distally shifted towards the apex (Figure 2.17A, D). Within the butterflies, the position of this band also separates the group into two inner clusters: the first,

where the yellow band has a medial position and goes up to the discal cell, and the second where the position is shifted towards the apex and does not include the discal cell. The first group includes *H. e. reductimacula*, *H. m. vicina*, *H. t. ssp. nov.*, *Eueides heliconioides* and some *H. elevatus*, and the second include *H. e. lativitta*, *H. m. malleti*, *H. timareta florencia* and some *H. x. melete* (Figure S17 A, D; Table S1.2 – Comparison 8). The PC2 revealed that *C. ithrana*, *E. heliconioides*, and some individuals of *H. m. malleti*, *H. t. florencia* and *H. e. lativitta* have relatively narrower bands (Figure 2.17A, D).

Interestingly, the individuals of these three species of *Heliconius* with narrower bands are those collected not in the Amazonian lowlands, but in the Andes foothills in the most northward distribution of these subspecies (Table S1.2 – Comparison 9; Figure 2.18). The dennis patch also separated *C. ithrana* from all other species both dorsally (in the PC1 and PC2) (Figure 2.17A) and ventrally (only in PC2) (Figure 2.17D). Dorsally, PC1 reveals that *C. ithrana* has a virtually absent dennis patch compared to all other species in this ring (Figure 2.17B; Table S1.2 – Comparison 8). On the other hand, PC2 (size) showed that *H. x. melete* has the bigger dennis patch and *E. heliconioides* has the smallest (Figure 2.17B, E; Table S1.2 - Comparison 8), while all other species vary in between (Figure 2.17B, E; Table S1.2 – Comparison 8). Ventrally, PC2 also separates *C. ithrana* from all other species since the patch in this moth locates towards the anal margin, while in the other species, it is located towards the coastal margin (Figure 2.17E, Table S1.2 – Comparison 8). PC1 recovered additional variation associated with the size of the dennis, showing that *H. erato* has a larger dennis compared to *H. elevatus*, *H. melpomene*, *H. timareta* and *E. heliconioides* (Table S1.2 – Comparison 8; Figure 2.17E). The dennis patch of the individuals and species that occur in the Andean foothills exhibits high phenotypic convergence (Figure 2.18B, E; Table S1.2 – Comparison 9), although the dennis of *H. x. melete* and *H. e. lativitta* is larger than that of *H. t. florencia* (Figure 2.18B, PC1). Also, the ventral side, *H. t. florencia* has a dennis in a “V” shape that differs from the other species (Table S1.2 – Comparison 9; Figure 2.18E, PC1). Individuals of *H. m. malleti* vary along with these two extremes (Table S1.2 – Comparison 9; Figure 2.18E).

In terms of the rays, the dorsal PC1 shows that they are wider in the proximal region, and as they approach the distal region, they become thinner and curved in *H. t. florencia*, *H. m. malleti*, *H. m. vicina* and *H. e. elevatus* (Figure 2.17C, F; Table S1.2 – Comparison 8). Also, in these species, the rays are separated from a band above them and have a slightly shifted angle of orientation (Figure 2.17C). In contrast, the rays of *H. erato* and *H. xanthocles* are thinner in the proximal region of the wing and thicker and rounded in the distal region (Figure 2.17C). The dorsal PC2 separates rays based on shape in three groups: the first composed by *C. ithrana*, the second that groups *E. heliconiodes* and *H. aoede*, and the third that includes all remaining species (Figure 2.17C). There *C. ithrana* has a broader base, while the rays are thinner in the proximal region and wider in the distal thus resembling a triangle (Figure 2.17C). Ventrally, both PC1 and PC2 show the same trend as in the dorsal surface (Figure 2.17F; Table S1.2). Individuals from the Andean foothills had rays similar in size and shape in both surfaces (Figure 2.18C, F; Table S1.2 – Comparison 9) but cluster in two groups. The first is composed by *H. melpomene* and *H. timareta*, and the second is composed by *H. erato* and *H. xanthocles* (Figure 2.18C, F, PC1). The differences between these groups in shape and size are consistent with those already described for the species in the Amazon ring.

I also analysed the similarity between yellow/white colour elements in *H. cydno* and co-mimics (*H. sapho*, *H. sara*, *H. eleuchia* and those from the tribe Ithomiini (Danainae). The FW band shows marked differences both dorsally and ventrally (Figure 2.19A, D; Table S1.2 – Comparison 10). The PC1 separated species with a solid band (*H. s. chocoensis*, *H. s. sapho*, *H. zelinde* and *H. c. cydno*) from those with a split band (*E. humboldt*, *H. hecuba*, *H. c. hermogenes*, *H. c. weymeri*, *H. c. cydnides*, *H. sara* and *H. e. eleuchia*; Figure 2.19A, D; Table S1.2 – Comparison 10). Other species are located in the middle, as they do not fit any extreme phenotypes (i.e., *H. c. waningeri* and *H. e. eleusinus*). The PC2 recovered variation by colour, where species with yellow bands were grouped in a cluster, while species with white bands were clustered apart (the exceptions were *H. c. spp. nov.* and *H. e. eleusinus*, where the size had a higher effect on their clustering than colour). In the HW, *H. cydno* has two elements: a medial yellow bar and submarginal white or yellow border.

These elements occur in repulsion (i.e., the presence of the bar only happens when the border is absent and vice versa).

The subspecies of *H. c. cydno* and their co-mimics grouped on PC1 based on the presence of the submarginal band both dorsally and ventrally (Table S1.2; Figure 2.19B, E). Also, PC2 grouped these taxa based on the position of this band in the HW. One of the groups is composed by *H. eleuchia eleuchia* and *H. sapho sapho*, which exhibit a broad white submarginal band that reaches the distal edge. A second group is formed by those subspecies that have a narrow submarginal band that is also slightly shifted towards the proximal edge of the HW (i.e., *H. c. hermogenes* and *H. h. tolima*; Table S1.2; Figure 2.19B). A third group was composed by subspecies whose submarginal band is not located at the edge of the wing but displaced towards the middle of it (i.e., *H. c. cydnides* and *H. c. waningeri*) (Figure 2.19E).

We observed the same three groups in the HW yellow bar, dorsally and ventrally (Figure 2.19C, F). PC1 grouped subspecies based on the presence/absence of this trait (Figure 2.19C, F; Table S1.2), while PC2 grouped them based on shape and position. A first group is formed solely by *Elzunia humboldt*, that has a short and wide yellow bar all along its length, and its blunt end reaches the androconial region between veins R and M1. The forms of *H. c. weymeri f. weymeri* formed a second group that has a wide yellow bar in the medial region, which includes the discal cell, and has a sharp end between veins R and M1. The third group, which is close to the latter, includes *H. e. chestertonii* and has a pointed bar that ends just before reaching the androconial region (dorsally) and reduces its size from M1 so at the end it is very narrow (ventrally).

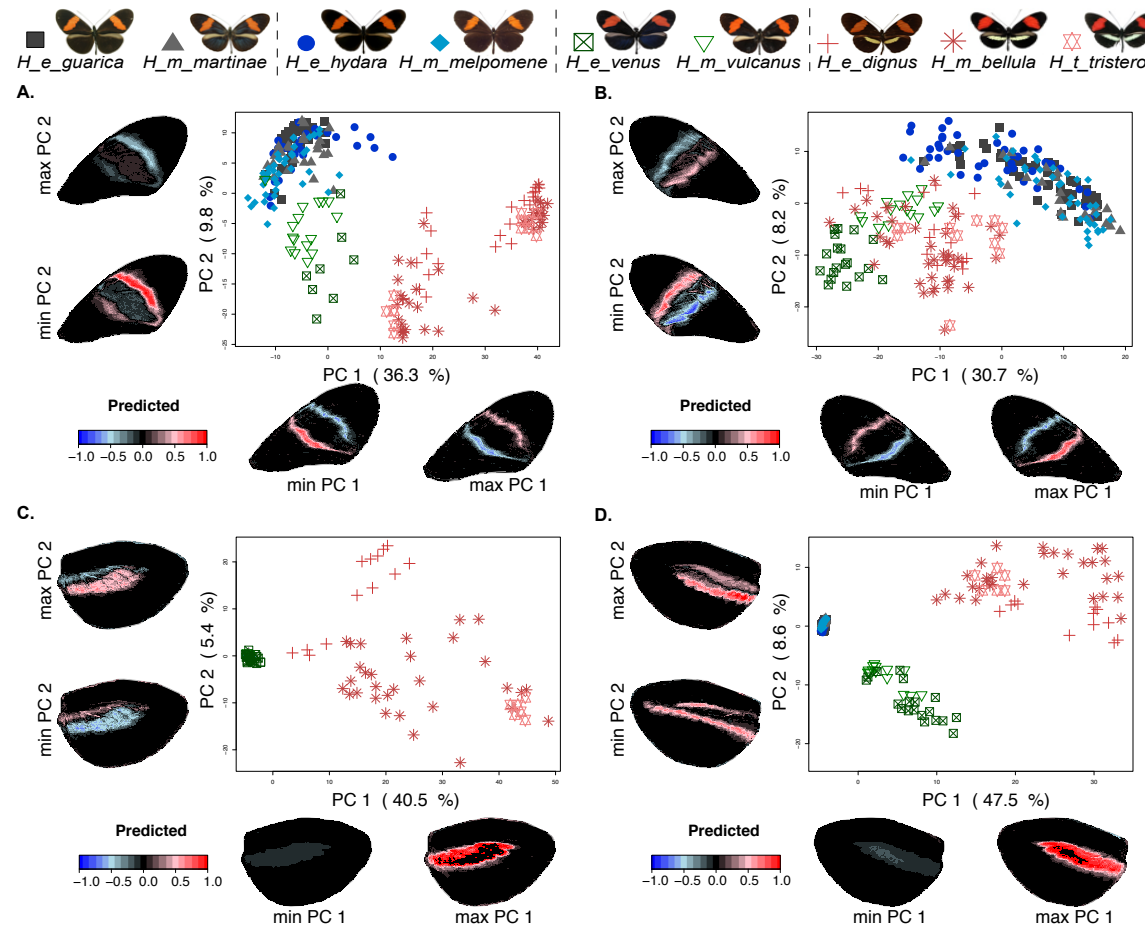


Figure 2.16. Comparison of colour pattern between subspecies exhibiting the red-banded phenotype. Scale of predicted values indicates the expression of colour pattern (positive/red: full presence, and negative/blue: full absence). Wing elements analysed: red band on the dorsal FW (**A**) and ventral FW (**B**); yellow bar on the dorsal HW (**C**) and ventral HW (**D**). MANCOVA test values are in Table S1.2 – Comparison 1. Dash lines indicate different geographic mimicry rings.



Chetone ithrana *Eueides heliconioides eanes* *H_aeode* *H_e_elevatus* *H_e_lativitta* *H_e_reductimacula* *H_m_malleti* *H_m_vicina* *H_t_ssp_nov* *H_t_florencia* *H_x_merete*

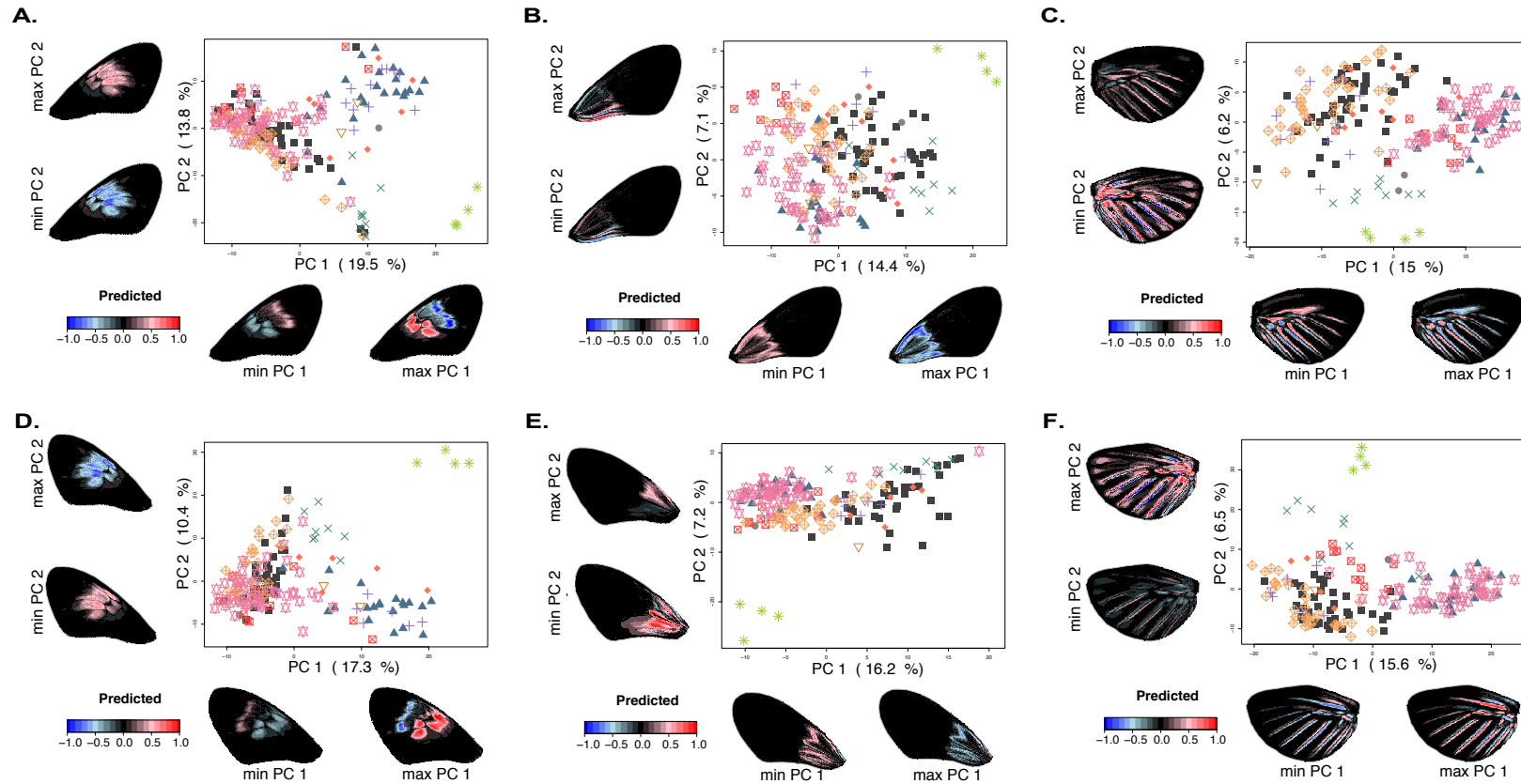


Figure 2.17. Comparison of colour pattern between species and subspecies exhibiting the dennis-ray phenotype in the Amazon. Scale of predicted values indicates the expression of colour pattern (positive/red: full presence, and negative/blue: full absence). Wing elements analysed: yellow band on the dorsal FW (A) and ventral FW (D); dennis pattern on the dorsal FW (B) and ventral FW (E); rays on the dorsal HW (C) and ventral HW (F). MANCOVA test values are in Table S1.2 – Comparison 8.

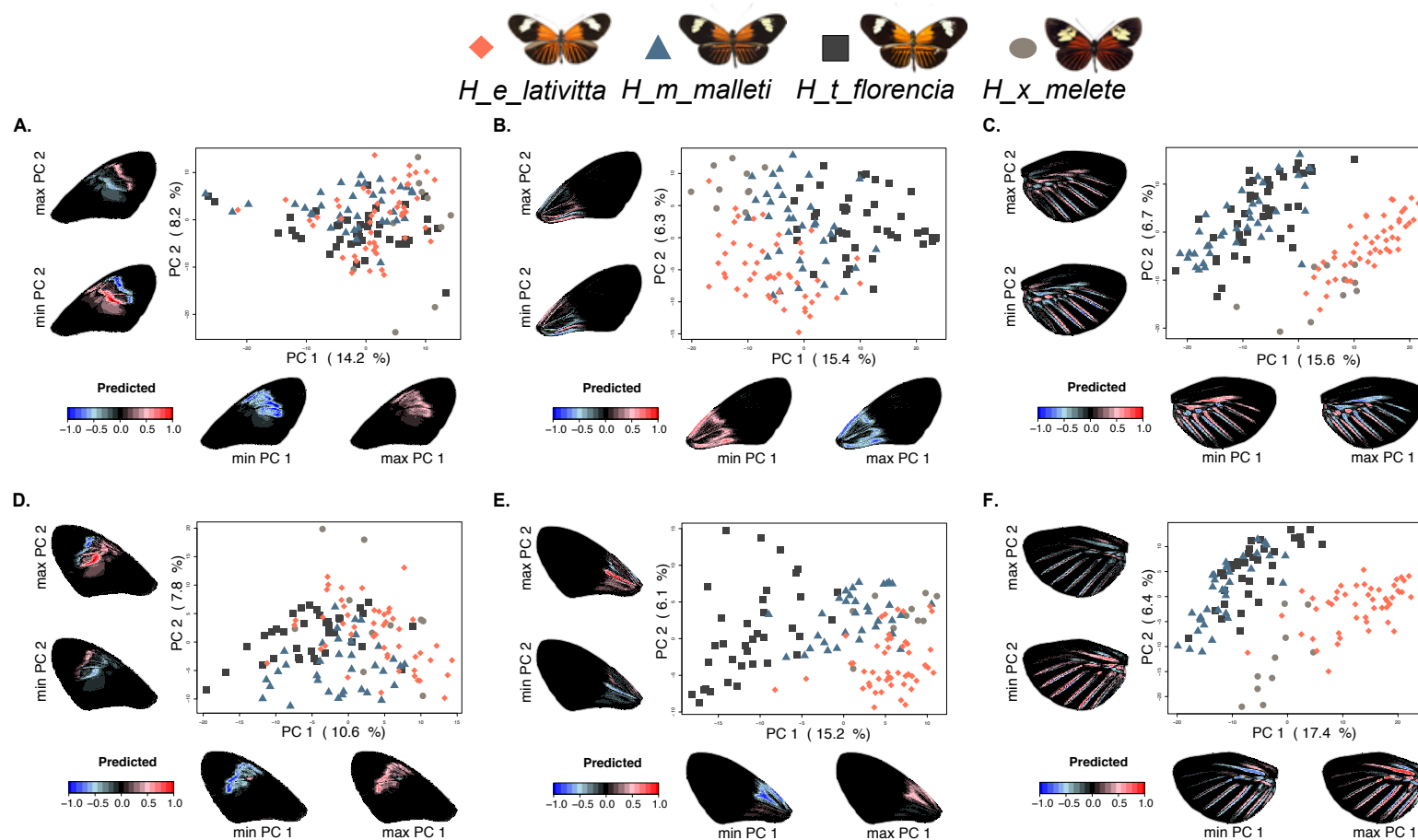


Figure 2.18. Comparison of colour pattern between subspecies exhibiting the dennis-ray phenotype in the southeast Andean foothills. Scale of predicted values indicates the expression of colour pattern (positive/red: full presence, and negative/blue: full absence). Wing elements analysed: yellow band on the dorsal FW (**A**) and ventral FW (**D**); dennis pattern on the dorsal FW (**B**) and ventral FW (**E**); rays' pattern on the dorsal HW (**C**) and ventral HW (**F**). MANCOVA test values indicated in Table S1.2 – Comparison 9.

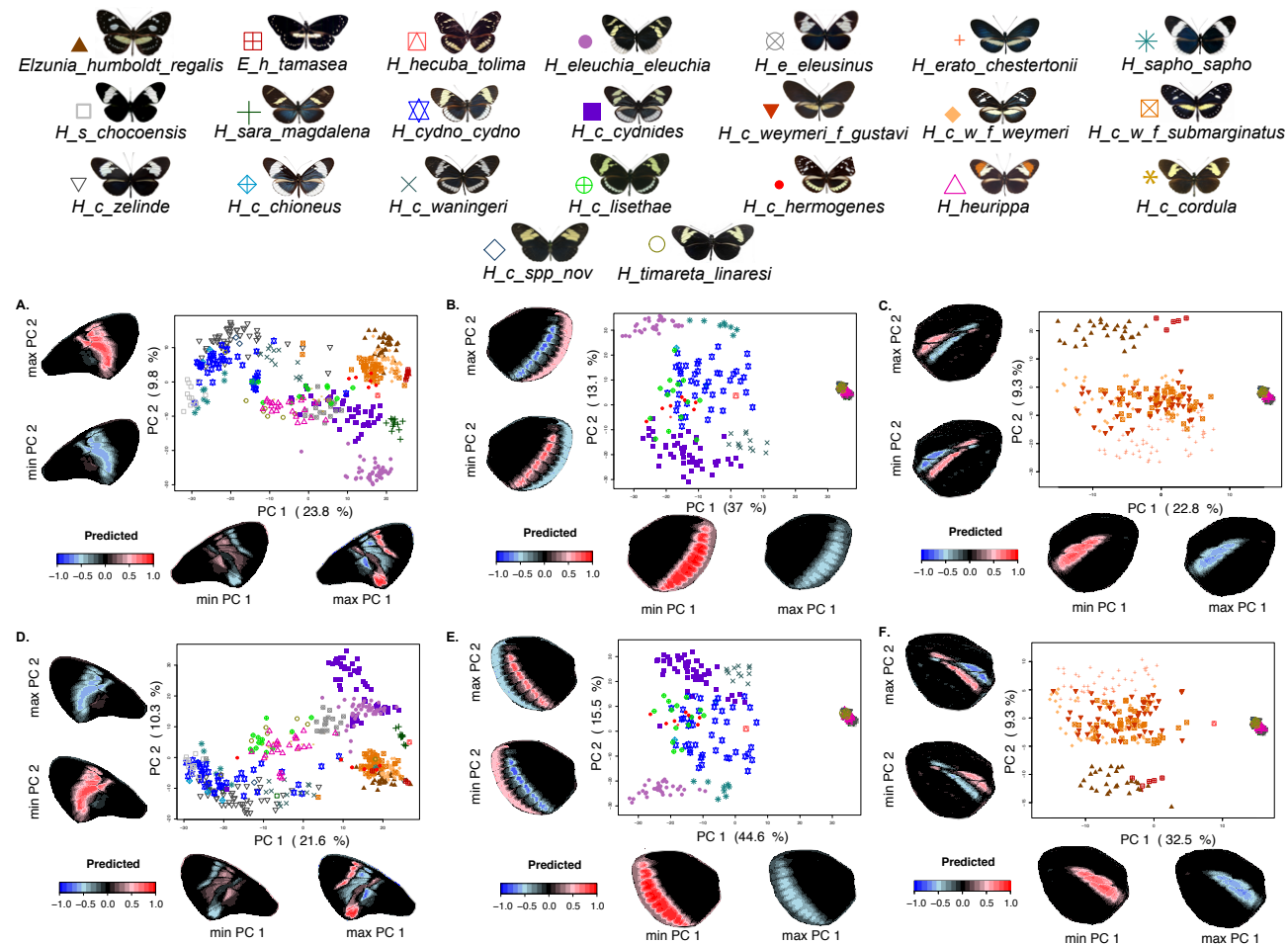


Figure 2.19. Comparison of colour pattern between subspecies exhibiting the yellow/white phenotype. Scale of predicted values indicates the expression of colour pattern (positive/red: full presence, and negative/blue: full absence). Wing elements analysed: yellow/white band on the dorsal FW (**A**) and ventral FW (**D**); yellow bar on the dorsal HW (**B**) and ventral HW (**E**); the white/yellow border on the dorsal HW (**C**) and ventral HW (**F**). MANCOVA test values are in Table S1.2 – Comparison 10.

DISCUSSION

Müllerian mimicry is one of the most spectacular and successful adaptations observed in nature. The phenotypic convergence and advergence to a given adaptive optimum have been widely documented in several organisms (20,203,212–216,204–211) and there is experimental evidence showing the efficiency of mimicry signals in warning local predators favouring the survival of species that participate in a mimicry ring. In butterflies, it has been suggested that the mimicry signal may be multifactorial, not only the wing colour pattern but also wing size and shape play a role. These traits display different ranges of variation and genetic architecture (i.e., major effect loci controlling colour pattern variation vs. a likely polygenic basis for wing shape and size) that must be shaped by natural selection to ensure mimetic convergence. In the present study, I quantified the similarity in wing size, shape and colour pattern in *Heliconius* in the *melpomene/cydno/timareta* clade and their co-mimics. The aim was to test the existence of a single multifactorial signal in each mimetic ring, or the existence of imperfect mimicry that may be explained by factors that limit the directionality of selection.

Overall, the mimicry rings I studied do not show convergence in wing size and shape. In terms of wing size, there is a considerable intra and interspecific variation with marked differences between members of a single mimicry ring. In terms of wing shape, variation is explained by species (for those taxa that have the red-band phenotype) or phylogenetic closeness (for *H. cydno* and its co-mimics, regardless of the inclusion of members of the tribe Ithomiini). The only case where wing shape may be partially contributing to mimicry is in the dennis/ray mimicry in the Amazon, the centroids of variation of most species participating in this ring overlap, except for *H. t. florenciana* and *C. ithrana*. This divergence in wing shape between co-mimics contrasts with previous findings in three red-banded mimetic pairs in Brazil, where there were no differences in wing shape and size (191). My findings also contrast the wing shape mimicry found between *H. numata* f. *silvana* and *Melinaea ludovica*, which has been suggested to contribute not only to phenotypic

convergence but also similarity in flight (217). A third study in *Heliconius* that compares wing shape and size between populations of *H. timareta thelxinoe* that coexist with different mimetic species found that wing shape is different between co-mimics in multiple geographic points (172), thus agreeing with my results.

Considering all evidence together, it seems that in *Heliconius*, natural selection tends to favour convergence, especially in wing shape, but other forces limit the perfection of such mimicry. As such, the heterogeneity I observed in wing size and shape between subspecies within a single species, and between mimetic pairs, may be due to causes other than selection for mimicry such as sexual selection, phylogenetic closeness and life-history traits. In particular, previous studies have reported that wing shape in *Heliconius* varies along an environmental gradient, where rounder wings are more common at higher elevations (218,219). The latter is supported by evidence in other butterflies, where groups that live at higher elevations have rounder wings because they favour flight manoeuvrability in low temperature and low-pressure environments (220,221). This is also observed in my study, particularly in *H. t. florenci* which lives at higher elevations than all other Amazonian dennis/ray species and has rounder wings than any of them.

Size was recently reported to present sexual dimorphism in *Heliconius* associated with mating type (pupal mating vs. adult mating) and with gregarious behaviour of immatures (218,222). Closely related species to *H. sara* (pupal mating and gregarious immatures) tend to have smaller males and bigger females, while species close to *H. melpomene* (adult mating and lonely immatures) tend to show bigger males and smaller females. This pattern is associated with intrasexual male competition and the reproductive costs of females, consequently, the contribution of wing size to mimicry is strongly constrained by the life-history of the species involved in the ring. Although I only measured males, I observed differences in this trait associated with the existence of this dimorphism. In particular, males of *H. e. eleuchia* (pupal mating and gregarious immatures) were smaller on average than those of its co-mimic *H. c. cydnides* (adult mating and lonely immatures).

The colouration pattern analysis revealed that phenotypic similarity in mimicry is complex and far from perfect. The extent of convergence in wing colour pattern varied between mimicry rings and in each of the wing colour elements analysed. The relative similarity (i.e., pigmented areas vs. the total area of the wing) were very similar for some wing colour traits, while others were much more variable.

The red-banded subspecies of *H. erato* and *H. melpomene* showed a considerable colour pattern accuracy between them, indicating that these two species are good co-mimics despite being distantly related. This agrees with a previous study of red-banded subspecies in South America (191), that only included the Colombian pair *H. m. vulcanus* and *H. e. venus*. In both studies, the wing element that showed the highest similarity was the FW red band, both between mimetic species and between subspecies within a single species. This holds true when evaluating the similarity of the HW yellow bar (ventrally or dorsally), thus suggesting that natural selection for mimicry is acting on all elements that compose a single local adaptive peak. The high similarity in wing colour pattern of races in the Magdalena Valley (*H. e. guarical/H. m. martinae*, and *H. m. melpomene/H. e. hy dara* from the north-eastern Andes) contrasts with previous analysis carried out with populations of *H. m. melpomene* and *H. e. hy dara* from Panama and Guiana (192). This discrepancy may be due to gene flow between red-banded subspecies in the northern Andes of Colombia, which may be enough to homogenise the variation in the FW red-band in the subspecies that live there thus favouring the existence of a single but widely distributed adaptive peak. An analysis that includes wings and genetic data from the entire distribution of *H. e. hy dara* and *H. m. melpomene* would help to determine whether gene flow explains local similarity vs. divergence within what is usually regarded as a single indistinguishable mimetic pair.

The widely distributed dennis-ray mimicry ring has little consistency in terms of similarity between co-mimics. First, I recovered *Chetone ithrana* as a highly divergent entity that differentiates from all other species and subspecies in all wing elements analysed. This is consistent with the mimicry in this ring being by advergence and with this moth being the model based on its high toxicity (177,223). However, the position of this species as

an independent entity may also be the result of phylogenetic divergence. Second, I observed high similarity in the FW yellow bar between *H. melpomene* and *H. erato*, although I recovered two phenotypic groups that differ in the morphology and position of such trait. The species *H. timareta* and *H. x. melete* distribute their variation in these two groups, and in a lesser extent, this also happens in *Eueides heliconiodes* and *H. elevatus*. In contrast, such grouping is not recovered by the dennis patch, where despite some variation in size, there is a general similarity among all species and subspecies participating in this ring. Lastly, the HW rays show less divergence between subspecies within a single species than between co-mimic species, especially in *H. erato* and *H. m. melpomene*. In this trait, *H. elevatus* and *H. timareta* are similar to *H. melpomene* while *H. x. melete* is more similar to *H. erato*.

The disparity in the groupings generated by each of the traits that constitute the dennis/ray phenotype may be explained by the presence of multiple adaptive peaks within what is usually regarded as a single widely distributed mimicry ring. It seems that the FW yellow band plays an important role in the mimicry signal perceived by local predators in two different habitats. Specifically, dennis-ray populations that occur at the foothills of the eastern Colombian Andes, at ~1000-1200 masl in a submontane tropical forest, have a FW yellow band slightly displaced distally and smaller than that of populations living at ~40-80 masl in the tropical jungle of the Amazon, where this band is displaced proximally and is bigger. Also, the higher similarity of the rays between subspecies within a single species and between closely related species suggest that this trait has more developmental constraints associated with the regulation of the expression of the transcription factor *optix* (responsible for red pattern variation in *Heliconius*, (95,224–227)), which limits mimetic convergence. In contrast, the genetic control underlying the formation of the yellow FW band seems more flexible in the regulation of *WntA* y *cortex* (responsible for delimiting the boundaries of pigmented vs. unpigmented wing scales, (227–234)) and this likely facilitates the convergence between distantly related taxa in a given mimetic context. When reanalysing the data but only including dennis-ray species from the Andes foothills, all species fell into a single group for the FW yellow band and dennis analyses, but not in the analysis of rays.

The red-band and dennis-ray phenotype, show that phenotypic similarity is higher when there are less species/subspecies that participate in the mimicry ring. Nonetheless, this does not mean that the presence of more species is detrimental to the effectiveness of the aposematic signal. As pointed by some studies, co-mimics could benefit from the presence of other species even when they exhibit a slightly different pattern because predators could generalise the signal (172,191,235–238). The latter is consistent with what found by Van Belleghem et al. (192), where the aposematic signal from the bands is more similar between co-mimics in relative terms than in absolute terms.

In the yellow/white phenotype, there is a high similarity between this *H. cydno* and members of the tribe Ithomiini (Danainae). This suggests phenotypic advergence, where the Ithomiini would be the model. Consistently, there is evidence of a recent introgression selective sweep around the gene *cortex* (that controls the FW white band and the HW yellow bar in *H. c. weymeri* (231). The phenotype of this species is *per se* an adaptive innovation within *H. cydno*, and, likely, the pattern of *H. c. hermogenes* (that mimics *E. h. tamasea* and *H. h. tolima*) is an innovation too. The same evolutionary mechanism may have operated in the only case where *H. erato* does not have *H. melpomene* as co-mimic, but *H. cydno*: *H. e. chestertonii* and *H. c. weymeri f. gustavi*, in this case, I also observed a considerable similarity in the HW yellow bar. The variation observed in the white FW band, together with the form and relative position of the HW submarginal bar, is explained by mimetic convergence. However, there is a slight grouping by subspecies within a single species rather than co-mimic species for the FW band in PC2 (9.8% of variation).

Usually, three *H. cydno* (*H. c. chineous*, *H. c. zelinde*, and *H. cydno cydno*) and *H. sapho* (*H. s. sapho*, *H. s. chocoensis*) mimicry rings are recognised based on the geographic variation of the elements that constitute this white pattern. However, the similarity in their FW band agrees with the existence of a single mimicry signal in all of these species that live in rainy forests in the Pacific, part of Central America and the northern Magdalena Valley. Even more, *H. c. waningeri*, which is restricted to the north-western side of the Eastern Cordillera of Colombia, participates in this phenotype. The presence of other wing

patterns and subspecies that are geographic replacements and/or have temporal and spatial variation in their occurrence may create conflict or competence between the selection that maintains the successful peak previously described and that favours the convergence or advergence to these new patterns.

As such, *H. c. zelinde* is much less divergent in the white FW band with *H. s. chocoensis* in the Colombian Pacific than with *H. e. eleusinus* in the western Andes (where *H. e. eleusinus* has a FW band split). Similarly, *H. sara magdalena* and *H. e. eleuchia*, both with a yellow and split FW band, constitute a second mimicry peak with *H. c. cydnides* where they are away to be perfect co-mimics as revealed in all colour pattern traits studied. It is possible that the aposematic signal of *H. e. eleuchia*, although sporadic, is effective enough to favour imperfect mimicry with *H. c. lisethae* at the South of the Magdallena Valley. This also would explain the maintenance of the yellow allele of *aristal-less* in populations of *H. cydno* in the North of this valley, thus generating colour polymorphism in the FW band.

Similarly, the submarginal bar also reveals imperfect mimicry. PC2, explains 13.1% of the variation of the position and size of this trait, slightly grouped subspecies by phylogenetic closeness. The differences in both, the forewing band and the submarginal bar between co-mimics that have yellow/white phenotype suggest, once again, that mimicry may be limited by developmental constraints. My analyses suggest that subspecies of *H. eleuchia* are less mimetic than other species. Other selection pressures may be shaping the size and position of the FW band and the submarginal bar. For example, the submarginal bar may be an anti-predatory mechanism, which, at flying, distorts the HW length making predators fail. This hypothesis, however, needs to be tested.

Multiple studies in butterflies show signal partitioning between dorsal and ventral wings surfaces (16,239–243). For example, in *Byciclus* and *Morpho* butterflies, dorsal surfaces are involved in sexual communication while eyespots on the ventral surfaces are selected against visual predation (241–244). Likewise, *Morpho* butterflies are iridescent on the dorsal surface involved in sexual selection while the ventral side, that as a role in avoiding

predation, has brown colouration with eyespots. In this study, although I detected minor differences in wing elements between dorsal and ventral surfaces, the analyses recovered the same phenotypic groups in both sides of the wings this suggesting that in *Heliconius* such signal partitioning is not as important as in other Lepidoptera.

Overall, the similarity in the traits studied (wing size, wing shape and colour pattern) in each of the mimicry rings analysed is far from being perfect and indicates that a single multifactorial signal does not occur and is not necessary to warn predators away. In the particular case of the colour pattern, conflicts between natural selection for mimicry (convergence) and sexual selection (divergence) may limit the similarity between co-mimics. Also, these forces may act differentially on each of the wing colouration elements thus leading to each of them having a different similarity level in response to how the receptor (partner or predator) perceives them (16,19,91,92,181,238,240,245). For instance, there is evidence in *H. erato* of the yellow FW band being more conspicuous for conspecifics than for birds (16), which may relax the effect of natural selection on this trait. Similarly, differences in the composition of the local community of predators may lead to different selective pressures on different localities thus facilitating variation in the convergence level between co-mimics (172,246). Predators may also choose and avoid preys based on a generalised wing colour pattern (less convergence) in some cases, but being more judicious in other cases (more convergence) based on their visual sensitivity (e.g. violet sensitive (VS) and ultraviolet sensitive (UVS) (92,240,247) and their ability to associate the colour signal to the butterflies' unpalatability (88,248).

At the genetic level, most of the phenotypic differences between co-mimics found here could be the result of divergence in the regulatory networks underlying the formation of the wing colour pattern, under the master control of the same four major effect genes *optix*, *WntA*, *aristal-less* and *cortex* (227). These networks should be highly polygenic and with complex connections, and in the evolutionary process, they were differentially rewired so they could meet the developmental constraints of each species while reaching a similar phenotypic outcome. Preliminary evidence supporting this hypothesis comes from *WntA* knockouts, where the resulting mutants showed different phenotypic effects

between co-mimics (234). In this way, the genetic architecture permits an imperfect convergence in the shape of the wing colour elements that are further 'tuned' by the relative amount of coloured wing scales relative to the entire wing as recently shown for the red FW band in *H. melpomene* and *H. erato* (192). However, the remarkable similarity I found between *H. cydno* and members of the tribe Ithomiini suggests that gene networks and major effect genes controlling colour wing phenotype in *Heliconius* are flexible enough to generate novel and advergent wing patterns rather than being the product of entirely different networks and genes (225,227).

Finally, my results are consistent with mimetic adaptation being a complex and dynamic process where the genetic architecture and its associated developmental constraints (and their flexibility) play a major role in the generation of convergent phenotypes. However, mimetic convergence is also shaped by predators (agents of selection), specifically by how they perceive signals, what is the composition of their community, and their ability to associate butterflies' wing pattern to their toxicity spectrum.

CHAPTER 2. REPRODUCTIVE ISOLATION DRIVEN BY PHEROMONES IN MIMETIC AND CLOSELY RELATED BUTTERFLIES

INTRODUCTION

The mechanisms by which species maintain their integrity are diverse and involve a combination of multiple signals of intra and inter-specific communication such as chemical, visual, auditory and tactile cues (3,4,123,249,250). In particular, sexual communication in insects involves long and short-range pheromones, which play multiple roles (64,123,249,251). For instance, pheromones can communicate the mating status of females (35,36), quality and age of males (37,38), quality and quantity of nuptial gifts (39), body size (40), dominance status (41), and degree of relatedness (42). Also, chemicals play an important role in mate choice and species recognition (15,67). In particular, pheromones mediate mate choice in many insects including flies (*Drosophila*), grasshoppers (*Chorthippus parallelus*), leaf beetles (*Chrisochus*) and stick insects (*Timema*) (15,43,47,48,67,124,125,252).

In Lepidoptera, males and females produce volatile and non-volatile compounds suggesting that chemical communication plays a critical role in inter and intra-specific communication (58,59,126). In *Bicyclus anynana*, visual and chemical cues are equally important for mate choice, and females recognise heterospecific males based on their pheromones (60). Also, males of *Heliconius charithonia* which engage in pupal mating by copulating with females as they eclose, can identify the sex of a conspecific pupa based on sex-specific compounds (135,253). Moreover, chemical cues seem to mediate species recognition among mimetic and distantly related *Heliconius* species

where conflicts between mimicry and sexual communication may arise (108,138,254). This is supported by the fact that males of *Heliconius* have species-specific mixtures in their wing androconia (i.e. specialised male wing scales that produce scents) (138,255).

In *Heliconius*, mate discrimination between closely related species relies on wing colour pattern (12,256). For example, the sister species *H. melpomene* and *H. cydno* (divergence ~1.5–2 Mya) (257), which are sympatric across Central America and the Andes, not only differ in habitat use but also in wing colouration (186,258,259). In fact, multiple experiments show that males prefer to court females exhibiting their own colour pattern (12,188,189). In contrast, the phylogenetically close *H. melpomene malleti* and *H. timareta florenci* mimic each other and coexist in sympatry in the South Eastern Andes of Colombia (Figure 3.1). Despite their phenotypic resemblance, this species pair shows strong pre-mating ecological isolation (differences in host plant preference) as well as strong reproductive isolation tested in no-choice experiments (188,260); even so, a low number of hybrids are found in nature (~2%) (188,254). Therefore, the strong reproductive isolation between *H. m. malleti* and *H. t. florenci* implies that sexual isolation is mediated by cues other than colour pattern, such as chemical cues (138,189,254).

Thus, the case of mimicry between the closely related *H. m. malleti* and *H. timareta* offers an ideal model to study the importance of visual and chemical cues in mate choice, and ultimately, reproductive isolation. In this chapter, I investigated through behavioural experiments whether chemical cues, specifically sex pheromones, mediate mate recognition and preference in *H. m. malleti* and *H. timareta*.

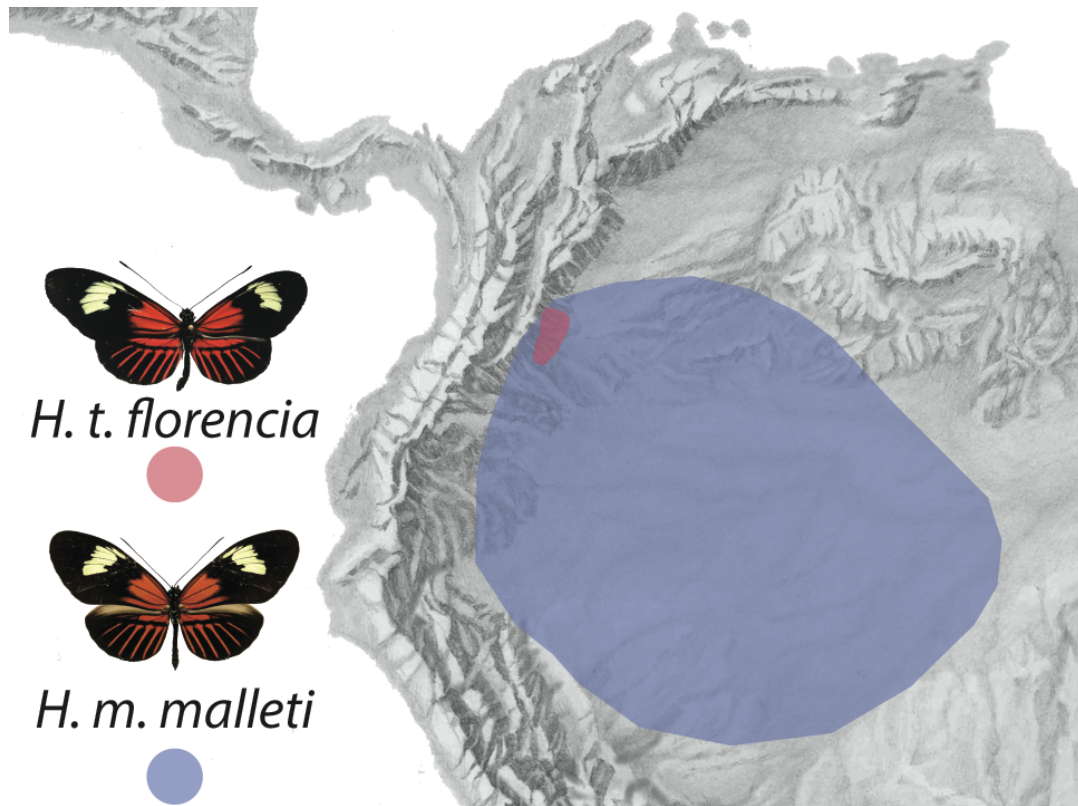


Figure 3.1. Map showing the geographic distribution and wing phenotype of *H. timareta florencia* and *H. melpomene malleti* in the South Eastern Andes of Colombia.

MATERIALS AND METHODS

QUANTIFICATION OF WING PHENOTYPE

To quantify colour, I used wings of wild males of *H. t. florencia* and *H. m. malleti* deposited in the 'Colección de Artrópodos de la Universidad del Rosario (CAUR229)' (Table S2.1). To evaluate whether *H. m. malleti* and *H. t. florencia* exhibit differences in wing phenotype, we scanned ventral and dorsal forewings (FW) and hindwings (HW) of 43 *H. m. malleti* and 45 *H. t. florencia* (Table S2.1) using a high-resolution flatbed scanner Epson Perfection V550, in RGB colour format with a resolution of 2400 dpi. Right side wings were always used. Then, we used ImageJ (202) to place a set of 34 landmark coordinates per individual (dorsally and ventrally; Figure 2.1A). These landmark coordinates were analysed in the R package Patternize (201) to quantify variation in wing colour

patterns (band size and shape). This package extracts, transforms and superimposes colour patterns to finely quantify the variation of colour pattern among species and performs a principal component analysis (PCA) on the binary representation of the aligned colour pattern obtained from each sample with the *sumRaster* function (201). We then tested differences in wing pattern among species using a multivariate analysis of variance (MANOVA) in R based on a subset of PCs (those that explain >95% of the variation).

In addition, we used *tpsDig2* (195) to place 32 landmark coordinates on the outline of both forewing and hindwing (dorsally; Figure 2.1B). These landmark coordinates were superimposed using a General Procrustes Analysis (GPA) in the R package 'geomorph' (196–198). The resulting coordinates in the tangent space were used as shape data, while the log-transformed centroid size (197) was used as a size estimate (220). Differences in wing size among species were investigated with a one-way ANOVA with size as a dependent variable and species as a factor, followed by Tukey's pairwise comparison test. Differences in wing shape among species were tested using a Procrustes MANOVA applied to the aligned landmark configurations. This was done using the *procD.lm* function in the 'geomorph' R package (196). For details see above (Chapter 1, Materials and Methods).

WILD SAMPLING

Wild individuals of *H. timareta florencica* and *H. melpomene malleti* were collected in the localities Sucre and Doraditas in Colombia (01°48'12" N - 75°39'19" W, 1200 m and 01°42'39" N - 75°42'32" W, 1400 m) that were taken to the insectaries of the Universidad del Rosario in La Vega (Colombia) to establish stock populations for the behavioural experiments. Larvae were reared on *Passiflora oerstedii* while adults were provided with *Psiguria* sp. as pollen source and supplied with ~20% sugar solution.

Field collections and insectary rearing were conducted under the permit #530 issued by the 'Autoridad Nacional de Licencias Ambientales' of Colombia

(ANLA). Rearing conditions were approved by the Ethics Committee of Universidad del Rosario (approval #CEI-ABN026-000155).

BEHAVIOURAL EXPERIMENTS

Behavioural experiments were conducted to test female preference for colour pattern and chemical cues of conspecific males. I conducted three types of triad experiments:

- ***Experiment 1: Altering the wing phenotype of males.*** This experiment investigated how the male's colour pattern affects mate preference in conspecific females. A total of 20 females per species were tested. In each case, a single one-day-old virgin female was presented with two conspecific males of at least ten days old (i.e., sexually mature). One of the males (treatment male) had his forewing and hindwing completely blacked out using a black marker (COPIC 100) thus hiding his wing colour pattern. The second male (control) had his forewing and hindwing painted with a colourless marker (COPIC 0), in this way, the male kept his phenotype unaltered, but I controlled for any odour effect of the marker.
- ***Experiment 2: Blocking the emission of chemical blends in males.*** This experiment investigated whether the male's chemical blend mediates recognition by conspecific females. A total of 18 females of *H. t. florencía* and 22 females of *H. m. malleti* were tested. In each case, a single one-day-old virgin female was presented with two conspecific males of at least ten days old (i.e., sexually mature): a control male and a 'pheromone blocked' male (treatment). Both males were treated with transparent nail varnish (Vogue Fantastic containing butyl acetate, ethyl acetate, nitrocellulose, adipic acid, neopentyl glycol, trimellitic anhydride copolymer, isopropyl alcohol, acetyl tributyl citrate, stearalkonium bentonite, styrene, acrylates copolymer, silica benzophenone-1, calcium sodium borosilicate, synthetic fluorphlogopite, polyethylene

terephthalate and polyurethane-11), following the protocol previously developed by Costanzo & Monteiro (2007)(60). Pheromone blocked males had the dorsal side of their hindwing androconia blocked, whilst control males had an adjacent area of the wing blocked.

- **Experiment 3: Perfuming males with the heterospecific chemical blends.** This experiment investigated whether the male's chemical bouquet affect the female's mate preference. A total of 19 females of *H. t. florenci*a and 18 females of *H. m. malleti* were tested. First, I prepared extracts from sexually mature males of each species by dissecting and mixing the androconia region of five conspecific individuals of the same age and soaking them in 200 μ L of hexane for 1 hour. After this incubation, the solvent was transferred to a new vial and stored at -20°C until needed. Then, a single one-day-old virgin female was presented with two sexually matured conspecific males. Both males were initially treated with transparent nail varnish applied on the dorsal side of their hindwing to block their androconia and thus, block their natural emission of chemicals. Then, one of the males (control) was perfumed by spreading the conspecific hexane extract in the androconia region, whereas the second male (treatment male) was perfumed by spreading the heterospecific hexane extract. In order to investigate how long the hexane extract remains in the wings of the perfumed males before completely evaporating (which can potentially affect the results), I blocked the HW androconia of nine males of each species using transparent nail varnish and then, re-perfumed this region by spreading the heterospecific hexane extract. I left these males fly in an insectary and dissected their androconia at 1 minute, 30 minutes or 60 minutes and soaked this tissue in 200 μ L of ultrapure dichloromethane (Merck UniSolv®) to be later analysed by gas chromatography/mass spectrometry (GC/MS; see below in Chapter 3, Materials and Methods).

All experiments were conducted from 7 am to 1 pm, checking every 30 minutes for mating; the experiments stopped when mating occurred. For each experiment, mature males (at least 10 days old) were randomly selected from

the stock population while females were used as soon as they become available. If no mating occurred on the first day, I repeated the experiment the next day using the same butterflies; in contrast, mated males or females were never reused. If no mating occurred after the second day, the experiment stopped. For the first hour of each experiment, I observed female behaviour towards the males. These behaviours were recorded only when a male was actively courting the female. Observations were divided into one-minute intervals and I recorded female behaviours of “acceptance” or “rejection” previously defined for *Heliconius* (81,261). Specifically, we recorded the following acceptance behaviours: flutter (slow and moderate wing flapping), fly towards (flight facing towards the male), slow flat (slow rhythmic flight), and wings open and exposed (wings open and abdomen relaxed). Similarly, we recorded the following rejection behaviours: fly away (flight away from the male), tucked up (alighted with wings closed and abdomen concealed within the wings), rapid and erratic flutter (high frequency flutter of her wings and abdomen raised when the male is in close proximity), and wings opened and abdomen bend (wings opened and abdomen raised, but without wing fluttering).

The mating outcome was analysed with binomial tests. Also, to test if females respond differently to control and treatment males, a generalized linear mixed model (GLMM) with a binomial error distribution and logit link function was used. The response variable was derived from those minutes where at least one of the males courted the female regardless of her response (either “acceptance” or “rejection”). Significance was determined by using likelihood ratio tests comparing models with and without male type included as an explanatory variable. In order to avoid pseudo-replication, individual female was included as a random effect in all models. All statistical analyses were performed with R version 3.3.2 (262), using the packages lme4 (263), ggplot2 (264), car (265) and binom (266).

RESULTS

QUANTIFICATION OF WING PHENOTYPE

H. m. malleti and *H. t. florencía* are significantly different in wing size, both in the FW and HW (ANOVA $F_{(1,82)}=63.894$, $p<0.01$ and $F_{(1,82)}=82.587$, $p<0.01$, respectively, Figure 3.2A,B). FW and HW of *H. t. florencía* are consistently larger than those of *H. m. malleti*. In terms of shape, the FW is statistically different between species (MANOVA $F_{(1,78)}=28.09$, $p=2.504e-12$), but not the HW (MANOVA $F_{(1,78)}=2.969$, $p=0.0371$; $\alpha=0.01$, Figure 3.2C and 3.2D). In the FW, the most variable landmark coordinates were LM3, LM4 (located in the distal part of the costal margin, near the wing apex; Figure 3.3A, 3.3B and 3.3E) and LM15 (located in the middle of the inner margin; Figure 3.3C, 3.3D and 3.3F). Thus, the significant shape variation between the two species appears to be linked with the length of the FW (longer in *H. t. florencía*) and the curvature of the inner margin (deeper in *H. t. florencía*).

The colour pattern comparison between the two species suggested subtle differences in wing colour pattern (Figure 4). The shape (PC2) of the three wing elements investigated (forewing band, forewing 'dennis' patch, and hindwing rays) did not differ between species, but their size (PC1) was slightly different (Figure 3.4). The edge of the yellow forewing band seemed more distally extended in *H. m. malleti* but only on the ventral side of the wing (Figure 3.4A and 3.4D). Also, the hindwing rays appeared thicker in *H. m. malleti*, but only on the dorsal side of the wing (Figure 3.4C and 3.4F). In contrast, the 'dennis' forewing patch is bigger in *H. m. malleti*, both dorsally and ventrally (Figure 3.4B and 3.4E). Despite this, none of these differences were statistically significant between species indicating that the two species are almost indistinguishable in terms of wing colour pattern.

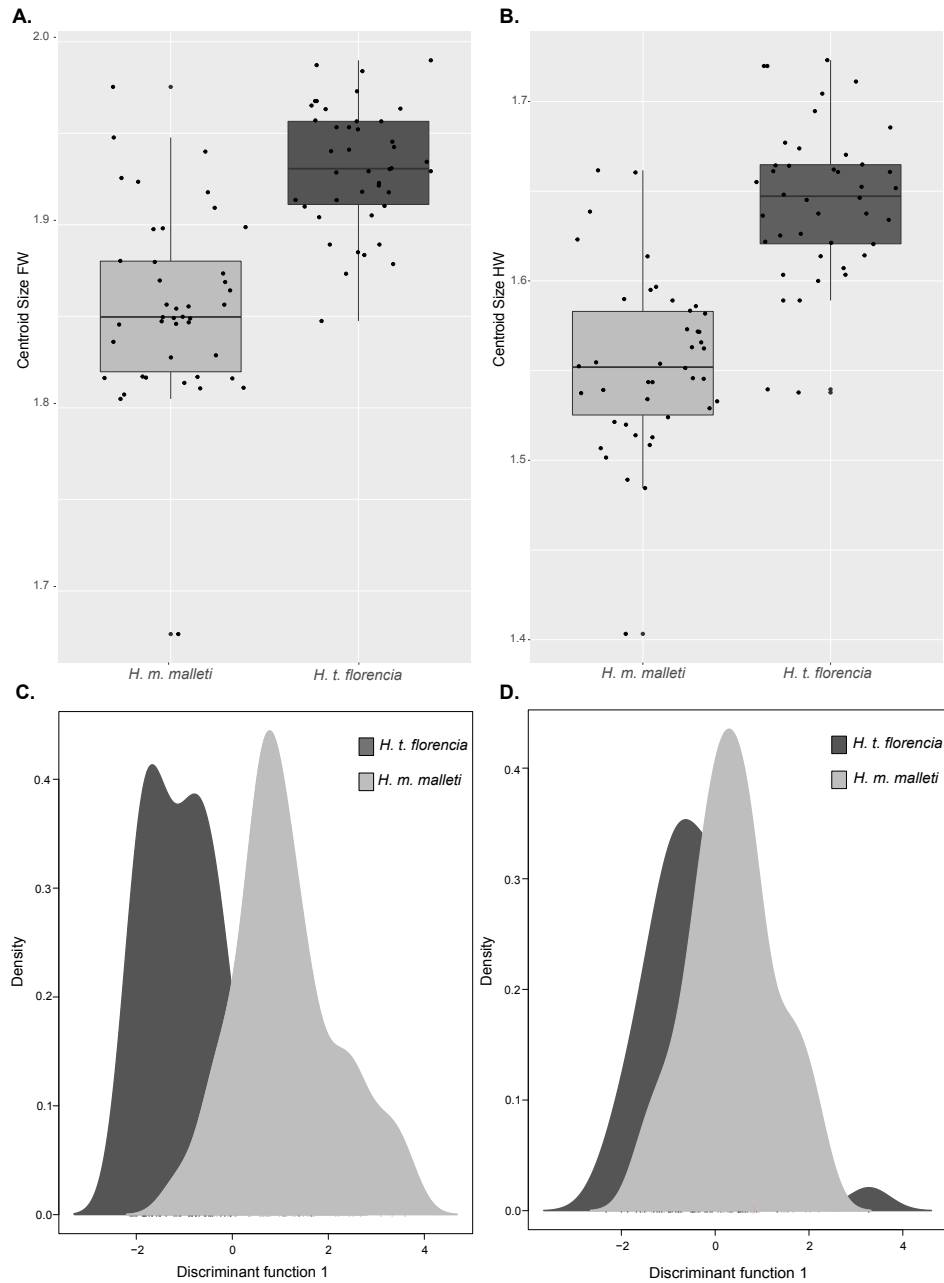


Figure 3.2. Species wing size and shape. Forewing (A) and hindwing (B) size variation. Density plots showing the variation in the shape of the forewing (C) and the hindwing (D). A total of 43 *H. m. malleti* and 45 *H. t. florentia* were analysed.

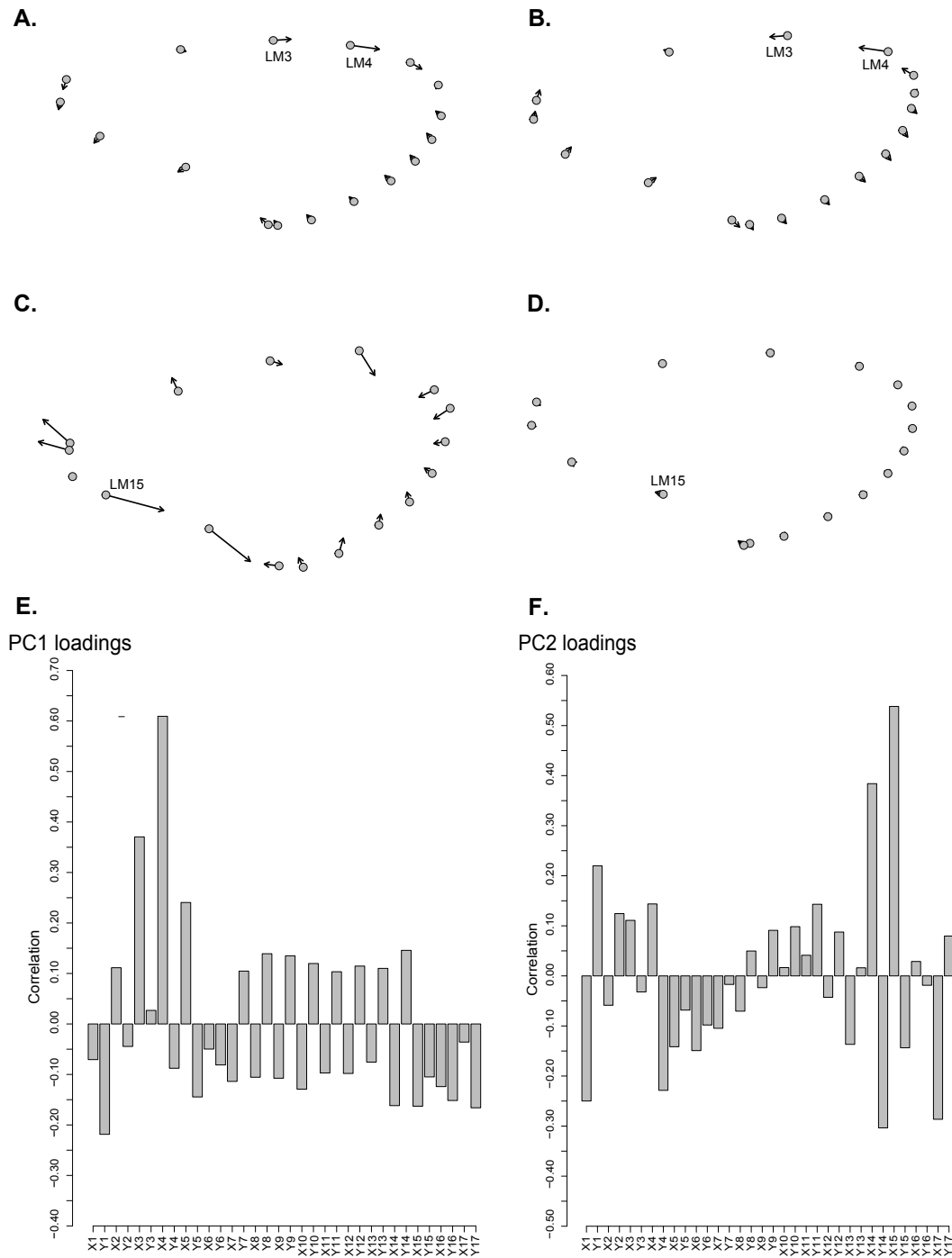


Figure 3.3. Shape variation of forewings of *H. melpomene malleti* and *H. timareta florencia*. Shape deformation (A) and (B) represents the shape at minimum values for PC1 and PC2, respectively. Shape deformation (C) and (D) represents maximum values for PC1 and PC2, respectively. Landmarks indicated (LM3, LM4 and LM15) are the one that varies the most. Panels (E) and (F) show the PC1 and PC2 loadings, respectively.

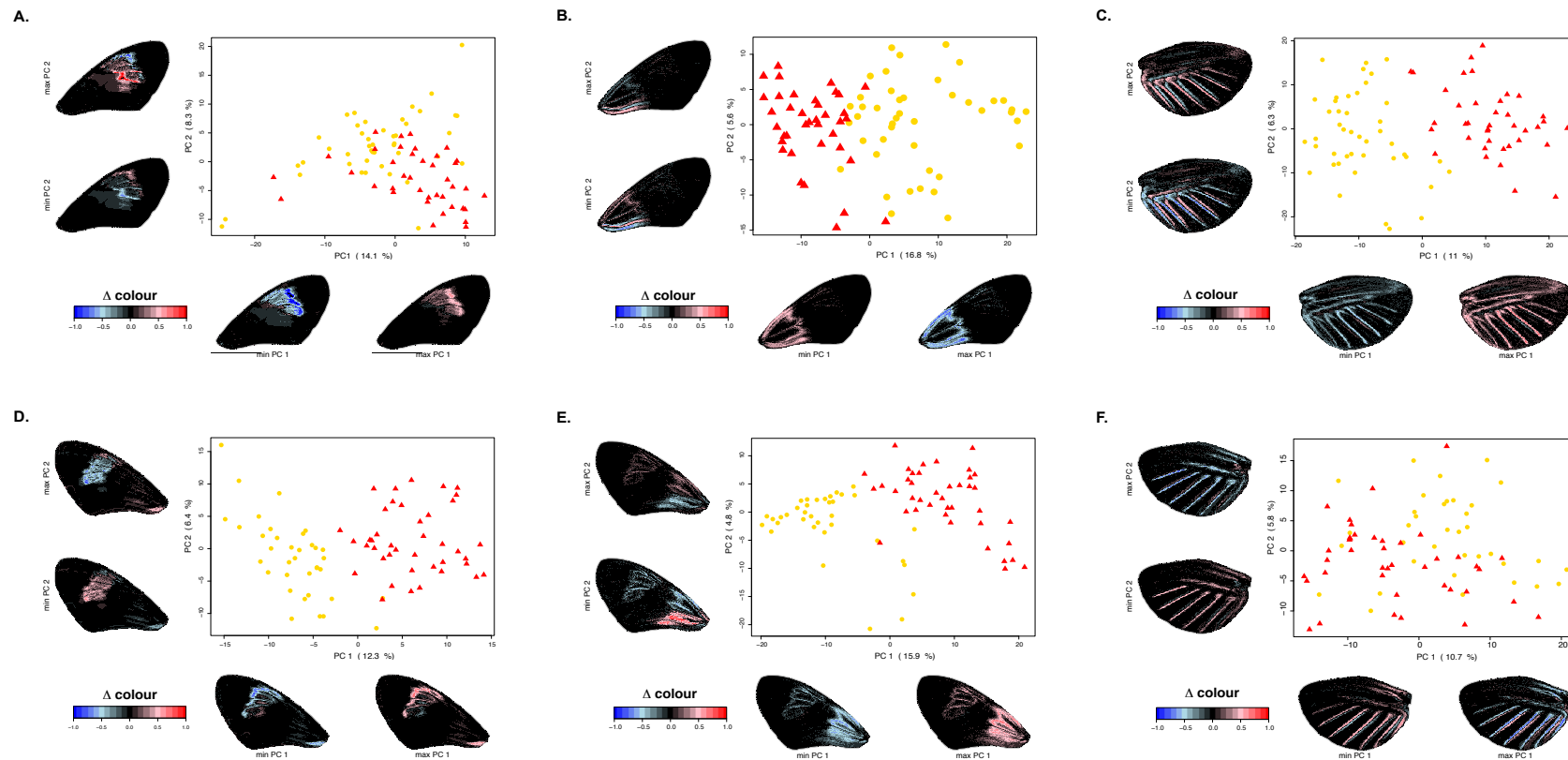


Figure 3.4. Colour pattern comparison between the two species. (A) Yellow patch on the dorsal forewing ($F_{(1,80)}=0.0647$, $p=0.978$); (B) Dennis on the dorsal forewing ($F_{(1,79)}=0.060$, $p=0.185$); (C) Ray on the dorsal hindwing ($F_{(1,80)}=0.592$, $p=0.621$); (D) Yellow patch on the ventral forewing ($F_{(1,74)}=0.619$, $p=0.604$); (E) Dennis on the ventral forewing ($F_{(1,74)}=1.259$, $p=0.294$) and (F) ray on the ventral hindwing ($F_{(1,74)}=0.658$, $p=0.580$). Yellow circles = *H. t. florenxia*. Red triangles = *H. m. malleti*. Only individuals with wings in good condition were used ($n=88$; Table S2.1). Predicted values scale indicates the expression of colour pattern, where positive values (red) represent higher presence and negative values (blue) represents lower presence or even absence. PC1 explains the variation in size and PC2 explains the variation in the shape of said colour pattern element.

BEHAVIOURAL EXPERIMENTS

Experiment 1: Altering the wing phenotype of males. Altering the wing pattern of males had no effect on mating probability. In all 40 experiments, both *H. t. florencia* and *H. m. malleti* females mated equally with conspecific males that had altered or normal wing colour pattern ($p=0.55$ in both cases; Figure 3.5).

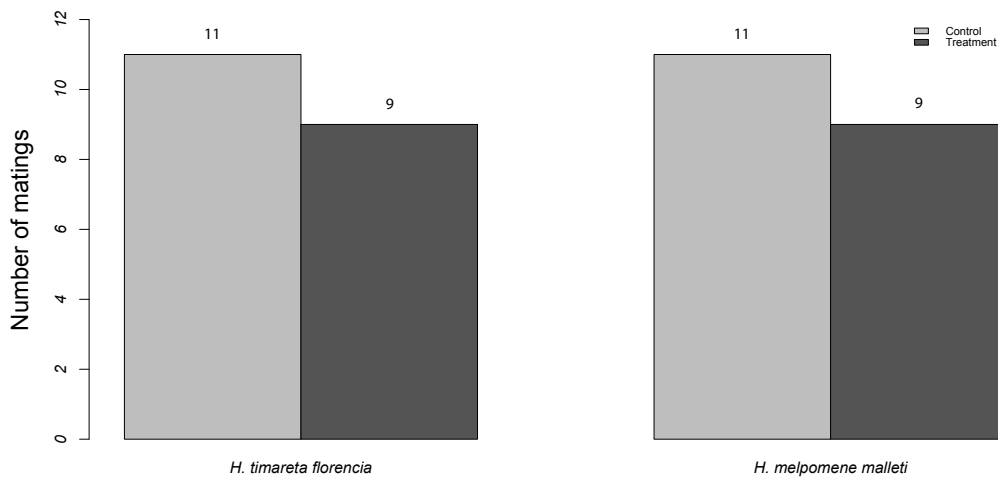


Figure 3.5. Mate choice triads testing the importance of wing colour pattern in mate preference. Number of matings obtained is indicated above each bar. Control males are represented in light grey and treatment males are represented in dark grey.

Consistent with this finding, I found no differences in female response towards control and treatment males in all but one of the behaviours assayed (Figure 3.6 and Table 3.1). The exception was the observation that females of *H. t. florencia* kept their wings open for a larger proportion of the time during courtship by control males relative to male whose wing patterns were eliminated ($\chi^2_{(1,216)}=6.905$, $p=0.008$) (Figure 3.6 and Table 3.1). This further suggests that, in these two species, the male's wing colour pattern is not a crucial cue for females to recognize their conspecific mate.

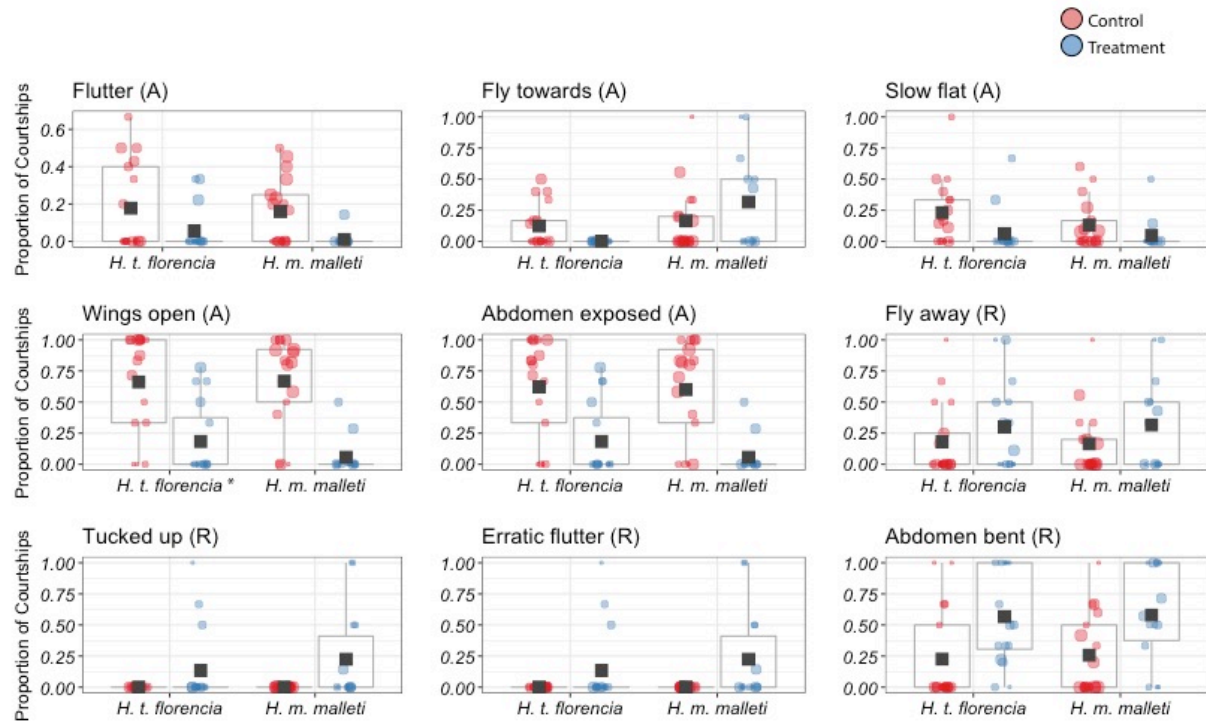


Figure 3.6. Proportion of courtships that resulted in female behavioural responses towards control and treatment males. Behaviours are classified as Acceptance (A) or Rejection (R). Control males are represented in red (left) and treatment males in blue (right). Means are marked with a black square and boxplots mark the inter-quartile ranges. Size of datapoint is proportional to the number of courtships by that male. Asterisk (*) next to the species' name is indicative of statistical significance ($\alpha=0.01$) according to GLMM.

Table 3.1. Female behavioural response towards males with normal (control) and altered (treatment) wing phenotype. Behaviours are classified as Acceptance or Rejection. Asterisk (*) indicates statistical significance ($\alpha=0.01$) according to GLMM.

Behaviour		<i>H. m. malleti</i>	<i>H. t. florencia</i>
Flutter	Acceptance	$\chi^2_{(1,326)}=0.646, p=0.421$	$\chi^2_{(1,216)}=4.734, p=0.029$
Fly towards	Acceptance	$\chi^2_{(1,326)}=0.877, p=0.349$	$\chi^2_{(1,216)}=0.090, p=0.764$
Slow flat	Acceptance	$\chi^2_{(1,326)}=0.608, p=0.435$	$\chi^2_{(1,216)}=1.223, p=0.268$
Wings open	Acceptance	$\chi^2_{(1,326)}=2.005, p=0.156$	$\chi^2_{(1,216)}=6.905, p=0.008^*$
Abdomen exposed	Acceptance	$\chi^2_{(1,326)}=0.215, p=0.642$	$\chi^2_{(1,216)}=0.067, p=0.795$
Fly away	Rejection	$\chi^2_{(1,326)}=2.353, p=0.125$	$\chi^2_{(1,216)}=1.474, p=0.224$
Tucked up	Rejection	$\chi^2_{(1,326)}=1.213, p=0.270$	$\chi^2_{(1,216)}=5.500, p=0.018$
Erratic flutter	Rejection	$\chi^2_{(1,326)}=1.723, p=0.189$	$\chi^2_{(1,216)}=2.495, p=0.114$
Abdomen bent	Rejection	$\chi^2_{(1,326)}=0.075, p=0.784$	$\chi^2_{(1,216)}=5.549, p=0.018$

Experiment 2: Blocking the emission of chemical blends. Blocking the emission of chemical blends in males showed an effect on mating probability. Females of both species discriminated against conspecific males in which the chemical bouquet emission was experimentally blocked ($p<0,001$ in both cases; Figure 3.7). In *H. t. florencia* only 16% of the matings occurred with the blocked male whilst in *H. m. malleti*, matings with the blocked male only occurred 13% of the times (Figure 3.7).

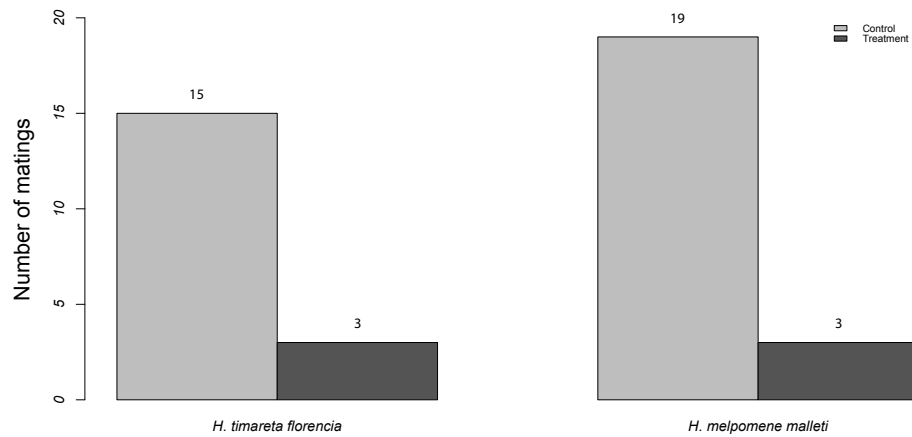


Figure 3.7. Mate choice triads in where male chemical blend was blocked. The number of matings obtained in each condition is indicated above each bar. Control males are represented in light grey and treatment males are represented in dark grey.

Consistent with these findings, behavioural observations revealed significant differences in female behavioural responses towards blocked and unblocked males (Figure 3.8). In both species, female acceptance behaviours (A) were observed more often towards control males while rejection behaviours (R) were more frequently observed towards treatment males. In particular, females of *H. m. malleti* were more receptive towards control males in all but two behaviours (slow flat and flutter; $p=0.042$ and $p=0.085$, respectively; Table 3.2). Likewise, *H. t. florenciae* females were more receptive towards control males in all but two behaviours (slow flat and fly towards, $p=0.209$ and $p=0.013$, respectively; Table 3.2). Both species consistently rejected the treatment (blocked) males (Figure 3.8). This suggests that the ability of a male to emit sexual pheromones is crucial for females to accept potential mates in both species.

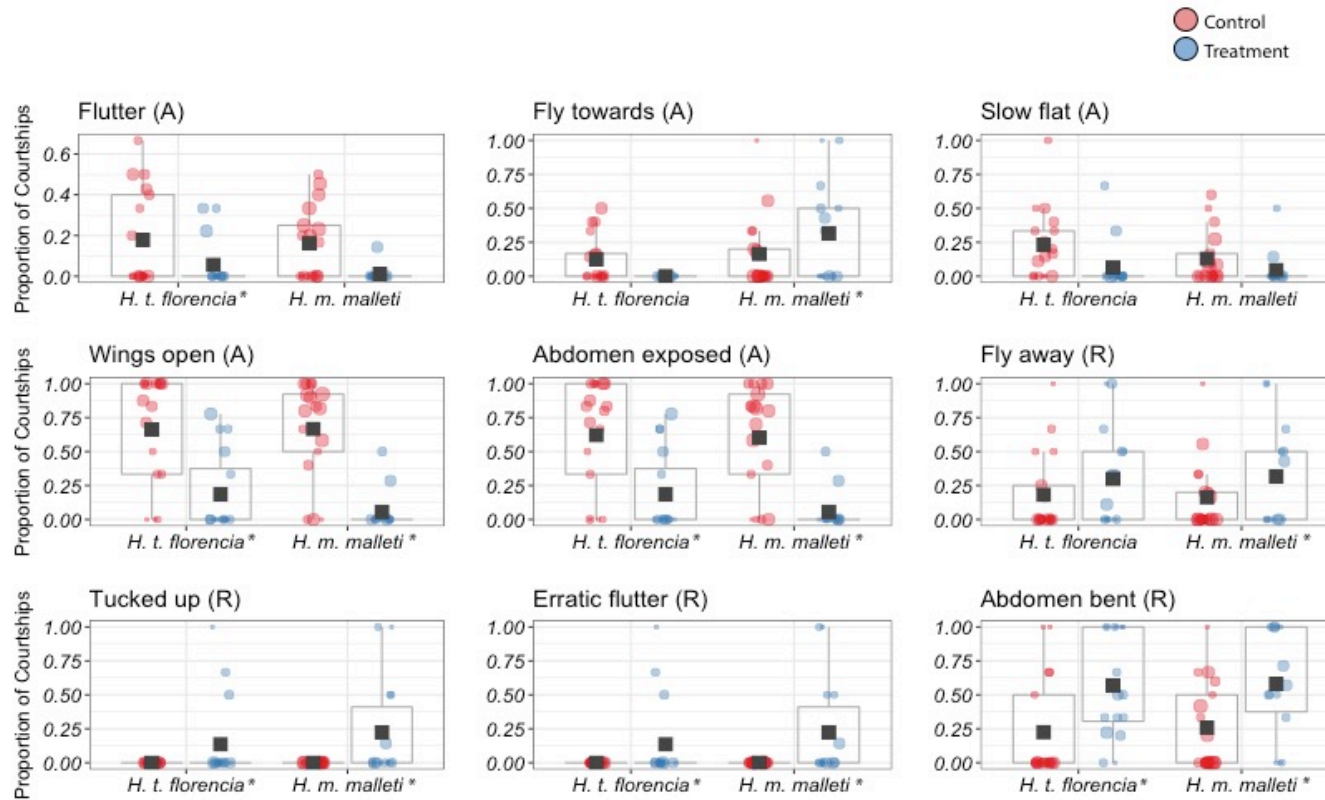


Figure 3.8. Female behavioural responses towards males with an altered capacity to emit sexual pheromones. Behaviours are classified as Acceptance (A) or Rejection (R). Control males are represented in red (left) and treatment males in blue (right). Means are marked with a black square and boxplots mark the inter-quartile ranges. Asterisk (*) next to the species' name is indicative of statistical significance ($\alpha=0.01$) according to GLMM.

Table 3.2. Female behavioural responses in triads that tested the female's preference for the male's sex pheromones. Asterisk (*) is indicative of statistical significance ($\alpha=0.01$) according to GLMM.

Behaviour		<i>H. m. malleti</i>	<i>H. t. florencia</i>
Flutter	Acceptance	$\chi^2_{(1,122)}=2.956$, $p=0.085$	$\chi^2_{(1,162)}=10.239$, $p=0.001^*$
Fly towards	Acceptance	$\chi^2_{(1,122)}=2.441$, $p=0.0004^*$	$\chi^2_{(1,162)}=6.136$, $p=0.013$
Slow flat	Acceptance	$\chi^2_{(1,122)}=4.100$, $p=0.042$	$\chi^2_{(1,162)}=1.576$, $p=0.209$
Wings open	Acceptance	$\chi^2_{(1,122)}=27.401$, $p=1.654e-07^*$	$\chi^2_{(1,162)}=50.523$, $p=1.178e-12^*$
Abdomen exposed	Acceptance	$\chi^2_{(1,122)}=22.453$, $p=2.153e-06^*$	$\chi^2_{(1,162)}=44.046$, $p=3.207e-11^*$
Fly away	Rejection	$\chi^2_{(1,122)}=8.035$, $p=0.004^*$	$\chi^2_{(1,162)}=6.136$, $p=0.013$
Tucked up	Rejection	$\chi^2_{(1,122)}=11.273$, $p=0.0007^*$	$\chi^2_{(1,162)}=18.078$, $p=2.121e-05^*$
Erratic flutter	Rejection	$\chi^2_{(1,122)}=15.823$, $p=6.954e-05^*$	$\chi^2_{(1,162)}=26.037$, $p=3.349e-07^*$
Abdomen bent	Rejection	$\chi^2_{(1,122)}=17.093$, $p=3.558e-05^*$	$\chi^2_{(1,162)}=22.909$, $p=1.698e-06^*$

Experiment 3: Perfuming males with the heterospecific chemical blends.

The triads testing female preference for perfumed males ($n= 37$) did not yield any matings. The failure to mate might reflect the rapid evaporation rate of the chemical extracts. For example, the concentration of octadecanal decreased by 25% in the first 30 minutes and 82% after 60 minutes (Figure S2.1 and Table S2.2). Similarly, the concentration of syringaldehyde decreased by 25% in the first 30 minutes and 47% after the first hour.

Nevertheless, I observed significant differences in female behavioural responses towards treatment and control males (Table 3.3 and Figure 3.9). Specifically, in all behaviours tested, females exhibited acceptance behaviours towards males perfumed with the hexane extract of their own species and consistently rejected males perfumed with that of the other species. This indicates that the composition of the male sex pheromone is important for females in order to recognize a male as conspecific and accept him to mate with her and implies that female preference plays a major role in reproductive isolation in *Heliconius*.

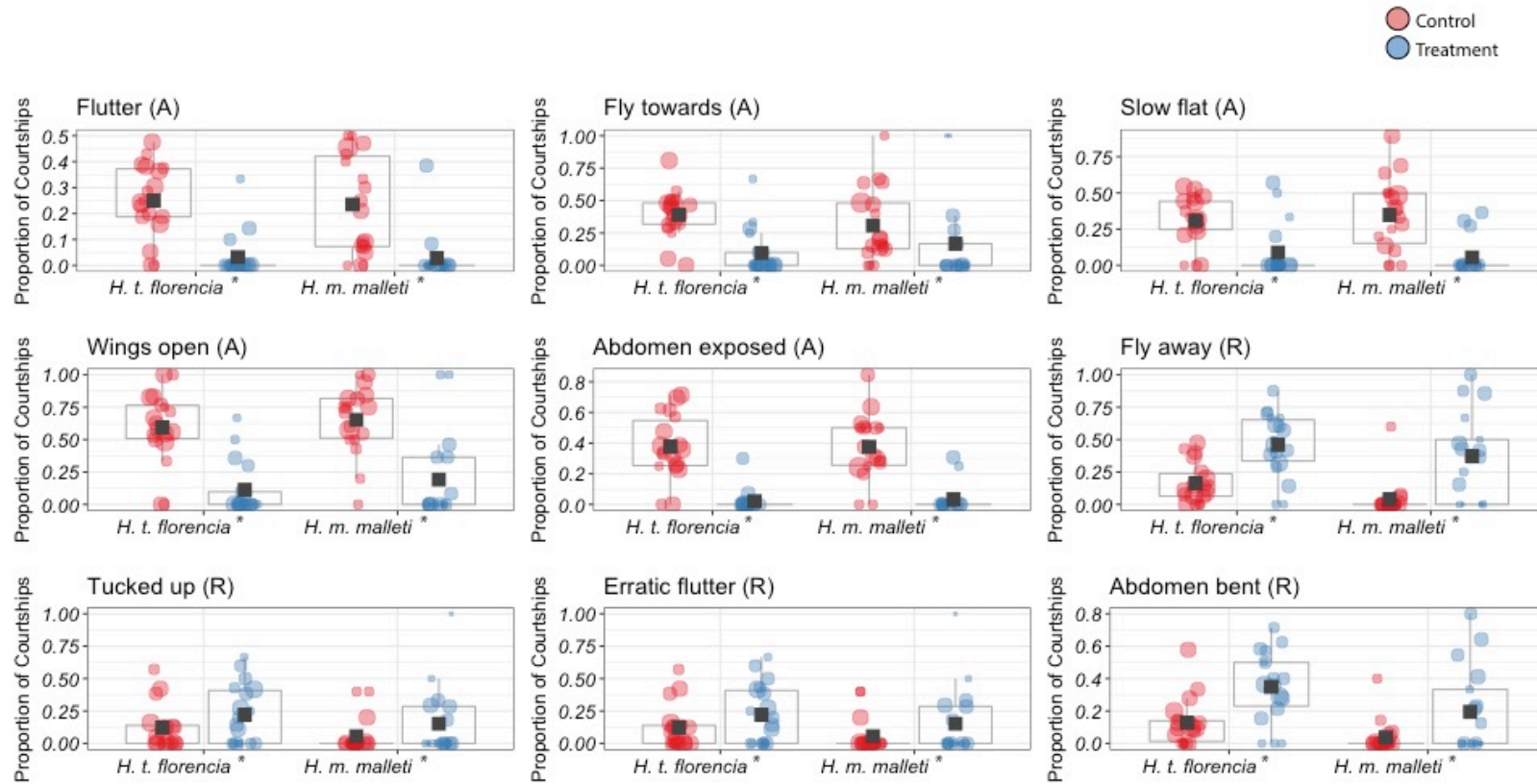


Figure 3.9. Female behavioural responses towards males “perfumed” with a hexane extract from five males either of *H. m. mallei* or *H. t. florenzia*. Behaviours are classified as Acceptance (A) or Rejection (R). Control males are represented in red (left) and treatment males in blue (right). Means are marked with a black square and boxplots mark the inter-quartile ranges. Asterisk (*) next to the species’ name is indicative of statistical significance ($\alpha=0.01$) according to GLMM.

Table 3.3. Female behavioural responses in triads that tested female preference for males “perfumed” with a hexanic extract from five either of conspecific or heterospecific male. The asterisk (*) indicates statistical significance ($\alpha=0.01$) according to the GLMM.

Behaviour		<i>H. m. malleti</i>	<i>H. t. florencia</i>
Flutter	Acceptance	$\chi^2_{(1,473)}=51.113, p=8.72e-13^*$	$\chi^2_{(1,354)}=25.476, p=4.48e-07^*$
Fly towards	Acceptance	$\chi^2_{(1,473)}=75.612, p=2.20e-16^*$	$\chi^2_{(1,354)}=32.715, p=1.06e-08^*$
Slow flat	Acceptance	$\chi^2_{(1,473)}=44.195, p=2.97e-11^*$	$\chi^2_{(1,354)}=48.501, p=3.30e-12^*$
Wings open	Acceptance	$\chi^2_{(1,473)}=139.04, p=2.20e-16^*$	$\chi^2_{(1,354)}=93.902, p<2.20e-16^*$
Abdomen exposed	Acceptance	$\chi^2_{(1,473)}=90.039, p=2.20e-16^*$	$\chi^2_{(1,354)}=60.483, p=7.48e-15^*$
Fly away	Rejection	$\chi^2_{(1,473)}=44.263, p=2.87e-11^*$	$\chi^2_{(1,354)}=109.41, p<2.20e-16^*$
Tucked up	Rejection	$\chi^2_{(1,473)}=13.629, p=2.23e-04^*$	$\chi^2_{(1,354)}=8.158, p=0.004^*$
Erratic flutter	Rejection	$\chi^2_{(1,473)}=43.539, p=4.16e-11^*$	$\chi^2_{(1,354)}=75.385, p<2.20e-16^*$
Abdomen bent	Rejection	$\chi^2_{(1,473)}=27.207, p=1.83e-07^*$	$\chi^2_{(1,354)}=47.357, p=5.91e-12^*$

DISCUSSION

Intersexual communication plays a crucial role in determining the outcome of mating attempts. Therefore, variation in sexual cues and preferences has major implications for speciation, as they can cause reproductive isolation. The role of visual cues and visual preference in triggering reproductive isolation has been well documented in animal taxa that have diverged in the presence of gene flow (85,267,268). In contrast, while it is widely acknowledged that chemical signals play a role in animal pre-mating isolation (269,270), their role as drivers of sympatric speciation is much less studied.

In *Heliconius* butterflies, reproductive and behavioural isolation usually follow a multimodal pattern where multiple traits such as wing colouration, pheromones, and habitat use, among others, are involved (254). For example, visual cues mediate the recognition of conspecific females by males across the entire spectrum of divergence in the *melpomene/cydno/timareta* clade with implications for reproductive isolation and

speciation (254). Thus, reproductive isolation between taxa with shifts in wing colour pattern, such as the species *H. m. rosina* and *H. c. chioneus* (high divergence) or the subspecies *H. t. linaresi* and *H. t. florencía* (low divergence), heavily relies on visual cues (254). In addition to wing colouration, chemicals seem to also contribute to species recognition (14,81,108). In fact, species identity largely explains the overall variation in chemical profiles in *Heliconius* (255).

To date, the contribution of visual cues to reproductive isolation in these butterflies has been deeply studied and experimentally tested, mainly in males (43,44,51,74–77; although see 78). However, the role of chemical cues and female preference in maintaining species integrity is far less understood. In this sense, the convergence in wing colouration between the sister and sympatric species *H. t. florencía* and *H. m. malleti* provides a natural experimental model to disentangle the effect of wing colour pattern and chemical signals, and to characterise the role of female preference in reproductive isolation. In this study, I confirmed the existence of strong mating preferences between *H. m. malleti* and *H. t. florencía*, and that this preference appears not to be related to the colour pattern, but chemically mediated.

I found that the mimetic and closely related species pair *H. t. florencía* and *H. m. malleti* are nearly identical in terms of wing patterning, and in consequence, altering this trait with black markers had little effect on the preference of females for mates. This accords with a previous study where experiments with wing models washed in hexane revealed that males of *H. t. florencía* approached and courted models of *H. m. malleti* as much as theirs (260). Although I detected some differences in size and wing shape between these species these did not seem to contribute to species recognition either. These results suggest that wing phenotype is not the cue that maintains species integrity between these mimetic pair. Instead, strong mating isolation appears to be largely driven by chemical signals.

In addition, I demonstrated that females of *H. m. malleti* and *H. t. florencía* strongly discriminated against conspecific males that have their wing androconia experimentally

blocked, affecting reproductive success with implications for reproductive isolation.

Consistent with this result, I found that females showed more acceptance behaviour and less rejection behaviour towards males perfumed with a conspecific extract relative to those perfumed with the heterospecific extract, demonstrating that pheromone composition is an important trait for species recognition that likely mediates reproductive isolation in this species pair. Intriguingly, no matings were observed in these perfuming experiments, which could be partly due to the rapid evaporation of the androconial perfume applied. However, since these experiments did not alter the chemicals in the abdominal gland, the lack of mating also indicates that the sole presence of the abdominal scent is not enough to ensure successful mating, and the androconial scent is always needed. Even more, the compound composition in each of these scents possibly needs to occur in specific mixture ratios. This would agree with recent findings in the butterfly *Pieris napi*, where the synergistic processing of two wing male volatile components in a 1:1 ratio is necessary for female acceptance (274). Also, in *Drosophila*, the disruption natural ratios in male cuticular hydrocarbons lead to aversion response in females (275) further suggesting that normal mixture ratios in the chemicals underlying mate acceptance and preference are required. Therefore, it is likely that the abdominal and androconial extracts, and their specific composition, play different roles at different stages of courtship (although this remains to be tested).

Heliconius females, as well as other butterfly systems such as *B. anynana* (13), are actively involved in mating decisions, demonstrating the potential for multimodal signals, especially visual and olfactory cues (273). This study shows that sexual chemicals are effective cues that contribute to mate recognition in day flying butterflies.

CHAPTER 3. MATE PREFERENCE AND PHEROMONE COMPOSITION IN A PAIR OF CLOSELY RELATED AND MIMETIC SPECIES OF THE GENUS *Heliconius*

INTRODUCTION

The evolution of different mating behaviours and mating cues between closely related species is recognized as an important mechanism that maintains reproductive isolation (276). This is because one or both of the sexes fail to identify the other species as a suitable mate. Therefore, characterising the behaviours and traits that influence mating preference as well as to understand their genetic basis is crucial to shed light on how species boundaries are formed and maintained.

In insects, and especially in Lepidoptera, several studies have demonstrated the importance of sex pheromones as a reproductive isolation mechanism between closely related species (58,126,277–279). However, the study of the composition, function and genetic basis of sex pheromones has been mainly addressed in insects with agricultural importance but not in adaptive radiations in nature (37,147,280–282). To date, the sex pheromones of more than 500 Lepidoptera are known, and the synthesis pathway of these compounds, as well as the participating enzymes, have been well characterized in moths (143–145). In contrast, much less is known about sexual olfactory communication in butterflies, where not only the female produces sex pheromones but, in some species, males produce sex pheromones that are perceived by females (38,51,138,140,141,163). Despite this, the chemical composition of sex pheromones in butterflies and moths is highly similar (15,138,139,145,147,156,283,284) and the sex pheromone biosynthetic pathways are conserved between moths and the butterfly *Bicyclus anynana* (139).

Even more, genomic comparisons have suggested the conservation of sex pheromone biosynthetic gene clades between moths and butterflies of the genera *Papilio*, *Danaus* and *Heliconius* (139,167). Despite this, the role of chemical cues as a reproductive isolation barrier in *Heliconius* has not been profoundly studied (but see 10 and 61).

The mimetic pair *H. melpomene malleti* and *H. timareta florencia* share the dennis-ray wing pattern in the south-eastern Andes of Colombia, and exhibits strong reproductive isolation, which suggests that in the absence of colour pattern differences that could be used as mate recognition cues other mechanisms such as chemical signals should mediate conspecific mate recognition. In agreement with this hypothesis, recent evidence indicates that reproductive isolation between *H. melpomene* and *H. timareta* is based on female response to species-specific chemical signals, indicating that chemical signalling is important in mate choice in *Heliconius* butterflies as I showed previously on Chapter 2 (108,138,172,254). Previous studies revealed that these two species differ in their androconia and genital chemical composition, suggesting that chemical signalling is important in mate choice in *Heliconius* butterflies (81). However, such studies included few individuals (108,138). Therefore, it is crucial to confirm these results and test the role of chemicals in maintaining reproductive isolation between *H. melpomene malleti* and *H. timareta florencia*. If such is the case, it is also necessary to investigate the inheritance patterns of both male chemical production and female preference to better understand of the genetic architecture of speciation in the face of gene flow.

Here I used a combined approach that includes chemical extraction, chemical characterization, genetic crosses and behavioural experiments to get a better understanding of reproductive isolation mediated by chemical signals in *Heliconius* butterflies, especially in the context of mimicry between sympatric and closely related species.

MATERIALS AND METHODS

WILD SAMPLING AND INTERSPECIFIC CROSSES

Wild specimens of *H. m. malleti* and *H. t. florencía* were collected in Sucre and Doraditas, Caquetá-Colombia (01°48'12" N - 75°39'19" W, 1200 m and 01°42'39" N - 75°42'32" W, 1400 m, respectively). For each species, wild males were preserved for chemical extraction (see below). The remaining wild individuals (males and females) were taken to the insectaries of Universidad del Rosario in La Vega (Colombia) to establish stock populations in 2×3×2 m insectaries for the behavioural and chemical analyses. Larva were reared on *Passiflora oerstedii* while adults were provided with *Psiguria* sp. as pollen source and supplied with ~20% sugar solution.

We also used the stock populations to perform interspecific crosses between *H. t. florencía* and *H. m. malleti*. To do so, a female of *H. t. florencía* was mated with an *H. m. malleti* male. The reciprocal cross was successful three times, but the female always died before laying eggs. Then, two F₁ males were backcrossed to pure *H. t. florencía* females (crosses towards females of *H. m. malleti* consistently failed). In all cases, eggs were collected daily and placed in small plastic pots. Larvae were reared individually to avoid cannibalism, and right before pupation, they were transferred to bigger plastic pots until eclosion. The two backcrosses towards *H. t. florencía* produced 25 males and 25 females: all males were processed to chemically characterise the composition of their chemical blends, while 24 females were used in behavioural experiments testing for female preference. The bodies of these offspring were preserved in 20% DMSO once data was collected.

Field collections and insectary rearing were conducted under the permit #530 issued by the "Autoridad Nacional de Licencias Ambientales" of Colombia (ANLA).

Rearing conditions and experimental crosses were approved by the Ethics Committee of Universidad del Rosario (approval #CEI-ABN026-000155).

In addition, to determine the hybrid ability to mate (F_1 and backcrosses), I performed no-choice mating experiments. For this, the success or failure of mating was recorded by direct observation in 80 control conspecific, 29 heterospecific and 112 hybrid mating attempts (i.e., F_1 and backcrosses). Then, the probability of mating ($P_{i \times j}$) between a female type i and a male type j was obtained by maximizing the \log_e of the likelihood (272,285) as follows:

$$ML (P_{i \times j}) = m_{i \times j} \log_e(P_{i \times j}) + (N_{i \times j} - m_{i \times j}) \log_e(1 - P_{i \times j})$$

Where m is the number of experiments involving a successful mating and n is the number of failed experiments. Likelihood maximization was carried out with the SOLVER algorithm of Microsoft Excel. Confidence intervals were obtained at the parameter values that led to a decrease in the \log_e of the likelihood of two units (286).

BEHAVIOURAL EXPERIMENTS

Behavioural triad experiments to study hybrid female preference were conducted with 18 F_1 one-day-old virgin females and 24 backcross one-day-old virgin females. In all cases, a single virgin hybrid female had to choose between two males, one *H. t. florencia* and one *H. m. malleti*. These triads were conducted in the same way as the previous behavioural experiments (for details see above, Chapter 2, Materials and Methods). Female acceptance or rejection behaviours were also recorded.

The mating outcome was analysed with a binomial test. I used a generalised linear mixed model (GLMM) with a binomial error distribution and logit link function to test

if females responded differently to control and treatment males. The response variable was derived from those minutes where at least one of the males courted the female regardless of her response (either “acceptance” or “rejection”). Significance was determined by using likelihood ratio tests comparing models with and without male type included as an explanatory variable. In order to avoid pseudoreplication, individual female was included as a random effect in all models. All statistical analyses were performed with R version 3.3.2 (262), using the packages lme4 (263), ggplot2 (264), car (265) and binom (266) following Darragh et al. 2017 (81).

CHARACTERIZATION OF CHEMICAL PROFILES

To determine the chemical composition of the volatile compounds of the androconia and genitalia in males of *H. m. malleti*, *H. t. florenci*a and their hybrids (F₁ and backcrosses), I dissected both tissues from adults and placed them individually in 200 µL of ultrapure dichloromethane (Merck UniSolv®) in 2 mL glass vials and soaked for 1 hour. After this incubation, the solvent was transferred to a new vial and stored at -20°C. Dichloromethane is a preferred solvent used for pheromone extraction since it is sufficiently volatile for extracts to be concentrated without exposing them to high temperatures, it is non-flammable, and penetrates scales better than hexane leading to higher extract titres (164,287).

These extracts were analysed by gas chromatography/mass spectrometry (GC/MS) at the Smithsonian Tropical Research Institute in Panama following the protocol of Mann et al., 2017 (138). Prior to the GC/MS, samples were evaporated under ambient air at room temperature. Then, I quantified the compounds found in the extracts using a Hewlett-Packard GC model 5977 mass-selective detector connected to a Hewlett-Packard GC model 7890B equipped with a Hewlett-Packard ALS 7693 autosampler. A BPX-5 fused silica capillary column (SGE, 25m x 0.22 mm, 0,25 µm) was used. Injection was performed in splitless mode (250°C

injector temperature) with helium as the carrier gas with a constant flow of 1.2 ml/min. The temperature programme started at 50°C, held for 5 min, and then rose to 320°C with a heating rate of 5°C/min. I used 2-tetradecyl acetate (200 ng) as an internal standard. Components were identified by comparison of mass spectra and gas chromatographic retention index with reference samples from the Schulz lab collection (Institute of Organic Chemistry, Technische Universität Braunschweig, Germany). Relative concentrations were determined by peak area analysis by GC/MS.

To evaluate species differences in compound composition I implemented a dimension reduction (PCAs) using the software Past v3.0 (288). I retained the components accounting for 95% of the variance, and those were used to conduct a Discriminant Analysis. A MANOVA was performed in candisc R package (200). Finally, using the means of the relative concentrations of each compound, I established the relationship among *H. t. florenci*a, *H. m. malleti*, F₁ and backcross males for androconia and genital bouquet (i.e., mixture of volatiles), calculating dendrograms using Euclidian distance. Both, dendrogram and compound composition were visualised using the function heatmap in R (version 3.5.0). GC/MS raw data is available in the public repository Zenodo: 10.1098/rspb.2020.0587.

RESULTS

WILD SAMPLING AND INTERSPECIFIC CROSSES

The frequency of successful mating in heterospecific and hybrid crosses was less than that of control crosses confirming the existence of prezygotic isolation barriers acting on these species (42; Table 4.1).

F₁ and BC females obtained from mating an F₁ female to a *H. t. florencica* male were reluctant to mate either parental species. In these trials, F₁ mated at 25% frequency and BC females at 37% frequency, always with *H. t. florencica* males (Figure 4.1, Table 4.1).

Table 4.1. Probability of mating in no-choice experiments. Hmm: *H. m. malleti*; Htf: *H. t. florencica*; F₁: Htf x Hmm; BC: backcrosses [Htf x Hmm] x Htf. Cross type is specified as female x male. [Confidence interval at 95%]. No-choice mating data was collected as in previous studies of *Heliconius* (272,285). This information allowed us to gain a better understanding of the premating barriers operating in this species pair (254). Mating probability for interspecific and hybrid trials was obtained by maximizing the loge of the likelihood function (for details see (108,260).

Cross type		N trials	Mating probability	Confidence interval	Source
Control (conspecific)	Htf x Htf	45	0.911	[0.82 - 0.971]	Merot et al. 2017
	Hmm x Hmm	35	0.857	[0.737 - 0.946]	Merot et al., 2017
Interspecific	Hmm x Htf	13	0.152	[0.04 - 0.363]	This study
	Htf x Hmm	16	0.188	[0.157 - 0.377]	This study
Hybrid crosses	F₁ x Hmm	18	0	[0 - 0.024]	Merot et al., 2017
	F₁ x Htf	24	0.249	[0.119 - 0.4]	Merot et al., 2017
	Hmm x F ₁	8	0	[0 - 0.011]	Merot et al., 2017
	Htf x F ₁	10	0.2	[0.04 - 0.45]	Merot et al., 2017
	F ₁ x F ₁	4	0	[0 - 0.0055]	This study
	BC x Htf	24	0.374	[0.225 - 0.56]	This study
	BC x Hmm	24	0	[0 - 0.033]	This study

BEHAVIOURAL EXPERIMENTS

Hybrid females (F₁ and BC) preferred males of *H. t. florencica* and discriminated against those of *H. m. malleti* (Figure 4.1). In addition, hybrid females were more likely to perform acceptance behaviours towards *H. t. florencica* males while rejection behaviours were observed more often towards *H. m. malleti* males (Figure 4.2, Table 4.2). This suggests that female preference is genetic and

perhaps dominant, although backcrosses to *H. m. malleti* are needed to gain more insights into the inheritance pattern of this trait.

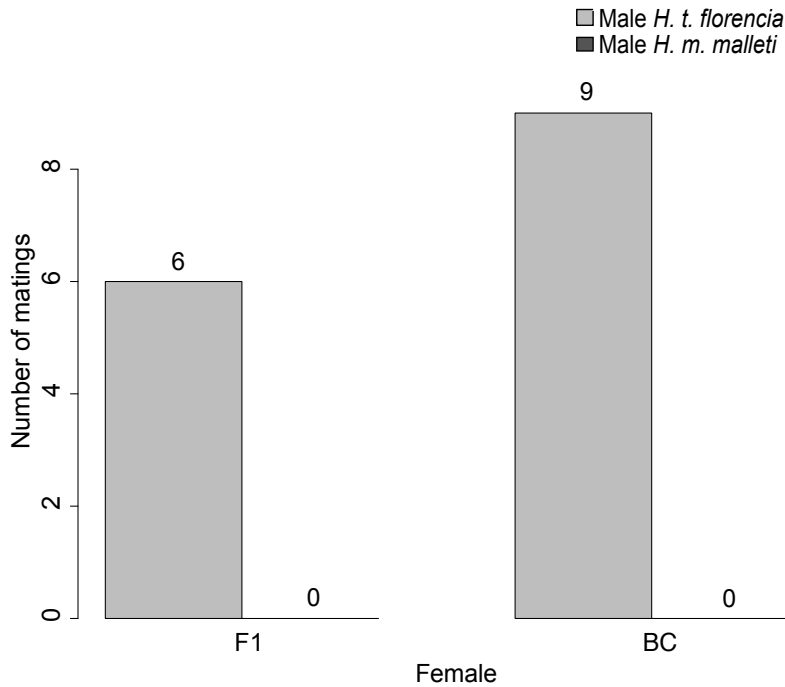


Figure 4.1. Mate choice triads testing behavioural responses in F_1 and backcross (BC) females. The number of matings obtained is indicated above each bar. *H. t. florenciae* males are represented in light grey and *H. m. malleti* males are represented in dark grey.

Table 4.2. Behavioural response of F_1 and BC females towards pure males of *H. m. malleti* and *H. t. florenciae*. The asterisk (*) indicates statistical significance ($\alpha=0.01$) according to GLMM.

Behaviour		F_1 Females	BC Females
Flutter	Acceptance	$\chi^2_{(1,561)}=2.103$, $p=0.147$	$\chi^2_{(1,468)}=0.101$, $p=0.75$
Fly towards	Acceptance	$\chi^2_{(1,561)}=3.184$, $p=0.074$	$\chi^2_{(1,468)}=37.345$, $p=9.90e-10^*$
Slow flat	Acceptance	$\chi^2_{(1,561)}=50.916$, $p=9.64e-13^*$	$\chi^2_{(1,468)}=259.210$, $p=2.20e-16^*$
Wings open	Acceptance	$\chi^2_{(1,561)}=62.043$, $p=3.30e-15^*$	$\chi^2_{(1,468)}=57.215$, $p=3.91e-14^*$
Abdomen exposed	Acceptance	$\chi^2_{(1,561)}=10.650$, $p=1.10e-03^*$	$\chi^2_{(1,468)}=309.720$, $p=2.20e-16^*$
Fly away	Rejection	$\chi^2_{(1,561)}=0.600$, $p=0.439$	$\chi^2_{(1,468)}=97.105$, $p=2.20e-16^*$
Tucked up	Rejection	$\chi^2_{(1,561)}=35.489$, $p=2.57e-09^*$	$\chi^2_{(1,468)}=106.420$, $p=2.20e-16^*$
Erratic flutter	Rejection	$\chi^2_{(1,561)}=44.106$, $p=3.11e-11^*$	$\chi^2_{(1,468)}=72.130$, $p=2.20e-16^*$
Abdomen bent	Rejection	$\chi^2_{(1,561)}=24.640$, $p=6.91e-07^*$	$\chi^2_{(1,468)}=4.630$, $p=0.031$

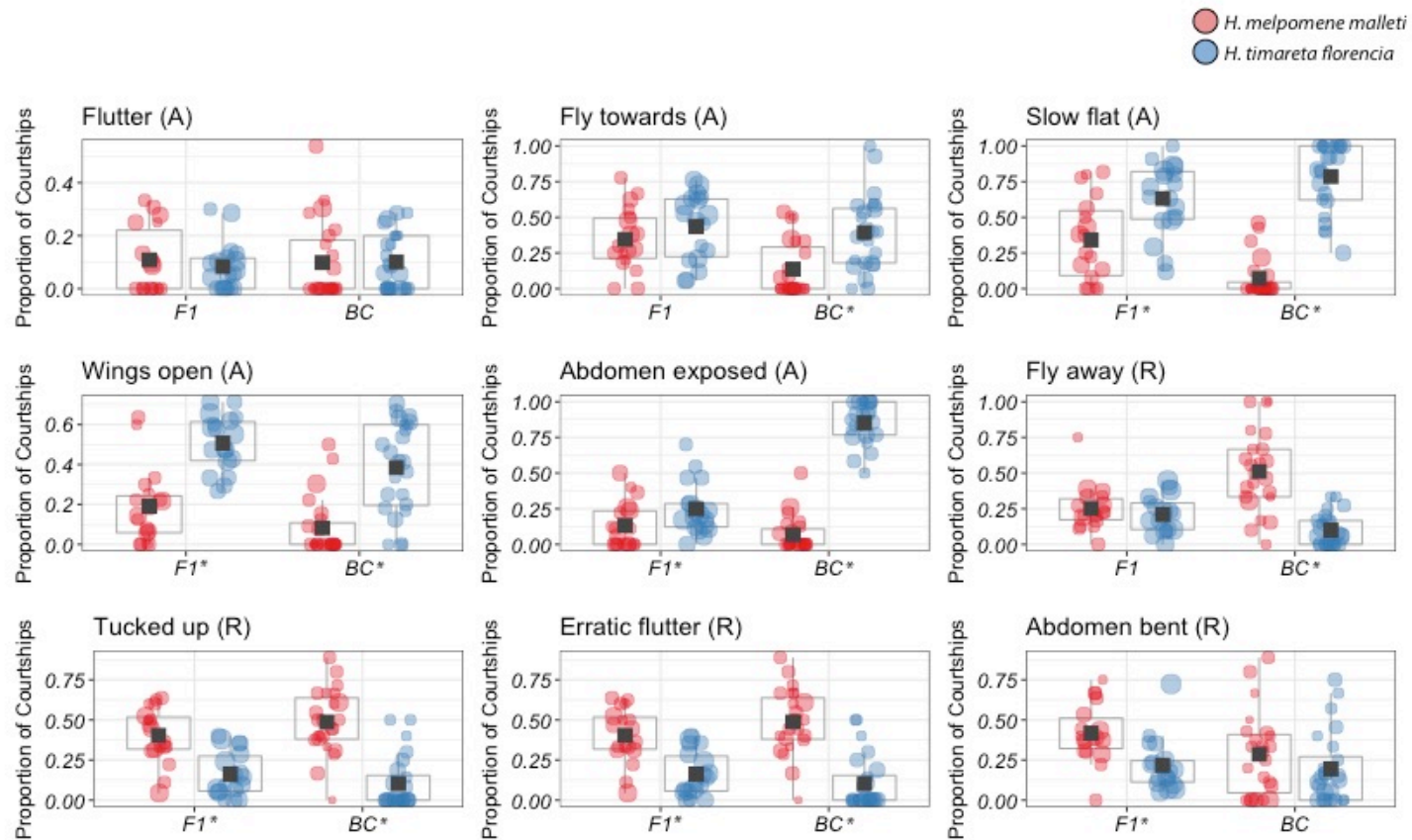


Figure 4.2. Proportion of courtships that resulted in behavioural responses in F_1 and BC females. Behaviours recorded were Acceptance (A) or Rejection (R) towards males of *H. m. malleti* (red, left) and *H. t. florenciae* (blue, right). Means are marked with a black square and boxplots mark the inter-quartile ranges. Size of datapoint is proportional to the number of courtships by that male. The asterisk (*) next to the female (F_1 /BC) is indicative of statistical significance ($\alpha=0.01$) according to GLMM.

CHARACTERISATION OF CHEMICAL PROFILES

I analysed a total of 100 wing androconia and 95 abdominal gland extracts from males of *H. m. malleti* ($n_{\text{and}}=31$, $n_{\text{gland}}=28$), *H. t. florencía* ($n_{\text{and}}=33$, $n_{\text{gland}}=32$), F_1 ($n_{\text{and}}=11$, $n_{\text{gland}}=11$) and backcrosses to *H. t. florencía* ($n_{\text{and}}=25$, $n_{\text{gland}}=24$). Males of both species presented a common composition in the wing androconia extract, and the most notable differences were in terms of the concentration of individual compounds in the mixture (Table S3.1). The compounds of the androconia region in *H. m. malleti* were mainly alkanes (28%), aldehydes (16.27%) and unknown compounds (18%), with octadecanal being the most abundant compound (1094.91 ng in *H. m. malleti* compared to 1.40 ng in *H. t. florencía*). In *H. t. florencía*, the androconia bouquet was composed of alkanes (37%) and esters (14%), with syringaldehyde and heneicosane being the most abundant compounds (Figure S3.1).

The androconia composition of F_1 and backcross males were very similar to that of *H. t. florencía* but showed higher individual variation (Figure S3.2, Figure S3.3, Table S3.1). Consistently, the discriminant analysis revealed a discrete group formed by *H. t. florencía*, F_1 and backcross males, while *H. m. malleti* formed an independent cluster (Figure 4.3A; MANOVA $F_{(1,3)}=13.347$, $p<2e-16$). A post-hoc Tukey test showed that F_1 and backcross males differed significantly from *H. m. malleti* males ($p<0.01$; in both cases) but not from those of *H. t. florencía* ($p=0.912$ and $p=0.891$; respectively).

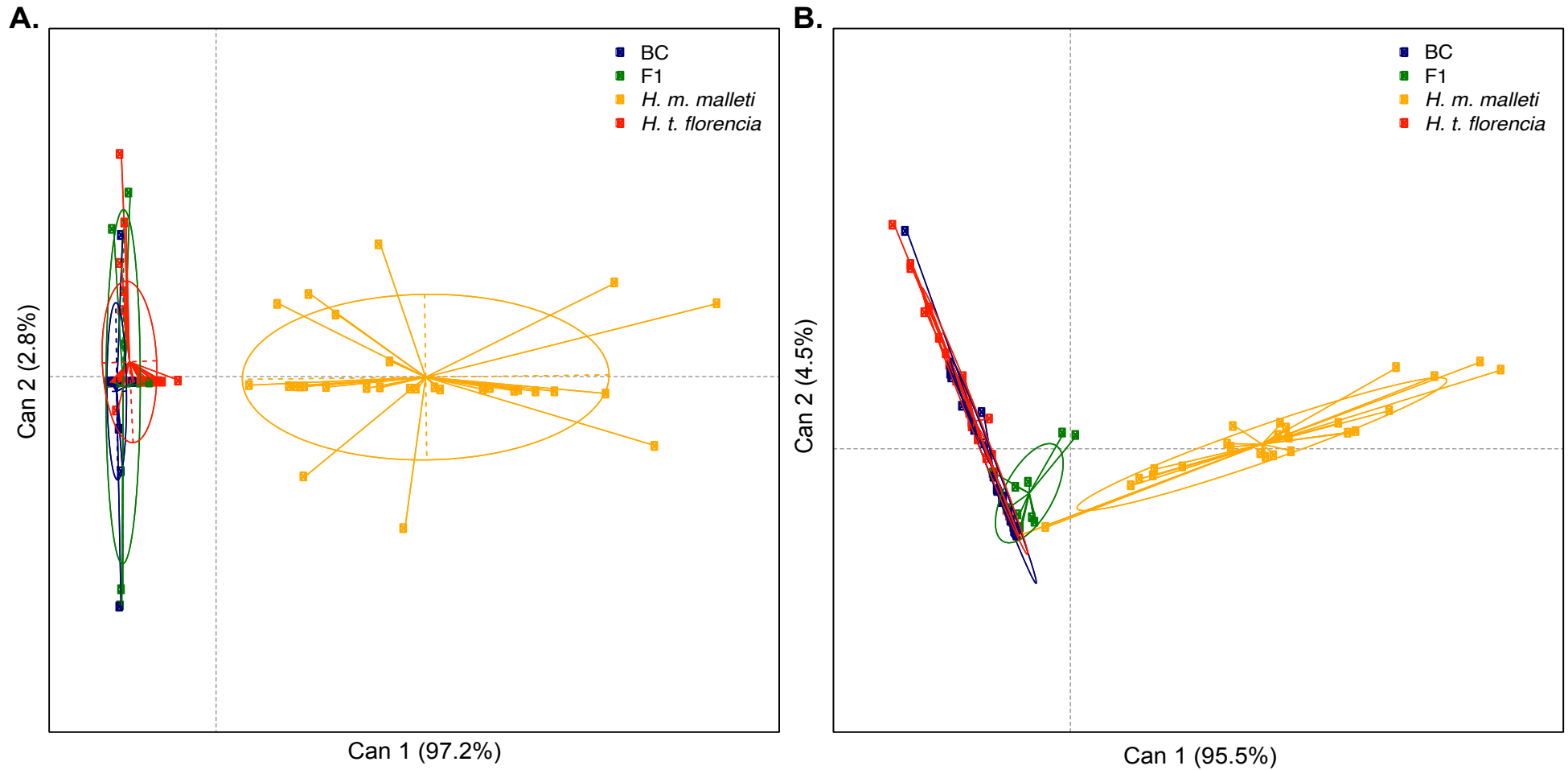


Figure 4.3. (A) Discriminant analysis based on individual composition of wing androconia extracts of males of *H. m. malleti*, *H. t. florencia*, F_1 and backcrosses (BC). (B) Discriminant analysis based on individual composition of abdominal gland extracts of males of *H. m. malleti*, *H. t. florencia*, F_1 and BC.

The abdominal gland bouquet of males was chemically more diverse than that of the androconia (Table S3.2). Alkanes, esters and lactones were the major compounds present in the abdominal gland bouquet of *H. m. malleti* and *H. t. florencía*. β -Ocimene and heneicosane largely dominated the abdominal gland bouquet of *H. m. malleti* males, while that of *H. t. florencía* was mainly composed of ethyl oleate, butyl oleate, isopropyl oleate and (Z)-9-octadecen-13-olide (Table S3.2, Figure S3.4). As in the androconia, the abdominal gland bouquet of F₁ and backcross males was more similar to *H. t. florencía* although some individuals had β -ocimene (Figure S3.5 and S3.6). The discriminant analysis revealed a discrete group composed of *H. t. florencía*, F₁ and backcross males which differentiate from a cluster formed only by *H. m. malleti* (Figure 4.3B; MANOVA $F_{(1,3)}=12.528$, $p<2e-16$). A post-hoc Tukey test showed that F₁ and backcross males differed significantly from *H. m. malleti* males ($p<0.01$; in both cases) but not from *H. t. florencía* males ($p=0.152$ and $p=0.777$; respectively). Interestingly, both species and their hybrids showed putative defensive secretions in their abdominal gland, namely 2-sec-butyl-3-methoxypyrazine in the abdominal gland extracts of *H. t. florencía*, F₁ and backcrosses and 2-isobutyl-3-methoxypyrazine in the abdominal gland extracts of *H. m. malleti*, F₁ and backcrosses (Table S3.2). These specific compounds are known to deter predators in the wood tiger moth (289), and in general, methoxypyrazines are compounds frequently found in the chemical defences of aposematic insects (128,290,291).

DISCUSSION

The importance of pre-zygotic reproductive barriers among the animal species is well known across the tree of life. In fact, the role they played in the diversification and maintenance of the species boundaries is well established (292). It is known, that closely related species often differ in traits important for mate choice in order to ensure assortative mating (12,43,52). These traits are predicted to be highly species-specific (293), such as the case of orchids bees, where *Euglossa dilemma* and *E. viridissima*, remain reproductively isolated according to their distinctive chemical signals (293).

Lepidoptera is the order that has the most information on volatiles involved in sexual recognition. For example, more than 2,000 sex pheromones have been identified in moths, and an additional eight in day flying butterflies (294,295). The function of sex chemicals in promoting species recognition and ensuring reproductive isolation in moths has been extensively demonstrated (296), while in butterflies, experimental evidence of such phenomena is less abundant (37,274,277,295). This is likely because researchers usually assumed that butterflies should mainly rely on mating systems based on visual signals suited to their diurnal habits.

In *Heliconius*, wing colour pattern has been identified as an important cue in speciation and mate preference (12,73,74,85,271). However, it has long been suggested that male pheromones play an important role that mediate species recognition (73,74,255), especially in cases where visual signals are compromised due to mimicry between closely related species. Previously, I demonstrated strong mating preferences between *H. t. florencía* and *H. m. malleti*; those preferences appear not to be related to colour pattern, but chemically mediated (Chapter 2). Consistent with those results, the androconia scale cells, as well as the abdominal glands of the two species had highly divergent profiles composed of differences in both the relative abundance and presence/absence of volatile chemicals. Therefore, this study along with previous findings show that assortative mating in *Heliconius* involves chemical signals (81,108).

In agreement with this hypothesis, I found that the composition of the male chemical bouquet of *H. m. malleti* and *H. t. florencía* is different, confirming the results previously reported in other studies that included a much lower sample size (108). The chemical signature of the two species is unique, not only in the androconia but also in the genitalia. This contrasts with the general pattern in Lepidoptera, where closely related species usually display similar chemical signatures, especially in pheromones (294). In particular, we identified octadecanal and β -ocimene as the main compounds in the androconia and genitalia bouquet of *H. m. malleti*, respectively. Even though octadecanal was also present in *H. t. florencía*, its abundance was much lower in this species. This agrees with recent findings, where octadecanal was found to be abundant in males of *H. m. rosina*

and almost absent in those of *H. c. chioneus* (295). Interestingly, octadecanal is electrophysiologically active in *Heliconius* (295) and β -ocimene is a known anti-aphrodisiac in the genus (36). Also, the most abundant compounds in the male androconia of *H. t. florencía* were syringaldehyde and heneicosane, known to act as long-range attraction molecules in multiple insect species (297–301). Similarly, the male bouquet of this species also contained phenylacetaldehyde and limonene, which act as copulating pheromones, hormones and defensive secretions in other Lepidoptera (298). The marked difference in chemical composition in the genital and wing extracts of males of *H. m. malleti* and *H. t. florencía* may be facilitated by the fact that these species have strong differences in larval host plant use (188), and larval diet is a known factor that affects adult pheromone composition in Lepidoptera (89,296).

Hybrid males (F_1 and backcrosses) had fewer and less abundant compounds in their blends compared with the parental species. Interestingly, both F_1 s and backcrosses had little octadecanal and some hybrid individuals even lacked it at all (just as pure *H. t. florencía* males do) suggesting that the low amount of this compound is heritable and possibly involving few major effect loci. This agrees with recent findings in *H. m. rosina* and *H. c. chioneus* that suggest a potential monogenic basis and dominant inheritance for octadecanal production (295). Similarly, hybrid females (F_1 and backcrosses) accepted better males of *H. t. florencía* more readily than those of *H. m. malleti*, and in some cases, we observed matings with the former species. This again suggests that female preference could be heritable and with a simple genetic basis. In fact, examples in orchid bees and *Drosophila* suggest that the genetics of chemical production and chemical preference have a simple genetics, where the same or few genes are involved (293,302). However, this data is not enough to draw definitive conclusions on the genetics of production of sexual chemical cues or female preference. To answer this question, it would be necessary to test the reciprocal F_1 (*H. m. malleti* mother \times *H. t. florencía* father) and backcrosses towards *H. m. malleti*. However, such crosses are extremely difficult to obtain, perhaps due to intrinsic behavioural sterility as reported for other Lepidoptera (303).

A previous QTL analysis in crosses between *H. melpomene* and *H. cydno* found no genetic linkage among colour pattern and/or colour preference loci with the locus underlying the production of octadecanal (295). This is unexpected if chemical cues play a major role in reproductive isolation, as theory predicts that traits under divergent selection and those that play a role in premating isolation should be tightly linked in order to facilitate speciation (85,304). In contrast, in cases where natural selection promotes mimicry convergence due to secondary introgression thus compromising visual recognition of conspecific mates, reproductive isolation should weaken possibly leading to species collapse (254,305). Yet, the total reproductive isolation between *H. m. malleti* and *H. t. florencía* is ~97% (254), implying that chemical barriers, along with other barriers such as habitat specialisation and host plant use, are sufficient to ensure species integrity. Our hybrid broods suggest that both sexual chemical production and preference for them likely have a simple genetic basis, and if they happen to be physically linked in the genome as in the case of visual cues and visual preference (85), then reproductive isolation is easily achieved and maintained.

Overall, this study corroborates the existence of chemical differences between male chemical signatures in a pair of closely related and mimetic species where wing phenotype is not a recognition trait. These chemical differences are used by females to effectively choose mates confirming that male sex compounds are necessary to mediate premating reproductive isolation between *H. m. malleti* and *H. t. florencía*. Also, my results suggest that both male chemical production and female preference in *Heliconius* are heritable traits with a simple genetic basis. In fact, recent studies have pinpointed candidate regions implicated in the production of male pheromones in *Heliconius* (295). However, to date, the genetic basis controlling female assortative mating behaviours remain largely unknown. In *Heliconius*, females exert choice based on multimodal signals, especially visual and olfactory cues (306). Therefore, in the absence of wing colour pattern divergence, the mimetic pair composed by *H. m. malleti* and *H. t. florencía* provides an excellent natural system to investigate the genetics of female preference based on pheromones and understand how species integrity is maintained in the presence of gene flow. It is possible that sexual signals and responses to those signals

involve the same gene, such as in the case of *Drosophila melanogaster* (307), or that both traits are controlled by independent loci, such as in *Heliothis* (308).

CONCLUSIONS

In this thesis, first I evaluated fine-scale morphological differences in wing size, shape, and colour pattern variation to investigate the degree of phenotypic resemblance between co-mimic species in multiple *Heliconius* mimetic rings. I found that wing size and shape do not contribute to mimicry as these traits vary between members of the same mimicry ring. These results suggest that natural selection pressures other than mimicry such as phylogenetic closeness, variation in life traits and sexual selection influence these traits. Colour phenotype is the main component of mimicry in *Heliconius*, but the mimicry in some phenotypes (i.e., rings) is better tuned than in others. For instance, the mimicry in red-banded phenotypes between subspecies of *H. erato* and *H. melpomene* is very accurate, indicating that these two species are good co-mimics across their distribution. In contrast, the mimicry in dennis-ray phenotypes is less precise and the colour elements that compose it significantly vary in terms of size and position, both dorsally and ventrally. This suggests the existence of multiple adaptive peaks across the mimicry landscape in the Amazon. Similarly, the mimicry in yellow/white phenotypes was also less accurate between co-mimics, which is especially due to variation in the FW band and the submarginal HW band, both dorsally and ventrally. The recovery of species typically regarded as the "model" (such as *C. ithrana* and Ithomiini butterflies) as highly divergent entities is consistent with mimicry being the result of phenotypic advergence. However, this result also may be explained by phylogenetic divergence. Finally, the number of species participating in a ring influences the extent of similarity among the members, with fewer participating species resulting in a much more similar phenotype. This does not mean that the signal is not as effective as the participation of multiple species may lead to its relaxation due to predators being able to generalize it. Overall, my results suggest that there is no perfect convergence in the mimicry rings of *Heliconius*. However, other aspects of mimicry such as geography, the community of predators and how they

perceive these signals are equally important. In fact, this is consistent with the idea that adaptation by mimicry is a complex and dynamic process affected by more than a single factor.

In strict terms, Müllerian mimicry rings are composed by phylogenetically distant species, where the convergence to colour pattern does not compromise reproductive isolation. In consequence, sympatric and closely related species usually exhibit different phenotypes, thus ensuring their reproductive isolation. However, the closely related pair *H. m. malleti* and *H. t. florencia* bear the same dennis-ray colour pattern and occur in the same geographical region, which may compromise their species integrity. In agreement with these species being nearly identical in terms of wing phenotype, I found that altering their colour pattern has no effect on the preference of females for mates, suggesting that wing phenotype is not the cue ensuring partner recognition. Instead, I found that androconial chemical compounds are important during courtship and subsequent mating. As such, females of both species discriminate against males with their androconia experimentally blocked and they accept better males perfumed with a conspecific scent, suggesting that the composition of those blends is an important trait for species recognition. In agreement with these results, the androconial and abdominal bouquets of males are highly divergent between the two species. Interspecific crosses, the composition of their androconial and abdominal bouquets and their preference behaviour suggest that both the production of chemical cues as well as the preference for them are heritable and possibly involve few major effect loci. Overall, this study confirms chemical differences in a pair of closely related and mimetic species where colour pattern seems not to be involved in reproductive isolation. Moreover, female choice is based on these chemical signals, demonstrating that *Heliconius* females are actively involved in mating decisions.

REFERENCES

1. Córdoba-Aguilar A, González-Tokman D, González-Santoyo I. Insect behavior: from mechanisms to ecological and evolutionary consequences. First Edit. Oxford, UK: Oxford University Press; 2018. 414 p.
2. Uetz GW, Roberts JA, Taylor PW. Multimodal communication and mate choice in wolf spiders: female response to multimodal versus unimodal signals. *Anim Behav* [Internet]. 2009;78:299–305. Available from: <http://dx.doi.org/10.1016/j.anbehav.2009.04.023>
3. Candolin U. The use of multiple cues in mate choice. *Biol Rev Camb Philos Soc* [Internet]. 2003;78:575–95. Available from: <http://www.ncbi.nlm.nih.gov/pubmed/14700392>
4. Chenoweth SF, Blows MW. Dissecting the complex genetic basis of mate choice. *Nat Rev Genet* [Internet]. 2006;7(9):681–92. Available from: <http://www.ncbi.nlm.nih.gov/pubmed/16921346>
5. Bímová B, Albrecht T, Macholán M, Piálek J. Signalling components of the house mouse mate recognition system. *Behav Processes*. 2009;80(1):20–7.
6. Wyatt TD. Pheromones and animal behaviour: communication by smell and taste. Cambridge: Cambridge University Press; 2003.
7. Greenspan RJ, Ferveur JF. Courtship in *Drosophila*. *Annu Rev Genet*. 2000;34:205–32.
8. Conner WE. “Un chant d’appel amoureux”: Acoustic communication in moths. *J Exp Biol*. 1999;202(13):1711–23.
9. Weller SJ, Jacobson NL, Conner WE. The evolution of chemical defences and mating systems in tiger moths (Lepidoptera: Arctiidae). *Biol J Linn Soc*. 1999;68(4):557–78.
10. Boppré M. Chemical communication, plant relationships, and mimicry in the evolution of Danaid butterflies. *Entomol Exp Appl*. 1978;24(3):64–77.
11. Eisner T, Meinwald J. The chemistry of sexual selection. *Proc Natl Acad Sci U S A*. 1995;92:50–5.
12. Jiggins CD, Naisbit RE, Coe RL, Mallet J. Reproductive isolation caused by colour pattern mimicry. *Nature*. 2001;411:302–305.
13. Nosil P, Crespi BJ, Sandoval CP. Host-plant adaptation drives the parallel evolution of reproductive isolation. *Nature*. 2002;417(6887):440–3.
14. Estrada C, Jiggins CD. Interspecific sexual attraction because of convergence in warning colouration: Is there a conflict between natural and sexual selection in mimetic species? *J Evol Biol*. 2008;21:749–60.
15. Buellesbach J, Vetter SG, Schmitt T. Differences in the reliance on cuticular hydrocarbons as sexual signaling and species discrimination cues in parasitoid wasps. *Front Zool*. 2018;15(22):1–11.
16. Dalbosco Dell’Aglío D, Troscianko J, McMillan WO, Stevens M, Jiggins CD. The appearance of mimetic *Heliconius* butterflies to predators and conspecifics. *Evolution (N Y)*. 2018;72(10):2156–66.
17. Finkbeiner SD, Briscoe AD, Reed RD. Warning signals are seductive: Relative contributions of color and pattern to predator avoidance and mate attraction in *Heliconius* butterflies. *Evolution (N Y)*. 2014;68(12):3410–20.
18. Endler. Natural selection on color patterns in *Poecilia reticulata*. *Evolution (N Y)*. 1980;34:76–91.
19. Ruxton GD, Sherratt TN, Speed MP. Avoiding attack: The evolutionary ecology of crypsis, warning signals and mimicry. Vol. 17, Oxford biology. New York: Oxford University Press Inc.; 2004. 249 p.
20. Sherratt TN. The evolution of Müllerian mimicry. *Naturwissenschaften*. 2008;95:681–95.
21. Kapan DD. Three-butterfly system provides a field test of Müllerian mimicry. 2001;409:338–40.
22. Elias M, Gompert Z, Jiggins C, Willmott K. Mutualistic interactions drive ecological niche convergence in a diverse butterfly community. *PLoS Biol* [Internet]. 2008;6(12):2642–9. Available from: <http://journals.plos.org/plosbiology/article?id=10.1371/journal.pbio.0060300>
23. Joron M. Polymorphic mimicry, microhabitat use, and sex-specific behaviour. *J Evol Biol*. 2005;18(3):547–56.
24. Rojas B, Burdfield-Steel E, De Pasqual C, Gordon S, Hernández L, Mappes J, et al. Multimodal aposematic signals and their emerging role in mate attraction. *Front Ecol Evol*. 2018;6(93).
25. De Bruyne M, Baker TC. Odor detection in insects: Volatile codes. *J Chem Ecol*. 2008;34(7):882–97.

26. Missbach C, Dweck HKM, Vogel H, Vilcinskas A, Stensmyr MC, Hansson BS, et al. Evolution of insect olfactory receptors. *Elife*. 2014;3(e02115):1–22.
27. Greenfield M. Signalers and receivers: mechanisms and evolution of arthropod communication. New York, USA: Oxford University Press; 2002.
28. Ehman KD, Scott ME. Urinary odour preferences of MHC congenic female mice, *Mus domesticus*: Implications for kin recognition and detection of parasitized males. *Anim Behav*. 2001;62(4):781–9.
29. Kavaliers M, Colwell DD, Braun WJ, Choleris E. Brief exposure to the odour of a parasitized male alters the subsequent mate odour responses of female mice. *Anim Behav*. 2003;65(1):59–68.
30. Kavaliers M, Choleris E, Ågmo A, Pfaff DW. Olfactory-mediated parasite recognition and avoidance: Linking genes to behavior. *Horm Behav*. 2004;46(3):272–83.
31. Kavaliers M, Choleris E, Ågmo A, Muglia LJ, Ogawa S, Pfaff DW. Involvement of the oxytocin gene in the recognition and avoidance of parasitized males by female mice. *Anim Behav*. 2005;70(3):693–702.
32. Rich TJ, Hurst JL. The competing countermarks hypothesis: Reliable assessment of competitive ability by potential mates. *Anim Behav*. 1999;58(5):1027–37.
33. Beynon RJ, Hurst JL. Multiple roles of major urinary proteins in the house mouse, *Mus domesticus*. *Biochem Soc Trans*. 2003;31(1):142–6.
34. Czaczkes TJ, Grüter C, Ratnieks FLW. Trail pheromones: An integrative view of their role in social insect colony organization. *Annu Rev Entomol*. 2015;60(1):581–99.
35. Estrada C, Schulz S, Yildizhan S, Gilbert LE. Sexual selection drives the evolution of antiaphrodisiac pheromones in butterflies. *Evolution (N Y)*. 2011;65(10):2843–54.
36. Schulz S, Estrada C, Yildizhan S, Boppré M, Gilbert LE. An antiaphrodisiac in *Heliconius melpomene* butterflies. *J Chem Ecol*. 2008;34(1):82–93.
37. Nieberding CM, de Vos H, Schneider M V., Lassance J-M, Estramil N, Andersson J, et al. The male sex pheromone of the butterfly *Bicyclus anynana*: Towards an evolutionary analysis. *PLoS One*. 2008;3(7):e2751.
38. Nieberding CM, Fischer K, Saastamoinen M, Allen CE, Wallin EA, Hedenström E, et al. Cracking the olfactory code of a butterfly: The scent of ageing. *Ecol Lett*. 2012;15(5):415–24.
39. Dussourd DE, Harvis CA, Meinwald J, Eisner T. Pheromonal advertisement of a nuptial gift by a male moth (*Utetheisa ornatrix*). *Proc Natl Acad Sci U S A* [Internet]. 1991;88:9224–7. Available from: <http://www.pnas.org/content/88/20/9224>
40. Shine R, Phillips B, Wayne HL, LeMaster MP, Mason RT. Chemosensory cues allow courting male garter snakes to assess body length and body condition of potential mates. *Behav Ecol*. 2003;54:162–6.
41. Moore PJ, Reagan-Wallin NL, Haynes KF, Moore AJ. Odour conveys status on cockroaches. *Nature* [Internet]. 1997;25–6. Available from: <http://www.nature.com/nature/journal/v389/n6646/full/389025a0.html>
42. Smith BH. Recognition of female kin by male bees through olfactory signals. *Proc Natl Acad Sci USA* [Internet]. 1983;80:4551–4553. Available from: <http://www.pnas.org/content/80/14/4551.full.pdf>
43. Mas F, Jallon J-M. Sexual isolation and cuticular hydrocarbon differences between *Drosophila santomea* and *Drosophila yakuba*. *J Chem Ecol*. 2005;31(11):2747–52.
44. Pardy JA, Rundle HD, Bernards MA, Moehring AJ. The genetic basis of female pheromone differences between *Drosophila melanogaster* and *D. simulans*. *Heredity (Edinb)* [Internet]. 2018;1. Available from: <http://www.nature.com/articles/s41437-018-0080-3>
45. Linn C, Feder JL, Nojima S, Dambroski HR, Berlocher SH, Roelofs W. Fruit odor discrimination and sympatric host race formation in *Rhagoletis*. *Proc Natl Acad Sci U S A*. 2003;100(20):11490–3.
46. Olsson SB, Linn CEJ, Feder JL, Michel A, Dambroski HR, Berlocher SH, et al. Comparing peripheral olfactory coding with host preference in the *Rhagoletis* species complex. *Chem Senses*. 2009;34:37–48.
47. Tregenza T, Pritchard VL, Butlin RK. Patterns of trait divergence between populations of the meadow grasshopper, *Chorthippus parallelus*. *Evolution (N Y)*. 2000;54(2):574–85.
48. Schwander T, Arbuthnott D, Gries R, Gries G, Nosil P, Crespi BJ. Hydrocarbon divergence and reproductive isolation in *Timema* stick insects. *BMC Evol Biol* [Internet]. 2013;13. Available from: *BMC Evolutionary Biology*
49. Liu Y, Hu Y, Bi J, Kong X, Long G, Zheng Y, et al. Odorant-binding proteins involved in sex pheromone and host-plant recognition of the sugarcane borer *Chilo infuscatellus* (Lepidoptera: Crambidae). *Pest Manag Sci*. 2020;10.1002/ps.5961.
50. Pelozuelo L, Malosse C, Genestier G, Guenego H, Frerot B. Host-plant specialization in pheromone strains of

- the European corn borer *Ostrinia nubilalis* in France. *J Chem Ecol.* 2004;30(2):335–52.
51. Ômura H, Yotsuzuka S. Male-specific epicuticular compounds of the sulfur butterfly *Colias erate poliographus* (Lepidoptera: Pieridae). *Appl Entomol Zool.* 2015;
 52. Saveer AM, Becher PG, Birgersson G, Hansson BS, Witzgall P, Bengtsson M. Mate recognition and reproductive isolation in the sibling species *Spodoptera littoralis* and *Spodoptera litura*. *Front Ecol Evol* [Internet]. 2014;2(18):1–7. Available from: <http://journal.frontiersin.org/article/10.3389/fevo.2014.00018/abstract>
 53. Sheck AL, Groot AT, Ward CM, Gemeno C, Wang J, Brownie C, et al. Genetics of sex pheromone blend differences between *Heliothis virescens* and *Heliothis subflexa*: A chromosome mapping approach. *J Evol Biol.* 2006;19(2):600–17.
 54. Marco A, Chivers DP, Kiesecker JM, Blaustein AR. Mate choice by chemical cues in Western Redback (*Plethodon vehiculum*) and Dunn's (*P. dunni*) salamanders. *Ethology* [Internet]. 1998;104:781–8. Available from: <http://onlinelibrary.wiley.com/doi/10.1111/j.1439-0310.1998.tb00111.x/abstract>
 55. Martín J, López P. Chemoreception, symmetry and mate choice in lizards. *Proc R Soc B Biol Sci* [Internet]. 2000;267:1265–9. Available from: <http://rspb.royalsocietypublishing.org/content/267/1450/1265>
 56. Novotny MV. Pheromones, binding proteins and receptor responses in rodents. *Biochem Soc.* 2003;117–22.
 57. Wyatt TD. Pheromones and animal behavior: chemical signals and signatures. Cambridge: Cambridge University Press; 2014.
 58. Phelan PL, Baker TC. Evolution of male pheromones in moths: reproductive isolation through sexual selection? *Science* (80-). 1987;235:205–7.
 59. Löfstedt C, Herrebut WM, Menken SBJ. Sex pheromones and their potential role in the evolution of reproductive isolation in small ermine moths (Yponomeutidae). *Chemoecology* [Internet]. 1991;2:20–8. Available from: <http://link.springer.com/article/10.1007/BF01240662> VN - readcube.com
 60. Costanzo K, Monteiro A. A The use of chemical and visual cues in female choice in the butterfly *Bicyclus anynana*. *Proc R Soc B Biol Sci.* 2007;274:845–51.
 61. Bigiani A, Mucignat-Caretta C, Montani G, Tirindelli R. Pheromone reception in mammals. *Rev Physiol Biochem Pharmacol.* 2005;155:1–35.
 62. Glover TJ, Tang XH, Roelofs WL. Sex-pheromone blend discrimination by male moths from E and Z-strains of European corn-borer. *J Chem Ecol.* 1987;13(1):143–51.
 63. Eltz T, Zimmermann Y, Pfeiffer C, Ramirez Pech J, Twele R, Francke W, et al. An olfactory shift is associated with male perfume differentiation and species divergence in orchid bees. *Curr Biol* [Internet]. 2008;18:1844–8. Available from: <http://dx.doi.org/10.1016/j.cub.2008.10.049>
 64. Symonds MRE, Elgar MA. The evolution of pheromonal diversity. *Trends Ecol Evol.* 2008;23:220–228.
 65. Tanigaki T, Yamaoka R, Sota T. The role of cuticular hydrocarbons in mating and conspecific recognition in the closely related Longicorn beetles *Pidonia grallatrix* and *P. takechii*. *Zoolog Sci.* 2007;24(1):39–45.
 66. Geiselhardt S, Otte T, Hilker M. Looking for a similar partner: host plants shape mating preferences of herbivorous insects by altering their contact pheromones. *Ecol Lett.* 2012;15(9):971–7.
 67. Peterson MA, Dobler S, Larson EL, Juárez D, Schlarbaum T, Monsen KJ, et al. Profiles of cuticular hydrocarbons mediate male mate choice and sexual isolation between hybridising *Chrysochus* (Coleoptera: Chrysomelidae). *Chemoecology.* 2007;17(2):87–96.
 68. Xue HJ, Wei JN, Magalhães S, Zhang B, Song KQ, Liu J, et al. Contact pheromones of 2 sympatric beetles are modified by the host plant and affect mate choice. *Behav Ecol.* 2016;27(3):895–902.
 69. South A, LeVan K, Leombruni L, Orians CM, Lewis SM. Examining the role of cuticular hydrocarbons in Firefly species recognition. *Ethology.* 2008;114(9):916–24.
 70. Hay-Roe MM, Lamas G, Nation JL. Pre- and postzygotic isolation and Haldane rule effects in reciprocal crosses of *Danaus erippus* and *Danaus plexippus* (Lepidoptera: Danainae), supported by differentiation of cuticular hydrocarbons, establish their status as separate species. *Biol J Linn Soc.* 2007;91(3):445–53.
 71. Syvertsen TC, Jackson LL, Blomquist GJ, Vinson SB. Alkadienes mediating courtship in the parasitoid *Cardiochiles nigriceps* (Hymenoptera: Braconidae). *J Chem Ecol.* 1995;21(12):1971–89.
 72. Howard RW. Comparative analysis of cuticular hydrocarbons from the Ectoparasitoids *Cephalonomia waterstoni* and *Laelius utilis* (Hymenoptera: Bethyilidae) and their respective hosts, *Cryptolestes ferrugineus* (Coleoptera: Cucujidae) and *Trogoderma*. *Ann Entomol Soc Am.* 1992;85(3):317–25.
 73. Merrill RM, Dasmahapatra KK, Davey JW, Dell'Aglio DD, Hanly JJ, Huber B, et al. The diversification of

- Heliconius* butterflies: What have we learned in 150 years? J Evol Biol. 2015;28(8):1417–38.
74. Jiggins CD. Ecological speciation in mimetic butterflies. Bioscience [Internet]. 2008;58(6):541–8. Available from: <http://bioscience.oxfordjournals.org/cgi/doi/10.1641/B580610>
 75. Mérot C. Speciation in *Heliconius* butterflies: the balance between mimicry convergence and ecological divergence. Muséum National d’Histoire Naturelle, Paris.; 2014.
 76. Brower LP, Brower JVZ, Collins CT. Experimental studies of mimicry. 7. Relative palatability and Mullerian mimicry among neotropical butterflies of the subfamily Heliconiinae. Zool Sci Contrib New York Zool Soc. 1963;48(7):65–84.
 77. Chai P, Srygley RB. Predation and the flight, morphology, and temperature of Neotropical rain-forest butterflies. Am Nat. 1990;135(6):748–65.
 78. Darragh K. Pheromones in *Heliconius* butterflies: Chemical ecology, genetics, and behaviour. University of Cambridge; 2019.
 79. Arias M, Davey JW, Martin S, Jiggins C, Nadeau N, Joron M, et al. How do predators generalize warning signals in simple and complex prey communities? Insights from a videogame. Proc R Soc B Biol Sci. 2020;287:e20200014.
 80. Merrill RM, Van Schooten B, Scott JA, Jiggins CD. Pervasive genetic associations between traits causing reproductive isolation in *Heliconius* butterflies. Proc R Soc B. 2011;278:511–8.
 81. Darragh K, Vanjari S, Mann F, González-Rojas MF, Morrison CR, Salazar C, et al. Male sex pheromone components in *Heliconius* butterflies released by the androconia affect female choice. PeerJ [Internet]. 2017;5:e3953. Available from: <https://peerj.com/articles/3953>
 82. Rutowski R. The evolution of male mate-locating behavior in butterflies. Am Nat. 1991;138(5):1121–39.
 83. Mavárez J, Salazar CA, Bermingham E, Salcedo C, Jiggins CD, Linares M. Speciation by hybridization in *Heliconius* butterflies. Nature. 2006;441(7095):868–71.
 84. Jiggins CD, Estrada C, Rodrigues A. Mimicry and the evolution of premating isolation in *Heliconius melpomene* Linnaeus. J Evol Biol. 2004;17:680–91.
 85. Merrill RM, Rastas P, Martin SH, Melo MC, Barker S, Davey J, et al. Genetic dissection of assortative mating behavior. PLoS Biol. 2019;17(2):1–21.
 86. Boppré M. Chemically mediated interactions between butterflies. The biology of butterflies. Vane-Wright R, Ackery P, editors. Academic Press, London; 1984. 259–275 p.
 87. Pinheiro de Castro ÉC, Zagrobely M, Zurano JP, Zikan Cardoso M, Feyereisen R, Bak S. Sequestration and biosynthesis of cyanogenic glucosides in passion vine butterflies and consequences for the diversification of their host plants. Ecol Evol. 2019;9:5079–93.
 88. Sculfort O, de Castro ECP, Kozak KM, Bak S, Elias M, Nay B, et al. Variation of chemical compounds in wild Heliconiini reveals ecological factors involved in the evolution of chemical defenses in mimetic butterflies. Ecol Evol. 2020;(November 2019):1–18.
 89. Darragh K, Byers KJR, Merrill RM, McMillan WO, Schulz S, Jiggins CD. Male pheromone composition depends on larval but not adult diet in *Heliconius melpomene*. Ecol Entomol. 2019;44(3):397–405.
 90. de Castro ÉCP, Musgrove J, Bak S, McMillan WO, Jiggins CD. Phenotypic plasticity in chemical defence allows butterflies to diversify host use strategies. bioRxiv Prepr. 2020;
 91. Langham GM. Specialized avian predators repeatedly attack novel color morphs of *Heliconius* butterflies. Evolution (N Y). 2004;58(12):2783–7.
 92. Finkbeiner SD, Fishman DA, Osorio D, Briscoe AD. Ultraviolet and yellow reflectance but not fluorescence is important for visual discrimination of conspecifics by *Heliconius erato*. J Exp Biol [Internet]. 2017;220(7):1267–76. Available from: <http://jeb.biologists.org/lookup/doi/10.1242/jeb.153593>
 93. Mallet J, Barton NH. Strong natural selection in a warning-color hybrid zone. Evolution (N Y). 1989;43(2):421–31.
 94. Kapan DD. Divergent natural selection and Müllerian mimicry in polymorphic *Heliconius cydno* (Lepidoptera:Nymphalidae). The University of British Columbia; 1998.
 95. Kronforst MR, Papa R. The functional basis of wing patterning in *Heliconius* butterflies: The molecules behind mimicry. Genetics. 2015;200:1–19.
 96. Linares M. The ghost of mimicry past: laboratory reconstitution of an extinct butterfly “race.” Heredity (Edinb). 1997;78:628–35.
 97. Mallet J. Shift happens! Shifting balance and the evolution of diversity in warning colour and mimicry. Ecol

- Entomol. 2010;35(SUPPL. 1):90–104.
98. Fisher R. The genetical theory of natural selection. Oxford, U.K.: Oxford Univ. Press; 1930.
 99. Chouteau M, Angers B. Wright's shifting balance theory and the diversification of aposematic signals. *PLoS One*. 2012;7(3):e34028.
 100. Márquez R, Linderoth TP, Mejía-Vargas D, Nielsen R, Amézquita A, Kronforst MR. Divergence, gene flow, and the origin of leapfrog geographic distributions: The history of colour pattern variation in *Phyllobates* poison-dart frogs. *Mol Ecol*. 2020;29:3702–19.
 101. Chouteau M, Laurens V, Piron-Prunier F, Joron M. Polymorphism at a mimicry supergene maintained by opposing frequency-dependent selection pressures. *Proc Natl Acad Sci [Internet]*. 2017;114(31):8325–9. Available from: <http://www.pnas.org/lookup/doi/10.1073/pnas.1702482114>
 102. Jamie GA, Meier JI. The persistence of polymorphisms across species radiations. *Trends Ecol Evol [Internet]*. 2020;35(9):795–808. Available from: <https://doi.org/10.1016/j.tree.2020.04.007>
 103. Nadeau NJ. Genes controlling mimetic colour pattern variation in butterflies. *Curr Opin Insect Sci [Internet]*. 2016;17:24–31. Available from: <http://dx.doi.org/10.1016/j.cois.2016.05.013>
 104. Lewis JJ, Reed RD. Genome-wide regulatory adaptation shapes population-level genomic landscapes in *Heliconius*. *Mol Biol Evol*. 2018;36(1):159–73.
 105. Orteu A, Jiggins CD. The genomics of coloration provides insights into adaptive evolution. *Nat Rev Genet [Internet]*. 2020;21(8):461–75. Available from: <http://dx.doi.org/10.1038/s41576-020-0234-z>
 106. Morris J, Hanly JJ, Martin SH, Van Belleghem SM, Salazar CA, Jiggins CD, et al. Deep convergence, shared ancestry, and evolutionary novelty in the genetic architecture of *Heliconius* mimicry. *Genetics*. 2020;216:765–80.
 107. Merrill RM, Wallbank RWR, Bull V, Salazar PCA, Mallet J, Stevens M, et al. Disruptive ecological selection on a mating cue. *Proc R Soc B*. 2012;279:4907–13.
 108. Mérot C, Frérot B, Leppik E, Joron M. Beyond magic traits: Multimodal mating cues in *Heliconius* butterflies. *Evolution (N Y)*. 2015;69(11):2891–904.
 109. Rossi M, Hausmann AE, Thurman TJ, Montgomery SH, Papa R, Jiggins CD, et al. Visual mate preference evolution during butterfly speciation is linked to neural processing genes. *Nat Commun [Internet]*. 2020;11(4763). Available from: <http://dx.doi.org/10.1038/s41467-020-18609-z>
 110. Armstrong EA. The ethology of bird display and behavior. New York, NY: Dover Publications.; 1965.
 111. Gilliard ET. Birds of paradise and bower birds. Press NH, editor. Garden City, NY; 1969.
 112. Jones TM, Hamilton JGC. A role for pheromones in mate choice in a lekking sandfly. *Anim Behav*. 1998;56:891–8.
 113. Kotiaho JS. Testing the assumptions of conditional handicap theory: costs and condition dependence of a sexually selected trait. *Behav Ecol Sociobiol*. 2000;48:188–94.
 114. Milinski M, Bakker TCM. Female sticklebacks use male coloration in mate choice and hence avoid parasitized males. *Nature*. 1990;344:330–3.
 115. Pivnick KA, Lavoie-Dornik J, McNeil J. The role of the androconia in the mating behaviour of the European skipper, *Thymelicus lineola*, and evidence for a male sex pheromone. *Physiol Entomol*. 1992;17(October):260–8.
 116. Snedden WA, Sakaluk SK. Acoustic signalling and its relation to male mating success in sagebrush crickets. *Anim Behav*. 1992;44(4):633–9.
 117. Wing L. Drumming flight in the blue grouse and courtship characters of the Tetraonidae. *Condor*. 1946;48:154–7.
 118. Wertheim B, van Baalen E-JA, Dicke M, Vet LEM. Pheromone mediated aggregation in nonsocial arthropods: An evolutionary ecological perspective. *Annu Rev Entomol*. 2005;50(1):321–46.
 119. Schiestl FP. The evolution of floral scent and insect chemical communication. *Ecol Lett*. 2010;13(5):643–56.
 120. Ali MF, Morgan ED. Chemical communication in insect communities: a guide to insect pheromones with special emphasis on social insects. *Biol Rev*. 1990;65:227–247.
 121. Butenandt VA, Beckmann R, Stamm D, Hecker E. Über den sexual-lockstoff des seidenspinners *Bombyx mori*. Reindarstellung und Konstitution. *Z Naturforsch*. 1959;14b:283–4.
 122. Löfstedt C. Moth pheromone genetics and evolution. *Philos Trans Biol Sci*. 1993;340(1292):167–77.
 123. Smadja C, Butlin RK. On the scent of speciation: the chemosensory system and its role in premating isolation. *Heredity (Edinb)*. 2009;102:77–97.

124. Wicker-Thomas C. Evolution of insect pheromones and their role in reproductive isolation and speciation. *Ann la Soc Entomol Fr* [Internet]. 2011;47(1–2):55–62. Available from: <http://www.scopus.com/inward/record.url?eid=2-s2.0-80053962352&partnerID=tZOtx3y1>
125. Grillet M, Everaerts C, Houot B, Ritchie MG, Cobb M, Ferveur JF. Incipient speciation in *Drosophila melanogaster* involves chemical signals. *Sci Rep*. 2012;2(i):1–11.
126. Vane-Wright RI, Boppré M. Visual and chemical signalling in butterflies: functional and phylogenetic perspectives. *Philos Trans R Soc L B Biol Sci*. 1993;340:197–205.
127. Jiggins CD. *The Ecology and Evolution of Heliconius Butterflies*. Oxford University Press; 2017. 330 p.
128. Rothschild M, Moore BP, Brown W V. Pyrazines as warning odour components in the Monarch butterfly, *Danaus plexippus*, and in moth of the genera *Zygaena* and *Amata* (Lepidoptera). *Biol J Linn Soc*. 1984;23:375–380.
129. Müller F. The scent-scales of the male “Maracujá butterflies.” In: Longstaff GB, editor. *Butterfly hunting in many lands*. New York, NY: Longmans, Green & Co; 1912. p. 655–659.
130. Eltringham H. On the abdominal glands in *Heliconius* (Lepidoptera). *Trans R Entomol Soc Lond*. 1925;73:269–275.
131. Barth R. Os órgãos odoríferos masculinos de alguns Heliconiinae do Brasil. *Mem Inst Oswaldo Cruz*. 1952;50:335–86.
132. Emsley M. A morphological study of imagine Heliconiinae (Lep.: Nymphalidae) with a consideration of the evolutionary relationships within the group. *Zool N Y*. 1963;48:85–130.
133. Klein AL, de Araújo AM. Courtship behavior of *Heliconius erato phyllis* (Lepidoptera, Nymphalidae) towards virgin and mated females: Conflict between attraction and repulsion signals? *J Ethol*. 2010;28(3):409–20.
134. Crane J. Imaginal behaviour of a Trinidad butterfly, *Heliconius erato hydara* Hewitson, with special reference to the social use of color. *Zool N Y*. 1955;40:167–196.
135. Estrada C, Yildizhan S, Schulz S, Gilbert LE. Sex-specific chemical cues from immatures facilitate the evolution of mate guarding in *Heliconius* butterflies. *Proc R Soc B Biol Sci* [Internet]. 2010;277:407–13. Available from: <http://rspb.royalsocietypublishing.org/cgi/doi/10.1098/rspb.2009.1476>
136. Gilbert LE. Postmating female odor in *Heliconius* butterflies: A male-contributed antiaphrodisia? *Science* (80-). 1976;193(4251):419–20.
137. Malouines C. Counter-perfume: using pheromones to prevent female remating. *Biol Rev*. 2016;92(3):1570–81.
138. Mann F, Vanjari S, Rosser N, Mann S, Dasmahapatra KK, Corbin C, et al. The scent chemistry of *Heliconius* wing androconia. *J Chem Ecol*. 2017;43(9):843–57.
139. Liénard MA, Wang H-L, Lassance J-M, Löfstedt C. Sex pheromone biosynthetic pathways are conserved between moths and the butterfly *Bicyclus anynana*. *Nat Commun* [Internet]. 2014;5:3957. Available from: <http://www.pubmedcentral.nih.gov/articlerender.fcgi?artid=4050330&tool=pmcentrez&rendertype=abstract>
140. Yildizhan S, Van Loon J, Sramkova A, Ayasse M, Arsene C, ten Broeke C, et al. Aphrodisiac pheromones from the wings of the small cabbage white and large cabbage white butterflies, *Pieris rapae* and *Pieris brassicae*. *ChemBioChem*. 2009;10:1666–77.
141. Andersson J, Borg-Karlson A-K, Vongvanich N, Wiklund C. Male sex pheromone release and female mate choice in a butterfly. *J Exp Biol*. 2007;210:964–70.
142. Nishida R, Schulz S, Kim CS, Fukami H, Kuwahara Y, Honda K, et al. Male sex pheromone of a giant danaine butterfly, *Idea leuconoe*. *J Chem Ecol* [Internet]. 1996;22(5):949–72. Available from: <http://dx.doi.org/10.1007/BF02029947>
143. Zhang YN, Xia YH, Zhu JY, Li SY, Dong SL. Putative pathway of sex pheromone biosynthesis and degradation by expression patterns of genes identified from female pheromone gland and adult antenna of *Sesamia inferens* (Walker). *J Chem Ecol*. 2014;40:439–51.
144. He P, Zhang Y-F, Hong D-Y, Wang J, Wang X-L, Zuo L-H, et al. A reference gene set for sex pheromone biosynthesis and degradation genes from the diamondback moth, *Plutella xylostella*, based on genome and transcriptome digital gene expression analyses. *BMC Genomics* [Internet]. 2017;18(219). Available from: <http://bmcgenomics.biomedcentral.com/articles/10.1186/s12864-017-3592-y>
145. Jurenka R. Insect pheromone biosynthesis. *Top Curr Chem*. 2004;239:97–131.
146. Ando T, Inomata S, Yamamoto M. Lepidopteran Sex Pheromones. *Top Curr Chem*. 2004;239:51–96.

147. Groot AT, Dekker T, Heckel DG. The genetic basis of pheromone evolution in moths. *Annu Rev Entomol* [Internet]. 2016;61:99–117. Available from: <http://www.annualreviews.org/doi/10.1146/annurev-ento-010715-023638>
148. Leary GP, Allen JE, Bungler PL, Luginbill JB, Linn CE, Macallister IE, et al. Single mutation to a sex pheromone receptor provides adaptive specificity between closely related moth species. *Proc Natl Acad Sci U S A*. 2012;109(35):14081–6.
149. Miura N, Nakagawa T, Touhara K, Ishikawa Y. Broadly and narrowly tuned odorant receptors are involved in female sex pheromone reception in *Ostrinia* moths. *Insect Biochem Mol Biol* [Internet]. 2010;40(1):64–73. Available from: <http://dx.doi.org/10.1016/j.ibmb.2009.12.011>
150. Leal WS. Odorant reception in insects: Roles of receptors, binding proteins, and degrading enzymes. *Annu Rev Entomol*. 2012;58:373–91.
151. Corcoran JA, Jordan MD, Thrimawithana AH, Crowhurst RN, Newcomb RD. The peripheral olfactory repertoire of the lightbrown apple moth, *Epiphyas postvittana*. *PLoS One*. 2015;10(5):e0128596.
152. Walker III WB, Gonzalez F, Garczynski SF, Witzgall P. The chemosensory receptors of codling moth *Cydia pomonella* – expression in larvae and adults. *Sci Rep*. 2016;6:23518.
153. De Fouchier A, Walker WB, Montagné N, Steiner C, Binyameen M, Schlyter F, et al. Functional evolution of Lepidoptera olfactory receptors revealed by deorphanization of a moth repertoire. *Nat Commun*. 2017;8(15709).
154. Zhang Y-N, Zhang L-W, Chen D-S, Liang S, Zhao-Qun L, Ye Z-F, et al. Molecular identification of differential expression genes associated with sex pheromone biosynthesis in *Spodoptera exigua*. *Mol Genet Genomics*. 2017;
155. Groot AT, Staudacher H, Barthel A, Inglis O, Schöfl G, Santangelo RG, et al. One quantitative trait locus for intra- and interspecific variation in a sex pheromone. *Mol Ecol*. 2013;22:1065–80.
156. Koutroumpa FA, Jacquin-Joly E. Sex in the night : Fatty acid-derived sex pheromones and corresponding membrane pheromone receptors in insects. *Biochimie* [Internet]. 2014;1–7. Available from: <http://dx.doi.org/10.1016/j.biochi.2014.07.018>
157. Liu Y, Gu S, Zhang Y, Guo Y, Wang G. Candidate olfaction genes identified within the *Helicoverpa armigera* antennal transcriptome. *PLoS One*. 2012;7(10):e48260.
158. Gu SH, Wu KM, Guo YY, Pickett JA, Field LM, Zhou JJ, et al. Identification of genes expressed in the sex pheromone gland of the black cutworm *Agrotis ipsilon* with putative roles in sex pheromone biosynthesis and transport. *BMC Genomics* [Internet]. 2013;14(636). Available from: *BMC Genomics*
159. Jung CR, Kim Y. Comparative transcriptome analysis of sex pheromone glands of two sympatric lepidopteran congener species. *Genomics* [Internet]. 2014;103(4):308–15. Available from: <http://dx.doi.org/10.1016/j.ygeno.2014.02.009>
160. Li RT, Ning C, Huang LQ, Dong JF, Li X, Wang CZ. Expressional divergences of two desaturase genes determine the opposite ratios of two sex pheromone components in *Helicoverpa armigera* and *Helicoverpa assulta*. *Insect Biochem Mol Biol* [Internet]. 2017;90:90–100. Available from: <https://doi.org/10.1016/j.ibmb.2017.09.016>
161. Vogel H, Heidel AJ, Heckel DG, Groot AT. Transcriptome analysis of the sex pheromone gland of the noctuid moth *Heliothis virescens*. *BMC Genomics*. 2010;11(29):16–8.
162. Xia YH, Zhang YN, Hou XQ, Li F, Dong SL. Large number of putative chemoreception and pheromone biosynthesis genes revealed by analyzing transcriptome from ovipositor-pheromone glands of *Chilo suppressalis*. *Sci Rep*. 2015;5:1–12.
163. Svensson M. Sexual selection in moths: the role of chemical communication. *Biol Rev* [Internet]. 1996;71:113–35. Available from: <http://onlinelibrary.wiley.com/doi/10.1111/j.1469-185X.1996.tb00743.x/full>
164. Yildizhan S, van Loon J, Sramkova A, Ayasse M, Arsene C, ten Broeke C, et al. Aphrodisiac pheromones from the wings of the small cabbage white and large cabbage white butterflies, *Pieris rapae* and *Pieris brassicae*. *ChemBioChem*. 2009;10(10):1666–77.
165. Mann F, Szczerbowski D, Silva L De, McClure M, Elias M, Schulz S. 3-Acetoxy-fatty acid isoprenyl esters from androconia of the ithomiine butterfly *Ithomia salapia*. *Beilstein J Org Chem*. 2020;16:2776–87.
166. Wang HL, Brattström O, Brakefield PM, Francke W, Löfstedt C. Identification and biosynthesis of novel male specific esters in the wings of the tropical butterfly, *Bicyclus martius sanaos*. *J Chem Ecol*. 2014;40(6):549–

- 59.
167. Ozaki K, Utoguchi A, Yamada A, Yoshikawa H. Identification and genomic structure of chemosensory proteins (CSP) and odorant binding proteins (OBP) genes expressed in foreleg tarsi of the swallowtail butterfly *Papilio xuthus*. *Insect Biochem Mol Biol* [Internet]. 2008;38(11):969–76. Available from: <http://dx.doi.org/10.1016/j.ibmb.2008.07.010>
 168. Byers KJRP, Darragh K, Garza SF, Almeida DA, Warren IA, Rastas PMA, et al. Clustering of loci controlling species differences in male chemical bouquets of sympatric *Heliconius* butterflies. *bioRxiv Prepr.* 2020;
 169. Beatty CD, Beirincx K, Sherratt TN. The evolution of Müllerian mimicry in multispecies communities. *Nature* [Internet]. 2004;431(7004):63–66. Available from: <http://www.nature.com/nature/journal/v431/n7004/abs/nature02818.html>
 170. Gavrillets S, Hastings A. Coevolutionary chase in two-species systems with applications to mimicry. *J Theor Biol.* 1998;191:415–27.
 171. Huheey JE. Studies in warning coloration and mimicry. VII. Evolutionary consequences of a Batesian-Müllerian spectrum: A model for Müllerian mimicry. *Evolution (N Y)* [Internet]. 1976;30(1):86–93. Available from: <http://www.jstor.org/stable/2407675>
<http://www.jstor.org/stable/pdfplus/2407675.pdf?acceptTC=true>
 172. Mérot C, Le Poul Y, Théry M, Joron M. Refining mimicry: phenotypic variation tracks the local optimum. *J Anim Ecol.* 2016;85(4):1056–69.
 173. Sheppard PM, Turner JRG. The existence of Müllerian Mimicry. *Evolution (N Y).* 1974;31:452–3.
 174. Joron M, Iwasa Y. The evolution of a Müllerian mimic in a spatially distributed community. *J Theor Biol.* 2005;237(1):87–103.
 175. Joron M. Mimicry. In: Cardé RT, Resh VH, editors. *Encyclopedia of Insects.* 2nd Editio. New York: Academic Press, New York.; 2009. p. 633–43.
 176. Joron M, Mallet JLB. Diversity in mimicry: Paradox or paradigm? *Trends Ecol Evol.* 1998;13(11):461–6.
 177. Mallet J, Joron M. Evolution of diversity in warning color and mimicry: Polymorphisms, shifting balance, and speciation. *Annu Rev Ecol Syst* [Internet]. 1999;30:201–33. Available from: <http://www.annualreviews.org/doi/10.1146/annurev.ecolsys.30.1.201>
 178. Ihalainen E, Lindström L, Mappes J, Puolakkainen S. Can experienced birds select for Müllerian mimicry? *Behav Ecol.* 2008;19(2):362–8.
 179. Langham GM. Rufous-tailed jacamars and aposematic butterflies: Do older birds attack novel prey? *Behav Ecol.* 2006;17(2):285–90.
 180. Ihalainen E, Rowland HM, Speed MP, Ruxton GD, Mappes J. Prey community structure affects how predators select for Müllerian mimicry. *Proc R Soc B Biol Sci* [Internet]. 2012;279(1736):2099–105. Available from: <http://www.pubmedcentral.nih.gov/articlerender.fcgi?artid=3321702&tool=pmcentrez&rendertype=abstract>
 181. Benson WW. Natural Selection for Müllerian mimicry in *Heliconius erato* in Costa Rica. *Science (80-).* 1972;176(4037):936–9.
 182. Chouteau M, Angers B. The role of predators in maintaining the geographic organization of aposematic signals. *Am Nat.* 2011;178(6):810–7.
 183. Owen DF, Smith DAS, Gordon IJ, Owixy AM. Polymorphic Müllerian mimicry in a group of African butterflies: a re-assessment of the relationship between *Danaus chrysippus*, *Acraea encedon* and *Acraea encedana* (Lepidoptera: Nymphalidae). *J Zool.* 1994;232(1):93–108.
 184. Gordon IJ, Smith DAS. Diversity in mimicry. *Trends Ecol Evol.* 1999;14(4):150–1.
 185. Chouteau M, Arias M, Joron M. Warning signals are under positive frequency-dependent selection in nature. *Proc Natl Acad Sci* [Internet]. 2016;113(8):2164–9. Available from: <http://www.pnas.org/lookup/doi/10.1073/pnas.1519216113>
 186. Mallet J, McMillan WO, Jiggins CD. Mimicry and warning colour at the boundary between races and species. In: Howard D, Berlocher S, editors. *Endless forms Species and speciation* [Internet]. Oxford, UK: Oxford University Press; 1998. p. 390–403. Available from: <http://discovery.ucl.ac.uk/67729/>
 187. Brower AVZ. A new mimetic species of *Heliconius* (Lepidoptera: Nymphalidae), from southeastern Colombia, revealed by cladistic analysis of mitochondrial DNA sequences. *Zool J Linn Soc.* 1996;116:317–32.
 188. Giraldo N, Salazar C, Jiggins CD, Bermingham E, Linares M. Two sisters in the same dress: *Heliconius* cryptic

- species. *BMC Evol Biol.* 2008;8(324).
189. Mérot C, Mavárez J, Evin A, Dasmahapatra KK, Mallet J, Lamas G, et al. Genetic differentiation without mimicry shift in a pair of hybridizing *Heliconius* species (Lepidoptera: Nymphalidae). *Biol J Linn Soc.* 2013;109:830–47.
 190. Nadeau NJ, Ruiz M, Salazar P, Counterman B, Medina JA, Ortiz-Zuazaga H, et al. Population genomics of parallel hybrid zones in the mimetic butterflies, *H. melpomene* and *H. erato*. *Genome Res* [Internet]. 2014;24:1316–33. Available from: <http://www.ncbi.nlm.nih.gov/pubmed/24823669>
 191. Rossato DO, Boligon D, Fornel R, Kronforst MR, Gonçalves GL, Moreira GRP. Subtle variation in size and shape of the whole forewing and the red band among co-mimics revealed by geometric morphometric analysis in *Heliconius* butterflies. *Ecol Evol* [Internet]. 2018;1–16. Available from: <http://doi.wiley.com/10.1002/ece3.3916>
 192. Van Belleghem SM, Alicea Roman PA, Carbia Gutierrez H, Counterman BA, Papa R. Perfect mimicry between *Heliconius* butterflies is constrained by genetics and development. *Proc R Soc B Biol Sci* [Internet]. 2020;287:20201267. Available from: <https://royalsocietypublishing.org/doi/10.1098/rspb.2020.1267>
 193. Rosser N. Speciation and biogeography of Heliconiine butterflies. 2012.
 194. de Castro ÉCP, Zagrobelny M, Cardoso MZ, Bak S. The arms race between heliconiine butterflies and *Passiflora* plants - new insights on an ancient subject. *Biol Rev* [Internet]. 2017; Available from: <http://doi.wiley.com/10.1111/brv.12357>
 195. Rohlf FJ. TPSDig. Stony Brook, NY: Department of Ecology and Evolution, State University of NY at Stony Brook; 2010.
 196. Adams D, Collyer M, Kaliontzopoulou A, Sherratt E. Geometric morphometric analyses of 2D/3D landmark data. [https://cran.r-project.org/package=geomorph.](https://cran.r-project.org/package=geomorph;); 2017.
 197. Bookstein F. Morphometrics tools for landmark data: Geometry and biology. New York, NY: Cambridge University Press; 1991.
 198. Zelditch ML, Swiderski DL, Sheets HD, Fink WL. Geometric morphometrics for biologist: a primer. San Diego, LA: Elsevier Academic Press; 2004.
 199. Hijmans RJ, Williams E, Vennes C. Package ‘geosphere.’ 2019.
 200. Friendly M, Fox J. Candisc: visualizing generalized canonical discriminant and canonical correlation analysis [Internet]. 2017. Available from: <https://cran.r-project.org/package=candisc>
 201. Van Belleghem SM, Papa R, Ortiz-Zuazaga H, Hendrickx F, Jiggins CD, McMillan WO, et al. Patternize : An R package for quantifying color pattern variation. *Methods Ecol Evol.* 2018;9:390–8.
 202. Schneider CA, Rasband WS, Eliceiri KW. NIH Image to ImageJ: 25 years of image analysis. *Nat Methods.* 2012;11(7):671–5.
 203. Müller F. Ituna and Thyridia: a remarkable case of mimicry in butterflies. *Trans Entomol Soc London.* 1879;1879:20–29.
 204. Sbordoni V, Bullini L, Scarpelli G, Forestiero S, Rampini M. Mimicry in the burnet moth *Zygaena ephialtes*: population studies and evidence of a Batesian—Müllerian situation. *Ecol Entomol.* 1979;4:83–93.
 205. Niehuis O, Hofmann A, Naumann CM, Misof B. Evolutionary history of the burnet moth genus *Zygaena* Fabricius, 1775 (Lepidoptera: Zygaenidae) inferred from nuclear and mitochondrial sequence data: phylogeny, host-plant association, wing pattern evolution and historical biogeography. *Biol J Linn Soc.* 2007;92:501–20.
 206. Plowright RC, Owen RE. The evolutionary significance of bumble bee color patterns: a mimetic interpretation. *Evolution (N Y).* 1980;34(4):622–37.
 207. Williams P. The distribution of bumblebee colour patterns worldwide: possible significance for thermoregulation, crypsis, and warning mimicry. *Biol J Linn Soc.* 2007;92:97–118.
 208. Zrzavý J, Nedvěd O. Evolution of mimicry in the New World *Dysdercus* (Hemiptera: Pyrrhocoridae). *J Evol Biol.* 1999;12:956–69.
 209. Symula R, Schulte R, Summers K. Molecular phylogenetic evidence for a mimetic radiation in Peruvian poison frogs supports a Müllerian mimicry hypothesis. *Proc R Soc B Biol Sci.* 2001;268:2415–21.
 210. Chiari Y, Vences M, Vieites DR, Rabemananjara F, Bora P, Ramilijaona Ravoahangimalala O, et al. New evidence for parallel evolution of colour patterns in Malagasy poison frogs (Mantella). *Mol Ecol.* 2004;13:3763–74.
 211. Sanders KL, Malhotra A, Thorpe RS. Evidence for a Müllerian mimetic radiation in Asian pitvipers. *Proc R Soc*

- B Biol Sci. 2006;273:1135–41.
212. Springer VG, Smith-Vaniz WF. Mimetic relationships involving fishes of the family Blenniidae. *Smithson Contrib to Zool.* 1972;(112):1–36.
 213. Dumbacher JP, Fleischer RC. Phylogenetic evidence for colour pattern convergence in toxic pitohuis: Müllerian mimicry in birds? *Proc R Soc B Biol Sci.* 2001;268:1971–6.
 214. Chittka L. Bee color vision is optimal for coding flower color, but flower colors are not optimal for being coded—why? *Isr J Plant Sci.* 1997;45:115–27.
 215. Roy BA, Widmer A. Floral mimicry: a fascinating yet poorly understood phenomenon. *Trends Plant Sci.* 1999;4(8):325–30.
 216. Benitez-Vieyra S, Hempel De Ibarra N, Wertlen AM, Cocucci AA. How to look like a mallow: Evidence of floral mimicry between Turneraceae and Malvaceae. *Proc R Soc B Biol Sci.* 2007;274:2239–48.
 217. Jones RT, Le Poul Y, Whibley AC, Mèrot C, Ffrench-Constant RH, Joron M. Wing shape variation associated with mimicry in butterflies. *Evolution (N Y).* 2013;67(8):2323–34.
 218. Montejo-Kovacevich G, Smith JE, Meier JI, Bacquet CN, Whiltshire-Romero E, Nadeau NJ, et al. Altitude and life-history shape the evolution of *Heliconius* wings. *Evolution (N Y).* 2019;73(12):2436–50.
 219. Mena S, Kozak KM, Cárdenas RE, Checa MF. Forest stratification shapes allometry and flight morphology of tropical butterflies. *Proc R Soc B Biol Sci [Internet].* 2020;287:20201071. Available from: <https://royalsocietypublishing.org/doi/10.1098/rspb.2020.1071>
 220. Chazot N, Panara S, Zilbermann N, Blandin P, Le Poul Y, Cornette R, et al. Morpho morphometrics: Shared ancestry and selection drive the evolution of wing size and shape in *Morpho* butterflies. *Evolution (N Y).* 2015;70(1):181–94.
 221. Cespedes A, Penz CM, DeVries PJ. Cruising the rain forest floor: Butterfly wing shape evolution and gliding in ground effect. *J Anim Ecol.* 2015;84(3):808–16.
 222. Mendoza-Cuenca L, Macías-Ordóñez R. Foraging polymorphism in *Heliconius charitonia* (Lepidoptera: Nymphalidae): morphological constraints and behavioural compensation. *J Trop Ecol.* 2005;21:407–15.
 223. Mallet JLB, Jackson DA. The ecology and social behaviour of the Neotropical butterfly *Heliconius xanthocles* Bates in Colombia. *Zool J Linn Soc.* 1980;70:1–13.
 224. Reed RD, Papa R, Martin A, Hines HM, Counterman BA, Pardo-Diaz GC, et al. *Optix* drives the repeated convergent evolution of butterfly wing pattern mimicry. *Science (80-).* 2011;333(6046):1137–41.
 225. Lewis JJ, Van Belleghem SM. Mechanisms of change: a population-based perspective on the roles of modularity and pleiotropy in diversification. *Front Ecol Evol.* 2020;8:1–12.
 226. Wallbank RWR, Baxter SW, Pardo-Diaz C, Hanly JJ, Martin SH, Mallet J, et al. Evolutionary Novelty in a Butterfly Wing Pattern through Enhancer Shuffling. *PLoS Biol.* 2016;14(1):1–16.
 227. McMillan WO, Livraghi L, Concha C, Hanly JJ. From patterning genes to process: unraveling the gene regulatory networks that pattern *Heliconius* wings. *Front Ecol Evol.* 2020;8(221):1–15.
 228. Nadeau NJ, Pardo-Diaz GC, Whibley A, Supple MA, Saenko S V., Wallbank RWR, et al. The gene *cortex* controls mimicry and crypsis in butterflies and moths. *Nature [Internet].* 2016;534(7605):106–10. Available from: <http://dx.doi.org/10.1038/nature17961>
 229. Martin A, Papa R, Nadeau NJ, Hill RI, Counterman BA, Halder G, et al. Diversification of complex butterfly wing patterns by repeated regulatory evolution of a *Wnt* ligand. *Proc Natl Acad Sci [Internet].* 2012;109(31):12632–7. Available from: <http://www.pnas.org/cgi/doi/10.1073/pnas.1204800109>
 230. Lewis JJ, Van Belleghem SM, Riccardo P, Danko CG, Reed RD. Many functionally connected loci foster adaptive diversification along a neotropical hybrid zone. *Sci Adv.* 2020;6:eabb8617.
 231. Moest M, Van Belleghem SM, James JE, Salazar C, Martin SH, Barker SL, et al. Selective sweeps on novel and introgressed variation shape mimicry loci in a butterfly adaptive radiation. Vol. 18, *PLOS Biology.* 2020. e3000597 p.
 232. Morris J, Navarro N, Rastas P, Rawlins LD, Sammy J, Mallet J, et al. The genetic architecture of adaptation: convergence and pleiotropy in *Heliconius* wing pattern evolution. *Heredity (Edinb) [Internet].* 2019;123(2):138–52. Available from: <http://dx.doi.org/10.1038/s41437-018-0180-0>
 233. Papa R, Kapan DD, Counterman BA, Maldonado K, Lindstrom DP, Reed RD, et al. Multi-Allelic Major Effect Genes Interact with Minor Effect QTLs to Control Adaptive Color Pattern Variation in *Heliconius erato*. *PLoS One.* 2013;8(3):e57033.
 234. Concha C, Wallbank RWR, Hanly JJ, Fenner J, Livraghi L, Rivera ES, et al. Interplay between developmental

- flexibility and determinism in the evolution of mimetic *Heliconius* wing patterns. *Curr Biol* [Internet]. 2019;29:1–14. Available from: <https://doi.org/10.1016/j.cub.2019.10.010>
235. Rowe C, Lindström L, Lyytinen A. The importance of pattern similarity between Müllerian mimics in predator avoidance learning. *Proc R Soc B Biol Sci*. 2004;271(1537):407–13.
 236. Ihalainen E, Lindström L, Mappes J. Investigating Müllerian mimicry: Predator learning and variation in prey defences. *J Evol Biol*. 2007;20(2):780–91.
 237. Rowland HM, Ihalainen E, Lindström L, Mappes J, Speed MP. Co-mimics have a mutualistic relationship despite unequal defences. *Nature*. 2007;448(7149):64–7.
 238. Finkbeiner SD, Briscoe AD, Mullen SP. Complex dynamics underlie the evolution of imperfect wing pattern convergence in butterflies. *Evolution (N Y)*. 2017;71(4):949–59.
 239. Rutowski RL, Nahm AC, Macedonia JM. Iridescent hindwing patches in the Pipevine Swallowtail: Differences in dorsal and ventral surfaces relate to signal function and context. *Funct Ecol*. 2010;24(4):767–75.
 240. Su S, Lim M, Kunte K. Prey from the eyes of predators: Color discriminability of aposematic and mimetic butterflies from an avian visual perspective. *Evolution (N Y)*. 2015;69(11):2985–94.
 241. Oliver JC, Robertson KA, Monteiro A. Accommodating natural and sexual selection in butterfly wing pattern evolution. *Proc R Soc B Biol Sci*. 2009;276(1666):2369–75.
 242. Robertson KA, Monteiro A. Female *Bicyclus anynana* butterflies choose males on the basis of their dorsal UV-reflective eyespot pupils. *Proc R Soc B Biol Sci*. 2005;272(1572):1541–6.
 243. De Bona S, Valkonen JK, López-Sepulcre A, Mappes J. Predator mimicry, not conspicuousness, explains the efficacy of butterfly eyespots. *Proc R Soc B Biol Sci*. 2015;282:20150202.
 244. DeVries PJ, Penz CM, Hill RI. Vertical distribution, flight behaviour and evolution of wing morphology in *Morpho* butterflies. *J Anim Ecol*. 2010;79:1077–85.
 245. Finkbeiner SD. Communal roosting in *Heliconius* butterflies (Nymphalidae): roost recruitment, establishment, fidelity, and resource use trends based on age and sex. *J Lepid Soc*. 2014;68(1):10–6.
 246. Willmott KR, Willmott JCR, Elias M, Jiggins CD. Maintaining mimicry diversity: optimal warning colour patterns differ among microhabitats in Amazonian clearwing butterflies. *Proc R Soc B*. 2017;284:20170744.
 247. Cuthill IC, Allen WL, Arbuckle K, Caspers B, Chaplin G, Hauber ME, et al. The biology of color. *Science (80-)*. 2017;357(6350):eaan0221.
 248. Arias M, Meichanetzoglou A, Elias M, Rosser N, De-Silva DL, Nay B, et al. Variation in cyanogenic compounds concentration within a *Heliconius* butterfly community: does mimicry explain everything? *BMC Evol Biol* [Internet]. 2016;16(272):1–10. Available from: <http://dx.doi.org/10.1186/s12862-016-0843-5>
 249. Coyne J., Orr H. Speciation. Sunderland, Massachusetts: Sinauer Associates Inc, Sunderland, MA, USA.; 2004. 545 p.
 250. Wang L, Anderson DJ. Identification of an aggression-promoting pheromone and its receptor neurons in *Drosophila*. *Nature* [Internet]. 2010;463(7278):227–31. Available from: <http://www.nature.com/doi/10.1038/nature08678>
 251. Hartlieb E, Anderson P. Olfactory-released behaviours. In: B.S. H, editor. *Insect Olfaction*. Berlin, Heidelberg: Springer; 1999. p. 315–49.
 252. Alves H, Rouault JD, Kondoh Y, Nakano Y, Yamamoto D, Kim YK, et al. Evolution of cuticular hydrocarbons of hawaiian *Drosophilidae*. *Behav Genet*. 2010;40(5):694–705.
 253. Estrada C, Gilbert LE. Host plants and immatures as mate-searching cues in *Heliconius* butterflies. *Anim Behav* [Internet]. 2010;80(2):231–9. Available from: <http://dx.doi.org/10.1016/j.anbehav.2010.04.023>
 254. Mérot C, Salazar C, Merrill RM, Jiggins CD, Joron M. What shapes the continuum of reproductive isolation? Lessons from *Heliconius* butterflies. *Proc R Soc B Biol Sci*. 2017;284:20170335.
 255. Darragh K, Montejo-Kovacevich G, Kozak KM, Morrison CR, Figueiredo CME, Ready JS, et al. Species specificity and intraspecific variation in the chemical profiles of *Heliconius* butterflies across a large geographic range. *Ecol Evol Press* [Internet]. 2019;00:1–25. Available from: <https://www.biorxiv.org/content/10.1101/573469v1>
 256. Merrill RM, Chia A, Nadeau NJ. Divergent warning patterns contribute to assortative mating between incipient *Heliconius* species. *Ecol Evol*. 2014;4(7):911–7.
 257. Kozak KM, Wahlberg N, Neild AFE, Dasmahapatra KK, Mallet J, Jiggins CD. Multilocus Species Trees Show the Recent Adaptive Radiation of the Mimetic *Heliconius* Butterflies. *Syst Biol*. 2015;64(3):505–24.
 258. Brower AVZ. Parallel race formation and the evolution of mimicry in *Heliconius* butterflies : A phylogenetic

- hypothesis from mitochondrial DNA sequences. *Evolution* (N Y). 1996;50(1):195–221.
259. Jiggins CD, Linares M, Naisbit RE, Salazar C, Yang ZH, Mallet J. Sex-linked hybrid sterility in a butterfly. *Evolution* (N Y). 2001;55(8):1631–8.
 260. Sanchez AP, Pardo-Diaz GC, Enciso-Romero J, Muñoz A, Jiggins CD, Salazar C, et al. An introgressed wing pattern acts as a mating cues. *Evolution* (N Y). 2015;69(6):1619–29.
 261. Vanjari S, Mann F, Merrill R, Schulz S, Jiggins C. Male sex pheromone components in the butterfly *Heliconius melpomene*. bioRxiv. 2015;
 262. R Core Team. R: A language and environment for statistical computing. Vienna, Austria: R Foundation for Statistical Computing; 2016.
 263. Bates D, Maechler M, Bolker B, Walker S, Bojesen Christensen RH, Singmann H, et al. Linear Mixed-Effects Models using “Eigen” and S4. *Journal of Statistical Software*. 2015. p. 1–48.
 264. Wickham H. ggplot2 - Elegant Graphics for Data Analysis. 2nd ed. New York, NY: Springer-Verlag; 2009. 260 p.
 265. Fox J, Weisberg S. An R companion to applied regression. 2nd ed. Sage, editor. Thousand Oaks, CA; 2011. 449 p.
 266. Dorai-Raj S. binom: Binomial confidence intervals for several parameterizations [Internet]. 2014. Available from: <http://cran.r-project.org/package=binom>
 267. Hench K, Vargas M, Höppner MP, McMillan WO, Puebla O. Inter-chromosomal coupling between vision and pigmentation genes during genomic divergence. *Nat Ecol Evol*. 2019;3(4):657–67.
 268. Bay RA, Arnegard ME, Conte GL, Best J, Bedford NL, McCann SR, et al. Genetic coupling of female mate choice with polygenic ecological divergence facilitates Stickleback speciation. *Curr Biol*. 2017;27(21):3344–3349.e4.
 269. Shahandeh MP, Pischedda A, Turner TL. Male mate choice via cuticular hydrocarbon pheromones drives reproductive isolation between *Drosophila* species. *Evolution* (N Y). 2017;72(1):123–35.
 270. Keller-Costa T, Canário AVM, Hubbard PC. Chemical communication in cichlids: A mini-review. *Gen Comp Endocrinol* [Internet]. 2015;221:64–74. Available from: <http://dx.doi.org/10.1016/j.yggen.2015.01.001>
 271. Merrill RM, Gompert Z, Dembeck LM, Kronforst MR, McMillan WO, Jiggins CD. Mate preference across the speciation continuum in a clade of mimetic butterflies. *Evolution* (N Y). 2011;65(5):1489–500.
 272. Muñoz AG, Salazar C, Castaño J, Jiggins CD, Linares M. Multiple sources of reproductive isolation in a bimodal butterfly hybrid zone. *J Evol Biol*. 2010;23(6):1312–20.
 273. Southcott L, Kronforst M. Female mate choice is a reproductive isolating barrier in *Heliconius* butterflies : *Ethology*. 2018;124:862–8659.
 274. Larsdotter-Mellström H, Eriksson K, Liblikas I, Wiklund C, Borg-Karlson AK, Nylin S, et al. It’s all in the mix: Blend-specific behavioral response to a sexual pheromone in a butterfly. *Front Physiol*. 2016;7(68):1–10.
 275. Snellings Y, Herrera B, Wildemann B, Beelen M, Zwartz L, Wenseleers T, et al. The role of cuticular hydrocarbons in mate recognition in *Drosophila sukukii*. *Sci Rep* [Internet]. 2018;8(4996):1–11. Available from: <http://dx.doi.org/10.1038/s41598-018-23189-6>
 276. Rundle HD, Chenoweth SF, Doughty P, Blows MW. Divergent selection and the evolution of signal traits and mating preferences. *PLoS Biol*. 2005;3(11):1988–95.
 277. Grula J, McChesney J, Taylor O. Aphrodisiac pheromones of the sulfur butterflies *Colias eurytheme* and *C. philodice* (Lepidoptera, Pieridae). *J Chem Ecol*. 1980;6:241–56.
 278. Wago H. Studies on the Mating Behavior of the Pale Grass Blue, *Zizeeria maha argia* (Lepidoptera : Lycaenidae) III. Olfactory Cues in Sexual Discrimination by Males. *Appl Ent Zool*. 1978;13:283–9.
 279. Koutroumpa FA, Monsempes C, François M-C, de Cian A, Royer C, Concordet J-P, et al. Heritable genome editing with CRISPR/Cas9 induces anosmia in a crop pest moth. *Sci Rep*. 2016;6:29620.
 280. Counterman BA, Araujo-Perez F, Hines HM, Baxter SW, Morrison CM, Lindstrom DP, et al. Genomic hotspots for adaptation: The population genetics of Müllerian mimicry in *Heliconius erato*. *PLoS Genet*. 2010;6(2):e1000796.
 281. Hillier NK, Vickers NJ. The role of Heliethine hairpencil compounds in female *Heliopsis virescens* (Lepidoptera: Noctuidae) behavior and mate acceptance. *Chem Senses*. 2004;29(6):499–511.
 282. Schulz S, Nishida R. The pheromone system of the male danaine butterfly, *Idea leuconoe*. *Bioorg Med Chem*. 1996;4(3):341–9.
 283. Albre J, Steinwender B, Newcomb RD. The evolution of desaturase gene regulation involved in sex pheromone production in Leafroller Moths of the genus *Planotortrix*. *J Hered*. 2013;104(5):627–38.

284. Dopman EB, Robbins PS, Seaman A. Components of reproductive isolation between North American pheromone strains of the European corn borer. *Evolution* (N Y). 2010;64(4):881–902.
285. Naisbit RE, Jiggins CD, Linares M, Salazar C, Mallet J. Hybrid sterility, Haldane’s rule and speciation in *Heliconius cydno* and *H. melpomene*. *Genet Soc Am*. 2002;161:1517–26.
286. Edwards AWF. *Likelihood*. Cambridge University Press; 1972.
287. Hummel HE, Miller T. *Techniques in pheromone research*. Springer Science and Business Media; 2012. 464 p.
288. Hammer Ø, Harper DAT, Ryan PD. PAST: Paleontological statistics software package for education and data analysis. *Palaeontol Electron* [Internet]. 2001;4(1)(1):1–9. Available from: http://palaeo-electronica.org/2001_1/past/issue1_01.htm
289. Burdfield-Steel E, Pakkanen H, Rojas B, Galarza JA, Mappes J. De novo synthesis of chemical defenses in an aposematic moth. *J Insect Sci*. 2018;18(2):1–4.
290. Moore BP, Brown WV, Rothschild M. Methylalkylpyrazines in aposematic insects, their hostplants and mimics. *Chemoecology*. 1990;1(2):43–51.
291. Kaye H, Mackintosh NJ, Rothschild M, Moore BP. Odour of pyrazine potentiates an association between environmental cues and unpalatable taste. *Anim Behav*. 1989;37:1–6.
292. Coyne J, Orr H. *Speciation*. Sinauer Associates Inc, Sunderland, MA, USA.; 2004.
293. Brand P, Hinojosa-Díaz IA, Ayala R, Daigle M, Yurrita Obiols CL, Eltz T, et al. The evolution of sexual signaling is linked to odorant receptor tuning in perfume-collecting orchid bees. *Nat Commun* [Internet]. 2020;11. Available from: <http://dx.doi.org/10.1038/s41467-019-14162-6>
294. Löfstedt C, Wahlberg N, Millar JG. Evolutionary Patterns of Pheromone Diversity in Lepidoptera. In: Berkeley ed. JARC, editor. *Pheromone Communication in Moths : Evolution, Behavior and Application*. University of California Press; 2016. p. 43-78.
295. Byers KJRP, Darragh K, Musgrove J, Abondano Almeida D, Garza SF, Warren IA, et al. A major locus controls a biologically active pheromone component in *Heliconius melpomene*. *Evolution* (N Y). 2020;1–16.
296. Conner W, Iyengar V. Male pheromones in moths. In *pheromone communication*. In: Allison J, Ring C, editors. *Evolution, Behavior and Application*. Berkeley: University of California Press; 2016. p. 191–208.
297. Aldrich JR, Blum MS, Duffey SS, Fales HM. Male specific natural products in the bug, *Leptoglossus phyllopus*: Chemistry and possible function. *J Insect Physiol*. 1976;22(9):1201–6.
298. Morgan ED. *Biosynthesis in insects: advanced edition*. Royal Society of Chemistry, editor. RSC Publishing; 2010. 362 p.
299. Meyer HJ, Norris DM. Vanillin and Syringaldehyde as attractants (Coleoptera: Scolytidae). *Ann Entomol Soc Am*. 1967;60(4):858–9.
300. Seenivasagan T, Sharma KR, Sekhar K, Ganesan K, Prakash S, Vijayaraghavan R. Electroantennogram, flight orientation, and oviposition responses of *Aedes aegypti* to the oviposition pheromone n-heneicosane. *Parasitol Res*. 2009;104:827–33.
301. Simmons LW, Alcock J, Reeder A. The role of cuticular hydrocarbons in male attraction and repulsion by female Dawson’s burrowing bee, *Amegilla dawsoni*. *Anim Behav*. 2003;66:677–85.
302. Combs PA, Krupp JJ, Khosla NM, Bua D, Petrov DA, Levine JD, et al. Tissue-specific cis-regulatory divergence implicates eloF in inhibiting interspecies mating in *Drosophila*. *Curr Biol*. 2018;28(24):3969-3975.e3.
303. Kost S, Heckel DG, Yoshido A, Groot AT. A Z-linked sterility locus causes sexual abstinence in hybrid females and facilitates speciation in *Spodoptera frugiperda*. *Evolution* (N Y). 2016;70(6):1418–27.
304. Smadja CM, Butlin RK. A framework for comparing processes of speciation in the presence of gene flow. *Mol Ecol*. 2011;20(24):5123–40.
305. Seehausen O, Takimoto G, Roy D, Jokela J. Speciation reversal and biodiversity dynamics with hybridization in changing environments. *Mol Ecol*. 2008;17:30 – 44.
306. Southcott L, Kronforst M. Female mate choice is a reproductive isolating barrier in *Heliconius* butterflies. *Ethology*. 2018;124:862–8659.
307. Gleason JM, James RA, Wicker-Thomas C, Ritchie MG. Identification of quantitative trait loci function through analysis of multiple cuticular hydrocarbons differing between *Drosophila simulans* and *Drosophila sechellia* females. *Heredity* (Edinb) [Internet]. 2009;103(5):416–24. Available from: <http://dx.doi.org/10.1038/hdy.2009.79>
308. Teal PEA, Tumlinson JH. Effects of interspecific hybridization between *Heliothis virescens* and *H. subflexa* on

- the sex pheromone communication system. *Insect Physiol.* 1997;41:519–25.
309. Constantino LM, Salazar JA. Natural hybridization of *Heliconius cydno* Doubleday from Western Colombia (Lepidoptera: Nymphalidae: Heliconiinae). *Bol Cient del Mus Hist Nat Univ Caldas.* 1998;2(June):41–5.

SUPPLEMENTARY INFORMATION

CHAPTER 1. PHENOTYPIC RESEMBLANCE ACROSS MULTIPLE MIMICRY RINGS IN *Heliconius*

Table S1.1. Samples included in the morphometric analyses. A total of 1102 individuals were used. The wings were obtained from “Colección de Artrópodos -Universidad del Rosario-CAUR229” (M), “Museo de Historia Natural” - Universidad de Los Andes (Andes), “Instituto de Ciencias Naturales – Universidad Nacional de Colombia (ICN-MHL-L), the Butterfly Genetics Group – University of Cambridge (CAM), and a private collection of Jean Francois Le Crom (JFLC). The last column indicates analysis in which that specimen was used, D, dorsal; V, ventral; HW, hindwing; FW, forewing; SS; size and shape analysis.

ID Wing Scan	ID Collection	Taxon	Locality	Analysis
LGE-WS-02451	M3994	<i>Chetone ithrana</i>	Amazonas, Puerto Nariño, Quebrada Aguas Rojas	SS-FW; SS-HW; D-FW; V-FW; D-HW; V-HW
LGE-WS-02452	M3987	<i>Chetone ithrana</i>	Amazonas, Puerto Nariño, Quebrada Aguas Rojas	SS-FW; SS-HW; D-FW; V-FW; D-HW; V-HW
LGE-WS-02453	M3986	<i>Chetone ithrana</i>	Amazonas, Puerto Nariño, Quebrada Aguas Rojas	SS-FW; SS-HW; D-FW; V-FW; D-HW; V-HW
LGE-WS-02454	M3983	<i>Chetone ithrana</i>	Amazonas, Puerto Nariño, Quebrada Aguas Rojas	SS-FW; SS-HW; D-FW; V-FW; D-HW; V-HW
LGE-WS-00151	N/A	<i>Elzunia humboldt regalis</i>	Valle del Cauca, La Cumbre	SS-FW; SS-HW; D-FW; V-FW; D-HW; V-HW
LGE-WS-00152	N/A	<i>Elzunia humboldt regalis</i>	Valle del Cauca, Quebrada La Vieja	SS-FW; SS-HW; D-FW; V-FW; D-HW; V-HW
LGE-WS-00153	N/A	<i>Elzunia humboldt regalis</i>	Valle del Cauca, Yumbo, La Cumbre	SS-FW; SS-HW; D-FW; V-FW; D-HW; V-HW
LGE-WS-00154	N/A	<i>Elzunia humboldt regalis</i>	Valle del Cauca, Yumbo, La Cumbre	SS-FW; SS-HW; D-FW; V-FW; D-HW; V-HW
LGE-WS-00155	N/A	<i>Elzunia humboldt regalis</i>	Valle del Cauca, Cartago, San José del Palmar	SS-FW; SS-HW; D-FW; V-FW; D-HW; V-HW
LGE-WS-00156	N/A	<i>Elzunia humboldt regalis</i>	Valle del Cauca, Buenaventura	SS-FW; SS-HW; D-FW; V-FW; D-HW
LGE-WS-00157	N/A	<i>Elzunia humboldt regalis</i>	Valle del Cauca, Vereda del Racio	SS-FW; SS-HW; D-FW; V-FW; D-HW; V-HW
LGE-WS-00158	N/A	<i>Elzunia humboldt regalis</i>	Valle del Cauca, Quebrada La Vigía	SS-FW; SS-HW; D-FW; V-FW; D-HW; V-HW
LGE-WS-00159	N/A	<i>Elzunia humboldt regalis</i>	Valle del Cauca, Quebrada La Vigía	SS-FW; SS-HW; D-FW; V-FW; D-HW; V-HW

LGE-WS-00160	N/A	<i>Elzunia humboldt regalis</i>	Valle del Cauca, Rio Bravo, Lago Calima	SS-FW; D-FW; V-FW; D-HW
LGE-WS-00161	N/A	<i>Elzunia humboldt regalis</i>	Valle del Cauca, Yumbo, La Cumbre	SS-FW; D-FW; V-FW; D-HW; V-HW
LGE-WS-00162	N/A	<i>Elzunia humboldt regalis</i>	Valle del Cauca, Yumbo, La Cumbre	SS-FW; SS-HW; D-FW; V-FW; D-HW; V-HW
LGE-WS-00163	N/A	<i>Elzunia humboldt regalis</i>	Valle del Cauca, Yumbo, La Cumbre	D-FW; V-FW; D-HW; V-HW
LGE-WS-00164	N/A	<i>Elzunia humboldt regalis</i>	Valle del Cauca, Yumbo, La Cumbre	SS-FW; SS-HW; D-FW; V-FW; D-HW
LGE-WS-00166	Andes-E11638	<i>Elzunia humboldt regalis</i>	Valle del Cauca, Bitaco	SS-FW; SS-HW; D-FW; D-HW
LGE-WS-00167	Andes-E12485	<i>Elzunia humboldt regalis</i>	Valle del Cauca, Atuncela	SS-FW; SS-HW; D-FW; V-FW; D-HW; V-HW
LGE-WS-00168	Andes-E12480	<i>Elzunia humboldt regalis</i>	Valle del Cauca, Atuncela	SS-FW; SS-HW; D-FW; V-FW; D-HW
LGE-WS-00169	Andes-E12481	<i>Elzunia humboldt regalis</i>	Valle del Cauca, Atuncela	SS-FW; SS-HW; D-FW; V-FW; D-HW
LGE-WS-00170	Andes-E10535	<i>Elzunia humboldt regalis</i>	Valle del Cauca, Atuncela	SS-FW; SS-HW; D-FW; V-FW; D-HW; V-HW
LGE-WS-00171	Andes-E12483	<i>Elzunia humboldt regalis</i>	Valle del Cauca, Bitaco	SS-FW; SS-HW; D-FW; V-FW; D-HW; V-HW
LGE-WS-00172	Andes-E10540	<i>Elzunia humboldt regalis</i>	Valle del Cauca, Atuncela	SS-FW; SS-HW; D-FW; V-FW; D-HW; V-HW
LGE-WS-00173	Andes-E12484	<i>Elzunia humboldt regalis</i>	Valle del Cauca, Km83 Vía Buenaventura	SS-FW; SS-HW; D-FW; V-FW; D-HW; V-HW
LGE-WS-00174	Andes-E10534	<i>Elzunia humboldt regalis</i>	Valle del Cauca, Atuncela	SS-FW; SS-HW; D-FW; V-FW; D-HW; V-HW
LGE-WS-00175	Andes-E10927	<i>Elzunia humboldt regalis</i>	Valle del Cauca, Bitaco	SS-FW; SS-HW; D-FW; V-FW; D-HW; V-HW
LGE-WS-00176	Andes-E10925	<i>Elzunia humboldt regalis</i>	Valle del Cauca, Bitaco	SS-FW; SS-HW; D-FW; V-FW; D-HW; V-HW
LGE-WS-00177	Andes-E11646	<i>Elzunia humboldt regalis</i>	Valle del Cauca, Atuncela	SS-FW; SS-HW; D-FW; V-FW; D-HW; V-HW
LGE-WS-00178	Andes-E11646	<i>Elzunia humboldt regalis</i>	Valle del Cauca, Km83 Vía Buenaventura	SS-FW; SS-HW; D-FW; V-FW; D-HW; V-HW
LGE-WS-00179	Andes-E11377	<i>Elzunia humboldt regalis</i>	Valle del Cauca, Km83 Vía Buenaventura	SS-FW; SS-HW; D-FW; V-FW; D-HW; V-HW
LGE-WS-00180	Andes-E10538	<i>Elzunia humboldt regalis</i>	Valle del Cauca, Atuncela	SS-FW; SS-HW; D-FW; V-FW; D-HW; V-HW
LGE-WS-00181	Andes-E10894	<i>Elzunia humboldt regalis</i>	Valle del Cauca, Queremal	SS-FW; SS-HW; D-FW; V-FW; D-HW; V-HW
LGE-WS-00182	Andes	<i>Elzunia humboldt regalis</i>	Valle del Cauca, Lago Calima	SS-FW; SS-HW; D-FW; V-FW; D-HW; V-HW
LGE-WS-00183	Andes-E10909	<i>Elzunia humboldt regalis</i>	Valle del Cauca, Río Barragan, La Vieja, Combarco	SS-FW; SS-HW; D-FW; V-FW; D-HW; V-HW
LGE-WS-00184	Andes-E10908	<i>Elzunia humboldt regalis</i>	Valle del Cauca, Río Barragan, La Vieja, Combarco	SS-FW; SS-HW; D-FW; V-FW; D-HW; V-HW
LGE-WS-00185	Andes	<i>Elzunia humboldt regalis</i>	Cauca, Popayán, Quebrada el Silencio, La Elvira, Cartón de Colombia	SS-FW; SS-HW; V-FW; V-HW
LGE-WS-02301	M5181	<i>Elzunia humboldt tamasea</i>	Huila, Vereda La Plata, Reserva Natural Santa Rosalia	SS-FW; SS-HW

LGE-WS-02302	M5070	<i>Elzunia humboldt tamasea</i>	Huila, Vereda La Plata, Reserva Natural Santa Rosalia	SS-FW; SS-HW; D-FW; D-HW
LGE-WS-02303	M5069	<i>Elzunia humboldt tamasea</i>	Huila, Vereda La Plata, Reserva Natural Santa Rosalia	SS-FW; SS-HW
LGE-WS-02304	M5068	<i>Elzunia humboldt tamasea</i>	Huila, Vereda La Plata, Reserva Natural Santa Rosalia	SS-FW; SS-HW; D-FW; D-HW
LGE-WS-02305	M5065	<i>Elzunia humboldt tamasea</i>	Huila, Vereda La Plata, Reserva Natural Santa Rosalia	SS-FW; SS-HW
LGE-WS-02306	M5058	<i>Elzunia humboldt tamasea</i>	Huila, Vereda La Plata, Reserva Natural Santa Rosalia	SS-FW; SS-HW
LGE-WS-02307	M5057	<i>Elzunia humboldt tamasea</i>	Huila, Vereda La Plata, Reserva Natural Santa Rosalia	SS-FW; SS-HW; D-FW; V-FW; D-HW; V-HW
LGE-WS-02308	M5066	<i>Elzunia humboldt tamasea</i>	Huila, Vereda La Plata, Reserva Natural Santa Rosalia	SS-FW; SS-HW; D-FW; V-FW; D-HW; V-HW
LGE-WS-02309	M5067	<i>Elzunia humboldt tamasea</i>	Huila, Vereda La Plata, Reserva Natural Santa Rosalia	SS-FW; SS-HW; D-FW; V-FW; D-HW; V-HW
LGE-WS-02800	M5350	<i>Eueides heliconioides eanes</i>	Amazonas, La Pedrera	SS-FW; SS-HW; D-FW; V-FW; D-HW; V-HW
LGE-WS-02801	M5351	<i>Eueides heliconioides eanes</i>	Amazonas, La Pedrera	SS-FW; SS-HW; D-FW; V-FW; D-HW; V-HW
LGE-WS-02802	M5391	<i>Eueides heliconioides eanes</i>	Amazonas, La Pedrera	SS-FW; SS-HW; D-FW; V-FW; D-HW; V-HW
LGE-WS-02803	M5390	<i>Eueides heliconioides eanes</i>	Amazonas, La Pedrera	SS-FW; SS-HW; D-FW; V-FW; D-HW; V-HW
LGE-WS-02804	M5349	<i>Eueides heliconioides eanes</i>	Amazonas, La Pedrera	SS-FW; SS-HW; D-FW; V-FW; D-HW; V-HW
LGE-WS-02805	M5345	<i>Eueides heliconioides eanes</i>	Amazonas, La Pedrera	SS-FW; SS-HW; D-FW; V-FW; D-HW; V-HW
LGE-WS-02806	M5346	<i>Eueides heliconioides eanes</i>	Amazonas, La Pedrera	SS-FW; SS-HW; D-FW; V-FW; D-HW; V-HW
LGE-WS-02807	M5347	<i>Eueides heliconioides eanes</i>	Amazonas, La Pedrera	SS-FW; SS-HW; D-FW; V-FW; D-HW; V-HW
LGE-WS-01801	M4854	<i>Heliconius aoede</i>	Meta, Lejanías, Río Guejar	SS-FW; SS-HW; D-FW; V-FW; D-HW; V-HW
LGE-WS-01802	M1503	<i>Heliconius aoede</i>	Caquetá, Florencia, Paraiso	SS-FW; SS-HW; V-FW; V-HW
LGE-WS-01803	M2348	<i>Heliconius aoede</i>	Caquetá, Florencia, Paraiso	SS-FW; SS-HW; D-FW; V-FW; D-HW; V-HW
LGE-WS-01150	M3075	<i>Heliconius cydno cydno</i>	Cundinamarca, La Cumbre	D-FW; V-FW; D-HW; V-HW
LGE-WS-01151	M2946	<i>Heliconius cydno cydno</i>	Cundinamarca, La Cumbre	SS-FW; SS-HW; D-FW; V-FW; D-HW; V-HW
LGE-WS-01152	M2797	<i>Heliconius cydno cydno</i>	Santander, Bucaramanga	SS-FW; SS-HW; D-FW; V-FW; D-HW
LGE-WS-01153	M3084	<i>Heliconius cydno cydno</i>	Cundinamarca, La Cumbre	SS-FW; SS-HW; D-FW; V-FW; D-HW; V-HW
LGE-WS-01154	M3092	<i>Heliconius cydno cydno</i>	Cundinamarca, La Cumbre	SS-FW; SS-HW; D-FW; V-FW; D-HW; V-HW
LGE-WS-01155	M3285	<i>Heliconius cydno cydno</i>	Cundinamarca, La Cumbre	SS-FW; SS-HW; D-FW; V-FW; D-HW; V-HW
LGE-WS-01156	M1694	<i>Heliconius cydno cydno</i>	Santander, Bucaramanga	SS-FW; SS-HW; D-FW; V-FW; D-HW; V-HW
LGE-WS-01157	M2125	<i>Heliconius cydno cydno</i>	Cundinamarca, Peru, Guaduas	SS-FW; SS-HW; D-FW; V-FW; D-HW; V-HW

LGE-WS-01158	M3082	<i>Heliconius cydno cydno</i>	Cundinamarca, La Cumbre	SS-FW; SS-HW; D-FW; V-FW; D-HW; V-HW
LGE-WS-01159	M2799	<i>Heliconius cydno cydno</i>	Santander, Bucaramanga	SS-FW; SS-HW; D-FW; V-FW; D-HW; V-HW
LGE-WS-01160	M3081	<i>Heliconius cydno cydno</i>	Cundinamarca, La Cumbre	SS-FW; SS-HW; D-FW; V-FW; D-HW; V-HW
LGE-WS-01161	M3079	<i>Heliconius cydno cydno</i>	Cundinamarca, La Cumbre	SS-FW; SS-HW; D-FW; V-FW; D-HW; V-HW
LGE-WS-01162	M3078	<i>Heliconius cydno cydno</i>	Cundinamarca, La Cumbre	SS-FW; SS-HW; D-FW; V-FW; D-HW; V-HW
LGE-WS-01163	M2787	<i>Heliconius cydno cydno</i>	Santander, Bucaramanga	SS-FW; SS-HW; D-FW; V-FW; D-HW; V-HW
LGE-WS-01164	M2788	<i>Heliconius cydno cydno</i>	Santander, Bucaramanga	SS-FW; SS-HW; D-FW; V-FW; D-HW; V-HW
LGE-WS-01165	M2455	<i>Heliconius cydno cydno</i>	Cundinamarca, Vereda Granada	SS-FW; SS-HW; D-FW; V-FW; D-HW; V-HW
LGE-WS-01166	M2452	<i>Heliconius cydno cydno</i>	Cundinamarca, Vereda Granada	SS-FW; SS-HW; D-FW; V-FW; D-HW; V-HW
LGE-WS-01167	M2457	<i>Heliconius cydno cydno</i>	Cundinamarca, Vereda Granada	SS-FW; SS-HW; D-FW; V-FW; D-HW; V-HW
LGE-WS-01168	M2244	<i>Heliconius cydno cydno</i>	Cundinamarca, Vereda Granada	SS-FW; SS-HW; D-FW; V-FW; D-HW; V-HW
LGE-WS-01169	M2141	<i>Heliconius cydno cydno</i>	Santander, Bucaramanga	SS-FW; SS-HW; D-FW; V-FW; D-HW; V-HW
LGE-WS-01170	M2139	<i>Heliconius cydno cydno</i>	Santander, Bucaramanga	SS-FW; SS-HW; D-FW; V-FW; D-HW; V-HW
LGE-WS-01171	M2138	<i>Heliconius cydno cydno</i>	Santander, Bucaramanga	SS-FW; SS-HW; D-FW; V-FW; D-HW; V-HW
LGE-WS-01172	M2137	<i>Heliconius cydno cydno</i>	Santander, Bucaramanga	SS-FW; SS-HW; D-FW; V-FW; D-HW; V-HW
LGE-WS-01173	M2431	<i>Heliconius cydno cydno</i>	Cundinamarca, Vereda Granada	SS-FW; SS-HW; D-FW; V-FW; D-HW; V-HW
LGE-WS-01175	M2078	<i>Heliconius cydno cydno</i>	Santander, Bucaramanga	SS-FW; SS-HW; D-FW; V-FW; D-HW; V-HW
LGE-WS-01176	M2079	<i>Heliconius cydno cydno</i>	Santander, Bucaramanga	SS-FW; SS-HW; D-FW; V-FW; D-HW; V-HW
LGE-WS-01177	M2440	<i>Heliconius cydno cydno</i>	Cundinamarca, Vereda Granada	SS-FW; SS-HW; D-FW; V-FW; D-HW; V-HW
LGE-WS-01178	M2135	<i>Heliconius cydno cydno</i>	Santander, Bucaramanga	SS-FW; SS-HW; D-FW; V-FW; D-HW; V-HW
LGE-WS-01179	M3076	<i>Heliconius cydno cydno</i>	Cundinamarca, La Cumbre	SS-FW; SS-HW; D-FW; V-FW; D-HW; V-HW
LGE-WS-01180	M2077	<i>Heliconius cydno cydno</i>	Santander, Bucaramanga	SS-FW; SS-HW; D-FW; V-FW; D-HW; V-HW
LGE-WS-01181	M3094	<i>Heliconius cydno cydno</i>	Cundinamarca, La Cumbre	SS-FW; SS-HW; D-FW; V-FW; D-HW; V-HW
LGE-WS-01182	M3077	<i>Heliconius cydno cydno</i>	Cundinamarca, La Cumbre	SS-FW; SS-HW; D-FW; V-FW; D-HW; V-HW
LGE-WS-01183	M2798	<i>Heliconius cydno cydno</i>	Santander, Bucaramanga	SS-FW; SS-HW; D-FW; V-FW; D-HW; V-HW
LGE-WS-01184	M2089	<i>Heliconius cydno cydno</i>	Santander, Bucaramanga	SS-FW; SS-HW; D-FW; V-FW; D-HW; V-HW

LGE-WS-01185	M2789	<i>Heliconius cydno cydno</i>	Santander, Bucaramanga	SS-FW; SS-HW; D-FW; V-FW; D-HW; V-HW
LGE-WS-01186	M2076	<i>Heliconius cydno cydno</i>	Santander, Bucaramanga	SS-FW; SS-HW; D-FW; V-FW; D-HW; V-HW
LGE-WS-01187	M4184	<i>Heliconius cydno cydno</i>	Valle del Cauca, Buenos Aires	SS-FW; SS-HW; D-FW; V-FW; D-HW; V-HW
LGE-WS-01188	M2145	<i>Heliconius cydno cydno</i>	Santander, Bucaramanga	SS-FW; SS-HW; D-FW; V-FW; D-HW; V-HW
LGE-WS-01189	M2080	<i>Heliconius cydno cydno</i>	Santander, Bucaramanga	SS-FW; SS-HW; D-FW; V-FW; D-HW; V-HW
LGE-WS-01190	M4398	<i>Heliconius cydno cydno</i>	Santander, Florencia	SS-FW; SS-HW; D-FW; V-FW; D-HW; V-HW
LGE-WS-01191	M2136	<i>Heliconius cydno cydno</i>	Santander, Bucaramanga	SS-FW; SS-HW; D-FW; V-FW; D-HW; V-HW
LGE-WS-01192	Andes	<i>Heliconius cydno cydno</i>	Tolima, Iconozo	SS-FW; SS-HW; D-FW; V-FW; D-HW; V-HW
LGE-WS-01193	Andes	<i>Heliconius cydno cydno</i>	Tolima, Iconozo	SS-FW; SS-HW
LGE-WS-01101	M3942	<i>Heliconius cydno chioneus</i>	Chocó, Paridera, Potes	SS-FW; SS-HW; D-FW; V-FW; D-HW; V-HW
LGE-WS-01102	M3888	<i>Heliconius cydno chioneus</i>	Chocó, Bahía Solano	SS-FW; SS-HW; D-FW; V-FW; D-HW; V-HW
LGE-WS-01103	M3923	<i>Heliconius cydno chioneus</i>	Chocó, Cocalito	SS-FW; SS-HW
LGE-WS-01104	M3886	<i>Heliconius cydno chioneus</i>	Chocó, Bahía Solano	SS-FW; SS-HW
LGE-WS-01550	M2834	<i>Heliconius cydno cordula</i>	Venezuela, San Cristobal	SS-FW; SS-HW; D-FW; V-FW; D-HW; V-HW
LGE-WS-01551	M3223	<i>Heliconius cydno cordula</i>	Venezuela, San Cristobal	SS-FW; SS-HW; D-FW; V-FW; D-HW; V-HW
LGE-WS-01552	M2259	<i>Heliconius cydno cordula</i>	Venezuela, San Cristobal	SS-FW; SS-HW; D-FW; V-FW; D-HW; V-HW
LGE-WS-01554	M2258	<i>Heliconius cydno cordula</i>	Venezuela, San Cristobal	SS-FW; SS-HW; D-FW; V-FW; D-HW; V-HW
LGE-WS-01555	M2255	<i>Heliconius cydno cordula</i>	Venezuela, San Cristobal	SS-FW; SS-HW; D-FW; V-FW; D-HW; V-HW
LGE-WS-01556	M2181	<i>Heliconius cydno cordula</i>	Venezuela, San Cristobal	SS-FW; SS-HW; D-FW; V-FW; D-HW; V-HW
LGE-WS-01557	M2186	<i>Heliconius cydno cordula</i>	Venezuela, San Cristobal	SS-FW; SS-HW; D-FW; V-FW; D-HW; V-HW
LGE-WS-01558	M2167	<i>Heliconius cydno cordula</i>	Venezuela, San Cristobal	SS-FW; SS-HW; D-FW; V-FW; D-HW; V-HW
LGE-WS-01559	M2178	<i>Heliconius cydno cordula</i>	Venezuela, San Cristobal	SS-FW; SS-HW; D-FW; V-FW; D-HW; V-HW
LGE-WS-01560	M2170	<i>Heliconius cydno cordula</i>	Venezuela, San Cristobal	SS-FW; SS-HW; D-FW; V-FW; D-HW; V-HW
LGE-WS-01561	M2168	<i>Heliconius cydno cordula</i>	Venezuela, San Cristobal	SS-FW; SS-HW; D-FW; V-FW; D-HW; V-HW
LGE-WS-01562	M2097	<i>Heliconius cydno cordula</i>	Venezuela, San Cristobal	SS-FW; SS-HW; D-FW; V-FW; D-HW; V-HW
LGE-WS-01563	M2100	<i>Heliconius cydno cordula</i>	Venezuela, San Cristobal	SS-FW; SS-HW; D-FW; V-FW; D-HW; V-HW

LGE-WS-01564	M2157	<i>Heliconius cydno cordula</i>	Venezuela, San Cristobal	SS-FW; SS-HW; D-FW; V-FW; D-HW; V-HW
LGE-WS-01565	M2166	<i>Heliconius cydno cordula</i>	Venezuela, San Cristobal	SS-FW; SS-HW; D-FW; V-FW; D-HW; V-HW
LGE-WS-01566	M2095	<i>Heliconius cydno cordula</i>	Venezuela, San Cristobal	SS-FW; SS-HW; D-FW; V-FW; D-HW; V-HW
LGE-WS-01567	M2096	<i>Heliconius cydno cordula</i>	Venezuela, San Cristobal	SS-FW; SS-HW; D-FW; V-FW; D-HW; V-HW
LGE-WS-00001	N/A	<i>Heliconius cydno cydnides</i>	Valle del Cauca, Km16 via Buga-Buenaventura	SS-FW; D-FW; V-FW; D-HW; V-HW
LGE-WS-00002	N/A	<i>Heliconius cydno cydnides</i>	Valle del Cauca, Restrepo	SS-FW; SS-HW; D-FW; V-FW; D-HW; V-HW
LGE-WS-00003	N/A	<i>Heliconius cydno cydnides</i>	Valle del Cauca, Vijes, Carbonero	SS-FW; SS-HW; D-FW; V-FW; D-HW; V-HW
LGE-WS-00004	N/A	<i>Heliconius cydno cydnides</i>	Valle del Cauca, Buenos Aires, Yotoco	SS-FW; SS-HW; D-FW; V-FW; D-HW; V-HW
LGE-WS-00005	N/A	<i>Heliconius cydno cydnides</i>	Valle del Cauca, Cartago	SS-FW; SS-HW; D-FW; V-FW; D-HW; V-HW
LGE-WS-00006	N/A	<i>Heliconius cydno cydnides</i>	Valle del Cauca, Buenos Aires, Yotoco	SS-FW; SS-HW; D-FW; V-FW; D-HW; V-HW
LGE-WS-00007	N/A	<i>Heliconius cydno cydnides</i>	Valle del Cauca, Buenos Aires, Yotoco	SS-FW; SS-HW; D-FW; V-FW; D-HW; V-HW
LGE-WS-00008	N/A	<i>Heliconius cydno cydnides</i>	Valle del Cauca, Buenos Aires, Yotoco	SS-FW; SS-HW; D-FW; V-FW; D-HW; V-HW
LGE-WS-00009	N/A	<i>Heliconius cydno cydnides</i>	Valle del Cauca, Buenos Aires, Yotoco	SS-FW; SS-HW; D-FW; V-FW; D-HW; V-HW
LGE-WS-00010	N/A	<i>Heliconius cydno cydnides</i>	Valle del Cauca, Buenos Aires, Yotoco	SS-FW; SS-HW; D-FW; V-FW; D-HW; V-HW
LGE-WS-00011	N/A	<i>Heliconius cydno cydnides</i>	Valle del Cauca, Buenos Aires, Yotoco	SS-FW; SS-HW; D-FW; V-FW; D-HW; V-HW
LGE-WS-00012	N/A	<i>Heliconius cydno cydnides</i>	Valle del Cauca, Buenos Aires, Yotoco	SS-FW; SS-HW; D-FW; V-FW; D-HW; V-HW
LGE-WS-00013	N/A	<i>Heliconius cydno cydnides</i>	Valle del Cauca, Restrepo, Carbonero	SS-FW; SS-HW; D-FW; V-FW; D-HW; V-HW
LGE-WS-00014	N/A	<i>Heliconius cydno cydnides</i>	Valle del Cauca, Buenos Aires, Yotoco	SS-FW; SS-HW; D-FW; V-FW; D-HW; V-HW
LGE-WS-00015	N/A	<i>Heliconius cydno cydnides</i>	Valle del Cauca, Santa María, Vijes	SS-FW; SS-HW; D-FW; V-FW; D-HW; V-HW
LGE-WS-00016	N/A	<i>Heliconius cydno cydnides</i>	Valle del Cauca, Santa María, Vijes	SS-FW; SS-HW; D-FW; V-FW; D-HW; V-HW
LGE-WS-00017	N/A	<i>Heliconius cydno cydnides</i>	Valle del Cauca, Buenos Aires, Yotoco	SS-FW; SS-HW; D-FW; V-FW; D-HW; V-HW
LGE-WS-00018	N/A	<i>Heliconius cydno cydnides</i>	Valle del Cauca, Restrepo, Carbonero	SS-FW; SS-HW; D-FW; V-FW; D-HW; V-HW
LGE-WS-00019	N/A	<i>Heliconius cydno cydnides</i>	Valle del Cauca, Buenos Aires, Yotoco	SS-FW; SS-HW; D-FW; V-FW; D-HW; V-HW
LGE-WS-00020	N/A	<i>Heliconius cydno cydnides</i>	Valle del Cauca, Buenos Aires, Yotoco	SS-FW; SS-HW; D-FW; V-FW; D-HW; V-HW
LGE-WS-00021	N/A	<i>Heliconius cydno cydnides</i>	Valle del Cauca, Vijes, Carbonero	SS-FW; SS-HW; D-FW; V-FW; D-HW; V-HW
LGE-WS-00022	N/A	<i>Heliconius cydno cydnides</i>	Valle del Cauca, Buenos Aires, Yotoco	SS-FW; SS-HW; D-FW; V-FW; D-HW; V-HW

LGE-WS-00049	N/A	<i>Heliconius cydno cydnides</i>	Valle del Cauca, Vijes, Carbonero	SS-FW; SS-HW; D-FW; V-FW; D-HW; V-HW
LGE-WS-00050	N/A	<i>Heliconius cydno cydnides</i>	Valle del Cauca, Buenos Aires, Yotoco	SS-FW; SS-HW; D-FW; V-FW; D-HW; V-HW
LGE-WS-01851	M3112	<i>Heliconius cydno hermogenes</i>	Tolima, Ibagué, Santafé de los Guaduales	SS-FW; SS-HW; D-FW; V-FW; D-HW; V-HW
LGE-WS-01852	M3113	<i>Heliconius cydno hermogenes</i>	Tolima, Ibagué, Santafé de los Guaduales	SS-FW; SS-HW; D-FW; V-FW; D-HW; V-HW
LGE-WS-01853	M3277	<i>Heliconius cydno hermogenes</i>	Tolima, Ibagué, Santafé de los Guaduales	SS-FW; SS-HW; D-FW; V-FW; D-HW; V-HW
LGE-WS-01854	M3117	<i>Heliconius cydno hermogenes</i>	Tolima, Ibagué, Santafé de los Guaduales	SS-FW; SS-HW; D-FW; V-FW; D-HW; V-HW
LGE-WS-01855	M3278	<i>Heliconius cydno hermogenes</i>	Tolima, Ibagué, Santafé de los Guaduales	SS-FW; SS-HW; D-FW; V-FW; D-HW; V-HW
LGE-WS-01856	M3281	<i>Heliconius cydno hermogenes</i>	Tolima, Ibagué, Santafé de los Guaduales	SS-FW; SS-HW
LGE-WS-01857	M3118	<i>Heliconius cydno hermogenes</i>	Tolima, Ibagué, Santafé de los Guaduales	SS-FW; SS-HW; D-FW; V-FW; D-HW; V-HW
LGE-WS-01751	M2378	<i>Heliconius cydno lisethae</i>	Huila, San Agustín	SS-FW; SS-HW; D-FW; V-FW; D-HW; V-HW
LGE-WS-01752	M2375	<i>Heliconius cydno lisethae</i>	Huila, San Agustín	SS-FW; SS-HW; D-FW; V-FW; D-HW; V-HW
LGE-WS-01753	M2376	<i>Heliconius cydno lisethae</i>	Huila, San Agustín	SS-FW; SS-HW; D-FW; V-FW; D-HW; V-HW
LGE-WS-01754	M2377	<i>Heliconius cydno lisethae</i>	Huila, San Agustín	SS-FW; SS-HW; D-FW; V-FW; D-HW; V-HW
LGE-WS-01755	M2380	<i>Heliconius cydno lisethae</i>	Huila, San Agustín	SS-FW; SS-HW; D-FW; V-FW; D-HW; V-HW
LGE-WS-01756	M3430	<i>Heliconius cydno lisethae</i>	Tolima, Iconozo	SS-FW; SS-HW; D-FW; V-FW; D-HW; V-HW
LGE-WS-01757	M3431	<i>Heliconius cydno lisethae</i>	Tolima, Iconozo	SS-FW; SS-HW; D-FW; V-FW; D-HW; V-HW
LGE-WS-01758	M2382	<i>Heliconius cydno lisethae</i>	Huila, San Agustín	SS-FW; SS-HW; D-FW; V-FW; D-HW; V-HW
LGE-WS-01760	M3390	<i>Heliconius cydno lisethae</i>	Tolima, Iconozo	SS-FW; SS-HW; D-FW; V-FW; D-HW; V-HW
LGE-WS-01761	M3387	<i>Heliconius cydno lisethae</i>	Tolima, Iconozo	SS-FW; SS-HW; D-FW; V-FW; D-HW; V-HW
LGE-WS-01762	M2372	<i>Heliconius cydno lisethae</i>	Huila, San Agustín	SS-FW; SS-HW; D-FW; V-FW; D-HW; V-HW
LGE-WS-01763	M2371	<i>Heliconius cydno lisethae</i>	Huila, San Agustín	SS-FW; SS-HW; D-FW; V-FW; D-HW; V-HW
LGE-WS-01764	M3378	<i>Heliconius cydno lisethae</i>	Tolima, Iconozo	SS-FW; SS-HW; D-FW; V-FW; D-HW; V-HW
LGE-WS-01250	M3316	<i>Heliconius cydno wanningeri</i>	Santander, Tolota	SS-FW; SS-HW; D-FW; V-FW; D-HW; V-HW
LGE-WS-01251	M3318	<i>Heliconius cydno wanningeri</i>	Santander, Tolota	V-FW; V-HW
LGE-WS-01252	M2963	<i>Heliconius cydno wanningeri</i>	Santander, Tolota	SS-FW; SS-HW; D-FW; V-FW; D-HW; V-HW
LGE-WS-01253	M2967	<i>Heliconius cydno wanningeri</i>	Santander, Tolota	SS-FW; SS-HW; D-FW; V-FW; D-HW; V-HW

LGE-WS-01254	M3315	<i>Heliconius cydno wanningeri</i>	Santander, Tolota	SS-FW; SS-HW; D-FW; V-FW; D-HW; V-HW
LGE-WS-01255	M3317	<i>Heliconius cydno wanningeri</i>	Santander, Tolota	V-FW; V-HW
LGE-WS-01256	M3314	<i>Heliconius cydno wanningeri</i>	Santander, Tolota	SS-FW; SS-HW; D-FW; V-FW; D-HW; V-HW
LGE-WS-01257	M2063	<i>Heliconius cydno wanningeri</i>	Santander, Tolota	SS-FW; SS-HW; D-FW; V-FW; D-HW; V-HW
LGE-WS-01258	M2970	<i>Heliconius cydno wanningeri</i>	Santander, Tolota	SS-FW; SS-HW; D-FW; V-FW; D-HW; V-HW
LGE-WS-01259	M2971	<i>Heliconius cydno wanningeri</i>	Santander, Tolota	V-FW; V-HW
LGE-WS-01260	M3003	<i>Heliconius cydno wanningeri</i>	Santander, Tolota	SS-FW; SS-HW; D-FW; V-FW; D-HW; V-HW
LGE-WS-01261	M3004	<i>Heliconius cydno wanningeri</i>	Santander, Tolota	SS-FW; SS-HW; D-FW; V-FW; D-HW; V-HW
LGE-WS-01262	M2958	<i>Heliconius cydno wanningeri</i>	Santander, Tolota	SS-FW; SS-HW; D-FW; V-FW; D-HW; V-HW
LGE-WS-01263	M1589	<i>Heliconius cydno wanningeri</i>	Santander, Tolota	SS-FW; SS-HW; D-FW; V-FW; D-HW; V-HW
LGE-WS-01264	M2959	<i>Heliconius cydno wanningeri</i>	Santander, Tolota	SS-FW; SS-HW; D-FW; V-FW; D-HW; V-HW
LGE-WS-00100	M2569	<i>Heliconius cydno weymeri</i> f. <i>gustavi</i>	Valle del Cauca, Montañitas	SS-FW; SS-HW; D-HW; V-HW
LGE-WS-00101	M2536	<i>Heliconius cydno weymeri</i> f. <i>gustavi</i>	Valle del Cauca, Pance, Topacio	SS-FW; SS-HW; D-HW; V-HW
LGE-WS-00102	M2566	<i>Heliconius cydno weymeri</i> f. <i>gustavi</i>	Valle del Cauca, Montañitas	SS-FW; SS-HW; D-HW; V-HW
LGE-WS-00103	M2535	<i>Heliconius cydno weymeri</i> f. <i>gustavi</i>	Valle del Cauca, Pance, Topacio	SS-FW; SS-HW; D-HW; V-HW
LGE-WS-00104	M954	<i>Heliconius cydno weymeri</i> f. <i>gustavi</i>	Vale del Cauca, El Saladito	SS-FW; SS-HW; D-HW; V-HW
LGE-WS-00105	M2670	<i>Heliconius cydno weymeri</i> f. <i>gustavi</i>	Valle del Cauca, Montañitas	SS-FW; SS-HW; D-HW; V-HW
LGE-WS-00106	M953	<i>Heliconius cydno weymeri</i> f. <i>gustavi</i>	Vale del Cauca, El Saladito	SS-FW; SS-HW; D-HW; V-HW
LGE-WS-00107	M874	<i>Heliconius cydno weymeri</i> f. <i>gustavi</i>	Vale del Cauca, El Saladito	SS-FW; SS-HW; D-HW; V-HW
LGE-WS-00108	N/A	<i>Heliconius cydno weymeri</i> f. <i>gustavi</i>	Cauca, Helechaux	SS-FW; SS-HW; D-HW; V-HW
LGE-WS-00109	N/A	<i>Heliconius cydno weymeri</i> f. <i>gustavi</i>	Cauca, Helechaux	SS-FW; SS-HW; D-HW; V-HW
LGE-WS-00110	N/A	<i>Heliconius cydno weymeri</i> f. <i>gustavi</i>	Cauca, Helechaux	SS-FW; SS-HW; D-HW; V-HW
LGE-WS-00111	N/A	<i>Heliconius cydno weymeri</i> f. <i>gustavi</i>	Cauca, Helechaux	SS-FW; SS-HW; D-HW; V-HW
LGE-WS-00112	N/A	<i>Heliconius cydno weymeri</i> f. <i>gustavi</i>	Cauca, Cartón de Colombia	SS-FW; SS-HW; D-HW; V-HW
LGE-WS-00113	N/A	<i>Heliconius cydno weymeri</i> f. <i>gustavi</i>	Cauca, Helechaux	SS-FW; SS-HW; D-HW; V-HW
LGE-WS-00114	N/A	<i>Heliconius cydno weymeri</i> f. <i>gustavi</i>	Cauca, Cartón de Colombia	SS-FW; SS-HW; D-HW; V-HW

LGE-WS-00115	N/A	<i>Heliconius cydno weymeri f. gustavi</i>	Cauca, Helechaux	SS-FW; SS-HW; D-HW; V-HW
LGE-WS-00116	N/A	<i>Heliconius cydno weymeri f. gustavi</i>	Cauca, Helechaux	SS-FW; SS-HW; D-HW
LGE-WS-00117	N/A	<i>Heliconius cydno weymeri f. gustavi</i>	Cauca, Helechaux	SS-FW; SS-HW; D-HW; V-HW
LGE-WS-00118	N/A	<i>Heliconius cydno weymeri f. gustavi</i>	Cauca, Helechaux	SS-FW; SS-HW; D-HW; V-HW
LGE-WS-00119	N/A	<i>Heliconius cydno weymeri f. gustavi</i>	Cauca, Helechaux	SS-FW; SS-HW; D-HW; V-HW
LGE-WS-00120	N/A	<i>Heliconius cydno weymeri f. gustavi</i>	Cauca, Helechaux	SS-FW; SS-HW; D-HW; V-HW
LGE-WS-00121	N/A	<i>Heliconius cydno weymeri f. gustavi</i>	Cauca, Cartón de Colombia	SS-FW; SS-HW; D-HW; V-HW
LGE-WS-00122	N/A	<i>Heliconius cydno weymeri f. gustavi</i>	Cauca, Helechaux	SS-FW; SS-HW; D-HW; V-HW
LGE-WS-00123	N/A	<i>Heliconius cydno weymeri f. gustavi</i>	Cauca, Helechaux	SS-FW; SS-HW; V-HW
LGE-WS-00124	N/A	<i>Heliconius cydno weymeri f. gustavi</i>	Cauca, Helechaux	SS-FW; SS-HW; V-HW
LGE-WS-00125	M1716	<i>Heliconius cydno weymeri f. gustavi</i>	Valle del Cauca, Pance, Topacio	SS-FW; SS-HW; D-HW; V-HW
LGE-WS-00126	M2676	<i>Heliconius cydno weymeri f. gustavi</i>	Valle del Cauca, Montañitas	SS-FW; SS-HW; D-HW; V-HW
LGE-WS-00128	M2677	<i>Heliconius cydno weymeri f. gustavi</i>	Valle del Cauca, Montañitas	SS-FW; SS-HW; D-HW; V-HW
LGE-WS-00129	N/A	<i>Heliconius cydno weymeri f. gustavi</i>	Cauca, Helechaux	SS-FW; SS-HW; D-HW; V-HW
LGE-WS-00131	N/A	<i>Heliconius cydno weymeri f. gustavi</i>	Cauca, Cartón de Colombia	SS-FW; SS-HW; D-HW; V-HW
LGE-WS-00132	N/A	<i>Heliconius cydno weymeri f. gustavi</i>	Cauca, Helechaux	SS-FW; SS-HW; D-HW; V-HW
LGE-WS-00133	M2045	<i>Heliconius cydno weymeri f. gustavi</i>	Valle del Cauca, Pance, Topacio	SS-FW; SS-HW; D-HW; V-HW
LGE-WS-00134	N/A	<i>Heliconius cydno weymeri f. gustavi</i>	Cauca, Helechaux	SS-FW; SS-HW; D-HW; V-HW
LGE-WS-00135	N/A	<i>Heliconius cydno weymeri f. gustavi</i>	Cauca, Helechaux	SS-FW; SS-HW; D-HW; V-HW
LGE-WS-00136	N/A	<i>Heliconius cydno weymeri f. gustavi</i>	Cauca, Popayán	SS-FW; SS-HW; D-HW; V-HW
LGE-WS-00137	N/A	<i>Heliconius cydno weymeri f. gustavi</i>	Cauca, Cartón de Colombia	SS-FW; SS-HW; D-HW; V-HW
LGE-WS-00138	M2532	<i>Heliconius cydno weymeri f. gustavi</i>	Valle del Cauca, Pance, Topacio	SS-FW; SS-HW; D-HW; V-HW
LGE-WS-00139	N/A	<i>Heliconius cydno weymeri f. gustavi</i>	Cauca, Cartón de Colombia	SS-FW; SS-HW; D-HW; V-HW
LGE-WS-00140	N/A	<i>Heliconius cydno weymeri f. gustavi</i>	Cauca, Cartón de Colombia	SS-FW; SS-HW; D-HW; V-HW
LGE-WS-00141	N/A	<i>Heliconius cydno weymeri f. gustavi</i>	Cauca, Helechaux	SS-FW; SS-HW; D-HW; V-HW
LGE-WS-00142	N/A	<i>Heliconius cydno weymeri f. gustavi</i>	Cauca, Helechaux	SS-FW; SS-HW; D-HW; V-HW

LGE-WS-00143	N/A	<i>Heliconius cydno weymeri f. gustavi</i>	Cauca, Helechaux	SS-FW; SS-HW; D-HW; V-HW
LGE-WS-00144	M952	<i>Heliconius cydno weymeri f. gustavi</i>	Vale del Cauca, El Saladito	SS-FW; SS-HW; D-HW; V-HW
LGE-WS-00145	N/A	<i>Heliconius cydno weymeri f. gustavi</i>	Cauca, Cartón de Colombia	SS-FW; SS-HW; D-HW; V-HW
LGE-WS-00146	N/A	<i>Heliconius cydno weymeri f. gustavi</i>	Cauca, Helechaux	SS-FW; SS-HW; D-HW
LGE-WS-00147	N/A	<i>Heliconius cydno weymeri f. gustavi</i>	Cauca, Helechaux	SS-FW; SS-H; D-HW; V-HW
LGE-WS-00148	N/A	<i>Heliconius cydno weymeri f. gustavi</i>	Cauca, Helechaux	SS-FW; SS-H; D-HW; V-HW
LGE-WS-00149	N/A	<i>Heliconius cydno weymeri f. gustavi</i>	Cauca, Helechaux	SS-FW; SS-H; D-HW; V-HW
LGE-WS-00150	M935	<i>Heliconius cydno weymeri f. gustavi</i>	Vale del Cauca, El Saladito	SS-FW; SS-H; D-HW; V-HW
LGE-WS-00751	N/A	<i>Heliconius cydno weymeri f. submarginatus</i>	Lab recreated	SS-FW; SS-HW; D-FW; V-FW; D-HW; V-HW
LGE-WS-00752	N/A	<i>Heliconius cydno weymeri f. submarginatus</i>	Lab recreated	SS-FW; SS-HW; D-FW; V-FW; D-HW; V-HW
LGE-WS-00753	N/A	<i>Heliconius cydno weymeri f. submarginatus</i>	Lab recreated	SS-FW; SS-HW
LGE-WS-00754	N/A	<i>Heliconius cydno weymeri f. submarginatus</i>	Lab recreated	SS-FW; SS-HW; D-FW; V-FW; D-HW; V-HW
LGE-WS-00755	N/A	<i>Heliconius cydno weymeri f. submarginatus</i>	Lab recreated	SS-FW; SS-HW; D-FW; V-FW; D-HW; V-HW
LGE-WS-00756	N/A	<i>Heliconius cydno weymeri f. submarginatus</i>	Lab recreated	SS-FW; SS-HW; D-FW; V-FW; D-HW; V-HW
LGE-WS-00757	N/A	<i>Heliconius cydno weymeri f. submarginatus</i>	Lab recreated	SS-FW; SS-HW; D-FW; V-FW; D-HW; V-HW
LGE-WS-00758	N/A	<i>Heliconius cydno weymeri f. submarginatus</i>	Lab recreated	SS-FW; SS-HW; D-FW; V-FW; D-HW; V-HW
LGE-WS-00759	N/A	<i>Heliconius cydno weymeri f. submarginatus</i>	Lab recreated	SS-FW; SS-HW; D-FW; V-FW; D-HW; V-HW
LGE-WS-00760	N/A	<i>Heliconius cydno weymeri f. submarginatus</i>	Lab recreated	SS-FW; SS-HW; D-FW; V-FW; D-HW; V-HW
LGE-WS-00761	N/A	<i>Heliconius cydno weymeri f. submarginatus</i>	Lab recreated	SS-FW; SS-HW; D-FW; V-FW; D-HW; V-HW
LGE-WS-00762	N/A	<i>Heliconius cydno weymeri f. submarginatus</i>	Lab recreated	SS-FW; SS-HW; D-FW; V-FW; D-HW; V-HW
LGE-WS-00763	N/A	<i>Heliconius cydno weymeri f. submarginatus</i>	Lab recreated	SS-FW; SS-HW; D-FW; V-FW; D-HW; V-HW
LGE-WS-00764	N/A	<i>Heliconius cydno weymeri f. submarginatus</i>	Lab recreated	SS-FW; SS-HW; V-HW
LGE-WS-00765	N/A	<i>Heliconius cydno weymeri f. submarginatus</i>	Lab recreated	SS-FW; SS-HW; D-FW; V-FW; D-HW; V-HW
LGE-WS-00766	N/A	<i>Heliconius cydno weymeri f. submarginatus</i>	Lab recreated	SS-FW; SS-HW; D-FW; V-FW; D-HW; V-HW
LGE-WS-00767	N/A	<i>Heliconius cydno weymeri f. submarginatus</i>	Lab recreated	SS-FW; SS-HW; D-FW; V-FW; D-HW; V-HW
LGE-WS-00768	N/A	<i>Heliconius cydno weymeri f. submarginatus</i>	Lab recreated	SS-FW; SS-HW; D-FW; V-FW; D-HW; V-HW

LGE-WS-00795	N/A	<i>Heliconius cydno weymeri</i> f. <i>submarginatus</i>	Lab recreated	SS-FW; SS-HW; D-FW; V-FW; D-HW; V-HW
LGE-WS-00796	N/A	<i>Heliconius cydno weymeri</i> f. <i>submarginatus</i>	Lab recreated	V-FW; V-HW
LGE-WS-00797	N/A	<i>Heliconius cydno weymeri</i> f. <i>submarginatus</i>	Lab recreated	SS-FW; SS-HW; D-FW; D-HW
LGE-WS-00798	N/A	<i>Heliconius cydno weymeri</i> f. <i>submarginatus</i>	Lab recreated	SS-FW; SS-HW; D-FW; D-HW
LGE-WS-00799	N/A	<i>Heliconius cydno weymeri</i> f. <i>submarginatus</i>	Lab recreated	SS-FW; SS-HW; D-FW; D-HW
LGE-WS-00800	N/A	<i>Heliconius cydno weymeri</i> f. <i>submarginatus</i>	Lab recreated	SS-FW; SS-HW; D-FW; D-HW
LGE-WS-00201	N/A	<i>Heliconius cydno weymeri</i> f. <i>weymeri</i>	Cauca, Helechaux	SS-FW; SS-HW; D-FW; V-FW; D-HW; V-HW
LGE-WS-00202	N/A	<i>Heliconius cydno weymeri</i> f. <i>weymeri</i>	Cauca, Helechaux	SS-FW; SS-HW; V-FW
LGE-WS-00203	N/A	<i>Heliconius cydno weymeri</i> f. <i>weymeri</i>	Cauca, Helechaux	SS-FW; SS-HW; V-FW; V-HW
LGE-WS-00204	N/A	<i>Heliconius cydno weymeri</i> f. <i>weymeri</i>	Cauca, Helechaux	SS-FW; SS-HW; D-FW; V-FW; D-HW; V-HW
LGE-WS-00205	N/A	<i>Heliconius cydno weymeri</i> f. <i>weymeri</i>	Cauca, Helechaux	SS-FW; SS-HW; D-FW; V-FW; D-HW; V-HW
LGE-WS-00206	N/A	<i>Heliconius cydno weymeri</i> f. <i>weymeri</i>	Cauca, Helechaux	SS-FW; SS-HW; D-FW; V-FW; D-HW; V-HW
LGE-WS-00207	N/A	<i>Heliconius cydno weymeri</i> f. <i>weymeri</i>	Cauca, Helechaux	SS-FW; SS-HW; V-FW; V-HW
LGE-WS-00208	N/A	<i>Heliconius cydno weymeri</i> f. <i>weymeri</i>	Cauca, Helechaux	SS-FW; SS-HW; D-FW; V-FW; D-HW; V-HW
LGE-WS-00209	N/A	<i>Heliconius cydno weymeri</i> f. <i>weymeri</i>	Cauca, Helechaux	SS-FW; SS-HW; D-FW; V-FW; D-HW; V-HW
LGE-WS-00210	N/A	<i>Heliconius cydno weymeri</i> f. <i>weymeri</i>	Cauca, Helechaux	SS-FW; SS-HW; D-FW; V-FW; D-HW; V-HW
LGE-WS-00211	N/A	<i>Heliconius cydno weymeri</i> f. <i>weymeri</i>	Cauca, Helechaux	SS-FW; SS-HW; D-FW; V-FW; D-HW; V-HW
LGE-WS-00212	N/A	<i>Heliconius cydno weymeri</i> f. <i>weymeri</i>	Vale del Cauca, El Saladito	SS-FW; SS-HW; D-FW; V-FW; D-HW; V-HW
LGE-WS-00213	N/A	<i>Heliconius cydno weymeri</i> f. <i>weymeri</i>	Vale del Cauca, El Saladito	SS-FW; SS-HW; D-FW; V-FW; D-HW; V-HW
LGE-WS-00214	N/A	<i>Heliconius cydno weymeri</i> f. <i>weymeri</i>	Vale del Cauca, El Saladito	SS-FW; SS-HW; D-FW; V-FW; D-HW; V-HW
LGE-WS-00215	N/A	<i>Heliconius cydno weymeri</i> f. <i>weymeri</i>	Vale del Cauca, El Saladito	SS-FW; SS-HW; D-FW; V-FW; D-HW; V-HW
LGE-WS-00216	N/A	<i>Heliconius cydno weymeri</i> f. <i>weymeri</i>	Vale del Cauca, El Saladito	SS-FW; SS-HW; D-FW; V-FW; D-HW; V-HW
LGE-WS-00217	N/A	<i>Heliconius cydno weymeri</i> f. <i>weymeri</i>	Vale del Cauca, El Saladito	SS-FW; SS-HW; D-FW; V-FW; D-HW; V-HW
LGE-WS-00218	N/A	<i>Heliconius cydno weymeri</i> f. <i>weymeri</i>	Vale del Cauca, El Saladito	SS-FW; SS-HW; V-FW; V-HW
LGE-WS-00219	N/A	<i>Heliconius cydno weymeri</i> f. <i>weymeri</i>	Vale del Cauca, El Saladito	SS-FW; SS-HW; D-FW; V-FW; D-HW; V-HW
LGE-WS-00220	N/A	<i>Heliconius cydno weymeri</i> f. <i>weymeri</i>	Vale del Cauca, El Saladito	SS-FW; SS-HW; D-FW; V-FW; D-HW; V-HW

LGE-WS-00221	N/A	<i>Heliconius cydno weymeri</i> f. <i>weymeri</i>	Vale del Cauca, El Saladito	SS-FW; SS-HW; D-FW; V-FW; D-HW; V-HW
LGE-WS-00222	N/A	<i>Heliconius cydno weymeri</i> f. <i>weymeri</i>	Vale del Cauca, El Saladito	SS-FW; SS-HW; D-FW; V-FW; D-HW; V-HW
LGE-WS-00223	N/A	<i>Heliconius cydno weymeri</i> f. <i>weymeri</i>	Vale del Cauca, El Saladito	SS-FW; SS-HW; D-FW; V-FW; D-HW; V-HW
LGE-WS-00224	N/A	<i>Heliconius cydno weymeri</i> f. <i>weymeri</i>	Vale del Cauca, El Saladito	SS-FW; SS-HW; D-FW; V-FW; D-HW; V-HW
LGE-WS-00225	N/A	<i>Heliconius cydno weymeri</i> f. <i>weymeri</i>	Valle del Cauca, Villa Carmelo, Río Melendez	SS-FW; SS-HW; D-FW; V-FW; D-HW; V-HW
LGE-WS-00226	N/A	<i>Heliconius cydno weymeri</i> f. <i>weymeri</i>	Valle del Cauca, Villa Carmelo, Río Melendez	SS-FW; SS-HW; V-FW
LGE-WS-00227	N/A	<i>Heliconius cydno weymeri</i> f. <i>weymeri</i>	Valle del Cauca, Villa Carmelo, Río Melendez	SS-FW; SS-HW; D-FW; V-FW; D-HW; V-HW
LGE-WS-00228	N/A	<i>Heliconius cydno weymeri</i> f. <i>weymeri</i>	Valle del Cauca, Monterrico, Tocota	SS-FW; SS-HW; D-FW; V-FW; D-HW; V-HW
LGE-WS-00229	N/A	<i>Heliconius cydno weymeri</i> f. <i>weymeri</i>	Valle del Cauca, Villa Carmelo, Río Melendez	SS-FW; SS-HW; D-FW; V-FW; D-HW; V-HW
LGE-WS-00230	N/A	<i>Heliconius cydno weymeri</i> f. <i>weymeri</i>	Valle del Cauca, Villa Carmelo, Río Melendez	SS-FW; SS-HW; D-FW; V-FW; D-HW; V-HW
LGE-WS-00231	N/A	<i>Heliconius cydno weymeri</i> f. <i>weymeri</i>	Valle del Cauca, Villa Carmelo, Río Melendez	SS-FW; SS-HW; D-FW; V-FW; D-HW; V-HW
LGE-WS-00232	N/A	<i>Heliconius cydno weymeri</i> f. <i>weymeri</i>	Valle del Cauca, Monterrico	SS-FW; SS-HW; D-FW; V-FW; D-HW; V-HW
LGE-WS-00233	N/A	<i>Heliconius cydno weymeri</i> f. <i>weymeri</i>	Vale del Cauca, El Saladito	
LGE-WS-00234	N/A	<i>Heliconius cydno weymeri</i> f. <i>weymeri</i>	Vale del Cauca, El Saladito	SS-FW; SS-HW; D-FW; V-FW; D-HW; V-HW
LGE-WS-00235	N/A	<i>Heliconius cydno weymeri</i> f. <i>weymeri</i>	Valle del Cauca, Monterrico, Tocota	SS-FW; SS-HW; D-FW; V-FW; D-HW; V-HW
LGE-WS-00236	N/A	<i>Heliconius cydno weymeri</i> f. <i>weymeri</i>	Valle del Cauca, Villa Carmelo, Río Melendez	SS-FW; SS-HW; D-FW; V-FW; D-HW; V-HW
LGE-WS-00237	N/A	<i>Heliconius cydno weymeri</i> f. <i>weymeri</i>	Valle del Cauca, Villa Carmelo, Río Melendez	SS-FW; SS-HW; D-FW; V-FW; D-HW; V-HW
LGE-WS-00238	N/A	<i>Heliconius cydno weymeri</i> f. <i>weymeri</i>	Valle del Cauca, Cali, Río Aguacatal	SS-FW; SS-HW; D-FW; V-FW; D-HW; V-HW
LGE-WS-00239	N/A	<i>Heliconius cydno weymeri</i> f. <i>weymeri</i>	Valle del Cauca, Jamundí, San Antonio	SS-FW; SS-HW; V-FW
LGE-WS-00240	N/A	<i>Heliconius cydno weymeri</i> f. <i>weymeri</i>	Valle del Cauca, Pance, La Voragine	SS-FW; SS-HW; D-FW; V-FW; D-HW; V-HW
LGE-WS-00241	N/A	<i>Heliconius cydno weymeri</i> f. <i>weymeri</i>	Valle del Cauca, Pance, La Voragine	SS-FW; SS-HW; D-FW; V-FW; D-HW; V-HW
LGE-WS-00242	N/A	<i>Heliconius cydno weymeri</i> f. <i>weymeri</i>	Valle del Cauca, Pance, La Voragine	SS-FW; SS-HW; D-FW; V-FW; D-HW; V-HW
LGE-WS-00243	N/A	<i>Heliconius cydno weymeri</i> f. <i>weymeri</i>	Valle del Cauca, Villa Carmelo, Río Melendez	SS-FW; SS-HW; D-FW; V-FW; D-HW; V-HW
LGE-WS-00244	N/A	<i>Heliconius cydno weymeri</i> f. <i>weymeri</i>	Cauca, Cartón de Colombia	SS-FW; SS-HW; V-FW; V-HW
LGE-WS-00245	N/A	<i>Heliconius cydno weymeri</i> f. <i>weymeri</i>	Valle del Cauca, Pance, La Voragine	V-FW; V-HW
LGE-WS-00246	N/A	<i>Heliconius cydno weymeri</i> f. <i>weymeri</i>	Cauca, Cartón de Colombia	SS-FW; SS-HW; D-FW; V-FW; D-HW; V-HW
LGE-WS-00247	N/A	<i>Heliconius cydno weymeri</i> f. <i>weymeri</i>	Vale del Cauca, El Saladito	SS-FW; SS-HW; D-FW; V-FW; D-HW

LGE-WS-00248	N/A	<i>Heliconius cydno weymeri</i> f. <i>weymeri</i>	Cauca, Cartón de Colombia	SS-FW; SS-HW; D-FW; V-FW; D-HW
LGE-WS-00249	N/A	<i>Heliconius cydno weymeri</i> f. <i>weymeri</i>	Cauca, Cartón de Colombia	SS-FW; SS-HW; D-FW; V-FW; D-HW
LGE-WS-00250	N/A	<i>Heliconius cydno weymeri</i> f. <i>weymeri</i>	Cauca, Cartón de Colombia	SS-FW; SS-HW; D-FW; V-FW; D-HW
LGE-WS-00251	N/A	<i>Heliconius cydno weymeri</i> f. <i>weymeri</i>	Cauca, Cartón de Colombia	SS-FW; SS-HW; V-FW
LGE-WS-00452	N/A	<i>Heliconius cydno zelinde</i>	Valle del Cauca, Atuncela	SS-FW; SS-HW; D-FW; V-FW
LGE-WS-00453	N/A	<i>Heliconius cydno zelinde</i>	Valle del Cauca, Rio Bravo, Lago Calima	SS-FW; SS-HW; D-FW; V-FW
LGE-WS-00454	N/A	<i>Heliconius cydno zelinde</i>	Valle del Cauca, Rio Bravo, Lago Calima	SS-FW; SS-HW; D-FW; V-FW
LGE-WS-00455	N/A	<i>Heliconius cydno zelinde</i>	Valle del Cauca, Atuncela	SS-FW; SS-HW; D-FW; V-FW
LGE-WS-00456	N/A	<i>Heliconius cydno zelinde</i>	Valle del Cauca, Atuncela	SS-FW; SS-HW; D-FW; V-FW
LGE-WS-00457	N/A	<i>Heliconius cydno zelinde</i>	Valle_del_Cauca, Quebrada La Cristalina	SS-FW; SS-HW; D-FW; V-FW
LGE-WS-00458	N/A	<i>Heliconius cydno zelinde</i>	Valle_del_Cauca, Quebrada La Cristalina	SS-FW; SS-HW; D-FW; V-FW
LGE-WS-00459	N/A	<i>Heliconius cydno zelinde</i>	Valle del Cauca, Cisneros	SS-FW; SS-HW; D-FW; V-FW
LGE-WS-00460	N/A	<i>Heliconius cydno zelinde</i>	Valle_del_Cauca, Quebrada La Cristalina	SS-FW; SS-HW; D-FW; V-FW
LGE-WS-00461	N/A	<i>Heliconius cydno zelinde</i>	Cauca, Playa Rica, 20 de Julio	SS-FW; D-FW; V-FW
LGE-WS-00462	N/A	<i>Heliconius cydno zelinde</i>	Cauca, Playa Rica, 20 de Julio	SS-FW; SS-HW; D-FW
LGE-WS-00463	N/A	<i>Heliconius cydno zelinde</i>	Valle del Cauca, Cartago, San José del Palmar	SS-FW; SS-HW; D-FW; V-FW
LGE-WS-00464	N/A	<i>Heliconius cydno zelinde</i>	Valle del Cauca, Quebrada La Vibora	SS-FW; SS-HW; D-FW; V-FW
LGE-WS-00465	N/A	<i>Heliconius cydno zelinde</i>	Valle_del_Cauca, Quebrada La Cristalina	SS-FW; SS-HW; D-FW; V-FW
LGE-WS-00466	N/A	<i>Heliconius cydno zelinde</i>	Valle del Cauca, Alto de Anchicayá	SS-FW; SS-HW; D-FW; V-FW
LGE-WS-00467	N/A	<i>Heliconius cydno zelinde</i>	Valle_del_Cauca, Queremal	V-FW
LGE-WS-00468	N/A	<i>Heliconius cydno zelinde</i>	Valle_del_Cauca, Queremal	SS-FW; SS-HW; D-FW; V-FW
LGE-WS-00469	N/A	<i>Heliconius cydno zelinde</i>	Valle_del_Cauca, Quebrada La Cristalina	SS-FW; SS-HW; D-FW; V-FW
LGE-WS-00470	N/A	<i>Heliconius cydno zelinde</i>	Valle del Cauca, Cartago, San José del Palmar	SS-FW; SS-HW; D-FW; V-FW
LGE-WS-00471	M3493	<i>Heliconius cydno zelinde</i>	Valle del Cauca, Cartago, San José del Palmar	SS-FW; SS-HW; D-FW; V-FW
LGE-WS-00472	N/A	<i>Heliconius cydno zelinde</i>	Valle del Cauca, San Pedro	SS-FW; SS-HW; D-FW; V-FW
LGE-WS-00473	N/A	<i>Heliconius cydno zelinde</i>	Cauca, Playa Rica, 20 de Julio	SS-FW; SS-HW; D-FW; V-FW

LGE-WS-00474	N/A	<i>Heliconius cydno zelinde</i>	Valle del Cauca, Rio Bravo, Lago Calima	SS-FW; SS-HW; D-FW; V-FW
LGE-WS-00475	N/A	<i>Heliconius cydno zelinde</i>	Valle_del_Cauca, Quebrada La Cristalina	SS-FW; SS-HW; D-FW; V-FW
LGE-WS-00476	N/A	<i>Heliconius cydno zelinde</i>	Valle_del_Cauca, Quebrada La Cristalina	SS-FW; SS-HW; D-FW; V-FW
LGE-WS-00477	N/A	<i>Heliconius cydno zelinde</i>	Cauca, Playa Rica, 20 de Julio	SS-FW; SS-HW; D-FW; V-FW
LGE-WS-00478	N/A	<i>Heliconius cydno zelinde</i>	Valle del Cauca, Cartago, San José del Palmar	SS-FW; SS-HW; D-FW; V-FW
LGE-WS-00479	N/A	<i>Heliconius cydno zelinde</i>	Valle_del_Cauca, Quebrada La Cristalina	SS-FW; SS-HW; D-FW; V-FW
LGE-WS-00480	N/A	<i>Heliconius cydno zelinde</i>	Valle del Cauca, San Pedro	SS-FW; SS-HW; D-FW; V-FW
LGE-WS-00481	N/A	<i>Heliconius cydno zelinde</i>	Valle del Cauca, Ladrilleros	SS-FW; SS-HW; D-FW; V-FW
LGE-WS-00482	N/A	<i>Heliconius cydno zelinde</i>	Valle del Cauca, Cartago, San José del Palmar	SS-FW; SS-HW; D-FW; V-FW
LGE-WS-00483	N/A	<i>Heliconius cydno zelinde</i>	Valle del Cauca, Cartago, San José del Palmar	SS-FW; SS-HW; D-FW; V-FW
LGE-WS-00484	M2264	<i>Heliconius cydno zelinde</i>	Valle del Cauca, Ladrilleros	SS-FW; SS-HW; D-FW; V-FW
LGE-WS-00485	N/A	<i>Heliconius cydno zelinde</i>	Valle del Cauca, Rio Bravo, Lago Calima	SS-FW; SS-HW; D-FW; V-FW
LGE-WS-00486	N/A	<i>Heliconius cydno zelinde</i>	Valle del Cauca, Rio Bravo, Lago Calima	SS-FW; SS-HW; D-FW; V-FW
LGE-WS-00487	N/A	<i>Heliconius cydno zelinde</i>	Valle_del_Cauca, Quebrada La Cristalina	SS-FW; SS-HW; D-FW; V-FW
LGE-WS-00488	N/A	<i>Heliconius cydno zelinde</i>	Valle del Cauca, Ladrilleros	SS-FW; SS-HW; D-FW; V-FW
LGE-WS-00489	N/A	<i>Heliconius cydno zelinde</i>	Valle del Cauca, Ladrilleros	SS-FW; SS-HW; D-FW; V-FW
LGE-WS-00490	N/A	<i>Heliconius cydno zelinde</i>	Valle del Cauca, Km55 vía Buenaventura-Queremal	SS-FW; SS-HW; D-FW; V-FW
LGE-WS-00492	N/A	<i>Heliconius cydno zelinde</i>	Valle_del_Cauca, Quebrada La Cristalina	SS-FW; SS-HW; D-FW
LGE-WS-00493	N/A	<i>Heliconius cydno zelinde</i>	Valle del Cauca, Cartago, San José del Palmar	SS-FW; SS-HW; D-FW; V-FW
LGE-WS-00494	N/A	<i>Heliconius cydno zelinde</i>	Valle_del_Cauca, Calima	SS-FW; SS-HW; D-FW; V-FW
LGE-WS-00495	N/A	<i>Heliconius cydno zelinde</i>	Valle del Cauca, Alto de Anchicayá	SS-FW; SS-HW; D-FW; V-FW
LGE-WS-00496	M3490	<i>Heliconius cydno zelinde</i>	Valle del Cauca, San Pedro	SS-FW; SS-HW; D-FW; V-FW
LGE-WS-00497	N/A	<i>Heliconius cydno zelinde</i>	Valle del Cauca, Cartago, San José del Palmar	SS-FW; SS-HW; D-FW
LGE-WS-00498	N/A	<i>Heliconius cydno zelinde</i>	Valle_del_Cauca, Quebrada La Cristalina	SS-FW; SS-HW; D-FW; V-FW
LGE-WS-00499	M2261	<i>Heliconius cydno zelinde</i>	Valle del Cauca, Ladrilleros	SS-FW; SS-HW; D-FW; V-FW
LGE-WS-00501	M3506	<i>Heliconius cydno zelinde</i>	Valle del Cauca, San Pedro	SS-FW; SS-HW; D-FW; V-FW

LGE-WS-02604	M1033	<i>Heliconius cydno zelinde</i>	Valle del Cauca, Ladrilleros	SS-FW; SS-HW; D-FW; V-FW
LGE-WS-02605	M1029	<i>Heliconius cydno zelinde</i>	Valle del Cauca, La Barra	SS-FW; SS-HW; D-FW; V-FW
LGE-WS-02606	M2270	<i>Heliconius cydno zelinde</i>	Valle del Cauca, Ladrilleros	SS-FW; SS-HW; D-FW; V-FW
LGE-WS-01650	M3853	<i>Heliconius cydno</i> spp. nov.	Cauca, Isla Gorgona	SS-FW; SS-HW; D-FW; V-FW; D-HW; V-HW
LGE-WS-01651	M3854	<i>Heliconius cydno</i> spp. nov.	Cauca, Isla Gorgona	SS-FW; SS-HW; D-FW; V-FW; D-HW; V-HW
LGE-WS-00051	N/A	<i>Heliconius eleuchia eleuchia</i>	Valle del Cauca, Buenos Aires, Yotoco	SS-FW; SS-HW; D-FW; V-FW; D-HW; V-HW
LGE-WS-00052	N/A	<i>Heliconius eleuchia eleuchia</i>	Valle del Cauca, Santa María, Vijes	SS-FW; SS-HW; D-FW; V-FW; D-HW; V-HW
LGE-WS-00053	N/A	<i>Heliconius eleuchia eleuchia</i>	Valle del Cauca, Santa María, Vijes	SS-FW; SS-HW; D-FW; D-HW
LGE-WS-00054	N/A	<i>Heliconius eleuchia eleuchia</i>	Valle del Cauca, Buenos Aires, Yotoco	SS-FW; SS-HW; D-FW; V-FW; D-HW; V-HW
LGE-WS-00055	N/A	<i>Heliconius eleuchia eleuchia</i>	Valle del Cauca, Buenos Aires, Yotoco	SS-FW; D-FW; D-HW
LGE-WS-00056	N/A	<i>Heliconius eleuchia eleuchia</i>	Valle del Cauca, Buenos Aires, Yotoco	SS-FW; SS-HW; D-FW; V-FW; D-HW; V-HW
LGE-WS-00057	N/A	<i>Heliconius eleuchia eleuchia</i>	Valle del Cauca, Buenos Aires, Yotoco	SS-FW; SS-HW; D-FW
LGE-WS-00058	N/A	<i>Heliconius eleuchia eleuchia</i>	Valle del Cauca, Buenos Aires	SS-FW; SS-HW; D-FW; V-FW; D-HW; V-HW
LGE-WS-00059	N/A	<i>Heliconius eleuchia eleuchia</i>	Valle del Cauca, Buenos Aires	SS-FW; SS-HW; D-FW; V-FW; D-HW; V-HW
LGE-WS-00060	N/A	<i>Heliconius eleuchia eleuchia</i>	Valle del Cauca, Buenos Aires	SS-FW; SS-HW; D-FW; D-HW
LGE-WS-00061	N/A	<i>Heliconius eleuchia eleuchia</i>	Valle del Cauca, Buenos Aires	SS-FW; SS-HW; D-FW; V-FW; D-HW; V-HW
LGE-WS-00062	N/A	<i>Heliconius eleuchia eleuchia</i>	Valle del Cauca, Montañitas	SS-FW; SS-HW; D-FW; V-FW; D-HW; V-HW
LGE-WS-00063	N/A	<i>Heliconius eleuchia eleuchia</i>	Valle del Cauca, Buenos Aires	SS-FW; SS-HW; D-FW; V-FW; D-HW; V-HW
LGE-WS-00064	N/A	<i>Heliconius eleuchia eleuchia</i>	Valle del Cauca, Montañitas	SS-FW; SS-HW; D-FW; V-FW; D-HW; V-HW
LGE-WS-00065	N/A	<i>Heliconius eleuchia eleuchia</i>	Valle del Cauca, Montañitas	SS-FW; SS-HW; D-FW; V-FW; D-HW; V-HW
LGE-WS-00066	N/A	<i>Heliconius eleuchia eleuchia</i>	Valle del Cauca, Montañitas	SS-FW; SS-HW; D-FW
LGE-WS-00067	N/A	<i>Heliconius eleuchia eleuchia</i>	Magdalena, Santa Marta, Minca	SS-FW; SS-HW; D-FW; V-FW; D-HW; V-HW
LGE-WS-00068	N/A	<i>Heliconius eleuchia eleuchia</i>	Valle del Cauca, Buenos Aires, Yotoco	SS-FW; D-FW
LGE-WS-00069	N/A	<i>Heliconius eleuchia eleuchia</i>	Valle del Cauca, Buenos Aires	V-FW; V-HW
LGE-WS-00070	N/A	<i>Heliconius eleuchia eleuchia</i>	Valle del Cauca, Vijes, Carbonero	SS-FW; SS-HW; D-FW; V-FW; D-HW; V-HW
LGE-WS-00071	N/A	<i>Heliconius eleuchia eleuchia</i>	Magdalena, Santa Marta, Minca	SS-FW; SS-HW; D-FW; V-FW; D-HW; V-HW

LGE-WS-00072	N/A	<i>Heliconius eleuchia eleuchia</i>	Valle del Cauca, Vijes, Carbonero	SS-FW; SS-HW; D-FW; V-FW; D-HW; V-HW
LGE-WS-00073	N/A	<i>Heliconius eleuchia eleuchia</i>	Valle del Cauca, Vijes, Carbonero	SS-FW; SS-HW; D-FW; V-FW; D-HW; V-HW
LGE-WS-00074	N/A	<i>Heliconius eleuchia eleuchia</i>	Valle del Cauca, Río Pichinde	SS-FW; SS-HW; D-FW; V-FW; D-HW; V-HW
LGE-WS-00075	N/A	<i>Heliconius eleuchia eleuchia</i>	Valle del Cauca, Río Pichinde	SS-FW; SS-HW; D-FW; V-FW; D-HW; V-HW
LGE-WS-00076	N/A	<i>Heliconius eleuchia eleuchia</i>	Valle del Cauca, Vijes, Carbonero	SS-FW; SS-HW; D-FW; V-FW; D-HW; V-HW
LGE-WS-00077	N/A	<i>Heliconius eleuchia eleuchia</i>	Vale del Cauca, El Saladito	SS-FW; SS-HW; D-FW; V-FW; D-HW; V-HW
LGE-WS-00078	N/A	<i>Heliconius eleuchia eleuchia</i>	Valle del Cauca, Buenos Aires	SS-FW; SS-HW; D-FW; V-FW; D-HW; V-HW
LGE-WS-00079	N/A	<i>Heliconius eleuchia eleuchia</i>	Valle del Cauca, Vijes, Carbonero	SS-FW; SS-HW; D-FW; D-HW
LGE-WS-00080	N/A	<i>Heliconius eleuchia eleuchia</i>	Valle del Cauca, Buenos Aires	SS-FW; SS-HW; D-FW; V-FW; D-HW; V-HW
LGE-WS-00081	N/A	<i>Heliconius eleuchia eleuchia</i>	Valle del Cauca, Vijes, Carbonero	SS-FW; SS-HW; D-FW
LGE-WS-00082	N/A	<i>Heliconius eleuchia eleuchia</i>	Magdalena, Santa Marta, Minca	SS-FW; SS-HW; D-FW; V-FW; D-HW; V-HW
LGE-WS-00083	N/A	<i>Heliconius eleuchia eleuchia</i>	Huila, Colombia	SS-FW; SS-HW; D-FW; V-FW; D-HW; V-HW
LGE-WS-00084	N/A	<i>Heliconius eleuchia eleuchia</i>	Huila, Colombia	SS-FW; SS-HW; D-FW
LGE-WS-00085	M2792	<i>Heliconius eleuchia eleuchia</i>	Santander, Bucaramanga, Manzanares	SS-FW; SS-HW; D-FW; V-FW; D-HW; V-HW
LGE-WS-00086	N/A	<i>Heliconius eleuchia eleuchia</i>	Valle del Cauca, Buenos Aires	SS-FW; SS-HW; D-FW; V-FW; D-HW; V-HW
LGE-WS-00087	N/A	<i>Heliconius eleuchia eleuchia</i>	Valle del Cauca, Buenos Aires	SS-FW; SS-HW; D-FW; V-FW; D-HW; V-HW
LGE-WS-00088	N/A	<i>Heliconius eleuchia eleuchia</i>	Valle del Cauca, Buenos Aires	SS-FW; SS-HW; D-FW; V-FW; D-HW; V-HW
LGE-WS-00089	N/A	<i>Heliconius eleuchia eleuchia</i>	Boyacá, Otanche	SS-FW; SS-HW; D-FW; V-FW; V-HW
LGE-WS-00092	N/A	<i>Heliconius eleuchia eleuchia</i>	Valle del Cauca, Buenos Aires, Yotoco	SS-FW; SS-HW; D-FW; V-FW; D-HW; V-HW
LGE-WS-00093	N/A	<i>Heliconius eleuchia eleuchia</i>	Valle del Cauca, Buenos Aires	SS-FW; SS-HW; D-FW
LGE-WS-00094	N/A	<i>Heliconius eleuchia eleuchia</i>	Valle del Cauca, Calima, El Pital	SS-FW; SS-HW; D-FW
LGE-WS-00095	N/A	<i>Heliconius eleuchia eleuchia</i>	Valle del Cauca, Buenos Aires	SS-FW; SS-HW; D-FW; V-FW; D-HW; V-HW
LGE-WS-00096	N/A	<i>Heliconius eleuchia eleuchia</i>	Vale del Cauca, El Saladito	SS-FW; SS-HW; D-FW; V-FW; D-HW; V-HW
LGE-WS-00097	M2793	<i>Heliconius eleuchia eleuchia</i>	Santander, Bucaramanga, Manzanares	SS-FW; SS-HW; D-FW; V-FW; D-HW; V-HW
LGE-WS-00099	M3106	<i>Heliconius eleuchia eleuchia</i>	Tolima, Ibagué, Santafé de los Guaduales	SS-FW; SS-HW; D-FW; V-FW; D-HW; V-HW
LGE_WS_02601	M3105	<i>Heliconius eleuchia eleuchia</i>	Tolima, Ibagué, Santafé de los Guaduales	SS-FW; SS-HW; D-FW; V-FW; V-HW

LGE_WS_02602	M4403	<i>Heliconius eleuchia eleuchia</i>	Santander, Florencia	SS-FW; SS-HW; D-FW; V-FW; V-HW
LGE_WS_02603	M2458	<i>Heliconius eleuchia eleuchia</i>	Cundinamarca, Peru, Guaduas	SS-FW; SS-HW; D-FW
LGE-WS-01349	M3670	<i>Heliconius eleuchia eleusinus</i>	Valle del Cauca, Rio Bravo, Lago Calima	SS-FW; SS-HW; D-FW; V-FW
LGE-WS-01350	M4871	<i>Heliconius eleuchia eleusinus</i>	Valle del Cauca, El Darién	SS-FW; SS-HW; D-FW; V-FW
LGE-WS-01351	JFLC	<i>Heliconius eleuchia eleusinus</i>	Nariño, Junín	SS-FW; SS-HW; D-FW; V-FW
LGE-WS-01353	JFLC	<i>Heliconius eleuchia eleusinus</i>	Valle_del_Cauca, Queremal	SS-FW; SS-HW; D-FW; V-FW
LGE-WS-01354	JFLC	<i>Heliconius eleuchia eleusinus</i>	Caldas, Taiba	SS-FW; SS-HW; D-FW; V-FW
LGE-WS-01355	JFLC	<i>Heliconius eleuchia eleusinus</i>	Valle del Cauca, El Danubio	SS-FW; SS-HW; D-FW; V-FW
LGE-WS-01356	JFLC	<i>Heliconius eleuchia eleusinus</i>	Nariño, Junín	SS-FW; SS-HW; D-FW; V-FW
LGE-WS-01357	JFLC	<i>Heliconius eleuchia eleusinus</i>	Nariño, Junín	SS-FW; SS-HW; D-FW; V-FW
LGE-WS-01358	M3476	<i>Heliconius eleuchia eleusinus</i>	Valle del Cauca, La Elsa	SS-FW; SS-HW; D-FW; V-FW
LGE-WS-01359	M3471	<i>Heliconius eleuchia eleusinus</i>	Valle_del_Cauca, Queremal	SS-FW; SS-HW; D-FW; V-FW
LGE-WS-01360	M3327	<i>Heliconius eleuchia eleusinus</i>	Valle_del_Cauca, Queremal	SS-FW; D-FW; V-FW
LGE-WS-01361	M3328	<i>Heliconius eleuchia eleusinus</i>	Valle_del_Cauca, Queremal	SS-FW; SS-HW; D-FW; V-FW
LGE-WS-01362	M3353	<i>Heliconius eleuchia eleusinus</i>	Valle_del_Cauca, Queremal	SS-FW; SS-HW; D-FW; V-FW
LGE-WS-01363	M533	<i>Heliconius eleuchia eleusinus</i>	Valle del Cauca, Rio Bravo, Lago Calima	SS-FW; SS-HW; D-FW; V-FW
LGE-WS-01365	N/A	<i>Heliconius eleuchia eleusinus</i>	Valle_del_Cauca, Queremal	SS-FW; SS-HW; D-FW; V-FW
LGE-WS-01366	N/A	<i>Heliconius eleuchia eleusinus</i>	Valle_del_Cauca, Queremal	SS-FW; SS-HW; D-FW; V-FW
LGE-WS-01367	N/A	<i>Heliconius eleuchia eleusinus</i>	Valle del Cauca, Rio Bravo, Lago Calima	SS-FW; SS-HW; D-FW; V-FW
LGE-WS-01368	N/A	<i>Heliconius eleuchia eleusinus</i>	Valle del Cauca, Rio Bravo, Lago Calima	SS-FW; SS-HW; D-FW; V-FW
LGE-WS-02001	ICN-MHN-L 31727	<i>Heliconius elevatus elevatus</i>	Amazonas, Leticia	SS-FW; SS-HW; D-FW; V-FW; D-HW
LGE-WS-02002	ICN-MHN-L 31738	<i>Heliconius elevatus elevatus</i>	Amazonas, Leticia	SS-FW; SS-HW; D-FW; V-FW; D-HW; V-HW
LGE-WS-02003	M4010	<i>Heliconius elevatus elevatus</i>	Amazonas, Leticia	SS-FW; SS-HW; D-FW; D-HW
LGE-WS-02004	ICN-MHN-L 31760	<i>Heliconius elevatus elevatus</i>	Amazonas, Leticia	SS-FW; SS-HW
LGE-WS-02005	M536	<i>Heliconius elevatus elevatus</i>	Amazonas, Leticia	SS-FW; SS-HW; D-FW; D-HW
LGE-WS-02006	M537	<i>Heliconius elevatus elevatus</i>	Amazonas, Leticia	V-FW; V-HW

LGE-WS-02007	M5023	<i>Heliconius elevatus elevatus</i>	Amazonas, Leticia	SS-FW; SS-HW; D-FW; D-HW
LGE-WS-02008	JFLC	<i>Heliconius elevatus elevatus</i>	Guaviare, San José del Guaviare	SS-FW; SS-HW; D-FW; V-FW; D-HW; V-HW
LGE-WS-02009	JFLC	<i>Heliconius elevatus elevatus</i>	Bolivia, Chapare	SS-FW; SS-HW
LGE-WS-02010	JFLC	<i>Heliconius elevatus elevatus</i>	Bolivia, Chapare	SS-FW; SS-HW; D-FW; V-FW; D-HW; V-HW
LGE-WS-02011	M5389	<i>Heliconius elevatus elevatus</i>	Amazonas, La Pedrera	SS-FW; SS-HW
LGE-WS-00252	N/A	<i>Heliconius erato chestertonii</i>	Valle del Cauca, Buenos Aires	D-HW; V-HW
LGE-WS-00253	N/A	<i>Heliconius erato chestertonii</i>	Valle del Cauca, San José del Salado	SS-FW; SS-HW; D-HW; V-HW
LGE-WS-00254	N/A	<i>Heliconius erato chestertonii</i>	Antioquia, Bolivar	SS-FW; SS-HW; D-HW; V-HW
LGE-WS-00255	N/A	<i>Heliconius erato chestertonii</i>	Valle del Cauca, Calima	SS-FW; SS-HW; D-HW; V-HW
LGE-WS-00256	N/A	<i>Heliconius erato chestertonii</i>	Vale del Cauca, El Saladito	D-HW; V-HW
LGE-WS-00257	N/A	<i>Heliconius erato chestertonii</i>	Antioquia, Bolivar	SS-FW; SS-HW; D-HW; V-HW
LGE-WS-00258	N/A	<i>Heliconius erato chestertonii</i>	Valle del Cauca, Vijes, Carbonero	SS-FW; SS-HW; D-HW; V-HW
LGE-WS-00259	N/A	<i>Heliconius erato chestertonii</i>	Vale del Cauca, El Saladito	D-HW; V-HW
LGE-WS-00260	N/A	<i>Heliconius erato chestertonii</i>	Valle del Cauca, Buenos Aires	D-HW; V-HW
LGE-WS-00261	N/A	<i>Heliconius erato chestertonii</i>	Valle del Cauca, Montañitas	D-HW; V-HW
LGE-WS-00262	N/A	<i>Heliconius erato chestertonii</i>	Valle del Cauca, Buenos Aires	D-HW; V-HW
LGE-WS-00263	N/A	<i>Heliconius erato chestertonii</i>	Valle del Cauca, San José del Salado	SS-FW; SS-HW; D-HW; V-HW
LGE-WS-00264	N/A	<i>Heliconius erato chestertonii</i>	Valle del Cauca, Buenos Aires	D-HW; V-HW
LGE-WS-00265	N/A	<i>Heliconius erato chestertonii</i>	Valle del Cauca, Buenos Aires	D-HW; V-HW
LGE-WS-00266	N/A	<i>Heliconius erato chestertonii</i>	Valle del Cauca, Santa Ines	SS-FW; SS-HW; D-HW; V-HW
LGE-WS-00267	N/A	<i>Heliconius erato chestertonii</i>	Valle del Cauca, Calima	SS-FW; SS-HW; D-HW; V-HW
LGE-WS-00268	N/A	<i>Heliconius erato chestertonii</i>	Vale del Cauca, El Saladito	D-HW; V-HW
LGE-WS-00269	N/A	<i>Heliconius erato chestertonii</i>	Vale del Cauca, El Saladito	D-HW; V-HW
LGE-WS-00270	N/A	<i>Heliconius erato chestertonii</i>	Valle del Cauca, Buenos Aires	D-HW; V-HW
LGE-WS-00271	N/A	<i>Heliconius erato chestertonii</i>	Valle del Cauca, Buenos Aires	D-HW; V-HW
LGE-WS-00272	N/A	<i>Heliconius erato chestertonii</i>	Valle del Cauca, Buenos Aires, Yotoco	D-HW; V-HW

LGE-WS-00273	N/A	<i>Heliconius erato chestertonii</i>	Valle del Cauca, Buenos Aires, Yotoco	D-HW; V-HW
LGE-WS-00274	N/A	<i>Heliconius erato chestertonii</i>	Valle del Cauca, San Antonio	D-HW; V-HW
LGE-WS-00275	N/A	<i>Heliconius erato chestertonii</i>	Cauca, Helechaux	SS-FW; SS-HW; D-HW; V-HW
LGE-WS-00276	N/A	<i>Heliconius erato chestertonii</i>	Valle del Cauca, Buenos Aires, Yotoco	SS-FW; SS-HW; D-HW; V-HW
LGE-WS-00277	N/A	<i>Heliconius erato chestertonii</i>	Valle del Cauca, San Antonio	SS-FW; SS-HW; D-HW; V-HW
LGE-WS-00278	N/A	<i>Heliconius erato chestertonii</i>	Valle del Cauca, San Antonio	SS-FW; SS-HW; D-HW; V-HW
LGE-WS-00279	N/A	<i>Heliconius erato chestertonii</i>	Vale del Cauca, El Saladito	SS-FW; SS-HW; D-HW; V-HW
LGE-WS-00280	N/A	<i>Heliconius erato chestertonii</i>	Cauca, Salvajina, Rio Inguito	SS-FW; SS-HW; D-HW; V-HW
LGE-WS-00281	N/A	<i>Heliconius erato chestertonii</i>	Cauca, Salvajina, Rio Inguito	SS-FW; SS-HW; D-HW; V-HW
LGE-WS-00282	N/A	<i>Heliconius erato chestertonii</i>	Cauca, Salvajina, Rio Inguito	SS-FW; SS-HW; D-HW; V-HW
LGE-WS-00283	N/A	<i>Heliconius erato chestertonii</i>	Vale del Cauca, El Saladito	SS-FW; SS-HW; D-HW; V-HW
LGE-WS-00284	N/A	<i>Heliconius erato chestertonii</i>	Valle del Cauca, La Meseta, Villa Colombia	SS-FW; SS-HW; D-HW; V-HW
LGE-WS-00285	N/A	<i>Heliconius erato chestertonii</i>	Valle del Cauca, La Meseta, Villa Colombia	SS-FW; SS-HW; D-HW; V-HW
LGE-WS-00286	N/A	<i>Heliconius erato chestertonii</i>	Valle_del_Cauca, Calima	SS-FW; SS-HW; D-HW; V-HW
LGE-WS-00287	N/A	<i>Heliconius erato chestertonii</i>	Valle del Cauca, Restrepo, Carbonero	SS-FW; SS-HW; D-HW; V-HW
LGE-WS-00288	M782	<i>Heliconius erato chestertonii</i>	Valle del Cauca, Montañitas	D-HW; V-HW
LGE-WS-00289	M784	<i>Heliconius erato chestertonii</i>	Valle del Cauca, Montañitas	D-HW; V-HW
LGE-WS-00290	M791	<i>Heliconius erato chestertonii</i>	Valle del Cauca, Montañitas	SS-FW; SS-HW; D-HW; V-HW
LGE-WS-00291	M789	<i>Heliconius erato chestertonii</i>	Valle del Cauca, Montañitas	SS-FW; SS-HW; D-HW; V-HW
LGE-WS-00292	M793	<i>Heliconius erato chestertonii</i>	Valle del Cauca, Montañitas	SS-FW; SS-HW; D-HW; V-HW
LGE-WS-00293	M560	<i>Heliconius erato chestertonii</i>	Valle del Cauca, Rio Bravo, Lago Calima	D-HW; V-HW
LGE-WS-00294	M515	<i>Heliconius erato chestertonii</i>	Valle del Cauca, Trujillo	SS-FW; SS-HW; D-HW; V-HW
LGE-WS-00295	M532	<i>Heliconius erato chestertonii</i>	Valle del Cauca, Rio Bravo, Lago Calima	D-HW; V-HW
LGE-WS-00296	M563	<i>Heliconius erato chestertonii</i>	Valle del Cauca, Rio Bravo, Lago Calima	SS-FW; SS-HW; D-HW; V-HW
LGE-WS-00297	M1962	<i>Heliconius erato chestertonii</i>	Valle del Cauca, Buenos Aires, Yotoco	SS-HW; D-HW; V-HW
LGE-WS-00298	M3678	<i>Heliconius erato chestertonii</i>	Valle del Cauca, Buenos Aires, Yotoco	SS-FW; SS-HW; D-HW; V-HW

LGE-WS-00299	M3682	<i>Heliconius erato chestertonii</i>	Valle del Cauca, Buenos Aires	SS-FW; SS-HW; D-HW; V-HW
LGE-WS-00300	M3677	<i>Heliconius erato chestertonii</i>	Valle del Cauca, Buenos Aires	SS-FW; SS-HW; D-HW; V-HW
LGE-WS-00301	M2735	<i>Heliconius erato chestertonii</i>	Valle del Cauca, Buenos Aires	SS-FW; SS-HW; D-HW; V-HW
LGE-WS-02615	M2849	<i>Heliconius erato chestertonii</i>	Valle del Cauca, Atuncela	SS-FW; SS-HW; D-HW; V-HW
LGE-WS-02616	M2855	<i>Heliconius erato chestertonii</i>	Valle del Cauca, Atuncela	SS-FW; SS-HW; D-HW; V-HW
LGE-WS-02617	M2841	<i>Heliconius erato chestertonii</i>	Vale del Cauca, El Saladito	SS-FW; SS-HW; D-HW; V-HW
LGE-WS-02618	M2843	<i>Heliconius erato chestertonii</i>	Vale del Cauca, El Saladito	SS-FW; SS-HW; D-HW; V-HW
LGE-WS-02619	M2862	<i>Heliconius erato chestertonii</i>	Valle del Cauca, Atuncela	D-HW; V-HW
LGE-WS-02620	M2839	<i>Heliconius erato chestertonii</i>	Vale del Cauca, El Saladito	SS-FW; SS-HW; D-HW; V-HW
LGE-WS-02621	M2704	<i>Heliconius erato chestertonii</i>	Vale del Cauca, El Saladito	SS-FW; SS-HW; D-HW; V-HW
LGE-WS-02622	M3307	<i>Heliconius erato chestertonii</i>	Risaralda, Marsella, El Nudo	D-HW; V-HW
LGE-WS-02623	M3295	<i>Heliconius erato chestertonii</i>	Risaralda, Marsella, El Nudo	SS-FW; SS-HW; D-HW; V-HW
LGE-WS-02624	M1334	<i>Heliconius erato chestertonii</i>	Risaralda, Marsella, EcoLagos	SS-FW; SS-HW; D-HW; V-HW
LGE-WS-02625	M1332	<i>Heliconius erato chestertonii</i>	Risaralda, Marsella, El Nudo	SS-FW; SS-HW; D-HW; V-HW
LGE-WS-02626	M2772	<i>Heliconius erato chestertonii</i>	Valle del Cauca, Montañitas	SS-FW; SS-HW; D-HW; V-HW
LGE-WS-02627	M1331	<i>Heliconius erato chestertonii</i>	Risaralda, Marsella, El Nudo	SS-FW; SS-HW; D-HW; V-HW
LGE-WS-02628	M2767	<i>Heliconius erato chestertonii</i>	Valle del Cauca, Montañitas	D-HW; V-HW
LGE-WS-02629	M2766	<i>Heliconius erato chestertonii</i>	Valle del Cauca, Montañitas	SS-FW; SS-HW; D-HW; V-HW
LGE-WS-02630	M2600	<i>Heliconius erato chestertonii</i>	Valle del Cauca, Montañitas	SS-FW; SS-HW; D-HW; V-HW
LGE-WS-02631	M2608	<i>Heliconius erato chestertonii</i>	Valle del Cauca, Montañitas	SS-FW; SS-HW; D-HW; V-HW
LGE-WS-02632	M2585	<i>Heliconius erato chestertonii</i>	Valle del Cauca, Montañitas	SS-FW; SS-HW; D-HW; V-HW
LGE-WS-02633	M2609	<i>Heliconius erato chestertonii</i>	Valle del Cauca, Montañitas	SS-FW; SS-HW; D-HW; V-HW
LGE-WS-02634	M2602	<i>Heliconius erato chestertonii</i>	Valle del Cauca, Montañitas	SS-FW; SS-HW; D-HW; V-HW
LGE-WS-02635	M2603	<i>Heliconius erato chestertonii</i>	Valle del Cauca, Montañitas	SS-FW; SS-HW; D-HW; V-HW
LGE-WS-00901	M1873	<i>Heliconius erato dignus</i>	Putumayo, San Antonio	D-HW
LGE-WS-00902	M1874	<i>Heliconius erato dignus</i>	Putumayo, San Antonio	SS-FW; SS-HW; D-FW; V-FW; D-HW; V-HW

LGE-WS-00903	M1871	<i>Heliconius erato dignus</i>	Putumayo, San Antonio	SS-FW; SS-HW; D-FW; V-FW; D-HW; V-HW
LGE-WS-00904	M1875	<i>Heliconius erato dignus</i>	Putumayo, San Antonio	SS-FW; SS-HW; D-FW; V-FW; D-HW; V-HW
LGE-WS-00905	M4481	<i>Heliconius erato dignus</i>	Putumayo, Mocoa, Campucana	SS-FW; SS-HW; D-FW
LGE-WS-00906	M4484	<i>Heliconius erato dignus</i>	Putumayo, Mocoa, Campucana	SS-FW; SS-HW; D-FW; V-FW; D-HW; V-HW
LGE-WS-00907	M4483	<i>Heliconius erato dignus</i>	Putumayo, Mocoa, Campucana	SS-HW; D-FW; V-FW; D-HW; V-HW
LGE-WS-00908	M4480	<i>Heliconius erato dignus</i>	Putumayo, Mocoa, Campucana	SS-FW; SS-HW; D-FW; V-FW; D-HW; V-HW
LGE-WS-00909	M4479	<i>Heliconius erato dignus</i>	Putumayo, Mocoa, Campucana	SS-FW; SS-HW; D-FW; V-FW; D-HW; V-HW
LGE-WS-00910	M4289	<i>Heliconius erato dignus</i>	Putumayo, Mocoa, Campucana	SS-FW; D-FW; V-FW; D-HW; V-HW
CAM040015	CAM040015	<i>Heliconius erato dignus</i>	Putumayo, Mocoa, Campucana	SS-FW; D-FW; V-FW
CAM040016	CAM040016	<i>Heliconius erato dignus</i>	Putumayo, Mocoa, Campucana	SS-FW; D-FW; V-FW
CAM040017	CAM040017	<i>Heliconius erato dignus</i>	Putumayo, Mocoa, Campucana	SS-FW; D-FW
CAM040018	CAM040018	<i>Heliconius erato dignus</i>	Putumayo, Mocoa, Campucana	SS-HW
CAM040039	CAM040039	<i>Heliconius erato dignus</i>	Putumayo, Mocoa, Campucana	SS-FW; D-FW; V-FW
CAM040041	CAM040041	<i>Heliconius erato dignus</i>	Putumayo, Mocoa, Campucana	SS-FW; D-FW; V-FW
CAM040042	CAM040042	<i>Heliconius erato dignus</i>	Putumayo, Mocoa, Campucana	SS-FW; D-FW; V-FW
CAM040077	CAM040077	<i>Heliconius erato dignus</i>	Putumayo, Mocoa, Campucana	SS-FW; D-FW; V-FW
CAM040078	CAM040078	<i>Heliconius erato dignus</i>	Putumayo, Mocoa, Campucana	SS-FW; D-FW; V-FW
CAM040101	CAM040101	<i>Heliconius erato dignus</i>	Putumayo, Mocoa, Sibundoy	SS-FW
CAM040108	CAM040108	<i>Heliconius erato dignus</i>	Putumayo, Mocoa, Sibundoy	SS-FW
CAM040111	CAM040111	<i>Heliconius erato dignus</i>	Putumayo, Mocoa, Campucana	SS-FW; SS-HW; D-FW; V-FW; D-HW; V-HW
CAM040112	CAM040112	<i>Heliconius erato dignus</i>	Putumayo, Mocoa, Campucana	SS-FW; SS-HW; D-FW; V-FW; D-HW; V-HW
CAM040113	CAM040113	<i>Heliconius erato dignus</i>	Putumayo, Mocoa, Campucana	SS-FW; SS-HW; D-FW; V-FW; D-HW; V-HW
CAM040114	CAM040114	<i>Heliconius erato dignus</i>	Putumayo, Mocoa, Campucana	SS-FW; SS-HW; D-FW; V-FW; D-HW; V-HW
LGE-WS-00552	M1233	<i>Heliconius erato guarica</i>	Cundinamarca, Peru, Guaduas	SS-FW; SS-HW; D-FW; V-FW; D-HW; V-HW
LGE-WS-00553	M1206	<i>Heliconius erato guarica</i>	Cundinamarca, Peru, Guaduas	SS-FW; SS-HW; D-FW; V-FW; D-HW; V-HW
LGE-WS-00554	M1201	<i>Heliconius erato guarica</i>	Cundinamarca, Peru, Guaduas	SS-FW; SS-HW; D-FW; V-FW; D-HW; V-HW

LGE-WS-00555	M1236	<i>Heliconius erato guarica</i>	Cundinamarca, Peru, Guaduas	SS-FW; SS-HW; D-FW; V-FW; D-HW; V-HW
LGE-WS-00556	M1211	<i>Heliconius erato guarica</i>	Cundinamarca, Peru, Guaduas	SS-FW; SS-HW; D-FW; V-FW; D-HW; V-HW
LGE-WS-00557	M1208	<i>Heliconius erato guarica</i>	Cundinamarca, Peru, Guaduas	SS-FW; SS-HW; D-FW; V-FW; D-HW; V-HW
LGE-WS-00558	M1205	<i>Heliconius erato guarica</i>	Cundinamarca, Peru, Guaduas	SS-FW; SS-HW; D-FW; V-FW; D-HW; V-HW
LGE-WS-00559	M1200	<i>Heliconius erato guarica</i>	Cundinamarca, Peru, Guaduas	SS-FW; SS-HW; D-FW; V-FW; D-HW; V-HW
LGE-WS-00560	M1217	<i>Heliconius erato guarica</i>	Cundinamarca, Peru, Guaduas	SS-FW; SS-HW; D-FW; V-FW; D-HW; V-HW
LGE-WS-00561	M1216	<i>Heliconius erato guarica</i>	Cundinamarca, Peru, Guaduas	SS-FW; SS-HW; D-FW; V-FW; D-HW; V-HW
LGE-WS-00562	M1214	<i>Heliconius erato guarica</i>	Cundinamarca, Peru, Guaduas	SS-FW; SS-HW; D-FW; V-FW; D-HW; V-HW
LGE-WS-00563	M1227	<i>Heliconius erato guarica</i>	Cundinamarca, Peru, Guaduas	SS-FW; SS-HW; D-FW; V-FW; D-HW; V-HW
LGE-WS-00564	M1223	<i>Heliconius erato guarica</i>	Cundinamarca, Peru, Guaduas	SS-FW; SS-HW; D-FW; V-FW; D-HW; V-HW
LGE-WS-00565	M1220	<i>Heliconius erato guarica</i>	Cundinamarca, Peru, Guaduas	SS-FW; SS-HW; D-FW; V-FW; D-HW; V-HW
LGE-WS-00566	M1218	<i>Heliconius erato guarica</i>	Cundinamarca, Peru, Guaduas	SS-FW; SS-HW; D-FW; V-FW; D-HW; V-HW
LGE-WS-00567	M1221	<i>Heliconius erato guarica</i>	Cundinamarca, Peru, Guaduas	SS-FW; SS-HW; D-FW; V-FW; D-HW; V-HW
LGE-WS-00568	M1226	<i>Heliconius erato guarica</i>	Cundinamarca, Peru, Guaduas	SS-FW; SS-HW; D-FW; V-FW; D-HW; V-HW
LGE-WS-00569	M1225	<i>Heliconius erato guarica</i>	Cundinamarca, Peru, Guaduas	SS-FW; SS-HW; D-FW; V-FW; D-HW; V-HW
LGE-WS-00570	M1231	<i>Heliconius erato guarica</i>	Cundinamarca, Peru, Guaduas	SS-FW; SS-HW; D-FW; V-FW; D-HW; V-HW
LGE-WS-00571	M1199	<i>Heliconius erato guarica</i>	Cundinamarca, Peru, Guaduas	SS-FW; SS-HW; D-FW; V-FW; D-HW; V-HW
LGE-WS-00572	M1212	<i>Heliconius erato guarica</i>	Cundinamarca, Peru, Guaduas	SS-FW; SS-HW; D-FW; V-FW; D-HW; V-HW
LGE-WS-00573	M1213	<i>Heliconius erato guarica</i>	Cundinamarca, Peru, Guaduas	SS-FW; SS-HW; D-FW; V-FW; D-HW; V-HW
LGE-WS-00574	M1224	<i>Heliconius erato guarica</i>	Cundinamarca, Peru, Guaduas	SS-FW; SS-HW; D-FW; V-FW; D-HW; V-HW
LGE-WS-00575	M3103	<i>Heliconius erato guarica</i>	Tolima, Ibagué, Santafé de los Guadales	SS-FW; SS-HW; D-FW; V-FW; D-HW; V-HW
LGE-WS-00576	M3104	<i>Heliconius erato guarica</i>	Tolima, Ibagué, Santafé de los Guadales	SS-FW; SS-HW; D-FW; V-FW; D-HW; V-HW
LGE-WS-00577	M3071	<i>Heliconius erato guarica</i>	Cundinamarca, La Vega	SS-FW; SS-HW; D-FW; V-FW; D-HW; V-HW
LGE-WS-00578	M3072	<i>Heliconius erato guarica</i>	Cundinamarca, La Vega	SS-FW; SS-HW; D-FW; V-FW; D-HW; V-HW
LGE-WS-00579	M3070	<i>Heliconius erato guarica</i>	Cundinamarca, La Vega	SS-FW; SS-HW; D-FW; V-FW; D-HW; V-HW
LGE-WS-00580	M3074	<i>Heliconius erato guarica</i>	Cundinamarca, La Vega	SS-FW; SS-HW; D-FW; V-FW; D-HW; V-HW

LGE-WS-00581	M3428	<i>Heliconius erato guarica</i>	Tolima, Iconozo	SS-FW; SS-HW; D-FW; V-FW; D-HW; V-HW
LGE-WS-00582	M3429	<i>Heliconius erato guarica</i>	Tolima, Iconozo	SS-FW; SS-HW; D-FW; V-FW; D-HW; V-HW
LGE-WS-00583	M1484	<i>Heliconius erato guarica</i>	Cundinamarca, Boquerón	V-FW; D-HW; V-HW
LGE-WS-00584	M1485	<i>Heliconius erato guarica</i>	Cundinamarca, Boquerón	SS-FW; SS-HW; D-FW; V-FW; D-HW; V-HW
LGE-WS-00585	M1486	<i>Heliconius erato guarica</i>	Cundinamarca, Boquerón	SS-FW; SS-HW; D-FW; V-FW; D-HW; V-HW
LGE-WS-00586	M1983	<i>Heliconius erato guarica</i>	Cundinamarca, Sasaima	SS-FW; SS-HW; D-FW; V-FW; D-HW; V-HW
LGE-WS-00587	M1993	<i>Heliconius erato guarica</i>	Cundinamarca, Sasaima	D-FW; V-FW; D-HW; V-HW
LGE-WS-00588	M3125	<i>Heliconius erato guarica</i>	Huila, Neiva, Santa María	SS-FW; SS-HW; D-FW; V-FW; D-HW; V-HW
LGE-WS-00589	M2942	<i>Heliconius erato guarica</i>	Cundinamarca, La Vega	SS-FW; SS-HW; D-FW; V-FW; D-HW; V-HW
LGE-WS-00590	M3124	<i>Heliconius erato guarica</i>	Huila, Neiva, Santa María	SS-FW; SS-HW; D-FW; V-FW; D-HW; V-HW
LGE-WS-00591	M2941	<i>Heliconius erato guarica</i>	Cundinamarca, La Vega	SS-FW; SS-HW; D-FW; V-FW; D-HW; V-HW
LGE-WS-00592	M3122	<i>Heliconius erato guarica</i>	Huila, Neiva, Santa María	SS-FW; SS-HW; D-FW; V-FW; D-HW; V-HW
LGE-WS-00593	M3123	<i>Heliconius erato guarica</i>	Huila, Neiva, Santa María	SS-FW; SS-HW; D-FW; V-FW; D-HW; V-HW
LGE-WS-00594	M3102	<i>Heliconius erato guarica</i>	Tolima, Ibagué, Santafé de los Guaduales	SS-FW; SS-HW; D-FW; V-FW; D-HW; V-HW
LGE-WS-00595	M3376	<i>Heliconius erato guarica</i>	Tolima, Iconozo	SS-FW; D-FW; V-FW; D-HW; V-HW
LGE-WS-00602	N/A	<i>Heliconius erato hydara</i>	Casanare, Morcote, Nunchia	SS-FW; SS-HW; D-FW; V-FW; D-HW; V-HW
LGE-WS-00603	N/A	<i>Heliconius erato hydara</i>	Casanare, Morcote, Nunchia	SS-FW; SS-HW; D-FW; V-FW; D-HW; V-HW
LGE-WS-00604	N/A	<i>Heliconius erato hydara</i>	Casanare, Morcote, Nunchia	SS-FW; SS-HW; D-FW; V-FW; D-HW; V-HW
LGE-WS-00605	N/A	<i>Heliconius erato hydara</i>	Casanare, Morcote, Nunchia	SS-FW; SS-HW; D-FW; V-FW; D-HW; V-HW
LGE-WS-00606	M1242	<i>Heliconius erato hydara</i>	Meta, Buenavista	D-FW; V-FW
LGE-WS-00607	M396	<i>Heliconius erato hydara</i>	Casanare, Morcote, Nunchia	D-FW; V-FW
LGE-WS-00608	M859	<i>Heliconius erato hydara</i>	Meta, Buenavista	SS-FW; SS-HW; D-FW; V-FW
LGE-WS-00609	N/A	<i>Heliconius erato hydara</i>	Casanare, Morcote, Nunchia	SS-FW; SS-HW; D-FW; V-FW
LGE-WS-00610	M393	<i>Heliconius erato hydara</i>	Casanare, Morcote, Nunchia	SS-FW; SS-HW; D-FW; V-FW; D-HW; V-HW
LGE-WS-00611	M858	<i>Heliconius erato hydara</i>	Meta, Buenavista	SS-FW; SS-HW; D-FW; V-FW; D-HW; V-HW
LGE-WS-00612	M1257	<i>Heliconius erato hydara</i>	Meta, Buenavista	SS-FW; SS-HW; D-FW; V-FW; D-HW; V-HW

LGE-WS-00613	M1259	<i>Heliconius erato hydara</i>	Meta, Buenavista	SS-FW; SS-HW; D-FW; V-FW; D-HW; V-HW
LGE-WS-00614	M1867	<i>Heliconius erato hydara</i>	Meta, Buenavista	SS-FW; SS-HW; D-FW; V-FW; D-HW; V-HW
LGE-WS-00615	M1256	<i>Heliconius erato hydara</i>	Meta, Buenavista	SS-FW; SS-HW; D-FW; V-FW; D-HW; V-HW
LGE-WS-00616	M1251	<i>Heliconius erato hydara</i>	Meta, Buenavista	SS-FW; SS-HW; D-FW; V-FW; D-HW; V-HW
LGE-WS-00617	M1248	<i>Heliconius erato hydara</i>	Meta, Buenavista	SS-FW; SS-HW; D-FW; V-FW; D-HW; V-HW
LGE-WS-00618	M1254	<i>Heliconius erato hydara</i>	Meta, Buenavista	SS-FW; SS-HW; D-FW; V-FW; D-HW; V-HW
LGE-WS-00619	M1249	<i>Heliconius erato hydara</i>	Meta, Buenavista	SS-FW; SS-HW; D-FW; V-FW; D-HW; V-HW
LGE-WS-00620	M1250	<i>Heliconius erato hydara</i>	Meta, Buenavista	SS-FW; SS-HW; D-FW; V-FW; D-HW; V-HW
LGE-WS-00621	M1252	<i>Heliconius erato hydara</i>	Meta, Buenavista	SS-FW; SS-HW; D-FW; V-FW; D-HW; V-HW
LGE-WS-00622	M1247	<i>Heliconius erato hydara</i>	Meta, Buenavista	SS-FW; SS-HW; D-FW; V-FW; D-HW; V-HW
LGE-WS-00623	M1182	<i>Heliconius erato hydara</i>	Meta, Buenavista	SS-FW; SS-HW; D-FW; V-FW; D-HW; V-HW
LGE-WS-00624	M1244	<i>Heliconius erato hydara</i>	Meta, Buenavista	SS-FW; SS-HW; D-FW; V-FW; D-HW; V-HW
LGE-WS-00625	M1243	<i>Heliconius erato hydara</i>	Meta, Buenavista	SS-FW; SS-HW; D-FW; V-FW; D-HW; V-HW
LGE-WS-00626	M3798	<i>Heliconius erato hydara</i>	Boyacá, Santa María, La Almenara	SS-FW; SS-HW; D-FW; V-FW; D-HW; V-HW
LGE-WS-00627	M3800	<i>Heliconius erato hydara</i>	Boyacá, Santa María, La Almenara	SS-FW; SS-HW; D-FW; V-FW; D-HW; V-HW
LGE-WS-00628	M3409	<i>Heliconius erato hydara</i>	Meta, Altos de Buenavista	SS-FW; SS-HW; D-FW; V-FW; D-HW; V-HW
LGE-WS-00629	M3402	<i>Heliconius erato hydara</i>	Meta, Altos de Buenavista	SS-FW; SS-HW; D-FW; V-FW; D-HW; V-HW
LGE-WS-00630	M3403	<i>Heliconius erato hydara</i>	Meta, Altos de Buenavista	SS-FW; SS-HW; D-FW; V-FW; D-HW; V-HW
LGE-WS-00631	M3405	<i>Heliconius erato hydara</i>	Meta, Altos de Buenavista	SS-FW; SS-HW; D-FW; V-FW
LGE-WS-00632	M3399	<i>Heliconius erato hydara</i>	Meta, Altos de Buenavista	SS-FW; SS-HW; D-FW; V-FW
LGE-WS-00633	M3401	<i>Heliconius erato hydara</i>	Meta, Altos de Buenavista	SS-FW; SS-HW; D-FW; V-FW; D-HW; V-HW
LGE-WS-00634	M3415	<i>Heliconius erato hydara</i>	Meta, Altos de Buenavista	SS-FW; SS-HW; D-FW; V-FW; D-HW; V-HW
LGE-WS-00635	M3412	<i>Heliconius erato hydara</i>	Meta, Altos de Buenavista	SS-FW; SS-HW; D-FW; V-FW; D-HW; V-HW
LGE-WS-00636	M3414	<i>Heliconius erato hydara</i>	Meta, Altos de Buenavista	SS-FW; SS-HW; D-FW; V-FW; D-HW; V-HW
LGE-WS-00637	M3411	<i>Heliconius erato hydara</i>	Meta, Altos de Buenavista	SS-FW; SS-HW; D-FW; V-FW
LGE-WS-00638	M3407	<i>Heliconius erato hydara</i>	Meta, Altos de Buenavista	SS-FW; SS-HW; D-FW; V-FW; D-HW; V-HW

LGE-WS-00639	M3406	<i>Heliconius erato hydara</i>	Meta, Altos de Buenavista	SS-FW; SS-HW; D-FW; V-FW; D-HW; V-HW
LGE-WS-00640	M3257	<i>Heliconius erato hydara</i>	Meta, Altos de Buenavista	SS-FW; SS-HW; D-FW; V-FW; D-HW; V-HW
LGE-WS-00641	M857	<i>Heliconius erato hydara</i>	Meta, Altos de Buenavista	SS-FW; SS-HW; D-FW; V-FW
LGE-WS-00642	M3410	<i>Heliconius erato hydara</i>	Meta, Altos de Buenavista	SS-FW; SS-HW; D-FW; V-FW; D-HW; V-HW
LGE-WS-00643	M389	<i>Heliconius erato hydara</i>	Casanare, Morcote, Nunchia	SS-FW; SS-HW; D-FW; V-FW; D-HW; V-HW
LGE-WS-00644	N/A	<i>Heliconius erato hydara</i>	Meta, Villavicencio, Bosques de Bavaria	SS-FW; SS-HW; D-FW; V-FW; D-HW; V-HW
LGE-WS-00645	M322	<i>Heliconius erato hydara</i>	Casanare, Morcote, Nunchia	SS-FW; SS-HW; D-FW; V-FW; D-HW; V-HW
LGE-WS-00646	M321	<i>Heliconius erato hydara</i>	Casanare, Morcote, Nunchia	SS-FW; SS-HW; D-FW; V-FW; D-HW; V-HW
LGE-WS-00647	N/A	<i>Heliconius erato hydara</i>	Meta, Villavicencio, Bosques de Bavaria	SS-FW; SS-HW; D-FW; V-FW; D-HW; V-HW
LGE-WS-00648	M3797	<i>Heliconius erato hydara</i>	Boyacá, Santa María	SS-FW; SS-HW; D-FW; V-FW; D-HW; V-HW
LGE-WS-00649	M3785	<i>Heliconius erato hydara</i>	Boyacá, Santa María	SS-FW; SS-HW; D-FW; V-FW; D-HW; V-HW
LGE-WS-00650	M3799	<i>Heliconius erato hydara</i>	Boyacá, Santa María	SS-FW; SS-HW; D-FW; V-FW
LGE-WS-00651	M3778	<i>Heliconius erato hydara</i>	Boyacá, Santa María	SS-FW; SS-HW; D-FW; V-FW; D-HW; V-HW
LGE-WS-02750	M549	<i>Heliconius erato lativitta</i>	Amazonas, San Martín	SS-FW; SS-HW; D-FW; V-FW; D-HW; V-HW
LGE-WS-02751	M4296	<i>Heliconius erato lativitta</i>	Putumayo, Vereda San Rafael, Finca El Escondite	SS-FW; SS-HW; D-FW; V-FW; D-HW; V-HW
LGE-WS-02752	M2993	<i>Heliconius erato lativitta</i>	Caquetá, Quebrada Las Doraditas	SS-FW; SS-HW; D-FW; V-FW; D-HW; V-HW
LGE-WS-02753	M539	<i>Heliconius erato lativitta</i>	Amazonas, San Martín	SS-FW; SS-HW; D-FW; V-FW; D-HW; V-HW
LGE-WS-02754	M1835	<i>Heliconius erato lativitta</i>	Caquetá, Suaza, Doradillas	SS-FW; SS-HW; D-FW; V-FW; D-HW; V-HW
LGE-WS-02755	M1832	<i>Heliconius erato lativitta</i>	Caquetá, Suaza, Doradillas	SS-FW; SS-HW; D-FW; V-FW; D-HW; V-HW
LGE-WS-02756	M1831	<i>Heliconius erato lativitta</i>	Caquetá, Suaza, Doradillas	SS-FW; SS-HW; D-FW; V-FW; D-HW; V-HW
LGE-WS-02757	M1834	<i>Heliconius erato lativitta</i>	Caquetá, Suaza, Doradillas	SS-FW; SS-HW; D-FW; V-FW; D-HW; V-HW
LGE-WS-02758	M1802	<i>Heliconius erato lativitta</i>	Caquetá, Suaza, Doradillas	D-FW; V-FW; D-HW; V-HW
LGE-WS-02759	M1800	<i>Heliconius erato lativitta</i>	Caquetá, Suaza, Doradillas	SS-FW; SS-HW; D-FW; V-FW; D-HW; V-HW
LGE-WS-02760	M1798	<i>Heliconius erato lativitta</i>	Caquetá, Suaza, Doradillas	SS-FW; SS-HW; D-FW; V-FW; D-HW; V-HW
LGE-WS-02761	M1799	<i>Heliconius erato lativitta</i>	Caquetá, Suaza, Doradillas	SS-FW; SS-HW; D-FW; V-FW; D-HW; V-HW
LGE-WS-02762	M1778	<i>Heliconius erato lativitta</i>	Caquetá, Florencia, Sucre	SS-FW; SS-HW; D-FW; V-FW; D-HW; V-HW

LGE-WS-02763	M1787	<i>Heliconius erato lativitta</i>	Caquetá, Suaza, Doradillas	SS-FW; SS-HW; D-FW; V-FW; D-HW; V-HW
LGE-WS-02764	M1795	<i>Heliconius erato lativitta</i>	Caquetá, Suaza, Doradillas	SS-FW; SS-HW; D-FW; V-FW; D-HW; V-HW
LGE-WS-02765	M1790	<i>Heliconius erato lativitta</i>	Caquetá, Suaza, Doradillas	SS-FW; SS-HW; D-FW; V-FW; D-HW; V-HW
LGE-WS-02766	M1445	<i>Heliconius erato lativitta</i>	Caquetá, Florencia, Paraiso	SS-FW; SS-HW; D-FW; V-FW; D-HW; V-HW
LGE-WS-02767	M1585	<i>Heliconius erato lativitta</i>	Caquetá, Florencia, Paraiso	SS-FW; SS-HW; D-FW; V-FW; D-HW; V-HW
LGE-WS-02768	M1786	<i>Heliconius erato lativitta</i>	Caquetá, Suaza, Doradillas	SS-FW; SS-HW; D-FW; V-FW; D-HW; V-HW
LGE-WS-02769	M1446	<i>Heliconius erato lativitta</i>	Caquetá, Florencia, Paraiso	SS-FW; SS-HW; D-FW; V-FW; D-HW; V-HW
LGE-WS-02770	M1396	<i>Heliconius erato lativitta</i>	Caquetá, Florencia, Sucre	SS-FW; SS-HW; D-FW; V-FW; D-HW; V-HW
LGE-WS-02771	M1427	<i>Heliconius erato lativitta</i>	Caquetá, Florencia, Sucre	SS-FW; SS-HW; D-FW; V-FW; D-HW; V-HW
LGE-WS-02772	M1395	<i>Heliconius erato lativitta</i>	Caquetá, Florencia, Sucre	SS-FW; SS-HW; D-FW; V-FW; D-HW; V-HW
LGE-WS-02773	M1425	<i>Heliconius erato lativitta</i>	Caquetá, Florencia, Sucre	SS-FW; D-FW; V-FW; D-HW; V-HW
LGE-WS-02774	M1392	<i>Heliconius erato lativitta</i>	Caquetá, Florencia, Sucre	SS-FW; SS-HW; D-FW; V-FW; D-HW; V-HW
LGE-WS-02775	M1388	<i>Heliconius erato lativitta</i>	Caquetá, Florencia, Sucre	SS-FW; SS-HW; D-FW; V-FW; D-HW; V-HW
LGE-WS-02776	M1389	<i>Heliconius erato lativitta</i>	Caquetá, Florencia, Sucre	SS-FW; SS-HW; D-FW; V-FW; D-HW; V-HW
LGE-WS-02777	M1380	<i>Heliconius erato lativitta</i>	Caquetá, Florencia, Paraiso	SS-FW; SS-HW; D-FW; V-FW; D-HW; V-HW
LGE-WS-02778	M1146	<i>Heliconius erato lativitta</i>	Caquetá, Puerto Rico	SS-FW; SS-HW; D-FW; V-FW; D-HW; V-HW
LGE-WS-02779	M1169	<i>Heliconius erato lativitta</i>	Caquetá, Florencia, Sucre	SS-FW; SS-HW; D-FW; V-FW; D-HW; V-HW
LGE-WS-02780	M1148	<i>Heliconius erato lativitta</i>	Caquetá, Puerto Rico	SS-FW; SS-HW; D-FW; V-FW; D-HW; V-HW
LGE-WS-02781	M1382	<i>Heliconius erato lativitta</i>	Caquetá, Florencia, Paraiso	D-FW; V-FW; D-HW; V-HW
LGE-WS-02782	M1128	<i>Heliconius erato lativitta</i>	Caquetá, Florencia, Sucre	SS-FW; SS-HW; D-FW; V-FW; D-HW; V-HW
LGE-WS-02783	M5020	<i>Heliconius erato lativitta</i>	Amazonas, Leticia	SS-FW; SS-HW; D-FW; V-FW; D-HW; V-HW
LGE-WS-02784	M3439	<i>Heliconius erato lativitta</i>	Caquetá, Quebrada Las Doraditas	SS-FW; SS-HW; D-FW; V-FW; D-HW; V-HW
LGE-WS-02785	M3065	<i>Heliconius erato lativitta</i>	Caquetá, Quebrada Las Doraditas	SS-FW; SS-HW; D-FW; V-FW; D-HW; V-HW
LGE-WS-02786	M1119	<i>Heliconius erato lativitta</i>	Caquetá, Florencia, Paraiso	SS-FW; SS-HW; D-FW; V-FW; D-HW; V-HW
LGE-WS-02787	M1071	<i>Heliconius erato lativitta</i>	Caquetá, Florencia, Sucre	SS-FW; SS-HW; D-FW; V-FW; D-HW; V-HW
LGE-WS-02788	M218	<i>Heliconius erato lativitta</i>	Caquetá, Florencia, Sucre	SS-FW; SS-HW; D-FW; V-FW; D-HW; V-HW

LGE-WS-02789	M1006	<i>Heliconius erato lativitta</i>	Caquetá, Florencia, Sucre	SS-FW; SS-HW; D-FW; V-FW; D-HW; V-HW
LGE-WS-02790	M300	<i>Heliconius erato lativitta</i>	Caquetá, Florencia, Sucre	SS-FW; SS-HW; D-FW; V-FW; D-HW; V-HW
LGE-WS-02791	M4067	<i>Heliconius erato lativitta</i>	Amazonas, Leticia	SS-FW; SS-HW; D-FW; V-FW; D-HW; V-HW
LGE-WS-02792	M539	<i>Heliconius erato lativitta</i>	Caquetá, Quebrada Las Doraditas	D-FW; V-FW; D-HW; V-HW
LGE-WS-02793	M4458	<i>Heliconius erato lativitta</i>	Caquetá, Florencia, Sucre	SS-FW; SS-HW; D-FW; V-FW; D-HW; V-HW
LGE-WS-02794	M4457	<i>Heliconius erato lativitta</i>	Caquetá, Florencia, Sucre	SS-FW; SS-HW
LGE-WS-02795	M4064	<i>Heliconius erato lativitta</i>	Amazonas, Leticia	SS-FW; SS-HW; D-FW; V-FW; D-HW; V-HW
LGE-WS-02796	M3440	<i>Heliconius erato lativitta</i>	Caquetá, Quebrada Las Doraditas	SS-FW; SS-HW; D-FW; V-FW; D-HW; V-HW
LGE-WS-02797	M4063	<i>Heliconius erato lativitta</i>	Amazonas, Leticia	SS-FW; SS-HW; D-FW; V-FW; D-HW; V-HW
LGE-WS-02798	M4047	<i>Heliconius erato lativitta</i>	Amazonas, Leticia	D-FW; V-FW; D-HW; V-HW
LGE-WS-02799	M4048	<i>Heliconius erato lativitta</i>	Amazonas, Leticia	D-FW; V-FW; D-HW; V-HW
LGE-WS-01951	M4056	<i>Heliconius erato reductimacula</i>	Amazonas, Leticia, Vereda San Jose	SS-FW; SS-HW; D-FW; V-FW; D-HW; V-HW
LGE-WS-01952	M4057	<i>Heliconius erato reductimacula</i>	Amazonas, Puerto Nariño, Quebrada Aguas Rojas	SS-FW; SS-HW; D-FW; V-FW; D-HW; V-HW
LGE-WS-01953	M4054	<i>Heliconius erato reductimacula</i>	Amazonas, Leticia	SS-FW; SS-HW; D-FW; V-FW; D-HW; V-HW
LGE-WS-01954	M5026	<i>Heliconius erato reductimacula</i>	Amazonas, Leticia, Reserva Cerca Viva	SS-FW; SS-HW; D-FW; V-FW; D-HW; V-HW
LGE-WS-01955	M4051	<i>Heliconius erato reductimacula</i>	Amazonas, Leticia, Vereda San Jose	SS-FW; SS-HW; D-FW; V-FW; D-HW; V-HW
LGE-WS-01956	M4050	<i>Heliconius erato reductimacula</i>	Amazonas, Leticia, Vereda San Jose	SS-FW; SS-HW
LGE-WS-01957	M4043	<i>Heliconius erato reductimacula</i>	Amazonas, Leticia	SS-FW; SS-HW; D-FW; V-FW; D-HW; V-HW
LGE-WS-01958	M4042	<i>Heliconius erato reductimacula</i>	Amazonas, Puerto Nariño, Quebrada Aguas Rojas	SS-FW; SS-HW; D-FW; V-FW; D-HW; V-HW
LGE-WS-01959	M4058	<i>Heliconius erato reductimacula</i>	Amazonas, Leticia, Vereda San Jose	SS-FW; SS-HW; D-FW; V-FW; D-HW; V-HW
LGE-WS-01960	M5175	<i>Heliconius erato reductimacula</i>	Amazonas, Vereda Vergel, Reserva Natura Park	SS-FW; SS-HW; D-FW; V-FW; D-HW; V-HW
LGE-WS-01962	M5402	<i>Heliconius erato reductimacula</i>	Amazonas, La Pedrera	SS-FW; SS-HW; D-FW; V-FW; D-HW; V-HW
LGE-WS-01963	M5405	<i>Heliconius erato reductimacula</i>	Amazonas, La Pedrera	SS-FW; SS-HW; D-FW; V-FW; D-HW; V-HW
LGE-WS-01964	M5404	<i>Heliconius erato reductimacula</i>	Amazonas, La Pedrera	SS-FW; SS-HW; D-FW; V-FW; D-HW; V-HW
LGE-WS-01965	M5403	<i>Heliconius erato reductimacula</i>	Amazonas, La Pedrera	SS-FW; SS-HW; D-FW; V-FW; D-HW; V-HW
LGE-WS-01966	M5304	<i>Heliconius erato reductimacula</i>	Amazonas, La Pedrera	SS-FW; SS-HW

LGE-WS-01967	M5323	<i>Heliconius erato reductimacula</i>	Amazonas, La Pedrera	SS-FW; SS-HW; D-FW; V-FW; D-HW; V-HW
LGE-WS-01968	M5306	<i>Heliconius erato reductimacula</i>	Amazonas, La Pedrera	SS-FW; SS-HW
LGE-WS-01969	M5307	<i>Heliconius erato reductimacula</i>	Amazonas, La Pedrera	SS-FW; SS-HW; D-FW; V-FW; D-HW; V-HW
LGE-WS-01970	M5399	<i>Heliconius erato reductimacula</i>	Amazonas, La Pedrera	SS-FW; SS-HW; D-FW; V-FW; D-HW; V-HW
LGE-WS-01971	M5398	<i>Heliconius erato reductimacula</i>	Amazonas, La Pedrera	SS-FW; SS-HW; D-FW; V-FW; D-HW; V-HW
LGE-WS-01972	M5400	<i>Heliconius erato reductimacula</i>	Amazonas, La Pedrera	SS-FW; SS-HW; D-FW; V-FW; D-HW; V-HW
LGE-WS-01973	M5401	<i>Heliconius erato reductimacula</i>	Amazonas, La Pedrera	SS-FW; SS-HW; D-FW; V-FW; D-HW; V-HW
LGE-WS-01974	M5369	<i>Heliconius erato reductimacula</i>	Amazonas, La Pedrera	SS-FW; SS-HW; D-FW; V-FW; D-HW; V-HW
LGE-WS-01975	M5368	<i>Heliconius erato reductimacula</i>	Amazonas, La Pedrera	SS-FW; SS-HW; D-FW; V-FW; D-HW; V-HW
LGE-WS-01976	M5325	<i>Heliconius erato reductimacula</i>	Amazonas, La Pedrera	SS-FW; SS-HW; D-FW; V-FW; D-HW; V-HW
LGE-WS-01977	M5326	<i>Heliconius erato reductimacula</i>	Amazonas, La Pedrera	SS-FW; SS-HW; D-FW; V-FW; D-HW; V-HW
LGE-WS-01978	M5397	<i>Heliconius erato reductimacula</i>	Amazonas, La Pedrera	SS-FW; SS-HW
LGE-WS-01979	M5396	<i>Heliconius erato reductimacula</i>	Amazonas, La Pedrera	SS-FW; SS-HW; V-FW; V-HW
LGE-WS-00951	M631	<i>Heliconius erato venus</i>	Valle del Cauca, Ladrilleros	SS-FW; SS-HW; D-FW; V-FW; D-HW; V-HW
LGE-WS-00952	M276	<i>Heliconius erato venus</i>	Valle del Cauca, Ladrilleros	SS-FW; SS-HW; D-FW; V-FW; D-HW; V-HW
LGE-WS-00953	M286	<i>Heliconius erato venus</i>	Valle del Cauca, La Barra	SS-FW; SS-HW; D-FW; V-FW; D-HW; V-HW
LGE-WS-00954	M284	<i>Heliconius erato venus</i>	Valle del Cauca, Ladrilleros	SS-FW; SS-HW; D-FW; V-FW; D-HW; V-HW
LGE-WS-00955	M4860	<i>Heliconius erato venus</i>	Valle_del_Cauca, Quebrada La Cristalina	SS-FW; SS-HW; D-FW; V-FW; D-HW; V-HW
LGE-WS-00956	M4873	<i>Heliconius erato venus</i>	Valle_del_Cauca, Quebrada La Cristalina	SS-FW; SS-HW; D-FW; V-FW; D-HW; V-HW
LGE-WS-00957	M4870	<i>Heliconius erato venus</i>	Valle_del_Cauca, Quebrada La Cristalina	SS-FW; SS-HW; D-FW; V-FW; D-HW; V-HW
LGE-WS-00958	M4869	<i>Heliconius erato venus</i>	Valle_del_Cauca, Quebrada La Cristalina	SS-FW; SS-HW; D-FW; V-FW; D-HW; V-HW
LGE-WS-00959	M1260	<i>Heliconius erato venus</i>	Valle del Cauca, Río Dagua, Sacarias	D-FW; V-FW; D-HW; V-HW
LGE-WS-00960	M1037	<i>Heliconius erato venus</i>	Valle del Cauca, Ladrilleros	SS-FW; SS-HW; D-FW; V-FW; D-HW; V-HW
LGE-WS-00961	M1039	<i>Heliconius erato venus</i>	Valle del Cauca, Ladrilleros	SS-FW; SS-HW; D-FW; V-FW; D-HW; V-HW
LGE-WS-00962	M639	<i>Heliconius erato venus</i>	Valle del Cauca, Ladrilleros	SS-FW; SS-HW; D-FW; V-FW; D-HW; V-HW
LGE-WS-00963	M2273	<i>Heliconius erato venus</i>	Valle del Cauca, Ladrilleros	SS-FW; SS-HW; D-FW; V-FW; D-HW; V-HW

LGE-WS-00964	M3127	<i>Heliconius erato venus</i>	Valle_del_Cauca, Queremal	SS-FW; SS-HW; D-FW; V-FW; D-HW; V-HW
LGE-WS-00965	M2280	<i>Heliconius erato venus</i>	Valle del Cauca, Ladrilleros	SS-FW; SS-HW; D-FW; V-FW; D-HW; V-HW
LGE-WS-00966	M2635	<i>Heliconius erato venus</i>	Valle del Cauca, La Barra	D-FW; V-FW; D-HW; V-HW
LGE-WS-00967	M3658	<i>Heliconius erato venus</i>	Valle_del_Cauca, Queremal	SS-FW; SS-HW; D-FW; V-FW; D-HW; V-HW
LGE-WS-00968	M4801	<i>Heliconius erato venus</i>	Valle del Cauca, Restrepo	SS-FW; SS-HW; D-FW; V-FW; D-HW; V-HW
LGE-WS-00969	M3349	<i>Heliconius erato venus</i>	Valle_del_Cauca, Queremal	SS-FW; SS-HW; D-FW; V-FW; D-HW; V-HW
LGE-WS-02401	Andes-E12497	<i>Heliconius hecuba tolima</i>	Nariño, Km59, vía Pasto-Mocoa	SS-FW; SS-HW; D-FW; V-FW; D-HW; V-HW
LGE-WS-02351	M1502	<i>Heliconius heurippa</i>	Meta, Buenavista	SS-FW; SS-HW; D-FW; V-FW
LGE-WS-02352	M1510	<i>Heliconius heurippa</i>	Meta, Buenavista	SS-FW; SS-HW; D-FW; V-FW
LGE-WS-02353	M2051	<i>Heliconius heurippa</i>	Meta, Buenavista	SS-FW; SS-HW; D-FW; V-FW
LGE-WS-02354	M2148	<i>Heliconius heurippa</i>	Meta, Cubarral, Vereda Vergel Alto	SS-FW; SS-HW; D-FW; V-FW
LGE-WS-02355	M2206	<i>Heliconius heurippa</i>	Meta, Buenavista	SS-FW; SS-HW; D-FW; V-FW
LGE-WS-02356	M2412	<i>Heliconius heurippa</i>	Meta, Buenavista	SS-FW; SS-HW; D-FW; V-FW
LGE-WS-02357	M2149	<i>Heliconius heurippa</i>	Meta, Cubarral, Vereda Vergel Alto	SS-FW; SS-HW; D-FW; V-FW
LGE-WS-02358	M2419	<i>Heliconius heurippa</i>	Meta, Buenavista	SS-FW; SS-HW; D-FW; V-FW
LGE-WS-02359	M3393	<i>Heliconius heurippa</i>	Meta, Buenavista	SS-FW; SS-HW; D-FW; V-FW
LGE-WS-02360	M3396	<i>Heliconius heurippa</i>	Meta, Buenavista	SS-FW; SS-HW; D-FW; V-FW
LGE-WS-02361	M3391	<i>Heliconius heurippa</i>	Meta, Buenavista	SS-FW; SS-HW; D-FW; V-FW
LGE-WS-02362	M3392	<i>Heliconius heurippa</i>	Meta, Buenavista	SS-FW; SS-HW; D-FW; V-FW
LGE-WS-02363	M3397	<i>Heliconius heurippa</i>	Meta, Buenavista	SS-FW; SS-HW; D-FW; V-FW
LGE-WS-02364	M3424	<i>Heliconius heurippa</i>	Meta, Buenavista	SS-FW; SS-HW; D-FW; V-FW
LGE-WS-02365	M4615	<i>Heliconius heurippa</i>	Meta, Lejanías, Río Guejar	SS-FW; SS-HW; D-FW; V-FW
LGE-WS-02366	M3844	<i>Heliconius heurippa</i>	Meta, Lejanías, Vereda Naranjal	SS-FW; SS-HW; D-FW; V-FW
LGE-WS-02367	M250	<i>Heliconius heurippa</i>	Meta, Buenavista	SS-FW; SS-HW; D-FW; V-FW
LGE-WS-02368	M3843	<i>Heliconius heurippa</i>	Meta, Lejanías, Río Guejar	SS-FW; SS-HW; D-FW; V-FW
LGE-WS-02369	M3423	<i>Heliconius heurippa</i>	Meta, Buenavista	SS-FW; SS-HW; D-FW; V-FW

LGE-WS-02370	M2962	<i>Heliconius heurippa</i>	Meta, Buenavista	SS-FW; SS-HW; D-FW; V-FW
LGE-WS-02371	M3394	<i>Heliconius heurippa</i>	Meta, Buenavista	SS-FW; SS-HW; D-FW; V-FW
LGE-WS-02372	N/A	<i>Heliconius heurippa</i>	Meta, Virgen de Chirajara	SS-FW; SS-HW; D-FW; V-FW
LGE-WS-02373	N/A	<i>Heliconius heurippa</i>	Meta, Virgen de Chirajara	SS-FW; SS-HW; D-FW; V-FW
LGE-WS-02374	N/A	<i>Heliconius heurippa</i>	Meta, Virgen de Chirajara	SS-FW; SS-HW; D-FW; V-FW
LGE-WS-02375	N/A	<i>Heliconius heurippa</i>	Meta, Buenavista	SS-FW; SS-HW; D-FW; V-FW
LGE-WS-02376	N/A	<i>Heliconius heurippa</i>	Meta, Buenavista	SS-FW; SS-HW; D-FW; V-FW
LGE-WS-00702	M821	<i>Heliconius melpomene melpomene</i>	Meta, Virgen de Chirajara	D-FW; V-FW; D-HW; V-HW
LGE-WS-00703	M663	<i>Heliconius melpomene melpomene</i>	Meta, Virgen de Chirajara	D-FW; V-FW; D-HW; V-HW
LGE-WS-00704	M390	<i>Heliconius melpomene melpomene</i>	Casanare, Morcote, Nunchia	SS-FW; SS-HW; D-FW; V-FW; D-HW; V-HW
LGE-WS-00705	M267	<i>Heliconius melpomene melpomene</i>	Meta, Virgen de Chirajara	SS-FW; SS-HW; D-FW; V-FW
LGE-WS-00706	M1475	<i>Heliconius melpomene melpomene</i>	Meta, Virgen de Chirajara	SS-FW; SS-HW; D-FW; V-FW; D-HW; V-HW
LGE-WS-00707	M822	<i>Heliconius melpomene melpomene</i>	Meta, Virgen de Chirajara	SS-FW; SS-HW; D-FW; V-FW; D-HW; V-HW
LGE-WS-00708	M823	<i>Heliconius melpomene melpomene</i>	Meta, Virgen de Chirajara	SS-FW; SS-HW; D-FW; V-FW; D-HW; V-HW
LGE-WS-00709	M825	<i>Heliconius melpomene melpomene</i>	Meta, Virgen de Chirajara	SS-FW; SS-HW; D-FW; V-FW; D-HW; V-HW
LGE-WS-00710	M826	<i>Heliconius melpomene melpomene</i>	Meta, Virgen de Chirajara	SS-FW; SS-HW; D-FW; V-FW
LGE-WS-00711	M828	<i>Heliconius melpomene melpomene</i>	Meta, Virgen de Chirajara	SS-FW; SS-HW; D-FW; V-FW; D-HW; V-HW
LGE-WS-00712	M829	<i>Heliconius melpomene melpomene</i>	Meta, Virgen de Chirajara	SS-FW; SS-HW; D-FW; V-FW; D-HW; V-HW
LGE-WS-00713	M830	<i>Heliconius melpomene melpomene</i>	Meta, Virgen de Chirajara	SS-FW; SS-HW; D-FW; V-FW; D-HW; V-HW
LGE-WS-00714	M832	<i>Heliconius melpomene melpomene</i>	Meta, Virgen de Chirajara	SS-FW; SS-HW; D-FW; V-FW; D-HW; V-HW
LGE-WS-00715	M831	<i>Heliconius melpomene melpomene</i>	Meta, Virgen de Chirajara	SS-FW; SS-HW; D-FW; V-FW; D-HW; V-HW
LGE-WS-00719	M325	<i>Heliconius melpomene melpomene</i>	Casanare, Morcote, Nunchia	SS-FW; SS-HW; D-FW; V-FW; D-HW; V-HW
LGE-WS-00720	M1737	<i>Heliconius melpomene melpomene</i>	Meta, Virgen de Chirajara	SS-FW; SS-HW; D-FW; V-FW; D-HW; V-HW
LGE-WS-00721	M1357	<i>Heliconius melpomene melpomene</i>	Meta, Virgen de Chirajara	SS-FW; SS-HW; D-FW; V-FW; D-HW; V-HW
LGE-WS-00722	M3256	<i>Heliconius melpomene melpomene</i>	Meta, Virgen de Chirajara	SS-FW; SS-HW; D-FW; V-FW; D-HW; V-HW
LGE-WS-00723	M2187	<i>Heliconius melpomene melpomene</i>	Meta, Villavicencio, Bosques de Bavaria	SS-FW; SS-HW; D-FW; V-FW; D-HW; V-HW

LGE-WS-00724	M2189	<i>Heliconius melpomene melpomene</i>	Meta, Villavicencio, Bosques de Bavaria	SS-FW; SS-HW; D-FW; V-FW; D-HW; V-HW
LGE-WS-00725	M824	<i>Heliconius melpomene melpomene</i>	Meta, Virgen de Chirajara	D-FW; V-FW; D-HW; V-HW
LGE-WS-00726	M2413	<i>Heliconius melpomene melpomene</i>	Meta, Virgen de Chirajara	SS-FW; SS-HW; D-FW; V-FW; D-HW; V-HW
LGE-WS-00727	M1057	<i>Heliconius melpomene melpomene</i>	Meta, Virgen de Chirajara	SS-FW; SS-HW; D-FW; V-FW; D-HW; V-HW
LGE-WS-00728	M1055	<i>Heliconius melpomene melpomene</i>	Meta, Villavicencio, El Carmen	SS-FW; SS-HW; D-FW; V-FW; D-HW; V-HW
LGE-WS-00729	M1061	<i>Heliconius melpomene melpomene</i>	Meta, Virgen de Chirajara	SS-FW; SS-HW; D-FW; V-FW; D-HW; V-HW
LGE-WS-00730	M1456	<i>Heliconius melpomene melpomene</i>	Meta, Villavicencio, Bosques de Bavaria	SS-FW; SS-HW; D-FW; V-FW; D-HW; V-HW
LGE-WS-00731	M1669	<i>Heliconius melpomene melpomene</i>	Meta, Virgen de Chirajara	SS-FW; SS-HW; D-FW; V-FW; D-HW; V-HW
LGE-WS-00732	M3759	<i>Heliconius melpomene melpomene</i>	Meta, Virgen de Chirajara	SS-FW; SS-HW; D-FW; V-FW; D-HW; V-HW
LGE-WS-00733	N/A	<i>Heliconius melpomene melpomene</i>	Meta, Virgen de Chirajara	SS-FW; SS-HW; D-FW; V-FW; D-HW; V-HW
LGE-WS-00734	N/A	<i>Heliconius melpomene melpomene</i>	Meta, Virgen de Chirajara	SS-FW; SS-HW; D-FW; V-FW; D-HW; V-HW
LGE-WS-00735	N/A	<i>Heliconius melpomene melpomene</i>	Meta, Virgen de Chirajara	SS-FW; SS-HW; D-FW; V-FW; D-HW; V-HW
LGE-WS-00736	N/A	<i>Heliconius melpomene melpomene</i>	Meta, Virgen de Chirajara	SS-FW; SS-HW; D-FW; V-FW; D-HW; V-HW
LGE-WS-00737	N/A	<i>Heliconius melpomene melpomene</i>	Meta, Virgen de Chirajara	SS-FW; SS-HW; D-FW; V-FW; D-HW; V-HW
LGE-WS-00738	N/A	<i>Heliconius melpomene melpomene</i>	Meta, Virgen de Chirajara	D-FW; V-FW
LGE-WS-00739	N/A	<i>Heliconius melpomene melpomene</i>	Meta, Virgen de Chirajara	SS-FW; SS-HW; D-FW; V-FW; D-HW; V-HW
LGE-WS-00740	N/A	<i>Heliconius melpomene melpomene</i>	Meta, Virgen de Chirajara	SS-FW; SS-HW; D-FW; V-FW; D-HW; V-HW
LGE-WS-00741	N/A	<i>Heliconius melpomene melpomene</i>	Meta, Virgen de Chirajara	D-FW; V-FW; D-HW; V-HW
LGE-WS-00742	N/A	<i>Heliconius melpomene melpomene</i>	Meta, Virgen de Chirajara	SS-FW; SS-HW; D-FW; V-FW; D-HW; V-HW
LGE-WS-00743	N/A	<i>Heliconius melpomene melpomene</i>	Meta, Virgen de Chirajara	SS-FW; SS-HW; D-FW; V-FW; D-HW; V-HW
LGE-WS-00744	N/A	<i>Heliconius melpomene melpomene</i>	Meta, Virgen de Chirajara	SS-FW; SS-HW; D-FW; V-FW; D-HW; V-HW
LGE-WS-00745	N/A	<i>Heliconius melpomene melpomene</i>	Meta, Virgen de Chirajara	SS-FW; SS-HW; D-FW; V-FW; D-HW; V-HW
LGE-WS-00746	N/A	<i>Heliconius melpomene melpomene</i>	Meta, Virgen de Chirajara	SS-FW; SS-HW; D-FW; V-FW; D-HW; V-HW
LGE-WS-00747	N/A	<i>Heliconius melpomene melpomene</i>	Meta, Virgen de Chirajara	SS-FW; SS-HW; D-FW; V-FW; D-HW; V-HW
LGE-WS-00748	N/A	<i>Heliconius melpomene melpomene</i>	Meta, Virgen de Chirajara	SS-FW; SS-HW; D-FW; V-FW; D-HW; V-HW
LGE-WS-00749	N/A	<i>Heliconius melpomene melpomene</i>	Meta, Virgen de Chirajara	SS-FW; SS-HW; D-FW; V-FW; D-HW; V-HW

LGE-WS-00750	N/A	<i>Heliconius melpomene melpomene</i>	Meta, Virgen de Chirajara	SS-FW; SS-HW; D-FW; V-FW
LGE-WS-01000	M231	<i>Heliconius melpomene bellula</i>	Putumayo, San Antonio	SS-FW; SS-HW; D-FW; V-FW; D-HW; V-HW
LGE-WS-01001	M4302	<i>Heliconius melpomene bellula</i>	Putumayo, Mocoa, Campucana	SS-FW; SS-HW; D-FW; V-FW; D-HW; V-HW
LGE-WS-01002	M4277	<i>Heliconius melpomene bellula</i>	Putumayo, Mocoa, Campucana	SS-FW; SS-HW; D-FW; V-FW; D-HW; V-HW
LGE-WS-01003	M229	<i>Heliconius melpomene bellula</i>	Putumayo, San Antonio	SS-FW; SS-HW; D-FW; V-FW; D-HW; V-HW
LGE-WS-01004	M4293	<i>Heliconius melpomene bellula</i>	Putumayo, Mocoa, Campucana	SS-FW; SS-HW; D-FW; V-FW; D-HW; V-HW
LGE-WS-01006	M4524	<i>Heliconius melpomene bellula</i>	Putumayo, Mocoa, Campucana	SS-FW; D-FW; V-FW
LGE-WS-01007	M226	<i>Heliconius melpomene bellula</i>	Putumayo, Mocoa	SS-FW; SS-HW; D-FW; V-FW; D-HW; V-HW
LGE-WS-01008	M4257	<i>Heliconius melpomene bellula</i>	Putumayo, Mocoa, Campucana	SS-FW; SS-HW; D-FW; V-FW
LGE-WS-01009	M4785	<i>Heliconius melpomene bellula</i>	Putumayo, Mocoa, Campucana	SS-FW; SS-HW; D-FW; V-FW; D-HW; V-HW
LGE-WS-01010	M240	<i>Heliconius melpomene bellula</i>	Putumayo, San Antonio	SS-FW; SS-HW; D-FW; V-FW; D-HW; V-HW
LGE-WS-01011	M239	<i>Heliconius melpomene bellula</i>	Putumayo, San Antonio	SS-FW; SS-HW; D-FW; V-FW
LGE-WS-01012	M4258	<i>Heliconius melpomene bellula</i>	Putumayo, Mocoa, Campucana	SS-FW; SS-HW; D-FW; V-FW; D-HW; V-HW
LGE-WS-01013	M4259	<i>Heliconius melpomene bellula</i>	Putumayo, Mocoa, Campucana	SS-FW; SS-HW; D-FW; V-FW; D-HW; V-HW
LGE-WS-01014	M4265	<i>Heliconius melpomene bellula</i>	Putumayo, Mocoa, Campucana	SS-FW; SS-HW; D-FW; V-FW; D-HW; V-HW
LGE-WS-01015	M4260	<i>Heliconius melpomene bellula</i>	Putumayo, Mocoa, Campucana	SS-FW; SS-HW; D-FW; V-FW; D-HW; V-HW
LGE-WS-01016	M4267	<i>Heliconius melpomene bellula</i>	Putumayo, Mocoa, Campucana	SS-FW; SS-HW; D-FW; V-FW; D-HW; V-HW
LGE-WS-01017	M4417	<i>Heliconius melpomene bellula</i>	Putumayo, Mocoa, Campucana	SS-FW; SS-HW; D-FW; V-FW; D-HW; V-HW
LGE-WS-01018	M4268	<i>Heliconius melpomene bellula</i>	Putumayo, Mocoa, Campucana	SS-FW; SS-HW; D-FW; V-FW; D-HW; V-HW
LGE-WS-01019	M4414	<i>Heliconius melpomene bellula</i>	Putumayo, Mocoa, Campucana	SS-FW; SS-HW; D-FW; V-FW; D-HW; V-HW
LGE-WS-01020	M4264	<i>Heliconius melpomene bellula</i>	Putumayo, Mocoa, Campucana	SS-FW; SS-HW; D-FW; V-FW
LGE-WS-01021	M4416	<i>Heliconius melpomene bellula</i>	Putumayo, Mocoa, Campucana	SS-FW; SS-HW; D-FW; V-FW; D-HW; V-HW
LGE-WS-01023	M238	<i>Heliconius melpomene bellula</i>	Putumayo, San Antonio	SS-FW; SS-HW; D-FW; V-FW; D-HW; V-HW
CAM040032	CAM040032	<i>Heliconius melpomene bellula</i>	Putumayo, Mocoa, Campucana	SS-FW; SS-HW; D-FW; V-FW; D-HW; V-HW
CAM040043	CAM040043	<i>Heliconius melpomene bellula</i>	Putumayo, Mocoa, Campucana	SS-FW; D-FW; V-FW; D-HW
CAM040054	CAM040054	<i>Heliconius melpomene bellula</i>	Putumayo, Mocoa, Campucana	SS-FW; D-FW; V-FW

CAM040057	CAM040057	<i>Heliconius melpomene bellula</i>	Putumayo, Mocoa, Campucana	SS-FW; SS-HW; D-FW; V-FW; D-HW; V-HW
CAM040058	CAM040058	<i>Heliconius melpomene bellula</i>	Putumayo, Mocoa, Campucana	SS-FW; SS-HW; D-FW; V-FW; D-HW; V-HW
CAM040059	CAM040059	<i>Heliconius melpomene bellula</i>	Putumayo, Mocoa, Campucana	SS-FW; SS-HW; D-FW; V-FW; D-HW; V-HW
CAM040061	CAM040061	<i>Heliconius melpomene bellula</i>	Putumayo, Mocoa, Campucana	SS-FW; SS-HW; D-FW; V-FW; D-HW; V-HW
CAM040062	CAM040062	<i>Heliconius melpomene bellula</i>	Putumayo, Mocoa, Campucana	SS-FW; SS-HW; D-FW; V-FW; D-HW; V-HW
CAM040064	CAM040064	<i>Heliconius melpomene bellula</i>	Putumayo, Mocoa, Campucana	SS-FW; SS-HW; D-FW; V-FW; D-HW; V-HW
CAM040065	CAM040065	<i>Heliconius melpomene bellula</i>	Putumayo, Mocoa, Campucana	SS-FW; SS-HW; D-FW; V-FW; D-HW; V-HW
CAM040080	CAM040080	<i>Heliconius melpomene bellula</i>	Putumayo, Mocoa, Campucana	SS-FW; D-FW
CAM040081	CAM040081	<i>Heliconius melpomene bellula</i>	Putumayo, Mocoa, Campucana	SS-FW; SS-HW; D-FW; V-FW; D-HW; V-HW
CAM040082	CAM040082	<i>Heliconius melpomene bellula</i>	Putumayo, Mocoa, Campucana	SS-FW; SS-HW; D-FW; V-FW; D-HW; V-HW
CAM040085	CAM040085	<i>Heliconius melpomene bellula</i>	Putumayo, Mocoa, Campucana	SS-FW; SS-HW; D-FW; V-FW; D-HW; V-HW
CAM040086	CAM040086	<i>Heliconius melpomene bellula</i>	Putumayo, Mocoa, Campucana	SS-FW; SS-HW; D-FW; D-HW
CAM040087	CAM040087	<i>Heliconius melpomene bellula</i>	Putumayo, Mocoa, Campucana	SS-FW; SS-HW; D-FW; V-FW; D-HW; V-HW
CAM040088	CAM040088	<i>Heliconius melpomene bellula</i>	Putumayo, Mocoa, Campucana	SS-FW; SS-HW; D-FW; V-FW; D-HW; V-HW
CAM040099	CAM040099	<i>Heliconius melpomene bellula</i>	Putumayo, Mocoa, Campucana	SS-FW; D-FW; V-FW
CAM040110	CAM040110	<i>Heliconius melpomene bellula</i>	Putumayo, Mocoa, Campucana	SS-FW; SS-HW; D-FW; V-FW
LGE-WS-02700	M4034	<i>Heliconius melpomene malleti</i>	Amazonas, Puerto Nariño	SS-FW; SS-HW
LGE-WS-02701	M3544	<i>Heliconius melpomene malleti</i>	Caquetá, Florencia, Paraiso	SS-FW; SS-HW; D-FW; V-FW; D-HW; V-HW
LGE-WS-02702	M3096	<i>Heliconius melpomene malleti</i>	Caquetá, Quebrada Las Doraditas	SS-FW; SS-HW; D-FW; V-FW; D-HW; V-HW
LGE-WS-02703	M3359	<i>Heliconius melpomene malleti</i>	Caquetá, Quebrada Las Doraditas	SS-FW; SS-HW; D-FW; V-FW; D-HW; V-HW
LGE-WS-02704	M1014	<i>Heliconius melpomene malleti</i>	Caquetá, Florencia, Paraiso	SS-FW; SS-HW; D-FW; V-FW; D-HW; V-HW
LGE-WS-02705	M614	<i>Heliconius melpomene malleti</i>	Caquetá, Florencia, Sucre	SS-FW; SS-HW; D-FW; V-FW; D-HW; V-HW
LGE-WS-02706	M1016	<i>Heliconius melpomene malleti</i>	Caquetá, Florencia, Sucre	SS-FW; SS-HW; D-FW; V-FW; D-HW; V-HW
LGE-WS-02707	M4298	<i>Heliconius melpomene malleti</i>	Putumayo, Vereda San Rafael, Finca El Escondite	SS-FW; SS-HW; D-FW; V-FW; D-HW; V-HW
LGE-WS-02708	M604	<i>Heliconius melpomene malleti</i>	Caquetá, Florencia, Sucre	SS-FW; SS-HW; D-FW; V-FW; D-HW; V-HW
LGE-WS-02709	M592	<i>Heliconius melpomene malleti</i>	Caquetá, Florencia, Sucre	SS-FW; SS-HW; D-FW; V-FW; D-HW; V-HW

LGE-WS-02710	M589	<i>Heliconius melpomene malleti</i>	Caquetá, Florencia, Sucre	SS-FW; SS-HW; D-FW; V-FW; D-HW; V-HW
LGE-WS-02711	M590	<i>Heliconius melpomene malleti</i>	Caquetá, Florencia, Sucre	SS-FW; SS-HW; D-FW; V-FW; D-HW; V-HW
LGE-WS-02712	M468	<i>Heliconius melpomene malleti</i>	Caquetá, Florencia, Sucre	SS-FW; SS-HW; D-FW; V-FW; D-HW; V-HW
LGE-WS-02713	M58	<i>Heliconius melpomene malleti</i>	Caquetá, Finca Piñacue	SS-FW; SS-HW; D-FW; V-FW; D-HW; V-HW
LGE-WS-02714	M426	<i>Heliconius melpomene malleti</i>	Caquetá, Florencia, Sucre	SS-FW; SS-HW; D-FW; V-FW; D-HW; V-HW
LGE-WS-02715	M434	<i>Heliconius melpomene malleti</i>	Caquetá, Florencia, Sucre	SS-FW; SS-HW; D-FW; V-FW; D-HW; V-HW
LGE-WS-02716	M2360	<i>Heliconius melpomene malleti</i>	Caquetá, Florencia, Paraiso	SS-FW; SS-HW; D-FW; V-FW; D-HW; V-HW
LGE-WS-02717	M2404	<i>Heliconius melpomene malleti</i>	Caquetá, Florencia, Paraiso	SS-FW; SS-HW; D-FW; V-FW; D-HW; V-HW
LGE-WS-02718	M2361	<i>Heliconius melpomene malleti</i>	Caquetá, Florencia, Paraiso	SS-FW; SS-HW; D-FW; V-FW; D-HW; V-HW
LGE-WS-02719	M302	<i>Heliconius melpomene malleti</i>	Caquetá, Florencia, Villaraz	SS-FW; SS-HW; D-FW; V-FW; D-HW; V-HW
LGE-WS-02720	M2352	<i>Heliconius melpomene malleti</i>	Caquetá, Quebrada Las Doraditas	SS-FW; SS-HW
LGE-WS-02721	M2311	<i>Heliconius melpomene malleti</i>	Caquetá, Florencia, Sucre	SS-FW; SS-HW; D-FW; V-FW; D-HW; V-HW
LGE-WS-02722	M2309	<i>Heliconius melpomene malleti</i>	Caquetá, Finca Piñacue	SS-FW; SS-HW; D-FW; V-FW; D-HW; V-HW
LGE-WS-02723	M2321	<i>Heliconius melpomene malleti</i>	Caquetá, Finca Piñacue	SS-FW; SS-HW; D-FW; V-FW; D-HW; V-HW
LGE-WS-02724	M2312	<i>Heliconius melpomene malleti</i>	Caquetá, Finca Piñacue	SS-FW; SS-HW; D-FW; V-FW; D-HW; V-HW
LGE-WS-02725	M2437	<i>Heliconius melpomene malleti</i>	Caquetá, Las Morras, Puerto Amor	SS-FW; SS-HW; D-FW; V-FW; D-HW; V-HW
LGE-WS-02726	M2316	<i>Heliconius melpomene malleti</i>	Caquetá, Finca Piñacue	SS-FW; SS-HW
LGE-WS-02727	M56	<i>Heliconius melpomene malleti</i>	Caquetá, Finca Piñacue	SS-FW; SS-HW; D-FW; V-FW; D-HW; V-HW
LGE-WS-02728	M2369	<i>Heliconius melpomene malleti</i>	Caquetá, Florencia, Paraiso	SS-FW; SS-HW; D-FW; V-FW; D-HW; V-HW
LGE-WS-02729	M1288	<i>Heliconius melpomene malleti</i>	Caquetá, Florencia, Paraiso	SS-FW; SS-HW; D-FW; V-FW; D-HW; V-HW
LGE-WS-02730	M2405	<i>Heliconius melpomene malleti</i>	Caquetá, Quebrada Las Doraditas	SS-FW; SS-HW
LGE-WS-02731	M1192	<i>Heliconius melpomene malleti</i>	Caquetá, Quebrada Las Doraditas	SS-FW; SS-HW; D-FW; V-FW; D-HW; V-HW
LGE-WS-02732	M1312	<i>Heliconius melpomene malleti</i>	Caquetá, Florencia, Paraiso	SS-FW; SS-HW; D-FW; V-FW; D-HW; V-HW
LGE-WS-02733	M1512	<i>Heliconius melpomene malleti</i>	Caquetá, Florencia, Paraiso	SS-FW; SS-HW; D-FW; V-FW; D-HW; V-HW
LGE-WS-02734	M1283	<i>Heliconius melpomene malleti</i>	Caquetá, Florencia, Paraiso	SS-FW; SS-HW; D-FW; V-FW; D-HW; V-HW
LGE-WS-02735	M1287	<i>Heliconius melpomene malleti</i>	Caquetá, Quebrada La Yuca	SS-FW; SS-HW; D-FW; V-FW; D-HW; V-HW

LGE-WS-02736	M1757	<i>Heliconius melpomene malleti</i>	Caquetá, Florencia, Sucre	SS-FW; SS-HW; D-FW; V-FW; D-HW; V-HW
LGE-WS-02737	M1823	<i>Heliconius melpomene malleti</i>	Caquetá, Florencia, Paraiso	SS-FW; SS-HW; D-FW; V-FW; D-HW; V-HW
LGE-WS-02738	M1827	<i>Heliconius melpomene malleti</i>	Caquetá, Santa Helena	SS-FW; SS-HW; D-FW; V-FW; D-HW; V-HW
LGE-WS-02739	M1196	<i>Heliconius melpomene malleti</i>	Caquetá, Florencia, Paraiso	SS-FW; SS-HW; D-FW; V-FW; D-HW; V-HW
LGE-WS-02740	M1757	<i>Heliconius melpomene malleti</i>	Caquetá, Florencia, Sucre	SS-FW; SS-HW; D-FW; V-FW; D-HW; V-HW
LGE-WS-00652	M3274	<i>Heliconius melpomene martiniae</i>	Cundinamarca, Peru, Guaduas	SS-FW; SS-HW; D-FW; V-FW; D-HW; V-HW
LGE-WS-00653	M1239	<i>Heliconius melpomene martiniae</i>	Cundinamarca, Peru, Guaduas	SS-FW; SS-HW; D-FW; V-FW; D-HW; V-HW
LGE-WS-00654	M1476	<i>Heliconius melpomene martiniae</i>	Cundinamarca, Boquerón	SS-FW; SS-HW; D-FW; V-FW; D-HW; V-HW
LGE-WS-00655	M1477	<i>Heliconius melpomene martiniae</i>	Cundinamarca, Boquerón	SS-FW; SS-HW; D-FW
LGE-WS-00656	M1478	<i>Heliconius melpomene martiniae</i>	Cundinamarca, Boquerón	SS-FW; SS-HW; D-FW; V-FW; D-HW; V-HW
LGE-WS-00657	M1479	<i>Heliconius melpomene martiniae</i>	Cundinamarca, Boquerón	SS-FW; SS-HW; D-FW; V-FW; D-HW; V-HW
LGE-WS-00658	M1480	<i>Heliconius melpomene martiniae</i>	Cundinamarca, Boquerón	SS-FW; SS-HW; D-FW; V-FW; D-HW; V-HW
LGE-WS-00659	M1488	<i>Heliconius melpomene martiniae</i>	Cundinamarca, Boquerón	SS-FW; SS-HW; D-FW; V-FW; D-HW; V-HW
LGE-WS-00660	M1483	<i>Heliconius melpomene martiniae</i>	Cundinamarca, Boquerón	SS-FW; SS-HW; D-FW
LGE-WS-00661	M1482	<i>Heliconius melpomene martiniae</i>	Cundinamarca, Boquerón	SS-FW; SS-HW; D-FW; V-FW; D-HW; V-HW
LGE-WS-00662	M1481	<i>Heliconius melpomene martiniae</i>	Cundinamarca, Boquerón	SS-FW; SS-HW; D-FW; V-FW; D-HW; V-HW
LGE-WS-00663	M1489	<i>Heliconius melpomene martiniae</i>	Cundinamarca, Boquerón	SS-FW; SS-HW; D-FW; V-FW; D-HW; V-HW
LGE-WS-00664	M1982	<i>Heliconius melpomene martiniae</i>	Cundinamarca, Sasaima	SS-FW; SS-HW; D-FW; V-FW; D-HW; V-HW
LGE-WS-00665	M2943	<i>Heliconius melpomene martiniae</i>	Cundinamarca, Quebrada Natauta	SS-FW; SS-HW; D-FW
LGE-WS-00666	M3101	<i>Heliconius melpomene martiniae</i>	Tolima, Ibagué, Santafé de los Guaduales	SS-FW; SS-HW; D-FW
LGE-WS-00667	M4195	<i>Heliconius melpomene martiniae</i>	Boyacá, Otanche, El Bajío	SS-FW; SS-HW; D-FW; V-FW; D-HW; V-HW
LGE-WS-00668	M4202	<i>Heliconius melpomene martiniae</i>	Boyacá, Otanche	V-FW; D-HW; V-HW
LGE-WS-00669	M4205	<i>Heliconius melpomene martiniae</i>	Boyacá, Otanche, El Bajío	SS-FW; SS-HW; D-FW; V-FW; D-HW; V-HW
LGE-WS-00670	M4217	<i>Heliconius melpomene martiniae</i>	Boyacá, Otanche	SS-FW; SS-HW; D-FW; V-FW; D-HW; V-HW
LGE-WS-00671	M4224	<i>Heliconius melpomene martiniae</i>	Boyacá, Otanche	SS-FW; SS-HW; D-FW; V-FW; D-HW; V-HW
LGE-WS-00672	M4230	<i>Heliconius melpomene martiniae</i>	Boyacá, Otanche	SS-FW; SS-HW; D-FW; V-FW; D-HW; V-HW

LGE-WS-00673	M4882	<i>Heliconius melpomene martinai</i>	Cundinamarca, Sasaima	D-FW; V-FW; D-HW; V-HW
LGE-WS-00674	M4190	<i>Heliconius melpomene martinai</i>	Boyacá, Otanche	SS-FW; SS-HW; D-FW; V-FW; D-HW; V-HW
LGE-WS-00675	M4191	<i>Heliconius melpomene martinai</i>	Boyacá, Otanche	SS-FW; SS-HW; D-FW; V-FW; D-HW; V-HW
LGE-WS-00717	M1979	<i>Heliconius melpomene martinai</i>	Cundinamarca, Sasaima	SS-FW; SS-HW; D-FW; V-FW
LGE-WS-00718	M2945	<i>Heliconius melpomene martinai</i>	Cundinamarca, La Vega	SS-FW; SS-HW; D-FW; V-FW; D-HW; V-HW
LGE-WS-00701	M1240	<i>Heliconius melpomene martinai</i>	Cundinamarca, Peru, Guaduas	SS-FW; SS-HW; D-FW; V-FW; D-HW; V-HW
LGE-WS-02201	M5033	<i>Heliconius melpomene vicina</i>	Amazonas, Leticia	SS-FW; SS-HW; D-FW; V-FW; D-HW; V-HW
LGE-WS-02202	M4035	<i>Heliconius melpomene vicina</i>	Amazonas, Leticia, Vereda San Jose	SS-FW; SS-HW; D-FW; V-FW; D-HW; V-HW
LGE-WS-02203	M4029	<i>Heliconius melpomene vicina</i>	Amazonas, Leticia, Vereda San Jose	SS-FW; SS-HW; D-FW; V-FW; D-HW; V-HW
LGE-WS-02204	M4033	<i>Heliconius melpomene vicina</i>	Amazonas, Leticia, Vereda San Jose	SS-FW; SS-HW
LGE-WS-02205	M4037	<i>Heliconius melpomene vicina</i>	Amazonas, Leticia	D-FW; V-FW; D-HW; V-HW
LGE-WS-02206	M5027	<i>Heliconius melpomene vicina</i>	Amazonas, Leticia, Resguardo San Antonio, Rio Yahuaraca	SS-FW; SS-HW; D-FW; V-FW; D-HW; V-HW
LGE-WS-02207	M4036	<i>Heliconius melpomene vicina</i>	Amazonas, Leticia	SS-FW; SS-HW; D-FW; V-FW; D-HW; V-HW
LGE-WS-02208	M5165	<i>Heliconius melpomene vicina</i>	Amazonas, Leticia, Río Tacana	SS-FW; SS-HW; D-FW; V-FW; D-HW; V-HW
LGE-WS-02209	M4040	<i>Heliconius melpomene vicina</i>	Amazonas, Leticia	SS-FW; SS-HW; D-FW; V-FW; D-HW; V-HW
LGE-WS-02210	M4041	<i>Heliconius melpomene vicina</i>	Amazonas, Leticia	SS-FW; SS-HW; D-FW; V-FW; D-HW; V-HW
LGE-WS-02211	M5407	<i>Heliconius melpomene vicina</i>	Amazonas, La Pedrera	SS-FW; SS-HW; V-FW; V-HW
LGE-WS-02213	M5408	<i>Heliconius melpomene vicina</i>	Amazonas, La Pedrera	SS-FW; SS-HW; D-FW; V-FW; D-HW; V-HW
LGE-WS-02214	M5409	<i>Heliconius melpomene vicina</i>	Amazonas, La Pedrera	SS-FW; SS-HW; D-FW; V-FW; D-HW; V-HW
LGE-WS-02215	M5321	<i>Heliconius melpomene vicina</i>	Amazonas, La Pedrera	SS-FW; SS-HW
LGE-WS-02216	M5338	<i>Heliconius melpomene vicina</i>	Amazonas, La Pedrera	SS-FW; SS-HW
LGE-WS-02217	M5378	<i>Heliconius melpomene vicina</i>	Amazonas, La Pedrera	SS-FW; SS-HW; D-FW; V-FW; D-HW; V-HW
LGE-WS-00801	M711	<i>Heliconius melpomene vulcanus</i>	Valle del Cauca, Rio Bravo, Lago Calima	SS-FW; SS-HW; D-FW; V-FW; D-HW; V-HW
LGE-WS-00802	M625	<i>Heliconius melpomene vulcanus</i>	Valle_del_Cauca, Quebrada La Cristalina	SS-FW; SS-HW; D-FW; V-FW; D-HW; V-HW
LGE-WS-00803	M4858	<i>Heliconius melpomene vulcanus</i>	Valle_del_Cauca, Quebrada La Cristalina	SS-FW; SS-HW; D-FW; V-FW; D-HW; V-HW

LGE-WS-00804	M647	<i>Heliconius melpomene vulcanus</i>	Valle del Cauca, Ladrilleros	SS-FW; SS-HW; D-FW; V-FW; D-HW; V-HW
LGE-WS-00805	M4868	<i>Heliconius melpomene vulcanus</i>	Valle_del_Cauca, Quebrada La Cristalina	SS-FW; SS-HW; D-FW; V-FW; D-HW; V-HW
LGE-WS-00806	M4867	<i>Heliconius melpomene vulcanus</i>	Valle_del_Cauca, Quebrada La Cristalina	SS-FW; SS-HW; D-FW; V-FW; D-HW; V-HW
LGE-WS-00807	M4878	<i>Heliconius melpomene vulcanus</i>	Valle_del_Cauca, Quebrada La Cristalina	SS-FW; SS-HW; D-FW; V-FW; D-HW; V-HW
LGE-WS-00808	M4866	<i>Heliconius melpomene vulcanus</i>	Valle_del_Cauca, Quebrada La Cristalina	SS-FW; SS-HW; D-FW; V-FW; D-HW; V-HW
LGE-WS-00809	M4865	<i>Heliconius melpomene vulcanus</i>	Valle_del_Cauca, Quebrada La Cristalina	SS-FW; SS-HW; D-FW; V-FW; D-HW; V-HW
LGE-WS-00810	M4599	<i>Heliconius melpomene vulcanus</i>	Valle del Cauca, Ladrilleros	SS-FW; SS-HW; D-FW; V-FW; D-HW; V-HW
LGE-WS-00811	M623	<i>Heliconius melpomene vulcanus</i>	Valle_del_Cauca, Quebrada La Cristalina	SS-FW; SS-HW; D-FW; V-FW; D-HW; V-HW
LGE-WS-00812	M712	<i>Heliconius melpomene vulcanus</i>	Valle del Cauca, Rio Bravo, Lago Calima	SS-FW; SS-HW; D-FW; V-FW; D-HW; V-HW
LGE-WS-00813	N/A	<i>Heliconius melpomene vulcanus</i>	Valle del Cauca, Rio Bravo, Lago Calima	SS-FW; SS-HW; V-FW
LGE-WS-00814	N/A	<i>Heliconius melpomene vulcanus</i>	Valle del Cauca, Rio Bravo, Lago Calima	SS-FW; SS-HW; D-FW; V-FW; D-HW; V-HW
LGE-WS-00815	N/A	<i>Heliconius melpomene vulcanus</i>	Valle del Cauca, Rio Bravo, Lago Calima	SS-FW; SS-HW; D-FW; V-FW; D-HW; V-HW
LGE-WS-00816	N/A	<i>Heliconius melpomene vulcanus</i>	Valle del Cauca, Rio Bravo, Lago Calima	SS-FW; SS-HW; D-FW; V-FW; D-HW; V-HW
LGE-WS-02051	M4435	<i>Heliconius sapho sapho</i>	Bolivar, Serranía de San Lucas, San Pedro, Vereda Ojos Claros	SS-FW; SS-HW; D-FW; V-FW; D-HW; V-HW
LGE-WS-02052	M2790	<i>Heliconius sapho sapho</i>	Santander, Mesa de los Santos, Vereda Volador	SS-FW; SS-HW; D-FW; V-FW; D-HW; V-HW
LGE-WS-02053	M2791	<i>Heliconius sapho sapho</i>	Santander, Mesa de los Santos, Vereda Volador	SS-FW; SS-HW; D-FW; V-FW; D-HW; V-HW
LGE-WS-02054	M4879	<i>Heliconius sapho sapho</i>	Caldas, Samaná, Tasajos, Río La Miel	SS-FW; SS-HW; D-FW; V-FW; D-HW; V-HW
LGE-WS-02055	M1997	<i>Heliconius sapho sapho</i>	Cundinamarca, Sasaima	SS-FW; SS-HW; D-FW; V-FW; D-HW; V-HW
LGE-WS-02056	JFLC	<i>Heliconius sapho sapho</i>	Risaralda, Bacari	SS-FW; SS-HW; D-FW; V-FW; D-HW; V-HW
LGE-WS-02057	JFLC	<i>Heliconius sapho sapho</i>	Chocó, Capurganá	SS-FW; SS-HW; D-FW; V-FW; D-HW; V-HW
LGE-WS-02058	JFLC	<i>Heliconius sapho sapho</i>	Boyacá, Otanche	SS-FW; SS-HW; D-FW; V-FW; D-HW; V-HW
LGE-WS-01300	M3529	<i>Heliconius sapho chocoensis</i>	Chocó, Amargal, Azurri	SS-FW; SS-HW; D-FW; V-FW
LGE-WS-01301	M3522	<i>Heliconius sapho chocoensis</i>	Chocó, Amargal	SS-FW; SS-HW; D-FW; V-FW
LGE-WS-01302	M3516	<i>Heliconius sapho chocoensis</i>	Chocó, Amargal	SS-FW; SS-HW; D-FW; V-FW
LGE-WS-01303	M3515	<i>Heliconius sapho chocoensis</i>	Chocó, Amargal	SS-FW; SS-HW; D-FW; V-FW
LGE-WS-01304	M3504	<i>Heliconius sapho chocoensis</i>	Valle del Cauca, San Pedro	SS-FW; SS-HW; D-FW; V-FW

LGE-WS-01305	M3507	<i>Heliconius sapho chocoensis</i>	Valle del Cauca, San Pedro	SS-FW; SS-HW; D-FW; V-FW
LGE-WS-01306	M3511	<i>Heliconius sapho chocoensis</i>	Valle del Cauca, Maguipi, Playa Dorada	SS-FW; SS-HW; D-FW; V-FW
LGE-WS-01307	M3509	<i>Heliconius sapho chocoensis</i>	Valle del Cauca, San Pedro	SS-FW; SS-HW; D-FW; V-FW
LGE-WS-01308	M3501	<i>Heliconius sapho chocoensis</i>	Valle del Cauca, San Pedro	SS-FW; SS-HW; D-FW; V-FW
LGE-WS-01309	M3497	<i>Heliconius sapho chocoensis</i>	Valle del Cauca, San Pedro	SS-FW; SS-HW; D-FW; V-FW
LGE-WS-01310	M3500	<i>Heliconius sapho chocoensis</i>	Valle del Cauca, San Pedro	SS-FW; SS-HW; D-FW; V-FW
LGE-WS-01311	M3498	<i>Heliconius sapho chocoensis</i>	Valle del Cauca, San Pedro	SS-FW; SS-HW; D-FW; V-FW
LGE-WS-01312	M3531	<i>Heliconius sapho chocoensis</i>	Chocó, Amargal, Azurri	SS-FW; SS-HW; D-FW; V-FW
LGE-WS-00502	M4518	<i>Heliconius sara magdalena</i>	Santander, La Joya	D-FW; V-FW; D-HW; V-HW
LGE-WS-00503	M4517	<i>Heliconius sara magdalena</i>	Santander, Girón	SS-FW; SS-HW; D-FW
LGE-WS-00504	M5171	<i>Heliconius sara magdalena</i>	Meta, Buenavista	SS-FW; D-FW; V-FW; D-HW; V-HW
LGE-WS-00505	M3943	<i>Heliconius sara magdalena</i>	Chocó, Paridera, Potes	SS-FW; SS-HW; D-FW; V-FW; D-HW; V-HW
LGE-WS-00506	M3533	<i>Heliconius sara magdalena</i>	Chocó, Amargal, Azurri	SS-FW; SS-HW; D-FW; V-FW; D-HW; V-HW
LGE-WS-00507	M3899	<i>Heliconius sara magdalena</i>	Chocó, Bahía Solano, Playa Flores	SS-FW; SS-HW; D-FW; V-FW; D-HW; V-HW
LGE-WS-00508	M3901	<i>Heliconius sara magdalena</i>	Chocó, Bahía Solano, Playa Flores	SS-FW; SS-HW; D-FW; V-FW; D-HW; V-HW
LGE-WS-00509	M3946	<i>Heliconius sara magdalena</i>	Chocó, Paridera, Potes	SS-FW; SS-HW; D-FW; V-FW; D-HW; V-HW
LGE-WS-00510	M2172	<i>Heliconius sara magdalena</i>	Venezuela, San Cristobal	SS-FW; SS-HW; D-FW; V-FW; D-HW; V-HW
LGE-WS-00511	M3532	<i>Heliconius sara magdalena</i>	Chocó, Amargal, Azurri	SS-FW; SS-HW; D-FW; V-FW; D-HW; V-HW
LGE-WS-00512	M3251	<i>Heliconius sara magdalena</i>	Antioquia, San Luis	SS-FW; SS-HW; D-FW; V-FW; D-HW; V-HW
LGE-WS-00513	M3512	<i>Heliconius sara magdalena</i>	Valle del Cauca, Quebrada La Cristalina	SS-FW; D-FW
LGE-WS-00514	M1989	<i>Heliconius sara magdalena</i>	Cundinamarca, Sasaima	SS-FW; SS-HW; D-FW; V-FW; D-HW; V-HW
LGE-WS-00302	M620	<i>Heliconius timareta florencia</i>	Caquetá, Florencia, Sucre	SS-FW; SS-HW; D-FW; V-FW; D-HW; V-HW
LGE-WS-00303	M602	<i>Heliconius timareta florencia</i>	Caquetá, Florencia, Sucre	SS-FW; SS-HW; D-FW; V-FW; D-HW; V-HW
LGE-WS-00304	M451	<i>Heliconius timareta florencia</i>	Caquetá, Florencia, Sucre	SS-FW; SS-HW; D-FW; V-FW; D-HW; V-HW
LGE-WS-00305	M418	<i>Heliconius timareta florencia</i>	Caquetá, Florencia, Sucre	SS-FW; SS-HW; D-FW; V-FW; D-HW; V-HW
LGE-WS-00306	M587	<i>Heliconius timareta florencia</i>	Caquetá, Florencia, Sucre	SS-FW; SS-HW; D-FW; V-FW; D-HW; V-HW

LGE-WS-00307	M471	<i>Heliconius timareta florencia</i>	Caquetá, Florencia, Sucre	D-FW; V-FW; D-HW; V-HW
LGE-WS-00308	M596	<i>Heliconius timareta florencia</i>	Caquetá, Florencia, Sucre	SS-FW; SS-HW; D-FW; V-FW; D-HW; V-HW
LGE-WS-00309	M593	<i>Heliconius timareta florencia</i>	Caquetá, Florencia, Sucre	SS-FW; SS-HW; D-FW; V-FW; D-HW; V-HW
LGE-WS-00310	M588	<i>Heliconius timareta florencia</i>	Caquetá, Florencia, Sucre	SS-FW; SS-HW; D-FW; V-FW; D-HW; V-HW
LGE-WS-00311	M472	<i>Heliconius timareta florencia</i>	Caquetá, Florencia, Sucre	SS-FW; SS-HW; D-FW; V-FW; D-HW; V-HW
LGE-WS-00313	M1010	<i>Heliconius timareta florencia</i>	Caquetá, Florencia, Sucre	SS-FW; SS-HW; D-FW; V-FW; D-HW; V-HW
LGE-WS-00314	M1075	<i>Heliconius timareta florencia</i>	Caquetá, Florencia, Sucre	SS-FW; SS-HW; D-FW; V-FW; D-HW; V-HW
LGE-WS-00315	M1074	<i>Heliconius timareta florencia</i>	Caquetá, Florencia, Sucre	SS-FW; SS-HW; D-FW; V-FW; D-HW; V-HW
LGE-WS-00316	M611	<i>Heliconius timareta florencia</i>	Caquetá, Florencia, Sucre	SS-FW; SS-HW; D-FW; V-FW; D-HW; V-HW
LGE-WS-00317	M607	<i>Heliconius timareta florencia</i>	Caquetá, Florencia, Sucre	SS-FW; SS-HW; D-FW; V-FW; D-HW; V-HW
LGE-WS-00318	M595	<i>Heliconius timareta florencia</i>	Caquetá, Florencia, Sucre	SS-FW; SS-HW; D-FW; V-FW; D-HW; V-HW
LGE-WS-00319	M612	<i>Heliconius timareta florencia</i>	Caquetá, Florencia, Sucre	SS-FW; SS-HW; D-FW; V-FW; D-HW; V-HW
LGE-WS-00320	M1805	<i>Heliconius timareta florencia</i>	Caquetá, Florencia, Sucre	SS-FW; SS-HW; D-FW; V-FW; D-HW; V-HW
LGE-WS-00321	M1772	<i>Heliconius timareta florencia</i>	Caquetá, Florencia, Sucre	SS-FW; SS-HW; D-FW; V-FW; D-HW; V-HW
LGE-WS-00322	M1808	<i>Heliconius timareta florencia</i>	Caquetá, Florencia, Sucre	D-FW; V-FW; D-HW; V-HW
LGE-WS-00323	M1817	<i>Heliconius timareta florencia</i>	Caquetá, Florencia, Sucre	SS-FW; SS-HW; V-FW; V-HW
LGE-WS-00324	M618	<i>Heliconius timareta florencia</i>	Caquetá, Florencia, Sucre	SS-FW; SS-HW; D-FW; V-FW; D-HW; V-HW
LGE-WS-00325	M259	<i>Heliconius timareta florencia</i>	Caquetá, Florencia, Sucre	D-FW; V-FW; D-HW; V-HW
LGE-WS-00326	M255	<i>Heliconius timareta florencia</i>	Caquetá, Florencia, Sucre	D-FW; V-FW; D-HW; V-HW
LGE-WS-00327	M3875	<i>Heliconius timareta florencia</i>	Caquetá, Florencia, Sucre	D-FW; V-FW; D-HW; V-HW
LGE-WS-00328	M1084	<i>Heliconius timareta florencia</i>	Caquetá, Florencia, Sucre	SS-FW; SS-HW; D-FW; V-FW; D-HW; V-HW
LGE-WS-00329	M1085	<i>Heliconius timareta florencia</i>	Caquetá, Florencia, Sucre	SS-FW; SS-HW; D-FW; V-FW; D-HW; V-HW
LGE-WS-00330	M1094	<i>Heliconius timareta florencia</i>	Caquetá, Florencia, Sucre	SS-FW; SS-HW; D-FW; V-FW; D-HW; V-HW
LGE-WS-00331	M1754	<i>Heliconius timareta florencia</i>	Caquetá, Florencia, Sucre	SS-FW; SS-HW; D-FW; V-FW; D-HW; V-HW
LGE-WS-00332	M622	<i>Heliconius timareta florencia</i>	Caquetá, Florencia, Sucre	D-FW; V-FW; D-HW; V-HW
LGE-WS-00333	M1009	<i>Heliconius timareta florencia</i>	Caquetá, Florencia, Sucre	SS-FW; SS-HW; D-FW; V-FW; D-HW; V-HW

LGE-WS-00334	M616	<i>Heliconius timareta florenzia</i>	Caquetá, Florencia, Sucre	SS-FW; SS-HW; D-FW; V-FW; D-HW; V-HW
LGE-WS-00336	M1846	<i>Heliconius timareta florenzia</i>	Caquetá, Florencia, Sucre	SS-FW; SS-HW; D-FW; V-FW; D-HW; V-HW
LGE-WS-00337	M462	<i>Heliconius timareta florenzia</i>	Caquetá, Florencia, Sucre	SS-FW; SS-HW; D-FW; V-FW; D-HW; V-HW
LGE-WS-00339	M3767	<i>Heliconius timareta florenzia</i>	Caquetá, Florencia, Sucre	SS-FW; SS-HW; D-FW; V-FW; D-HW; V-HW
LGE-WS-00341	M3874	<i>Heliconius timareta florenzia</i>	Caquetá, Florencia, Sucre	SS-FW; SS-HW; D-FW; V-FW; D-HW; V-HW
LGE-WS-00343	M1769	<i>Heliconius timareta florenzia</i>	Caquetá, Florencia, Sucre	SS-FW; SS-HW; D-FW; V-FW; D-HW; V-HW
LGE-WS-00344	M1771	<i>Heliconius timareta florenzia</i>	Caquetá, Florencia, Sucre	SS-FW; SS-HW; D-FW; V-FW; D-HW; V-HW
LGE-WS-00345	M1758	<i>Heliconius timareta florenzia</i>	Caquetá, Florencia, Sucre	SS-FW; SS-HW; D-FW; V-FW; D-HW; V-HW
LGE-WS-00346	M257	<i>Heliconius timareta florenzia</i>	Caquetá, Florencia, Sucre	SS-FW; SS-HW; D-FW; V-FW; D-HW; V-HW
LGE-WS-00347	M3765	<i>Heliconius timareta florenzia</i>	Caquetá, Florencia, Sucre	SS-FW; SS-HW; D-FW; V-FW; D-HW; V-HW
LGE-WS-00348	M1079	<i>Heliconius timareta florenzia</i>	Caquetá, Florencia, Sucre	SS-FW; SS-HW; D-FW; V-FW; D-HW; V-HW
LGE-WS-00349	M63	<i>Heliconius timareta florenzia</i>	Caquetá, Finca Piñacue	SS-FW; SS-HW; D-FW; V-FW; D-HW; V-HW
LGE-WS-00350	M64	<i>Heliconius timareta florenzia</i>	Caquetá, Finca Piñacue	SS-FW; SS-HW; D-FW; V-FW; D-HW; V-HW
LGE-WS-01600	M2435	<i>Heliconius timareta linaresi</i>	Caquetá, Las Morras, Puerto Amor	SS-FW; SS-HW; D-FW; V-FW
LGE-WS-01601	M2434	<i>Heliconius timareta linaresi</i>	Caquetá, Las Morras, Puerto Amor	SS-FW; SS-HW; D-FW; V-FW
LGE-WS-01602	M2409	<i>Heliconius timareta linaresi</i>	Caquetá, Las Morras, Puerto Amor	SS-FW; SS-HW; D-FW; V-FW
LGE-WS-01603	M5164	<i>Heliconius timareta linaresi</i>	Caquetá, San Vicente del Caguan, Guayabal	SS-FW; SS-HW; D-FW; V-FW
LGE-WS-01604	M3762	<i>Heliconius timareta linaresi</i>	Caquetá, San Vicente del Caguan, Guayabal	SS-FW; SS-HW; D-FW; V-FW
LGE-WS-01605	M3761	<i>Heliconius timareta linaresi</i>	Caquetá, San Vicente del Caguan, Guayabal	SS-FW; SS-HW; D-FW; V-FW
LGE-WS-01606	M3881	<i>Heliconius timareta linaresi</i>	Caquetá, San Vicente del Caguan, Guayabal	SS-FW; SS-HW; D-FW; V-FW
LGE-WS-02151	ICN-31733	<i>Heliconius timareta</i> spp. nov.	Amazonas, Puerto Nariño, Quebrada Aguas Rojas	SS-FW; SS-HW
LGE-WS-02152	ICN-31711	<i>Heliconius timareta</i> spp. nov.	Amazonas, Puerto Nariño, Quebrada Aguas Rojas	SS-FW; SS-HW
LGE-WS-02153	ICN-32537	<i>Heliconius timareta</i> spp. nov.	Amazonas, Leticia, vereda Macedonia	SS-FW; SS-HW; D-FW; V-FW; D-HW; V-HW
LGE-WS-02154	ICN-32535	<i>Heliconius timareta</i> spp. nov.	Amazonas, Leticia, vereda Arará	SS-FW; SS-HW; D-FW; V-FW; D-HW; V-HW
LGE-WS-00852	M4261	<i>Heliconius tristero</i>	Putumayo, Mocoa, Campucana	SS-HW; D-FW; V-FW; D-HW; V-HW
LGE-WS-00853	M4303	<i>Heliconius tristero</i>	Putumayo, Mocoa, Campucana	SS-HW; D-FW; V-FW; D-HW; V-HW
LGE-WS-00854	M4266	<i>Heliconius tristero</i>	Putumayo, Mocoa, Campucana	SS-HW; D-FW; V-FW; D-HW; V-HW

LGE-WS-00855	M4311	<i>Heliconius tristero</i>	Putumayo, Mocoa, Campucana	SS-HW; D-FW; V-FW; D-HW; V-HW
LGE-WS-00856	M4384	<i>Heliconius tristero</i>	Putumayo, Mocoa, Campucana	SS-HW; D-FW; V-FW; D-HW; V-HW
LGE-WS-00858	M4525	<i>Heliconius tristero</i>	Putumayo, Mocoa, Campucana	SS-HW; D-FW; D-HW
LGE-WS-00859	M4412	<i>Heliconius tristero</i>	Putumayo, Mocoa, Campucana	V-HW
CAM040012	CAM040012	<i>Heliconius tristero</i>	Putumayo, Mocoa, Campucana	SS-FW; D-FW; V-FW
CAM040013	CAM040013	<i>Heliconius tristero</i>	Putumayo, Mocoa, Campucana	SS-FW; D-FW; V-FW
CAM040033	CAM040033	<i>Heliconius tristero</i>	Putumayo, Mocoa, Campucana	SS-FW; D-FW; V-FW
CAM040034	CAM040034	<i>Heliconius tristero</i>	Putumayo, Mocoa, Campucana	SS-FW
CAM040035	CAM040035	<i>Heliconius tristero</i>	Putumayo, Mocoa, Campucana	SS-FW; D-FW; V-FW
CAM040036	CAM040036	<i>Heliconius tristero</i>	Putumayo, Mocoa, Campucana	SS-FW; D-FW; V-FW
CAM040037	CAM040037	<i>Heliconius tristero</i>	Putumayo, Mocoa, Campucana	SS-FW; D-FW; V-FW
CAM040079	CAM040079	<i>Heliconius tristero</i>	Putumayo, Mocoa, Campucana	SS-FW; D-FW; V-FW
CAM040100	CAM040100	<i>Heliconius tristero</i>	Putumayo, Mocoa, Campucana	SS-FW; D-FW; V-FW
LGE-WS-02551	M3452	<i>Heliconius xanthocles melete</i>	Caquetá, Florencia, Paraiso	SS-FW; SS-HW; D-FW; V-FW; D-HW; V-HW
LGE-WS-02552	M3717	<i>Heliconius xanthocles melete</i>	Caquetá, Florencia, Paraiso	SS-FW; SS-HW; D-FW; V-FW; D-HW; V-HW
LGE-WS-02553	M3953	<i>Heliconius xanthocles melete</i>	Meta, Lejanías, Río Guejar	SS-FW; SS-HW
LGE-WS-02554	M4269	<i>Heliconius xanthocles melete</i>	Putumayo, Mocoa, Campucana	SS-FW; SS-HW; D-FW; V-FW; D-HW; V-HW
LGE-WS-02555	M1500	<i>Heliconius xanthocles melete</i>	Caquetá, Florencia, Paraiso	SS-FW; SS-HW; D-FW; V-FW; D-HW; V-HW
LGE-WS-02556	M1504	<i>Heliconius xanthocles melete</i>	Caquetá, Florencia, Paraiso	SS-FW; SS-HW; D-FW; V-FW; D-HW; V-HW
LGE-WS-02557	M1587	<i>Heliconius xanthocles melete</i>	Caquetá, Florencia, Paraiso	SS-FW; SS-HW; D-FW; V-FW; D-HW; V-HW
LGE-WS-02558	M1509	<i>Heliconius xanthocles melete</i>	Caquetá, Florencia, Paraiso	SS-FW; SS-HW; D-FW; V-FW; D-HW; V-HW
LGE-WS-02559	M306	<i>Heliconius xanthocles melete</i>	Caquetá, Florencia, Sucre	SS-FW; SS-HW
LGE-WS-02561	M420	<i>Heliconius xanthocles melete</i>	Caquetá, Florencia, Sucre	SS-FW; SS-HW; D-FW; V-FW; D-HW; V-HW
LGE-WS-02562	M305	<i>Heliconius xanthocles melete</i>	Caquetá, Florencia, Sucre	SS-FW; SS-HW
LGE-WS-02563	M3717	<i>Heliconius xanthocles melete</i>	Caquetá, Florencia, Paraiso	SS-FW; SS-HW

The Red-banded phenotype

Some subspecies of *H. melpomene* mimics *H. erato* with a large medial red mid-forewing band, known as the red-banded phenotype.

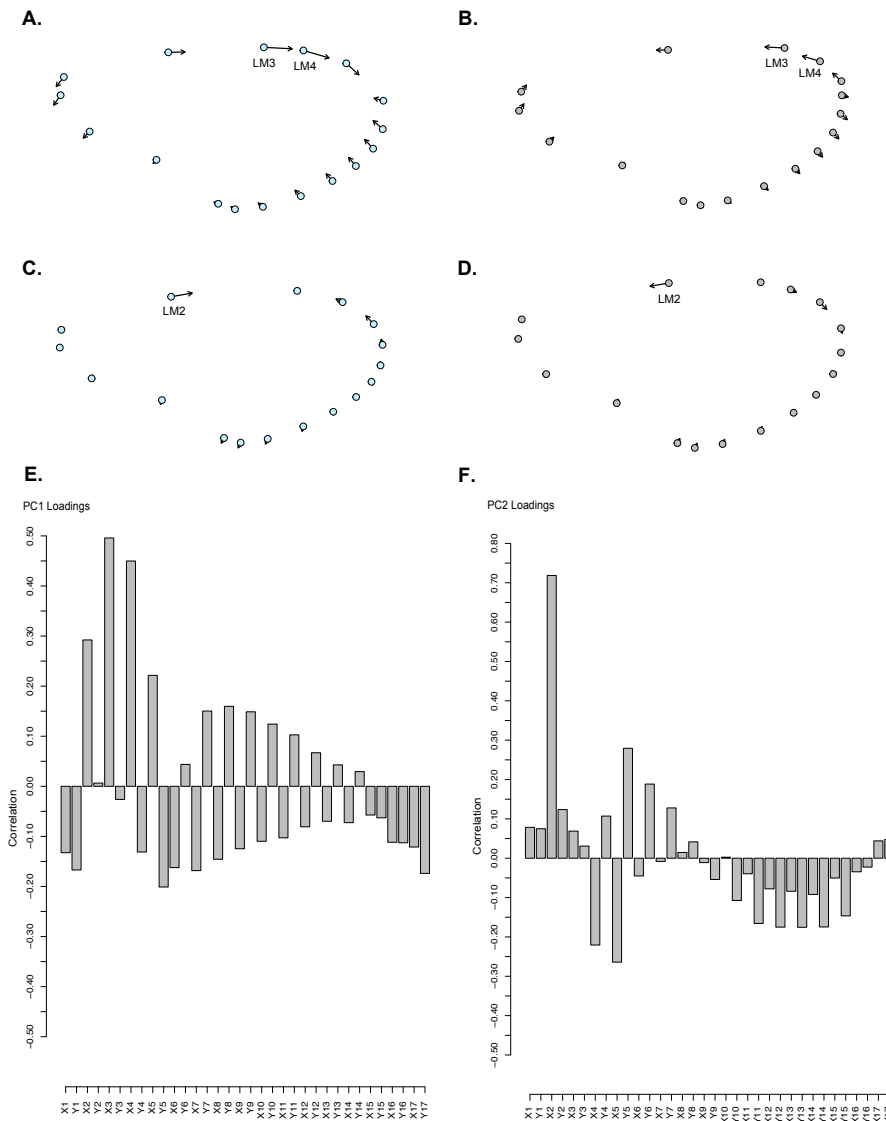


Figure S1.1. Shapes deformation and PC loadings representing the shape variation in the forewing between subspecies with the red-band phenotype. Shapes deformation (A) and (C) represents the shape at minimum values for PC1 and PC2, respectively. Shapes deformation (B) and (D), represents the maximum values for PC1 and PC2, respectively. Panels (E) and (F) shows the PC1 and PC2 loadings, respectively. The landmark coordinates (LMs) that vary the most in the FW are LM2, LM3 and LM4, located in the distal part of the costal margin, near the wing apex. *H. erato* tend to the minimum values of shape deformation while *H. melpomene* tend to the maximum values of shape deformation indicating that *H. erato* has wings more elongated than those of *H. melpomene*.

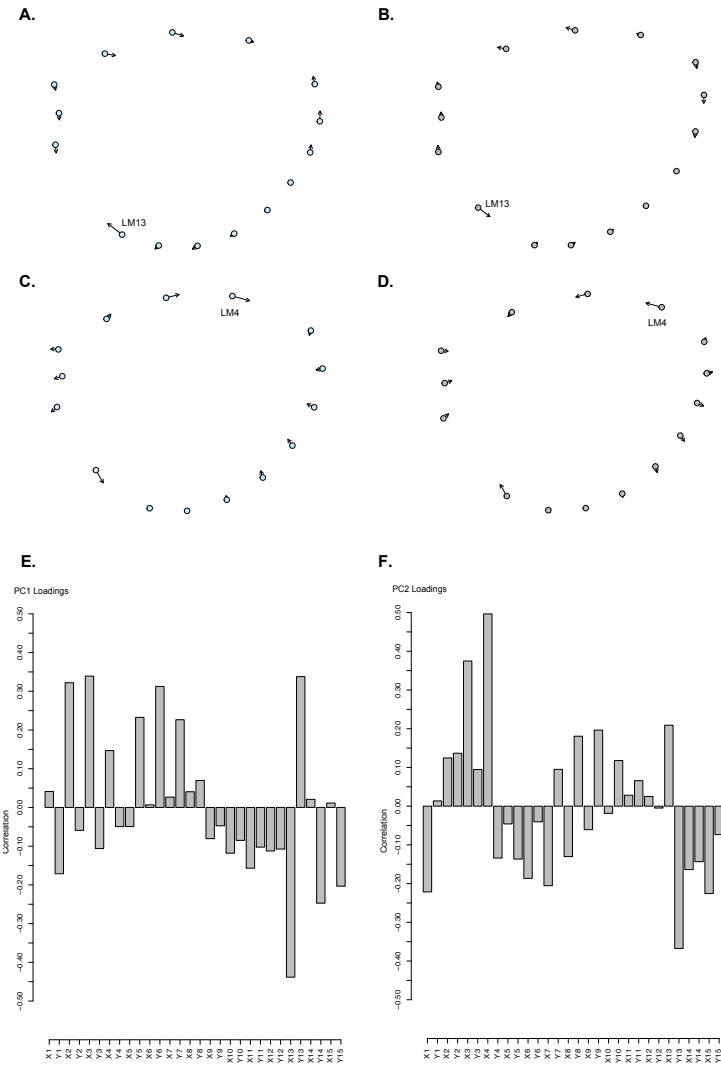


Figure S1.2. Shapes deformation and PC loadings representing the shape variation in the hindwing between subspecies with the red-band phenotype. Shapes deformation (A) and (C) represents the shape at minimum values for PC1 and PC2, respectively. Shapes deformation (B) and (D), represents the maximum values for PC1 and PC2, respectively. Panels (E) and (F) shows the PC1 and PC2 loadings, respectively. The landmark coordinates (LMs) that vary the most in the HW are LM4 located in the distal part of the coastal margin, near the apex, and LM13, located in the anal margin. *H. erato* tend to the minimum values of shape deformation while *H. melpomene* tend to the maximum values of shape deformation indicating that the HW of *H. erato* are not as rounded as the ones of *H. melpomene*.

The Dennis-Ray phenotype

One of the most remarkable examples of phenotypic convergence is known as “dennis-ray”. This phenotype is spread continuously across the Amazon basin (223), where *Heliconius* species, including among others *H. melpomene* and *H. erato*, converge on the same dennis-ray wing pattern with other butterflies and even diurnal moths (mimetic model) (177). Specifically, “dennis” refers to an orange/red basal patch on the forewing; “ray” refers to the radiate orange/red hindwing pattern, and there is also a yellow bar on the anteromedial part of the forewing (223).

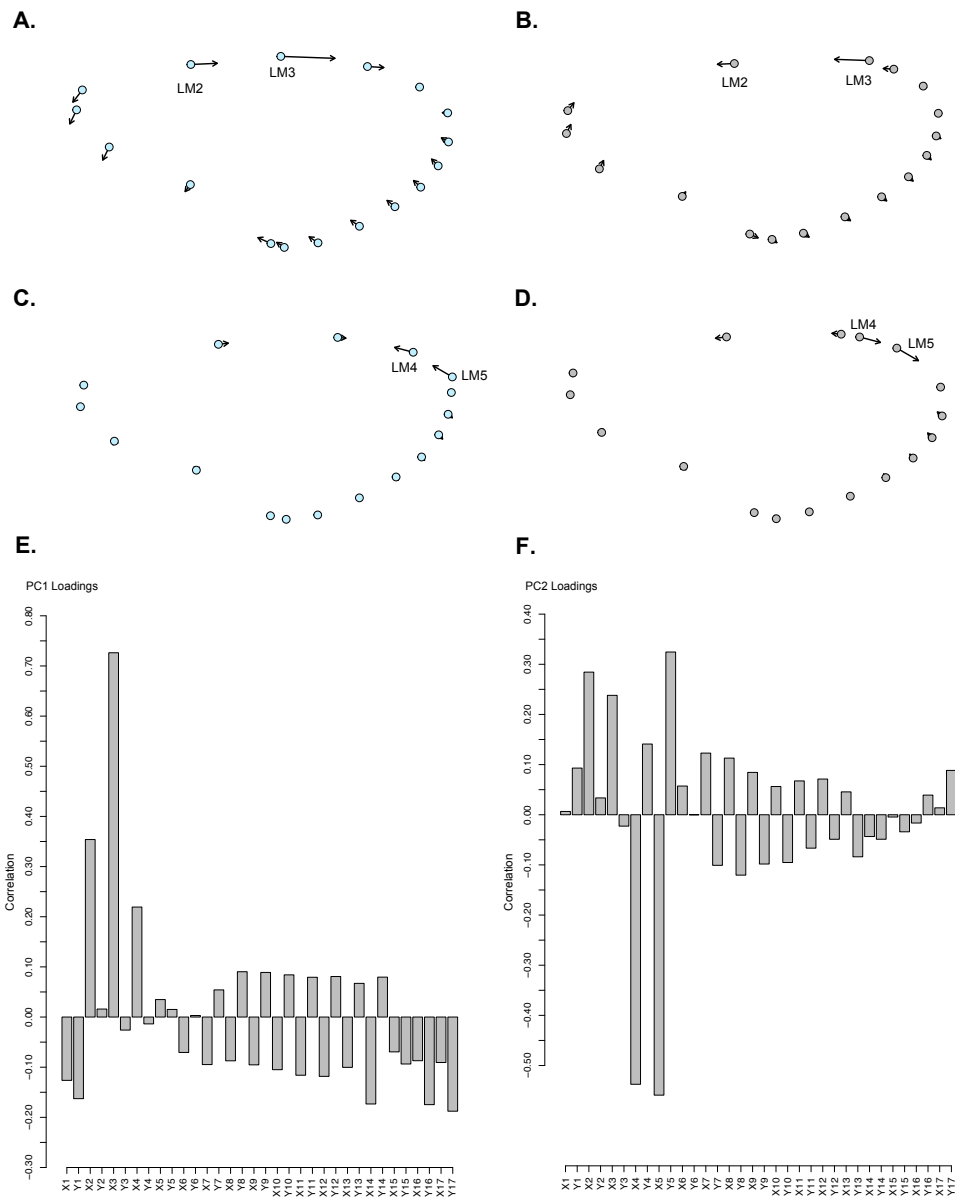


Figure S1.3. Shapes deformation and PC loadings representing the shape variation in the forewing between species and subspecies with the dennis-ray mimetic ring in the Amazon. The analysis included members of *Heliconius*, *Eueides heliconioides* and the moth *Chetone ithrana*. Shapes deformation (A) and (C) represents the shape at minimum values for PC1 and PC2, respectively. Shapes deformation (B) and (D), represents the maximum values for PC1 and PC2, respectively. Panels (E) and (F) shows the PC1 and PC2 loadings, respectively. The landmark coordinates (LMs) that vary the most in the FW are LM2, LM3, LM4 and LM5, located in the distal part of the costal margin, near the wing apex. *H. aoede* and *H. timareta florencia* tends to the minimum values of deformation for PC1 but to the maximum values of deformation for PC2, which would indicate that their wings are more elongated towards the apex than those of the other members of the mimetic ring analysed.

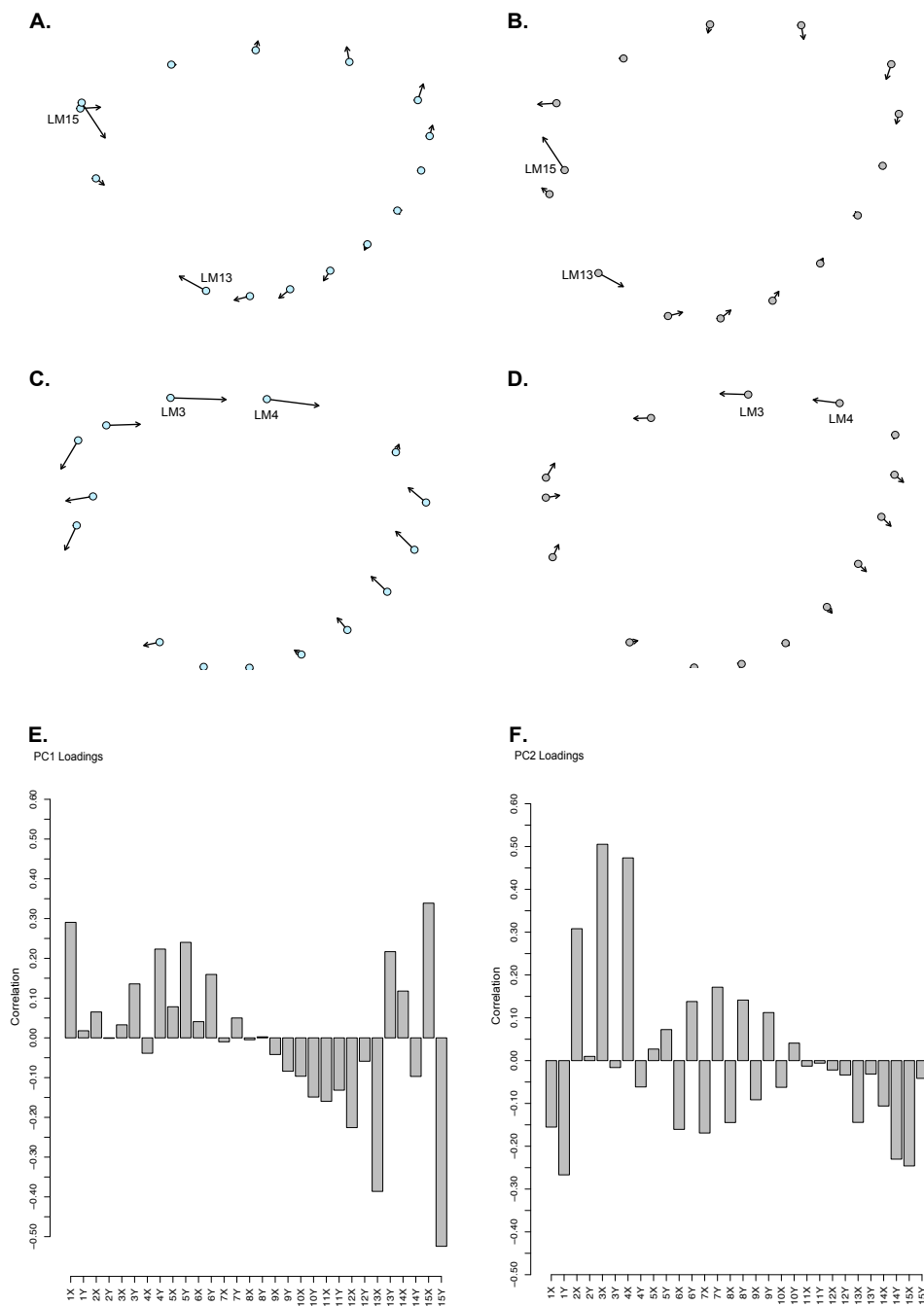


Figure S1.4. Shapes deformation and PC loadings representing the shape variation in the hindwing between species and subspecies with the dennis-ray mimetic ring in the Amazon. This analysis included members of *Heliconius*, *Eueides heliconioides* and the moth *Chetone ithrana*. Shapes deformation (A) and (C) represents the shape at minimum values for PC1 and PC2, respectively. Shapes deformation (B) and (D), represents the maximum values for PC1 and PC2, respectively. Panels (E) and (F) shows the PC1 and PC2 loadings, respectively. The landmark coordinates (LMs) that vary the most are LM13, LM15, both located in the anal margin, LM3 and LM4, located in the costal margin, near the wing apex. The HW of *Chetone ithrana* and *H. timareta florenci* tends to the minimum values of shape deformation, indicating that the HW of *C. ithrana* and to a certain extent those of *H. t. florenci*, have an inner border with a steep angle and are less rounded than those of the remaining members of the mimetic ring.

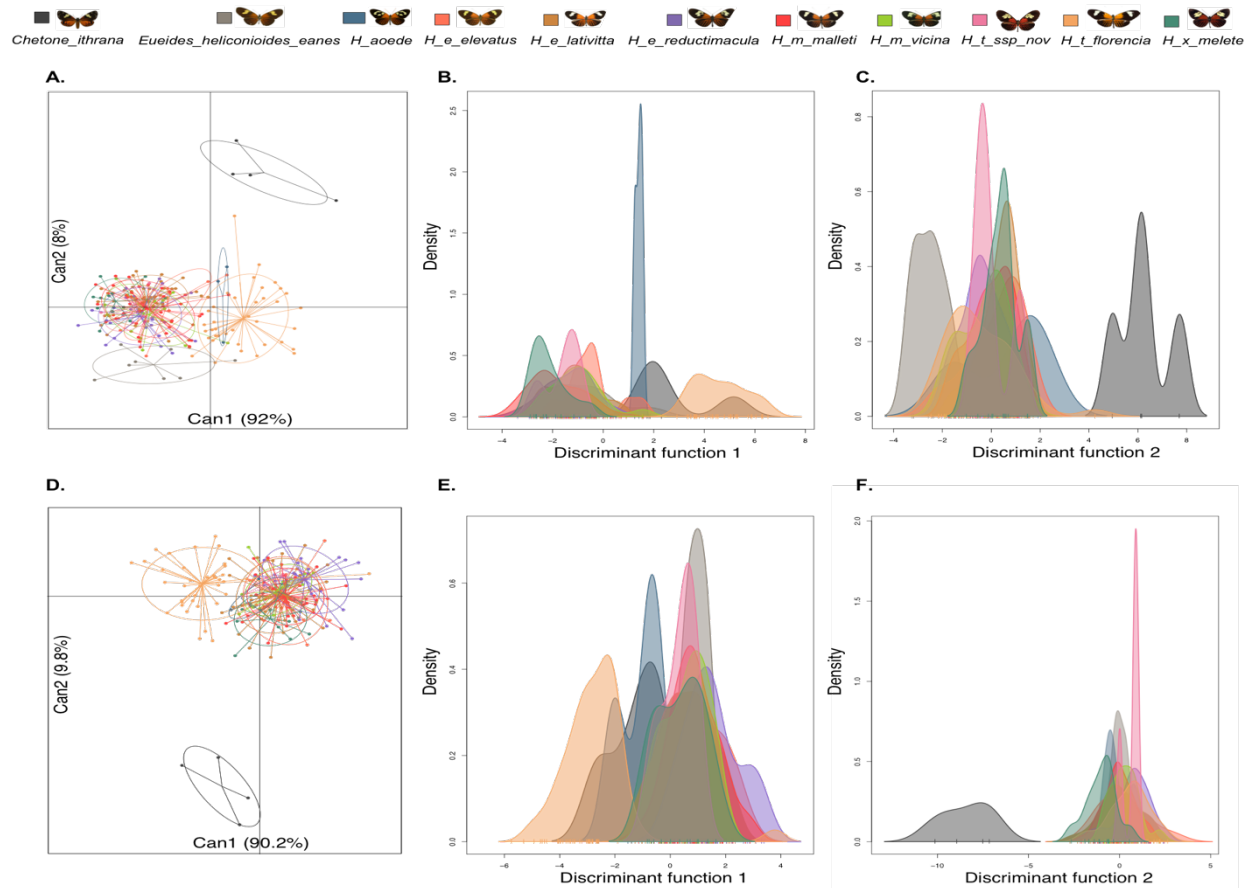


Figure S1.5. Comparison of wing shape between species and subspecies that participate in the dennis-ray mimicry ring in the Amazon including non-*Heliconius* species. This analysis included members of *Heliconius*, *Eueides heliconioides* and the moth *Chetone ithrana*. Discriminant analysis (A, D) and density plots (B-C, E-F) showing the variation in the shape of the FW (top row) and HW (bottom row). The MANCOVA test showed a significant main effect of subspecies (FW: $F_{(10,191)}=40.58$, $p=2.2e-16^*$; HW: $F_{(10,190)}=22.30$, $p=2.2e-16^*$), a non-significant effect of geographic distance (FW: $F_{(1,191)}=1.31$, $p=0.26$; HW: $F_{(1,190)}=0.36$, $p=0.69$), and a non-significant interaction between factors (FW: $F_{(6,191)}=1.15$, $p=0.31$; HW: $F_{(6,190)}=0.80$, $p=0.64$).

The White/Yellow phenotype

H. cydno are usually involved in Müllerian mimicry rings within species from the *sara/sapho* clade and in some cases with the Ithomiinae butterfly *Elzunia humboldt* (95,96). These species exhibit remarkable variation and are distributed along the Cauca and Magdalena Valley, as well as the western Cordillera (309).

In general, they display the yellow/white phenotype composed of a band in the medial part of the forewing, which could be a fully band, a “broken band”, “split band” (two bands running from the costal margin to the inner angle) or even a series of submarginal dots with a few “bands” in the post-medial area of the forewing known as Belem spot, cell spot and Ecuador triangle. In the hindwing two different phenotypes can be present, a white border intersected by the black nervature or a yellow bar in the post-medial area of the hindwing.

Moreover, *H. cydno weymeri* f. *gustavi* mimics *H. erato chestertonii* in the Cauca Valley (96). Typically, they have black forewings and the presence of a yellow band in the distal area of the hindwing.

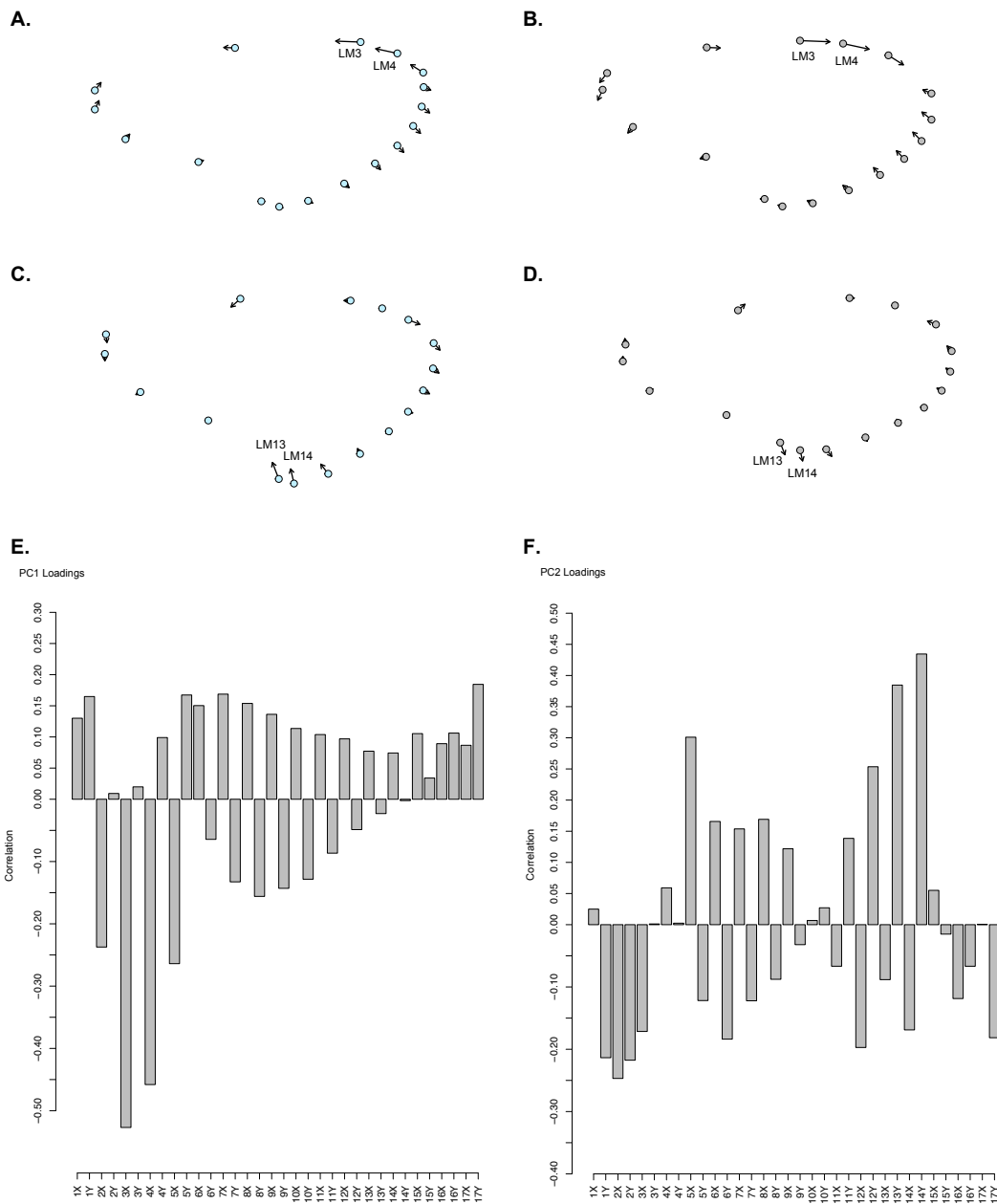


Figure S1.6. Shapes deformation and PC loadings representing the shape variation in the forewing between subspecies with the yellow/white phenotype. Shapes deformation (A) and (C) represents the shape at minimum values for PC1 and PC2, respectively. Shapes deformation (B) and (D), represents the maximum values for PC1 and PC2, respectively. Panels (E) and (F) shows the PC1 and PC2 loadings, respectively. The landmark coordinates (LMs) that vary the most in the FW are LM3, LM4, located in the distal part of the costal margin, near the wing apex and LM13 and LM14, located in the distal part of the anal margin, close to the tornus. The FW of the Ithomiinae butterfly *Elzunia* exhibits a typical triangle shape, and it is wider towards the apex and apical margin; meanwhile, the wings of *H. cydno* are more rounded.

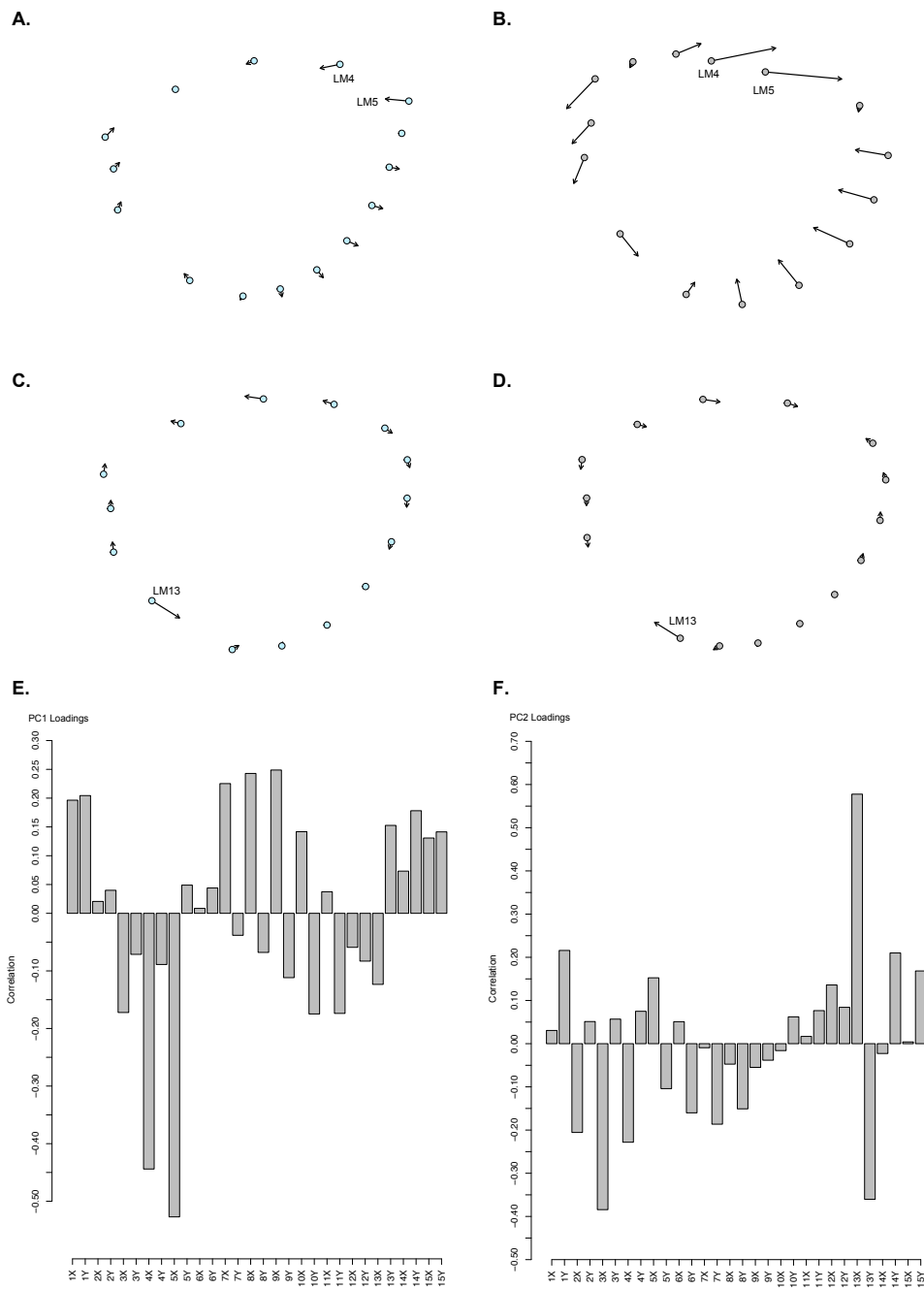


Figure S1.7. Shapes deformation and PC loadings representing the shape variation in the hindwing between subspecies with the yellow/white phenotype. Shapes deformation (A) and (C) represents the shape at minimum values for PC1 and PC2, respectively. Shapes deformation (B) and (D), represents the maximum values for PC1 and PC2, respectively. Panels (E) and (F) shows the PC1 and PC2 loadings, respectively. The landmark coordinates (LMs) that vary the most in the HW are LM4, LM5 and LM13. The first two placed in the most distal part of the costal margin and the latter, in the middle of the anal margin of the HW. Hence, the HW of *Elzunia* and *H. hecuba* are wider than the one of *Heliconius*, and particularly, the coastal margin is not straight but exhibits a notable downward deviation in the middle of it.

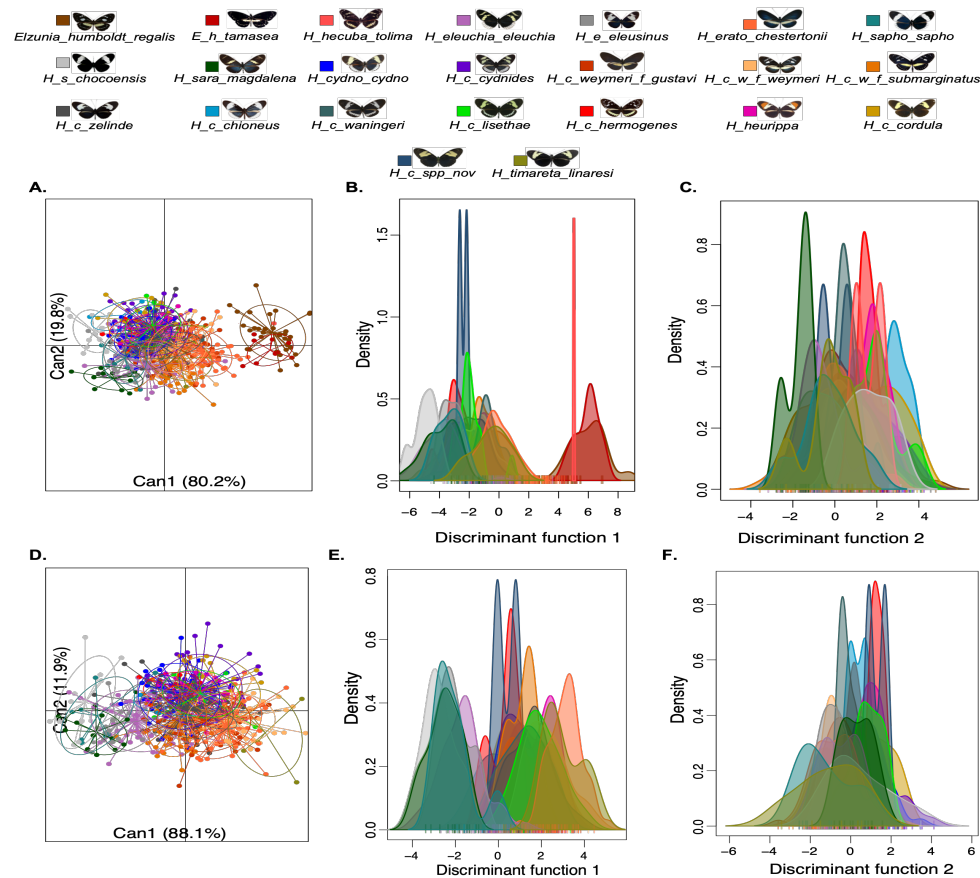







Figure S1.8. Comparison of forewing shape between subspecies with the yellow/white phenotype. Discriminant analysis (A, D) and density plots (B-C, E-F) showing the variation in the shape of the FW of the yellow/white phenotype. In the top row, the analysis included non-*Heliconius* species, as well as individuals from the mimetic ring *H. erato chestertonii* and *H. cydno weymeri f. gustavi*. In the bottom row, the analysis included the mimetic ring *H. erato chestertonii* and *H. cydno weymeri f. gustavi*, but without the presence of *H. hecuba tolima* and the Ithomiinae genus *Elzunia*. The MANCOVA test showed a significant main effect of subspecies ($F_{(22,526)}=23.12$, $p<2.2e-16^*$; and $F_{(19,487)}=17.11$, $p<2.2e-16^*$), a non-significant effect of geographic distance ($F_{(1,526)}=0.11$, $p=0.89$; $F_{(1,487)}=0.10$, $p=0.89$), and a non-significant interaction between factors ($F_{(15,526)}=1.11$, $p=0.31$; $F_{(14,487)}=0.97$, $p=0.49$), respectively.


Table S1.2. Statistical analyses. A total of 22 comparisons, each one corresponding to a particular mimicry ring (sympatric) and geographic (allopatric) comparisons. Numbers on parentheses indicate the number of individuals scanned. C: Comparison. Simpatry (S), Allopatry (A). Forewing (FW), hindwing (HW). **Lab recreated. Dash lines indicate different geographical mimicry rings. Differences in wing size were investigated with a one-way ANOVA with log-transformed centroid size (as a size estimate) as a dependent variable and subspecies as a factor. A multivariate analysis of covariance (MANCOVA) was performed to test for differences in wing shape and wing pattern, with subspecies as an explanatory variable, geographic distance was included as a covariable, as well as their interaction. Asterisk (*) is indicative of statistical significance ($\alpha=0.01$).









C	Phenotype	Location/ Occurrence	Mimicry ring						
1	Red-band	Magdalena Valley/ North-East Andean foothills/ Pacific/ Putumayo	A						
				Wing Size	FW	Subspecies	F(8,247)=5.18, p=5.33e-6*		
						DistGeo	F(1,247)=3.02, p=0.08		
						Subspecies:DistGeo	F(8,247)=2.61, p=0.009*		
					HW	Subspecies	F(8,225)=4.98, p=1.05e-5*		
						DistGeo	F(1,225)=2.48, p=0.11		
						Subspecies:DistGeo	F(8,225)=2.18, p=0.02		
				Wing Shape	FW	Subspecies	F(8,247)=6.81, p=3.65e-14*		
						DistGeo	F(1,247)=1.74, p=0.17		
						Subspecies:DistGeo	F(8,247)=0.91, p=0.54		
					HW	Subspecies	F(8,225)=10.03, p=2.2e-16*		
						DistGeo	F(1,225)=0.89, p=4.11		
						Subspecies:DistGeo	F(8,225)=0.84, p=0.63		
				Wing Pattern (Figure 2.16)	FW	Red-band	Dorsal	Subspecies	F(8,212)=1.24, p=0.22
								DistGeo	F(1,212)=0.03, p=0.96
							Ventral	Subspecies:DistGeo	F(8,212)=0.37, p=0.70
Subspecies	F(8,235)=0.19, p=0.99								

							DistGeo	F(1,235)=0.35, p=0.67
							Subspecies:DistGeo	F(8,235)=1.23, p=0.23
				HW	Yellow-bar	Dorsal	Subspecies	F(8,220)=10.24, p<2e-16*
							DistGeo	F(1,220)=0.001, p=0.99
							Subspecies:DistGeo	F(8,220)=11.68, p<2e-16*
						Ventral	Subspecies	F(8,215)=9.34, p<2e-16*
							DistGeo	F(1,215)=0.17, p=0.83
							Subspecies:DistGeo	F(8,215)=2.56, p=0.0008*
				 <i>H. erato venus</i> (19) <i>H. melpomene vulcanus</i> (16)				
2	Pacific	S	Wing Size	FW	Subspecies	F(1,29)=5.05, p=0.03		
					DistGeo	F(1,29)=5.29, p=0.02		
					Subspecies:DistGeo	F(1,29)=4.23, p=0.04		
				HW	Subspecies	F(1,29)=3.31, p=0.07		
					DistGeo	F(1,29)=4.29, p=0.04		
					Subspecies:DistGeo	F(1,29)=3.88, p=0.05		
			Wing Shape	FW	Subspecies	F(1,29)=2.93, p=0.07		
					DistGeo	F(1,29)=0.58, p=0.56		
					Subspecies:DistGeo	F(1,29)=1.34, p=0.27		
				HW	Subspecies	F(1,29)=25.77, p=4e-7*		
					DistGeo	F(1,29)=0.64, p=0.53		
					Subspecies:DistGeo	F(1,29)=1.10, p=0.34		
			Wing Pattern (Figure S1.10)	FW	Red-band	Dorsal	Subspecies	F(1,30)=1.55, p=0.22
						DistGeo	F(1,30)=0.47, p=0.62	
						Subspecies:DistGeo	F(1,30)=2.46, p=0.10	
						Ventral	Subspecies	F(1,29)=1.72, p=0.19
HW	Yellow-bar	DistGeo		F(1,29)=1.08, p=0.35				
		Subspecies:DistGeo		F(1,29)=2.00, p=0.15				
		Subspecies		F(1,29)=3.46, p=0.05				
		DistGeo		F(1,29)=0.64, p=0.54				
			Subspecies:DistGeo	F(1,29)=0.02, p=0.97				

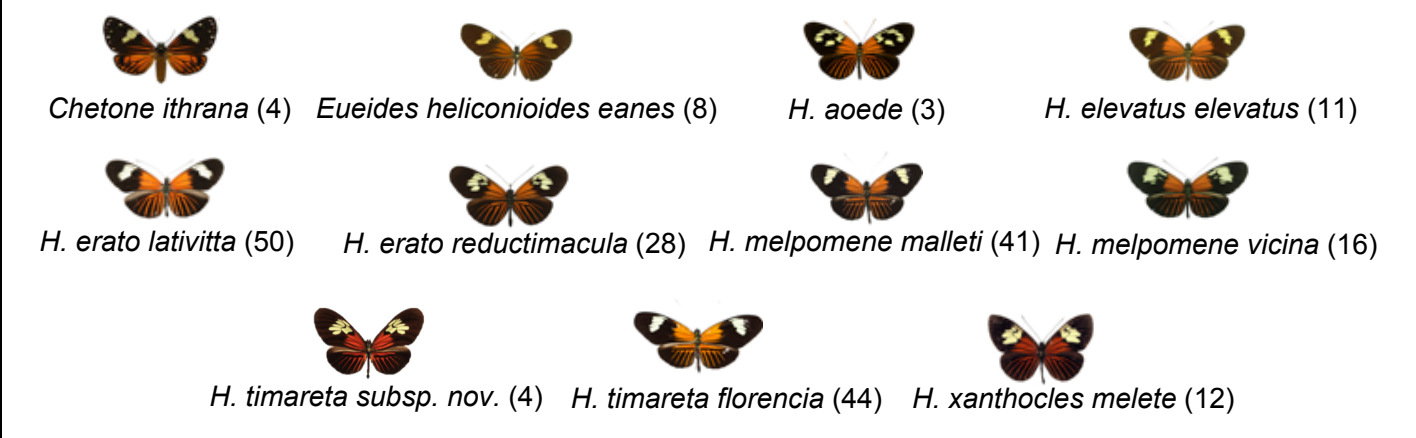
3	Magdalena Valley	S	  <i>H. erato guarica</i> (44) <i>H. melpomene martinae</i> (27)						
			Wing Size	FW	Subspecies	F(1,63)=18.31, p=6.49e-5*			
					DistGeo	F(1,63)=0.56, p=0.45			
					Subspecies:DistGeo	F(1,63)=0.01, p=0.91			
				HW	Subspecies	F(1,63)=22.15, p=1.42e-5*			
					DistGeo	F(1,63)=0.76, p=0.38			
					Subspecies:DistGeo	F(1,63)=0.06, p=0.80			
			Wing Shape	FW	Subspecies	F(1,63)=17.85, p=7.51e-7*			
					DistGeo	F(1,63)=6.23, p=0.003*			
					Subspecies:DistGeo	F(1,63)=1.92, p=0.15			
				HW	Subspecies	F(1,63)=48.47, p=2.11e-13*			
					DistGeo	F(1,63)=0.42, p=0.65			
					Subspecies:DistGeo	F(1,63)=0.49, p=0.61			
			Wing Pattern (Figure S1.11)	FW	Red-band	Dorsal	Subspecies	F(1,63)=1.08, p=0.34	
							DistGeo	F(1,63)=1.47, p=0.23	
							Subspecies:DistGeo	F(1,63)=0.35, p=0.70	
Ventral	Subspecies	F(1,61)=1.04, p=0.35							
	DistGeo	F(1,61)=0.73, p=0.48							
	Subspecies:DistGeo	F(1,61)=0.17, p=0.84							


4	North-East Andean foothills	S	  <i>H. erato hydara</i> (50) <i>H. melpomene melpomene</i> (46)					
			Wing Size	FW	Subspecies	F(1,85)=12.06, p=0.0008*		
					DistGeo	F(1,85)=3.72, p=0.05		
					Subspecies:DistGeo	F(1,85)=0.47, p=0.49		
				HW	Subspecies	F(1,85)=16.23, p=0.0001*		
					DistGeo	F(1,85)=5.51, p=0.02		
					Subspecies:DistGeo	F(1,85)=0.14, p=0.70		
			Wing Shape	FW	Subspecies	F(1,85)=15.58, p=1.74e-6*		
					DistGeo	F(1,85)=0.38, p=0.67		
Subspecies:DistGeo	F(1,85)=0.68, p=0.50							

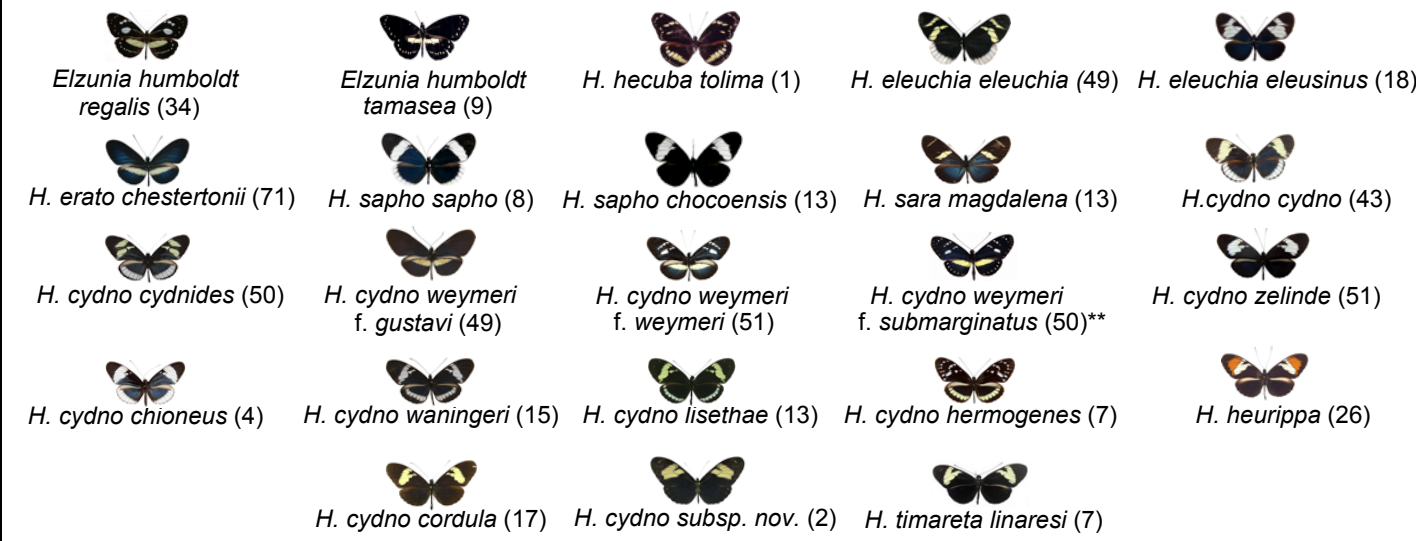
5	Putumayo	S	Wing Pattern (Figure S1.12)	HW	Subspecies	F(1,85)=25.18, p=2.69e-9*				
					DistGeo	F(1,85)=4.13, p=0.02				
					Subspecies:DistGeo	F(1,85)=0.40, p=0.67				
				FW	Red-band	Dorsal	Subspecies	F(1,84)=0.06, p=0.93		
							DistGeo	F(1,84)=4.78, p=0.01*		
							Subspecies:DistGeo	F(1,84)=1.07, p=0.34		
					Ventral	Subspecies	F(1,79)=0.55, p=0.57			
						DistGeo	F(1,79)=3.39, p=0.03			
						Subspecies:DistGeo	F(1,79)=1.86, p=0.16			
			 <i>H. erato dignus</i> (25) <i>H. melpomene bellula</i> (41) <i>H. tristero</i> (16)							
			Wing Size	FW	Subspecies	F(2,73)=3.22, p=0.04*				
					DistGeo	F(1,73)=4.31, p=0.04				
					Subspecies:DistGeo	F(1,73)=1.61, p=0.20				
				HW	Subspecies	F(2,49)=1.54, p=0.22				
					DistGeo	F(1,49)=0.07, p=0.78				
					Subspecies:DistGeo	F(1,49)=0.97, p=0.38				
			Wing Shape	FW	Subspecies	F(2,73)=4.10, p=0.003*				
					DistGeo	F(1,73)=0.88, p=0.41				
					Subspecies:DistGeo	F(1,73)=0.84, p=0.50				
				HW	Subspecies	F(2,49)=6.76, p=7.65e-5*				
DistGeo	F(1,49)=2.78, p=0.07									
Subspecies:DistGeo	F(1,49)=0.03, p=0.99									
Wing Pattern (Figure S1.13)	FW	Red-band	Dorsal	Subspecies	F(2,76)=2.00, p=0.09					
				DistGeo	F(1,76)=0.83, p=0.43					
				Subspecies:DistGeo	F(2,76)=0.92, p=0.45					
		Ventral	Subspecies	F(2,69)=0.50, p=0.73						
			DistGeo	F(1,69)=0.39, p=0.67						
			Subspecies:DistGeo	F(2,69)=0.74, p=0.48						
	HW	Yellow-bar	Dorsal	Subspecies	F(2,49)=7.31, p=3.45e-5*					
				DistGeo	F(1,49)=3.26, p=0.04					
				Subspecies:DistGeo	F(2,49)=0.83, p=0.50					
Ventral	Subspecies	F(2,42)=17.85, p=1.41e-10*								


						DistGeo		(1,42)=2.72, p=0.07		
						Subspecies:DistGeo		F(2,42)=4.84, p=0.001*		
6	Magdalena Valley/ North-East Andean foothills/ Pacific/ Putumayo	A	    <i>H. melpomene bellula</i> (41) <i>H. melpomene martinae</i> (27) <i>H. melpomene melpomene</i> (46) <i>H. melpomene vulcanus</i> (16)							
			Wing Size	FW	Subspecies		F(3,115)=1.45, p=0.22			
					DistGeo		F(1,115)=1.82, p=0.17			
					Subspecies:DistGeo		F(2,115)=1.20, p=0.30			
				HW	Subspecies		F(3,110)=2.23, p=0.08			
					DistGeo		F(1,115)=2.96, p=0.08			
					Subspecies:DistGeo		F(2,115)=1.88, p=0.13			
			Wing Shape	FW	Subspecies		F(3,116)=14.72, p=0.31			
					DistGeo		F(1,116)=0.40, p=0.66			
					Subspecies:DistGeo		F(2,116)=1.09, p=0.36			
				HW	Subspecies		F(3,111)=2.12, p=0.05			
					DistGeo		F(1,111)=2.29, p=0.10			
					Subspecies:DistGeo		F(2,111)=0.02, p=0.99			
			Wing Pattern (Figure S1.14)	FW	Red-band	Dorsal	Subspecies		F(3,91)=0.17, p=0.98	
							DistGeo		F(1,91)=1.92, p=0.15	
						Subspecies:DistGeo		F(2,91)=1.55, p=0.18		
Ventral	Subspecies					F(3,87)=0.54, p=0.77				
	DistGeo			F(1,87)=0.93, p=0.39						
Subspecies:DistGeo		F(3,87)=1.61, p=0.14								
HW	Yellow-bar	Dorsal		Subspecies		F(3,90)=181.4, p<2e-16*				
				DistGeo		F(1,90)=1.57, p=0.21				
		Subspecies:DistGeo		F(3,90)=2.39, p=0.03						
		Ventral	Subspecies		F(3,87)=2.82, p=0.01*					
DistGeo			F(1,87)=1.84, p=0.16							
Subspecies:DistGeo		F(3,87)=2.74, p=0.01*								
7	Magdalena Valley/ North-East Andean foothills/	A	    <i>H. erato dignus</i> (25) <i>H. erato guarica</i> (44) <i>H. erato hydara</i> (50) <i>H. erato venus</i> (19)							
			FW	Subspecies		F(3,119)=0.67, p=0.57				


		Pacific/ Putumayo	Wing Size	HW	DistGeo	F(1,119)=1.19, p=0.27			
					Subspecies:DistGeo	F(3,119)=0.91, p=0.43			
					Subspecies	F(3,111)=0.68, p=0.56			
				DistGeo	F(1,111)=1.79, p=0.18				
				Subspecies:DistGeo	F(3,111)=1.21, p=0.30				
				Subspecies	F(3,119)=7.33, p=0.33				
	Wing Shape		FW	DistGeo	F(1,119)=6.74, p=0.16				
					Subspecies:DistGeo	F(3,119)=2.25, p=0.38			
			HW	Subspecies	F(3,111)=4.44, p=0.28				
					DistGeo	F(1,111)=1.03, p=0.35			
				Subspecies:DistGeo	F(3,111)=0.49, p=0.81				
	Wing Pattern (Figure S1.15)		FW	Red-band	Dorsal	Subspecies	F(3,46)=0.35, p=0.70		
							DistGeo	F(1,46)=0.16, p=0.85	
						Ventral	Subspecies:DistGeo	F(3,46)=0.16, p=0.32	
							Subspecies	F(3,113)=0.19, p=0.97	
				DistGeo	F(1,113)=0.25, p=0.77				
				Subspecies:DistGeo	F(3,113)=0.06, p=0.99				
		HW	Yellow-bar	Dorsal	Subspecies	F(3,111)=11.68, p=1.03e-8*			
						DistGeo	F(1,111)=0.01, p=0.98		
				Ventral	Subspecies:DistGeo	F(3,111)=2.07, p=0.06			
					Subspecies	F(3,107)=6.15, p=6.4e-4*			
			DistGeo	F(1,107)=3.59, p=0.04					
			Subspecies:DistGeo	F(3,107)=8.44, p=0.03					





8	Dennis-Ray	Amazon	S					
				Wing Size	FW	Subspecies	F(10,188)=4.00, p=1.04e-4*	
						DistGeo	F(1,188)=2.06, p=0.15	
						Subspecies:DistGeo	F(6,188)=0.70, p=0.70	
					HW	Subspecies	F(10,187)=4.91, p=2.6e-6*	
						DistGeo	F(1,187)=0.69, p=0.40	
						Subspecies:DistGeo	F(6,187)=0.54, p=0.83	
				Wing Shape	FW	Subspecies	F(10,191)=40.58, p=2.2e-16*	
						DistGeo	F(1,191)=1.31, p=0.26	
						Subspecies:DistGeo	F(6,191)=1.15, p=0.31	
					HW	Subspecies	F(10,190)=22.30, p=2.2e-16*	
						DistGeo	F(1,190)=0.36, p=0.69	
Subspecies:DistGeo	F(6,190)=0.80, p=0.64							
Wing Pattern (Figure 2.17)	FW	Yellow-band	Dorsal	Subspecies	F(10,176)=4.65, p=1.40e-5*			
			Ventral	DistGeo	F(1,176)=2.07, p=0.14			
				Subspecies:DistGeo	F(7,176)=2.06, p=0.05			
		Dennis		Subspecies	F(10,156)=4.54, p=9.01e-7*			
			DistGeo	F(1,156)=1.52, p=0.22				
			Subspecies:DistGeo	F(7,156)=0.58, p=0.59				
	Dorsal	Subspecies	F(10,176)=5.66, p=3.39e-7*					
		DistGeo	F(1,176)=0.34, p=0.71					



							Subspecies:DistGeo	F(7,176)=1.33, p=0.23		
						Ventral	Subspecies	F(10,156)=5.35, p=9.08e-8*		
							DistGeo	F(1,156)=0.10, p=0.90		
							Subspecies:DistGeo	F(7,156)=1.57, p=0.11		
				HW	Ray	Dorsal	Subspecies	F(10,176)=3.69, p=1.01e-4*		
									DistGeo	F(1,176)=0.88, p=0.42
									Subspecies:DistGeo	F(7,176)=0.88, p=0.53
				HW	Ray	Ventral	Subspecies	F(10,153)=3.13, p=0.001*		
									DistGeo	F(1,153)=0.32, p=0.72
									Subspecies:DistGeo	F(9,153)=0.71, p=0.64
9	South-East Andean foothills	S	 <i>H. erato lativitta</i> (50) <i>H. melpomene malleti</i> (41) <i>H. timareta florencia</i> (44) <i>H. xanthocles melete</i> (12)							
			Wing Size	FW	Subspecies	F(3,129)=29.26, p=1.68e-14*				
					DistGeo	F(1,129)=3.24, p=0.07				
					Subspecies:DistGeo	F(2,130)=0.29, p=0.74				
				HW	Subspecies	F(3,127)=19.90, p=1.22e-10*				
					DistGeo	F(1,127)=3.24, p=0.07				
					Subspecies:DistGeo	F(2,127)=0.52, p=0.59				
			Wing Shape	FW	Subspecies	F(3,129)=97.08, p=2.2e-16*				
					DistGeo	F(1,129)=1.06, p=0.34				
					Subspecies:DistGeo	F(2,129)=1.73, p=0.14				
				HW	Subspecies	F(3,128)=49.66, p=2.2e-16*				
					DistGeo	F(1,128)=0.18, p=0.82				
					Subspecies:DistGeo	F(2,128)=1.77, p=0.13				
			Wing Pattern (Figure 2.18)	FW	Yellow-band	Dorsal	Subspecies	F(8,163)=0.77, p=0.71		
							DistGeo	F(1,163)=0.01, p=0.98		
							Subspecies:DistGeo	F(6,163)=0.08, p=1.00		
					Ventral	Subspecies	F(8,147)=0.73, p=0.75			
						DistGeo	F(1,147)=0.02, p=0.97			
						Subspecies:DistGeo	F(6,147)=1.18, p=0.29			
			Dennis	Dorsal	Subspecies	F(8,147)=0.64, p=0.84				
DistGeo	F(1,147)=0.01, p=0.98									


									Subspecies:DistGeo	F(6,147)=0.36, p=0.97		
									Ventral	Subspecies	F(9,152)=0.89, p=0.58	
								DistGeo		F(1,152)=0.04, p=0.95		
								Dorsal	Subspecies:DistGeo	F(8,152)=0.56, p=0.91		
										Subspecies	F(8,163)=1.18, p=0.28	
								DistGeo		F(1,163)=0.04, p=0.95		
				HW	Ray				Subspecies:DistGeo	F(6,163)=0.76, p=0.68		
									Ventral	Subspecies	F(8,145)=0.86, p=0.60	
										DistGeo	F(1,145)=0.002, p=0.98	
									Subspecies:DistGeo	F(7,145)=0.08, p=1.00		
10	Yellow/White	Cauca Valley/ Magdalena Valley/ Pacific/ North-East Andean foothills	A									
				Wing Size	FW	Subspecies	F(20,431)=6.51, p=5.38e-12*					
						DistGeo	F(1,431)=0.17, p=0.67					
						Subspecies:DistGeo	F(13,431)=1.64, p=0.07					
				HW	HW	Subspecies	F(20,422)=3.67, p=8.11e-6*					
						DistGeo	F(1,422)=1.21, p=0.27					
						Subspecies:DistGeo	F(13,422)=1.46, p=0.12					
					FW	Subspecies	F(20,431)=21.41, p<2.2e-16*					


				Wing Shape	HW	DistGeo	F(1,431)=0.16, p=0.84			
						Subspecies:DistGeo	F(13,431)=1.06, p=0.38			
						Subspecies	F(20,431)=29.73, p<2.2e-16*			
						DistGeo	F(1,431)=1.37, p=0.25			
						Subspecies:DistGeo	F(13,431)=0.77, p=0.78			
				Wing Pattern (Figure 2.19)	FW	Yellow/White band	Dorsal	Subspecies	F(20,414)=4.88, p<2e-16*	
								DistGeo	F(1,414)=2.22, p=0.11	
								Subspecies:DistGeo	F(13,414)=0.99, p=0.46	
							Ventral	Subspecies	F(20,426)=2.77, p=1.098e-6*	
								DistGeo	F(1,426)=0.12, p=0.88	
								Subspecies:DistGeo	F(13,426)=0.75, p=0.78	
					HW	Yellow bar	Dorsal	Subspecies	F(16,300)=0.57, p=0.01*	
								DistGeo	F(1,300)=0.58, p=0.55	
								Subspecies:DistGeo	F(11,300)=0.33, p=0.99	
							Ventral	Subspecies	F(16,275)=0.40, p=0.01*	
								DistGeo	F(1,275)=0.65, p=0.60	
								Subspecies:DistGeo	F(11,275)=0.65, p=0.85	
						White/Yellow border	Dorsal	Subspecies	F(13,328)=0.89, p=0.06*	
								DistGeo	F(1,328)=0.72, p=0.86	
								Subspecies:DistGeo	F(8,328)=0.72, p=0.77	
Ventral	Subspecies	F(14,300)=0.28, p=0.01*								
	DistGeo	F(1,300)=0.82, p=0.43								
	Subspecies:DistGeo	F(8,300)=1.77, p=0.30								
11	Pacific	S	 <i>H. cydno zelinde</i> (51) <i>H. eleuchia eleusinus</i> (18) <i>H. sapho chocoensis</i> (13)							
			Wing Size	FW	Subspecies	F(2,75)=24.06, p=8.43e-9*				
					DistGeo	F(1,75)=0.01, p=0.92				
					Subspecies:DistGeo	F(2,75)=1.66, p=0.19				
				HW	Subspecies	F(2,73)=20.98, p=6.32e-8*				
					DistGeo	F(1,73)=0.003, p=0.95				
					Subspecies:DistGeo	F(2,73)=2.92, p=0.05				
			FW	Subspecies	F(2,75)=42.67, p=2.0e-16*					

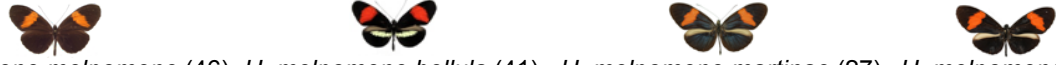
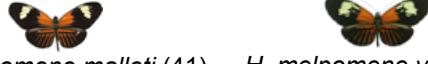
12	Magdalena Valley	S	Wing Shape	HW	DistGeo	F(1,75)=3.42, p=0.03						
					Subspecies:DistGeo	F(2,75)=0.70, p=0.58						
					Subspecies	F(2,73)=20.52, p=2.10e-13*						
					DistGeo	F(1,75)=0.44, p=0.64						
					Subspecies:DistGeo	F(2,75)=0.93, p=0.44						
			Wing Pattern (Figure S1.16)	FW	White band	Dorsal	Subspecies	F(2,74)=1.96, p=0.12				
							DistGeo	F(1,74)=0.66, p=0.52				
						Ventral	Subspecies:DistGeo	F(2,74)=0.20, p=0.81				
							Subspecies	F(2,72)=0.83, p=0.06				
					DistGeo	F(1,72)=0.15, p=0.85						
						Subspecies:DistGeo	F(2,72)=0.02, p=0.63					
					 <i>H. cydno wanningeri</i> (15) <i>H. sapho sapho</i> (8)							
					Wing Size	FW	Subspecies	F(1,15)=10.37, p=0.005*				
			DistGeo	F(1,15)=3.06, p=0.10								
			Subspecies:DistGeo	F(1,15)=3.06, p=0.10								
HW	Subspecies	F(1,16)=12.31, p=0.002*										
	DistGeo	F(1,16)=0.09, p=0.76										
	Subspecies:DistGeo	F(1,16)=0.10, p=0.76										
Wing Shape	FW	Subspecies	F(1,16)=61.55, p=5.87e-8*									
		DistGeo	F(1,16)=4.50, p=0.03									
		Subspecies:DistGeo	F(1,16)=0.70, p=0.32									
	HW	Subspecies	F(1,16)=11.40, p=8.33e-4*									
		DistGeo	F(1,16)=0.41, p=0.66									
		Subspecies:DistGeo	F(1,16)=0.90, p=0.44									
Wing Pattern (Figure S1.17)	FW	White band	Dorsal	Subspecies	F(1,16)=0.09, p=0.009*							
				DistGeo	F(1,16)=0.01, p=0.98							
			Ventral	Subspecies:DistGeo	F(1,16)=0.02, p=0.97							
				Subspecies	F(1,19)=1.65, p=0.02							
		DistGeo	F(1,19)=0.08, p=0.91									
			Subspecies:DistGeo	F(1,19)=0.06, p=0.93								
		HW	White border	Dorsal	Subspecies	F(1,16)=3.38, p=0.07						



14	Magdalena Valley	S	    <i>H. sara magdalena</i> (13) <i>H. eleuchia eleuchia</i> (49) <i>H. cydno lisethae</i> (13) <i>H. sapho sapho</i> (8)					
			Wing Size	FW	Subspecies	F(3,73)=7.81, p=0.0001*		
					DistGeo	F(1,73)=0.95, p=0.33		
					Subspecies:DistGeo	F(3,73)=1.15, p=0.33		
				HW	Subspecies	F(3,69)=11.60, p=3.01e-6*		
					DistGeo	F(1,69)=1.83, p=0.18		
					Subspecies:DistGeo	F(3,69)=1.67, p=0.18		
			Wing Shape	FW	Subspecies	F(3,73)=18.15, p=1.25e-15*		
					DistGeo	F(1,73)=0.11, p=0.89		
					Subspecies:DistGeo	F(3,73)=1.22, p=0.29		
				HW	Subspecies	F(3,69)=23.75, p=2.2e-16*		
					DistGeo	F(1,69)=0.99, p=0.37		
					Subspecies:DistGeo	F(3,69)=0.29, p=0.93		
			Wing Pattern (Figure S1.19)	FW	Yellow / White band	Dorsal	Subspecies	F(3,73)=0.02, p=0.009*
						Ventral	DistGeo	F(1,73)=0.41, p=0.66
							Subspecies:DistGeo	F(3,73)=0.15, p=0.98
							Subspecies	F(3,70)=0.42, p=0.008*
HW	White border	Dorsal		DistGeo	F(1,70)=0.22, p=0.79			
				Subspecies:DistGeo	F(3,70)=0.17, p=0.98			
		Ventral		Subspecies	F(3,59)=0.49, p=0.008*			
				DistGeo	F(1,59)=0.47, p=0.62			
Subspecies:DistGeo	F(3,59)=0.21, p=0.97							
Subspecies	F(3,61)=6.68, p=0.001*							
DistGeo	F(1,61)=1.02, p=0.40							
Subspecies:DistGeo	F(3,61)=2.52, p=0.06							



15	Cauca Valley	S	  <i>H. cydno cydnides</i> (50) <i>H. eleuchia eleuchia</i> (49)			
			Wing Size	FW	Subspecies	F(1,93)=10.98, p=0.001*
					DistGeo	F(1,93)=1.46, p=0.22
					Subspecies:DistGeo	F(1,93)=1.54, p=0.21

				Wing Shape	HW	Subspecies	F(1,90)=9.35, p=0.002*			
						DistGeo	F(1,90)=1.90, p=0.17			
						Subspecies:DistGeo	F(1,90)=1.98, p=0.16			
					FW	Subspecies	F(1,93)=65.09, p=2.2e-16*			
						DistGeo	F(1,93)=0.37, p=0.68			
						Subspecies:DistGeo	F(1,93)=0.57, p=0.57			
					HW	Subspecies	F(1,90)=205.51, p=2.2e-16*			
						DistGeo	F(1,90)=0.99, p=0.88			
						Subspecies:DistGeo	F(1,90)=2.28, p=0.10			
				Wing Pattern (Figure S1.20)	FW	Yellow / White band	Dorsal	Subspecies	F(1,93)=6.23, p=0.01*	
								DistGeo	F(1,93)=0.22, p=0.80	
							Subspecies:DistGeo	F(1,93)=1.50, p=0.25		
						Ventral	Subspecies	F(1,90)=11.49, p=0.003*		
							DistGeo	F(1,90)=1.95, p=0.19		
							Subspecies:DistGeo	F(1,90)=6.39, p=0.01*		
					HW	White border	Dorsal	Subspecies	F(1,81)=15.60, p=1.13e-5*	
								DistGeo	F(1,81)=0.11, p=0.89	
							Subspecies:DistGeo	F(1,81)=4.06, p=0.02		
				Ventral	Subspecies		F(1,82)=9.34, p=0.0005*			
					DistGeo		F(1,82)=0.40, p=0.67			
Subspecies:DistGeo	F(1,82)=1.04, p=0.36									
16		Magdalena Valley	S	 <i>Elzunia humboldt tamasea</i> (9) <i>H. cydno hermogenes</i> (7) <i>H. hecuba tolima</i> (1)						
				Wing Size	FW	Subspecies	F(2,12)=11.81, p=0.0009*			
						DistGeo	F(1,12)=0.02, p=0.87			
						Subspecies:DistGeo	F(2,12)=0.24, p=0.62			
					HW	Subspecies	F(2,13)=13.19, p=0.003*			
						DistGeo	F(1,13)=0.30, p=0.58			
						Subspecies:DistGeo	F(2,13)=1.41, p=0.25			
				Wing Shape	FW	Subspecies	F(2,14)=2.55, p=0.03*			
						DistGeo	F(1,14)=2.40, p=0.13			
						Subspecies:DistGeo	F(2,14)=29.74, p=0.54			
					HW	Subspecies	F(2,13)=62.30, p=2.52e-12*			

							DistGeo	F(1,121)=2.01, p=0.13		
							Subspecies:DistGeo	F(1,121)=0.50, p=0.60		
				HW	White border	Dorsal	Subspecies	F(2,117)=4.41, p=0.001*		
							DistGeo	F(1,117)=19.13, p=6.55e-8		
							Subspecies:DistGeo	F(1,117)=4.31, p=0.01*		
						Ventral	Subspecies	F(2,109)=5.00, p=0.0007*		
							DistGeo	F(1,109)=14.68, p=2.2e-6		
							Subspecies:DistGeo	F(1,109)=13.11, p=7.93e-6		
18	Cauca Valley	S	 <i>H. cydno weymeri f. gustavi</i> (49) <i>H. erato chesteronii</i> (71)							
			Wing Size	FW	Subspecies	F(1,96)=124.28, p<2.2e-16*				
					DistGeo	F(1,96)=1.10, p=0.29				
					Subspecies:DistGeo	F(1,96)=2.00, p=0.15				
			HW	Subspecies	F(1,96)=88.99, p=2.45e-15*					
				DistGeo	F(1,96)=2.23, p=0.13					
				Subspecies:DistGeo	F(1,96)=2.95, p=0.08					
			Wing Shape	FW	Subspecies	F(1,95)=10.64, p=6.81e-5*				
					DistGeo	F(1,95)=0.28, p=0.75				
					Subspecies:DistGeo	F(1,95)=0.41, p=0.66				
			HW	Subspecies	F(1,95)=53.23, p=3.4e-16*					
				DistGeo	F(1,95)=1.09, p=0.33					
				Subspecies:DistGeo	F(1,95)=0.01, p=0.99					
			Wing Pattern (Figure 2.20)	FW	Yellow bar	Dorsal	Subspecies	F(1,113)=5.42, p=0.005*		
							DistGeo	F(1,113)=0.55, p=0.57		
Ventral	Subspecies:DistGeo	F(1,113)=6.33, p=0.002*								
	Subspecies	F(1,113)=0.20, p=0.008*								
DistGeo	F(1,113)=0.92, p=0.40									
Subspecies:DistGeo	F(1,113)=5.81, p=0.003*									

19	<i>H. melpomene</i> subspecies Red-banded/ Dennis-ray	Magdalena Valley/ North-East Andean foothills/ Pacific/ Putumayo/ Amazon	A	 <i>H. melpomene melpomene</i> (46) <i>H. melpomene bellula</i> (41) <i>H. melpomene martinae</i> (27) <i>H. melpomene vulcanus</i> (16)			
				 <i>H. melpomene malleti</i> (41) <i>H. melpomene vicina</i> (16)			
				Wing Size	FW	Subspecies	F(5,169)=88.99, p=2.45e-15*
						DistGeo	F(1,169)=4.49, p=0.03
						Subspecies:DistGeo	F(5,169)=2.95, p=0.08
					HW	Subspecies	F(5,163)=7.27, p=3.39e-06*
						DistGeo	F(1,163)=3.01, p=0.08
						Subspecies:DistGeo	F(5,163)=2.02, p=0.07
				Wing Shape	FW	Subspecies	F(5,168)=6.19, p=0.10
						DistGeo	F(1,168)=2.34, p=0.09
						Subspecies:DistGeo	F(5,168)=0.41, p=0.10
					HW	Subspecies	F(5,163)=2.16, p=0.06
DistGeo	F(1,163)=1.02, p=0.36						
Subspecies:DistGeo	F(5,163)=1.19, p=0.29						

20	<i>H. erato</i> subspecies Red-banded/ Dennis-ray/ White/Yellow	Magdalena Valley/ North-East Andean foothills/ Pacific/ Putumayo/ Amazon/ Cauca Valley	A	 <i>H. erato hydara</i> (50) <i>H. erato dignus</i> (25) <i>H. erato guarica</i> (44) <i>H. erato venus</i> (19)			
				 <i>H. erato lativitta</i> (50) <i>H. erato reductimacula</i> (28) <i>H. erato chestertonii</i> (71)			
				Wing Size	FW	Subspecies	F(6,236)=17.66, p<2e-16*
						DistGeo	F(1,236)=4.12, p=0.04
						Subspecies:DistGeo	F(6,236)=2.27, p=0.03
					HW	Subspecies	F(6,226)=12.79, p=1.74e-12*
						DistGeo	F(1,226)=0.65, p=0.41
						Subspecies:DistGeo	F(6,226)=1.93, p=0.07
				Wing Shape	FW	Subspecies	F(6,235)=6.37, p=1.62e-10*
						DistGeo	F(1,235)=0.19, p=0.82

					Subspecies:DistGeo	F(6,235)=1.25, p=0.24				
				HW	Subspecies	F(6,226)=7.30, p=0.26				
					DistGeo	F(1,226)=0.82, p=0.43				
					Subspecies:DistGeo	F(6,226)=0.92, p=0.52				
21	<i>H. cydno</i> subspecies Yellow/White	South-East Andean foothills/ Cauca Valley/ Magdalena Valley/ Pacific/ North-East Andean foothills	A	 <p><i>H. cydno cydnides</i> (50) <i>H. cydno chioneus</i> (4) <i>H. cydno cydno</i> (43) <i>H. cydno waningeri</i> (15) <i>H. cydno lisethae</i> (13) <i>H. cydno hermogenes</i> (7)</p> <p><i>H. cydno cordula</i> (17) <i>H. cydno subsp. nov.</i> (2) <i>H_c_ weymeri</i> f. <i>weymeri</i> (51) <i>H. cydno zelinde</i> (51) <i>H. cydno weymeri</i> f. <i>submarginatus</i> (50)** <i>H. cydno weymeri</i> f. <i>gustavi</i> (49)</p>			Wing Size	FW	Subspecies	F(11,323)=6.95, p=1.01e-7*
				DistGeo	F(1,323)=0.05, p=0.81					
				Subspecies:DistGeo	F(6,323)=1.93, p=0.07					
				HW	Subspecies	F(11,321)=7.16, p=5.75e-8*				
					DistGeo	F(1,321)=2.67, p=0.10				
					Subspecies:DistGeo	F(6,321)=1.42, p=0.20				
				Wing Shape	FW	Subspecies		F(11,323)=13.87, p<2.2e-16*		
						DistGeo		F(1,323)=0.35, p=0.70		
						Subspecies:DistGeo		F(6,323)=1.05, p=0.39		
				HW	Subspecies	F(11,226)=8.46, p<2.2e-16*				
					DistGeo	F(1,226)=1.09, p=0.33				
					Subspecies:DistGeo	F(6,226)=1.03, p=0.41				
22	<i>H. timareta</i> subspecies Red- banded/ Dennis-ray/ White/Yellow	Putumayo/ Amazon/ Eastern slopes of the Andes	A	 <p><i>H. tristero</i> (16) <i>H. timareta florencea</i> (44) <i>H. timareta subsp. nov.</i> (4) <i>H. timareta linaresi</i> (7) <i>H. heurippa</i> (26)</p>			Wing Size	FW	Subspecies	F(4,81)=3.70, p=0.007*
				DistGeo	F(1,81)=0.13, p=0.71					
				Subspecies:DistGeo	F(2,81)=0.56, p=0.57					
				HW	Subspecies	F(4,72)=1.86, p=0.16				
					DistGeo	F(1,72)=1.37, p=0.24				
					Subspecies:DistGeo	F(2,72)=0.78, p=0.46				
				FW	Subspecies	F(4,81)=41.42, p<2.2e-16*				

				Wing Shape		DistGeo	F(1,81)=3.12, p=0.05	
						Subspecies:DistGeo	F(2,81)=0.23, p=0.91	
					HW	Subspecies	F(4,72)=24.49, p<2.2e-16*	
							DistGeo	F(1,72)=0.25, p=0.77
							Subspecies:DistGeo	F(2,72)=11.30, p=5.08e-8*

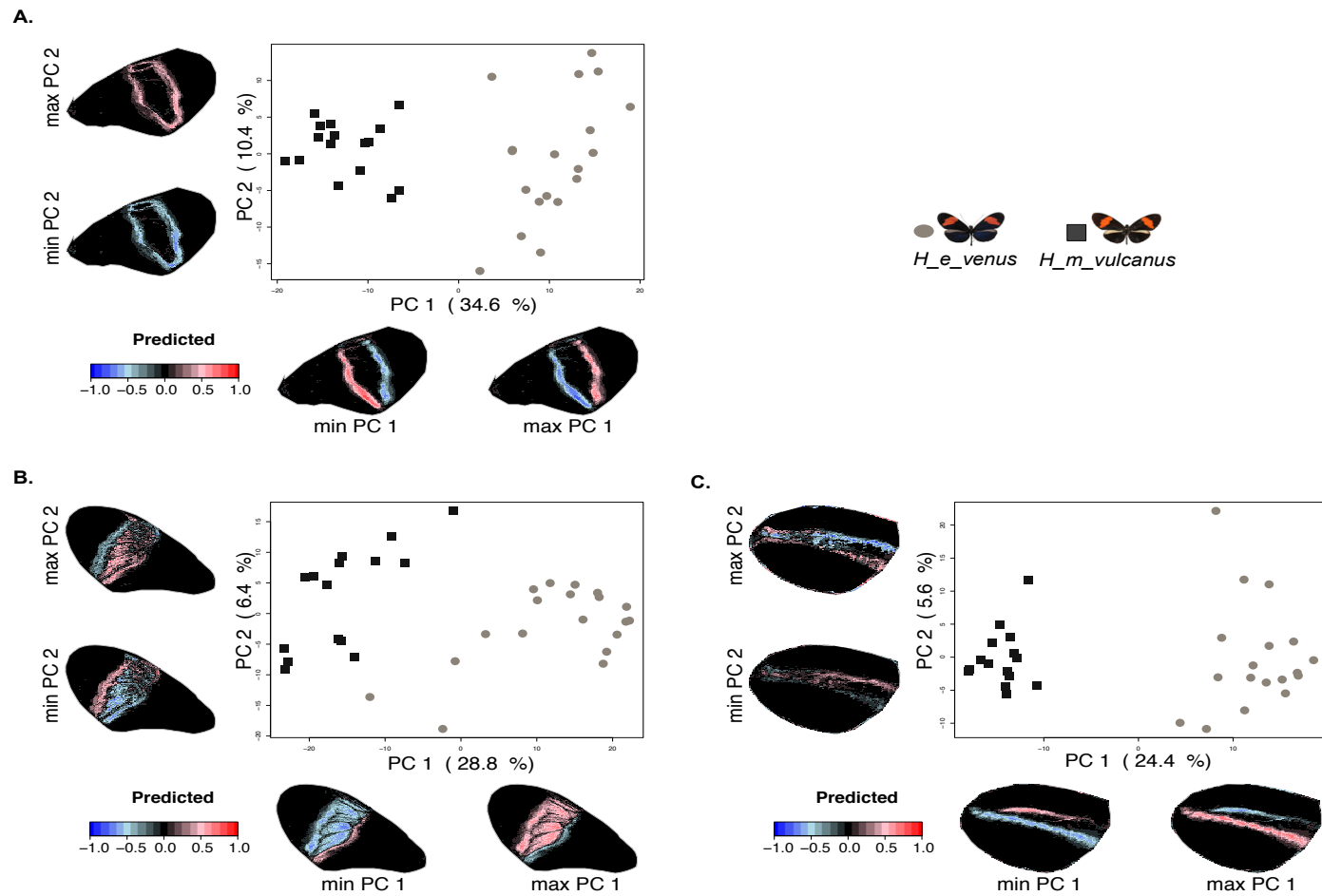


Figure S1.10. Comparison of colour pattern between *H. erato venus* and *H. melpomene vulcanus*, subspecies exhibiting the red-banded phenotype. Scale of predicted values indicates the expression of colour pattern (positive/red: full presence and negative/blue: full absence). Wing elements analysed: red band on the dorsal FW (A) and ventral FW (B); yellow bar on the ventral HW (C). MANCOVA test values are in in Table S1.2 – Comparison 2.

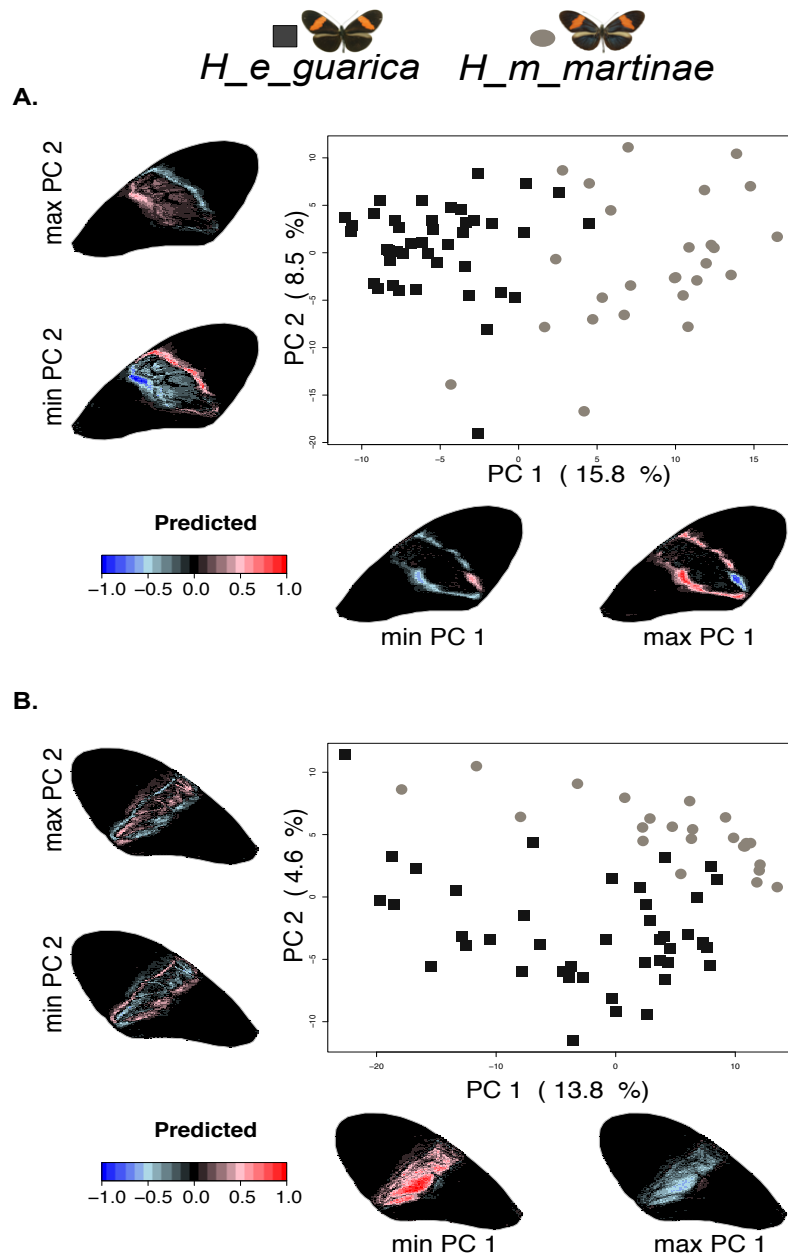




Figure S1.11. Comparison of colour pattern between *H. erato guarica* and *H. melpomene martinae*, subspecies exhibiting the red-banded phenotype. Scale of predicted values indicates the expression of colour pattern, where positive (positive/red: full presence, and negative/blue: full absence). Wing elements analysed: red band on the dorsal FW (**A**) and ventral FW (**B**). MANCOVA test values are in Table S1.2 – Comparison 3.

 *H_e_nydaara*  *H_m_melpomene*

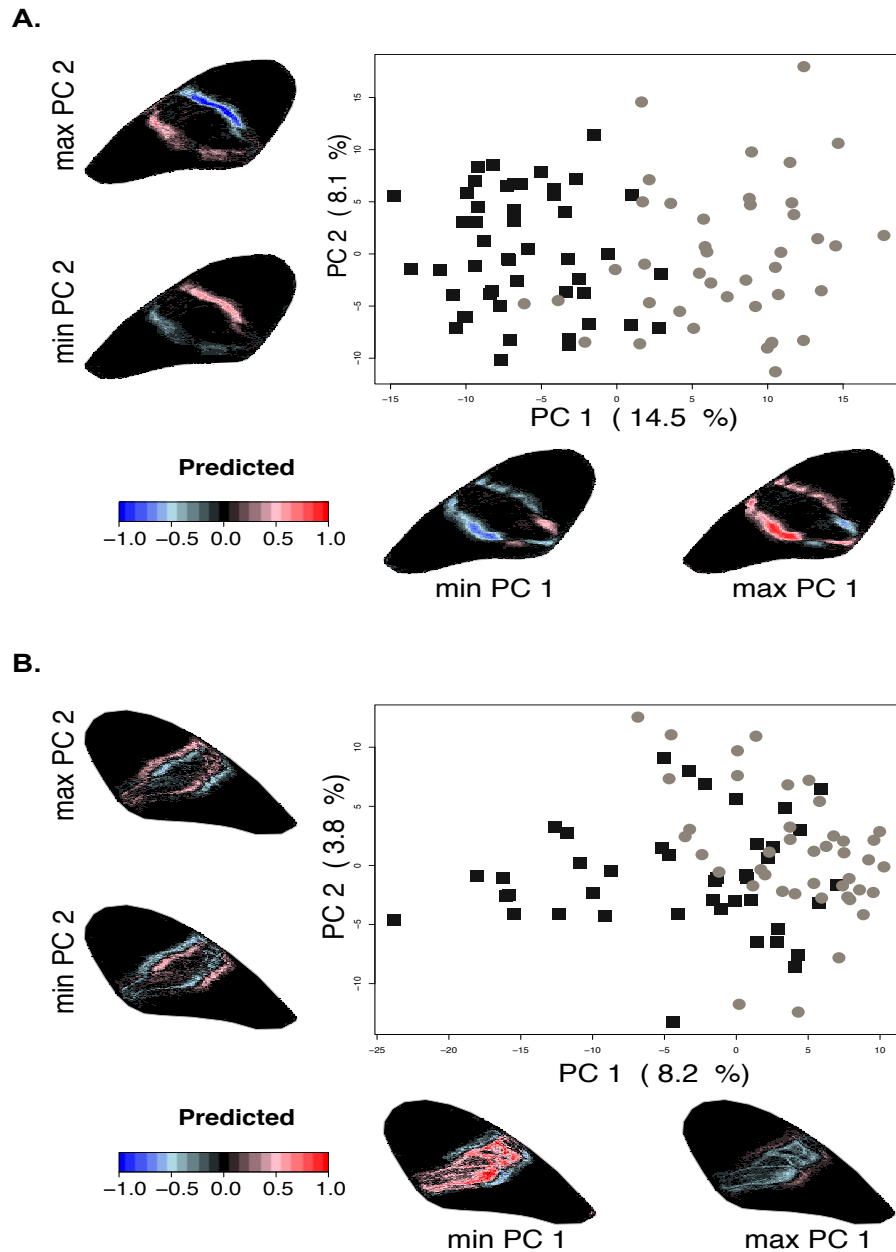


Figure S1.12. Comparison of colour pattern between *H. erato nydaara* and *H. melpomene melpomene*, subspecies exhibiting the red-banded phenotype. Scale of predicted values indicates the expression of colour pattern (positive/red: full presence, and negative/blue: full absence). Wing elements analysed: red band on the dorsal FW (**A**) and ventral FW (**B**). MANCOVA test values are in Table S1.2 – Comparison 4.

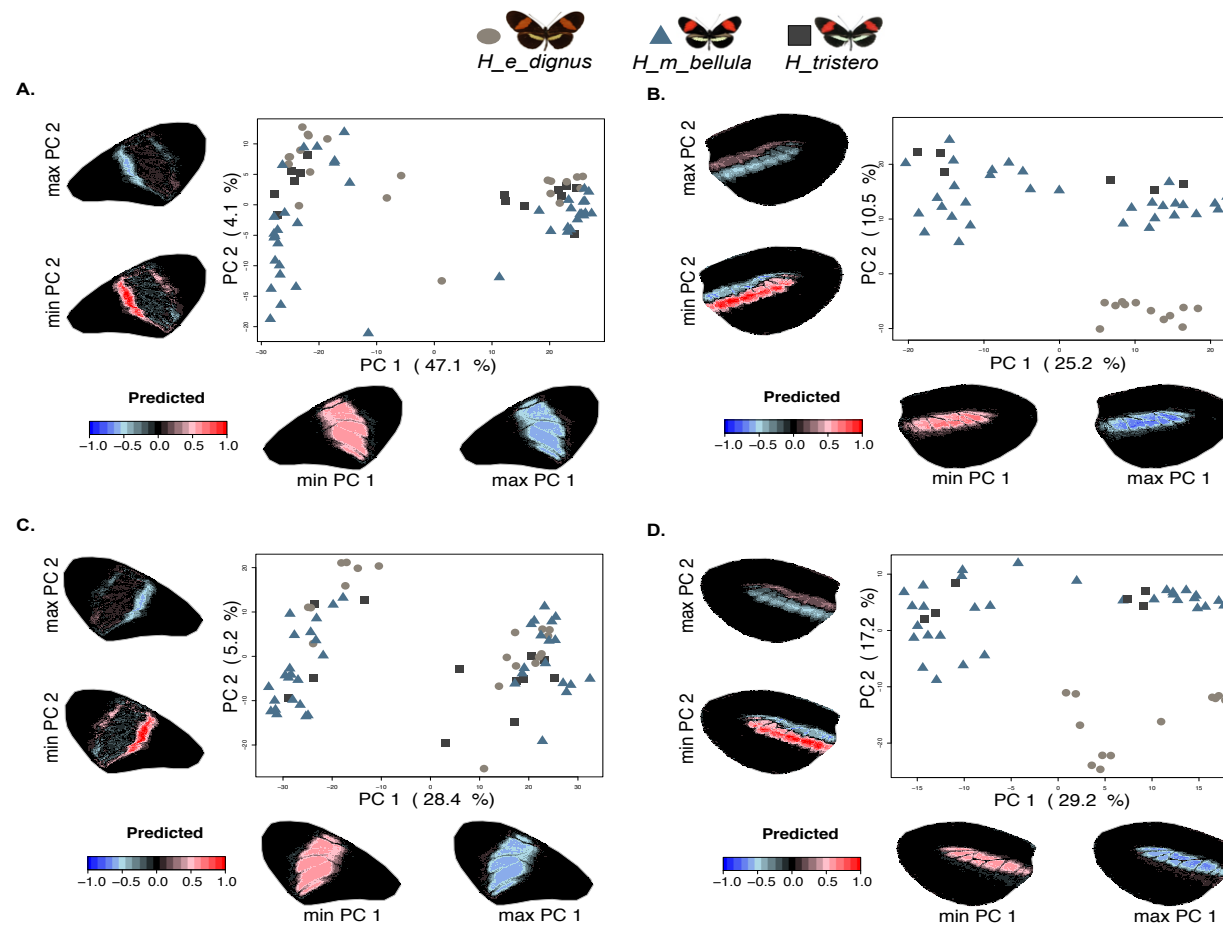


Figure S1.13. Comparison of colour pattern between *H. erato dignus*, *H. melpomene bellula* and *H. tristero*, subspecies exhibiting the red-banded phenotype. Scale of predicted values indicates the expression of colour pattern (positive/red: full presence, and negative/blue: full absence). Wing elements analysed: red band on the dorsal FW (A) and ventral FW (C); yellow bar on the dorsal HW (B) and ventral HW (D). MANCOVA test values are in Table S1.2 – Comparison 5.

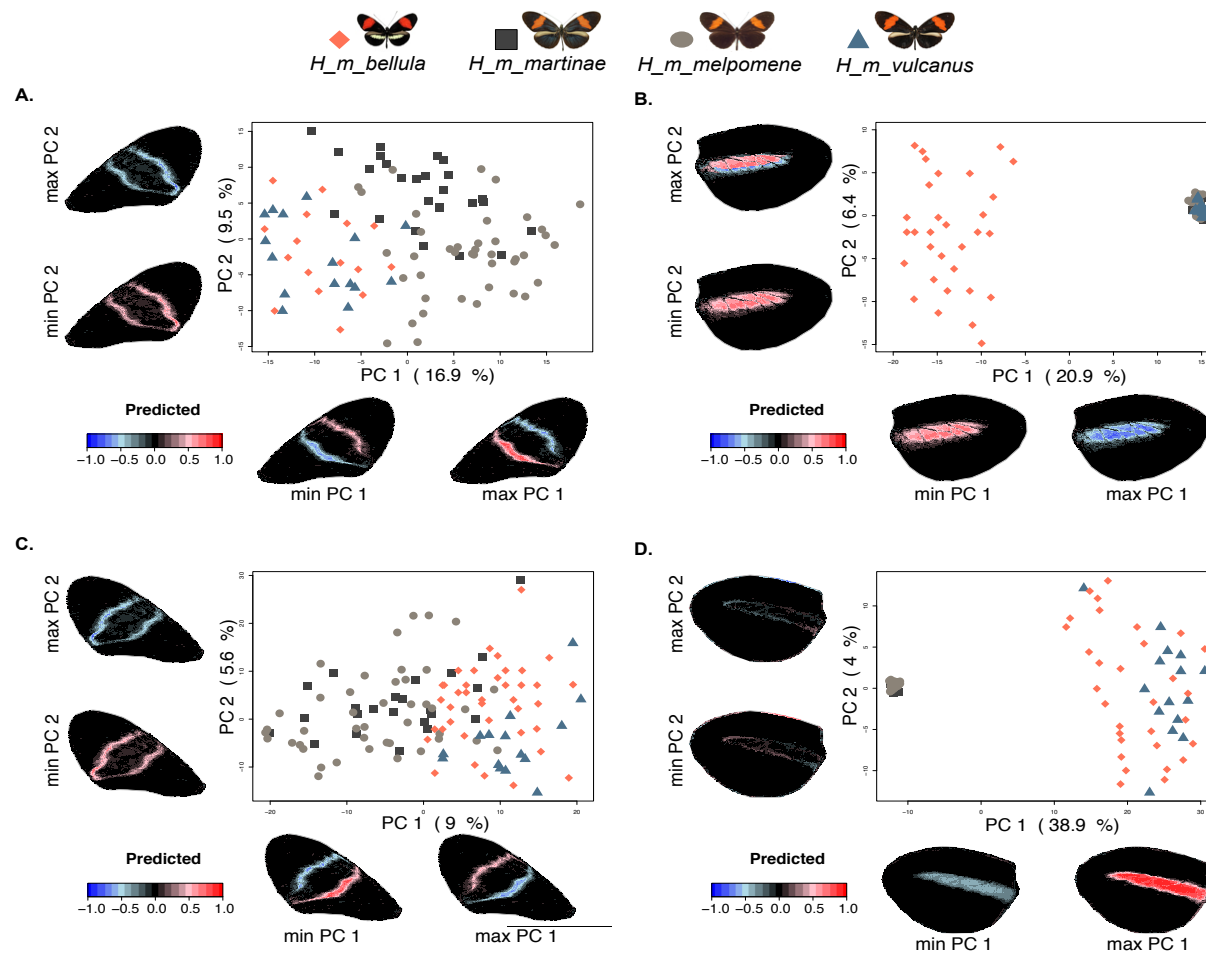


Figure S1.14. Comparison of colour pattern between subspecies of *H. melpomene* with the red-banded phenotype. Scale of predicted values indicates the expression of colour pattern (positive/red: full presence, and negative/blue: full absence). Wing elements analysed: red band on the dorsal FW (**A**) and ventral FW (**C**); yellow bar on the dorsal HW (**B**) and ventral HW (**D**). MANCOVA test values are in Table S1.2 – Comparison 6.

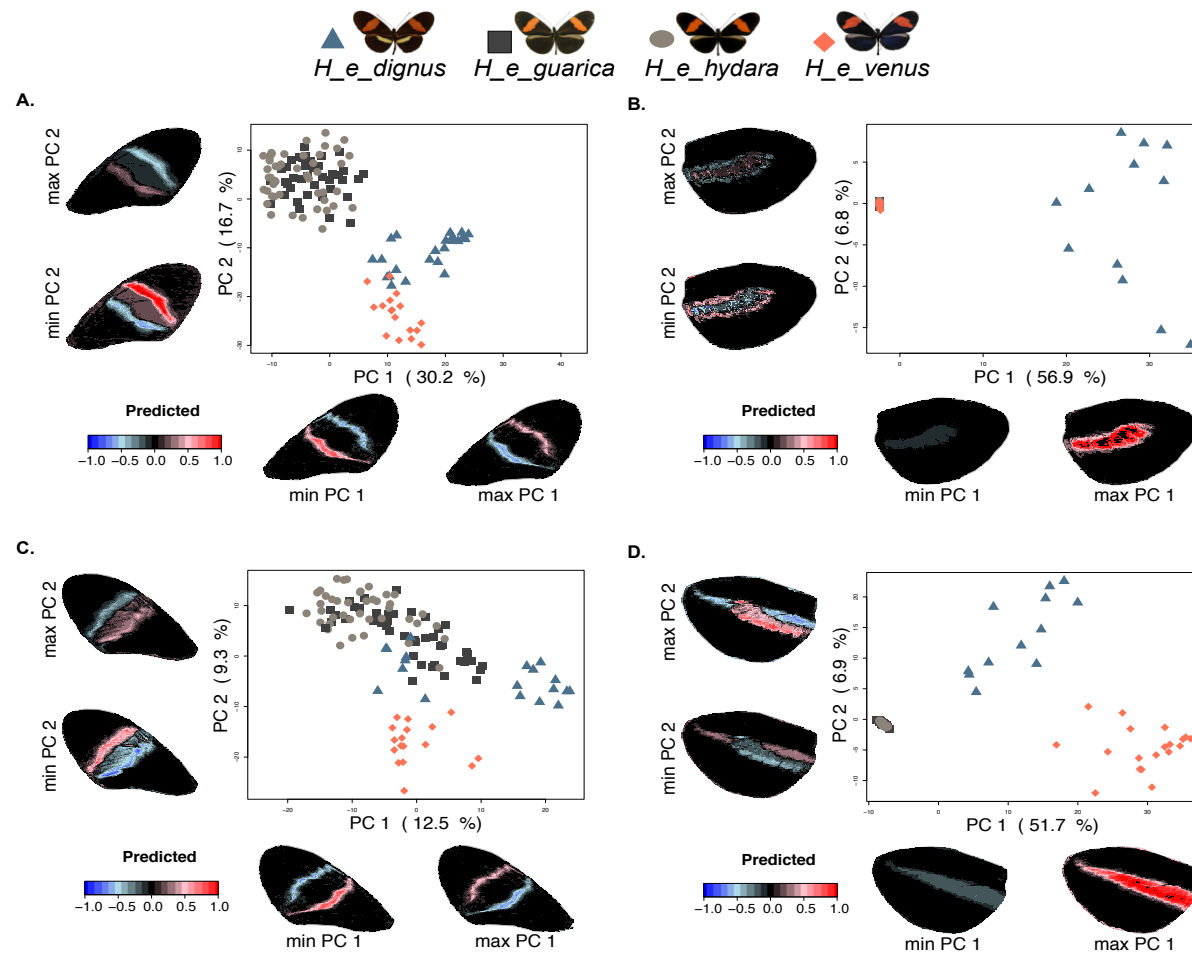


Figure S1.15. Comparison of colour pattern between subspecies of *H. erato* with the red-banded phenotype. Scale of predicted values indicates the expression of colour pattern (positive/red: full presence, and negative/blue: full absence). Wing elements analysed: red band on the dorsal FW (A) and ventral FW (C); yellow bar on the dorsal HW (B) and ventral HW (D). MANCOVA test values are in Table S1.2 – Comparison 7.





H_c_zelinde *H_eleuchia_eleusinus* *H_s_chocoensis*

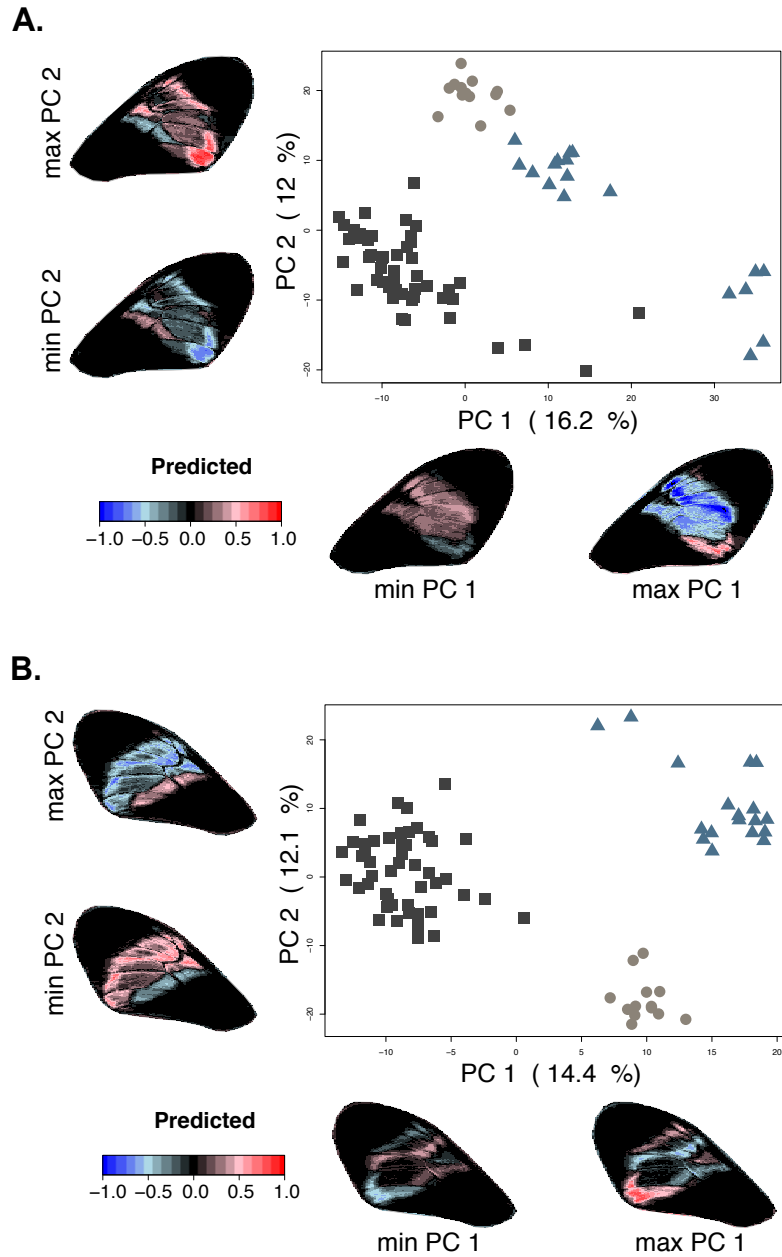


Figure S1.16. Comparison of colour pattern between *H. cydno zelinde*, *H. eleuchia eleusinus* and *H. sapho chocoensis*, subspecies exhibiting the yellow/white phenotype. Scale of predicted values indicates the expression of colour pattern (positive/red: full presence, and negative/blue: full absence). Wing elements analysed: white band on the dorsal FW (**A**) and ventral FW (**B**). MANCOVA test values are in Table S1.2 – Comparison 11.

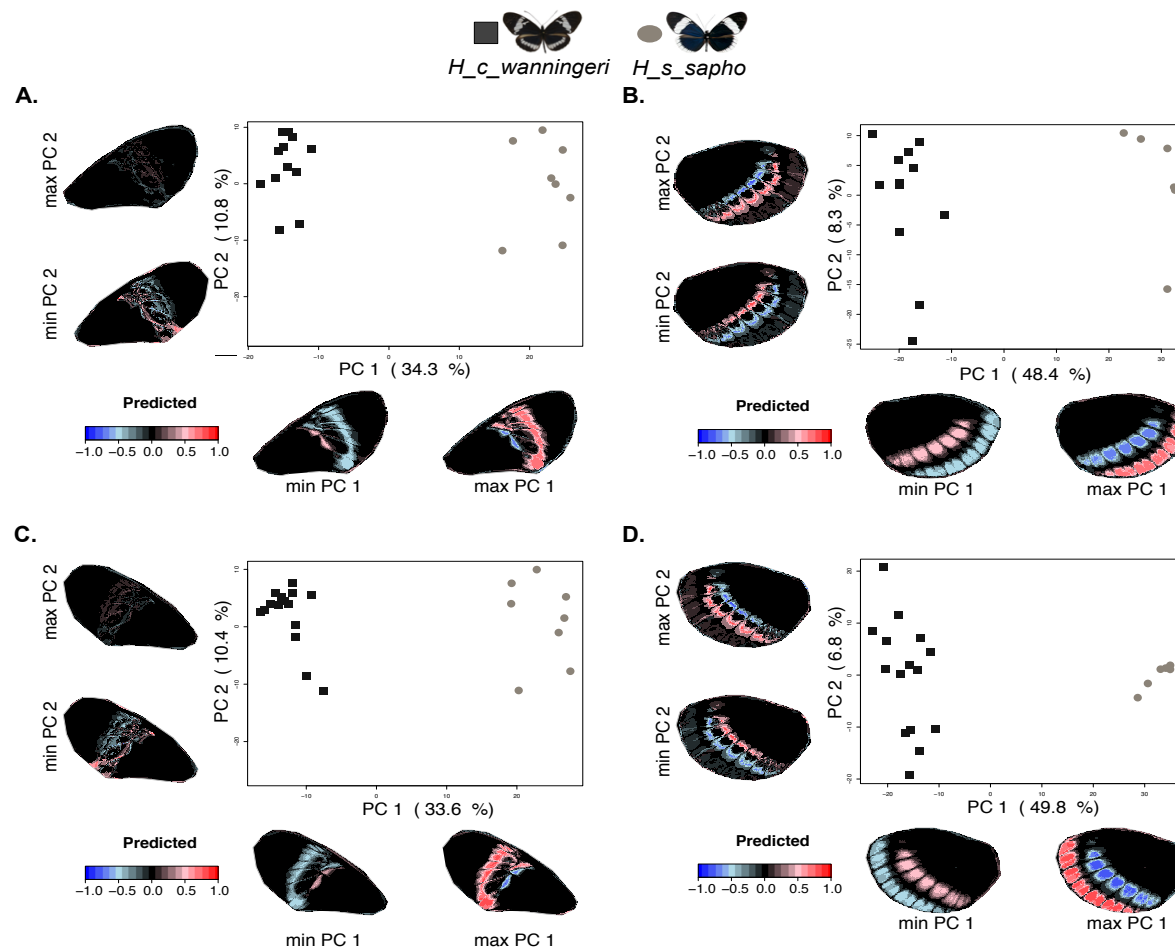


Figure S1.17. Comparison of colour pattern between *H. cydno wanningeri* and *H. sapho sapho*, subspecies exhibiting the yellow/white phenotype. Scale of predicted values indicates the expression of colour pattern (positive/red: full presence, and negative/blue: full absence). Wing elements analysed: white band on the dorsal FW (**A**) and ventral FW (**C**); white border on the dorsal HW (**B**) and ventral HW (**D**). MANCOVA test values are in Table S1.2 – Comparison 12.

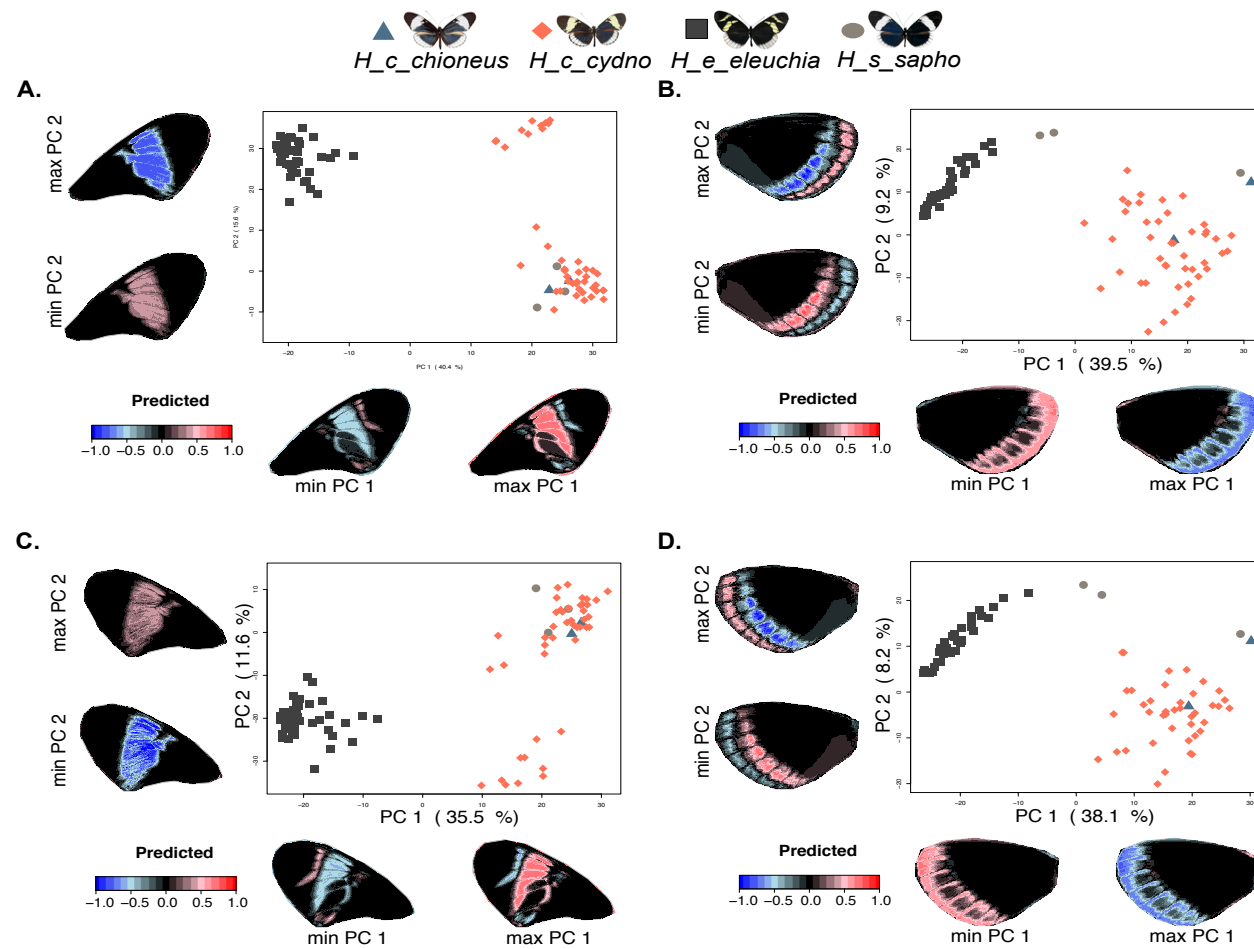


Figure S1.18. Comparisons of colour pattern between *H. cydno chioneus*, *H. cydno cydno*, *H. eleuchia eleuchia* and *H. sapho sapho*. Scale of predicted values indicates the expression of colour pattern (positive/red: full presence, and negative/blue: full absence). Wing elements analysed: yellow/white band on the dorsal FW (**A**) and ventral FW (**C**); white border on the dorsal HW (**B**) and ventral HW (**D**). MANCOVA test values are in Table S1.2 – Comparison 13.

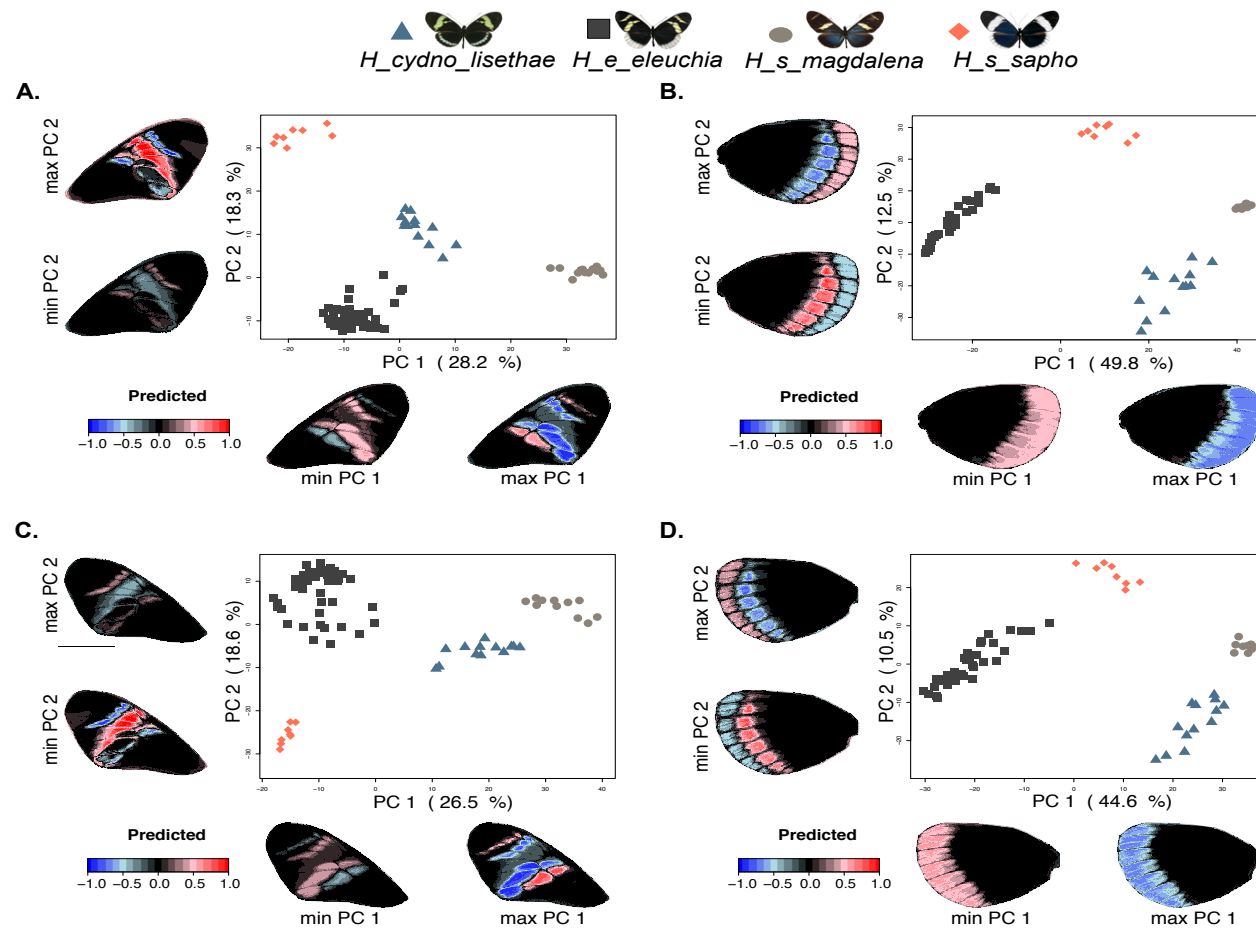


Figure S1.19. Comparison of colour pattern between *H. sara magdalena*, *H. sapho sapho*, *H. eleuchia eleuchia* and *H. cydno lisethae*, subspecies exhibiting the yellow/white phenotype. Scale of predicted values indicates the expression of colour pattern (positive/red: full presence, and negative/blue: full absence). Wing elements analysed: yellow/white band on the dorsal FW (A) and ventral FW (C); white border on the dorsal HW (B) and ventral HW (D). MANCOVA test values are in Table S1.2 – Comparison 14.

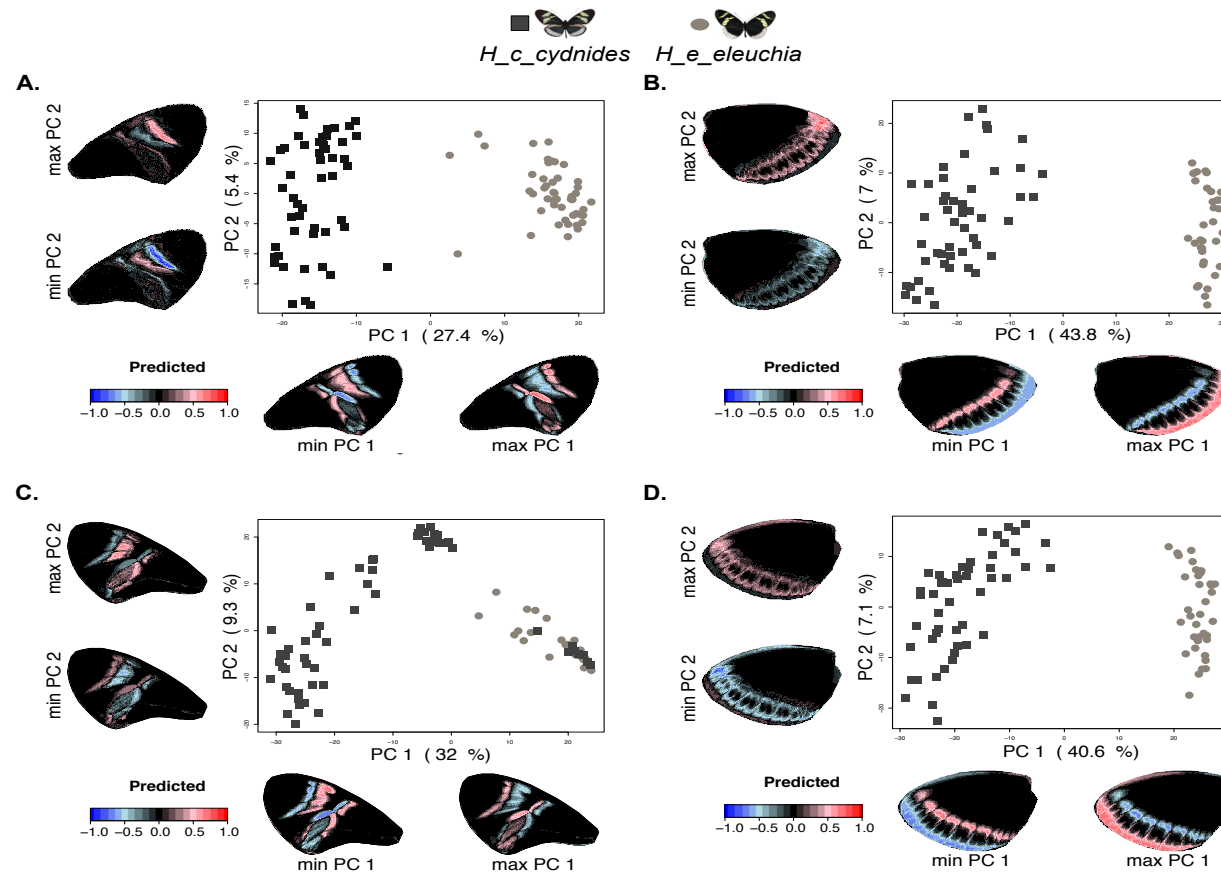


Figure S1.20. Comparison of colour pattern between *H. cydno cydnides* and *H. eleuchia eleuchia*, subspecies exhibiting the yellow/white phenotype. Scale of predicted values indicates the expression of colour pattern (positive/red: full presence, and negative/blue: full absence). Wing elements analysed: split band on the dorsal FW (A) and ventral FW (C); white border on the dorsal HW (B) and ventral HW (D). MANCOVA test values are in Table S1.2 – Comparison 15.

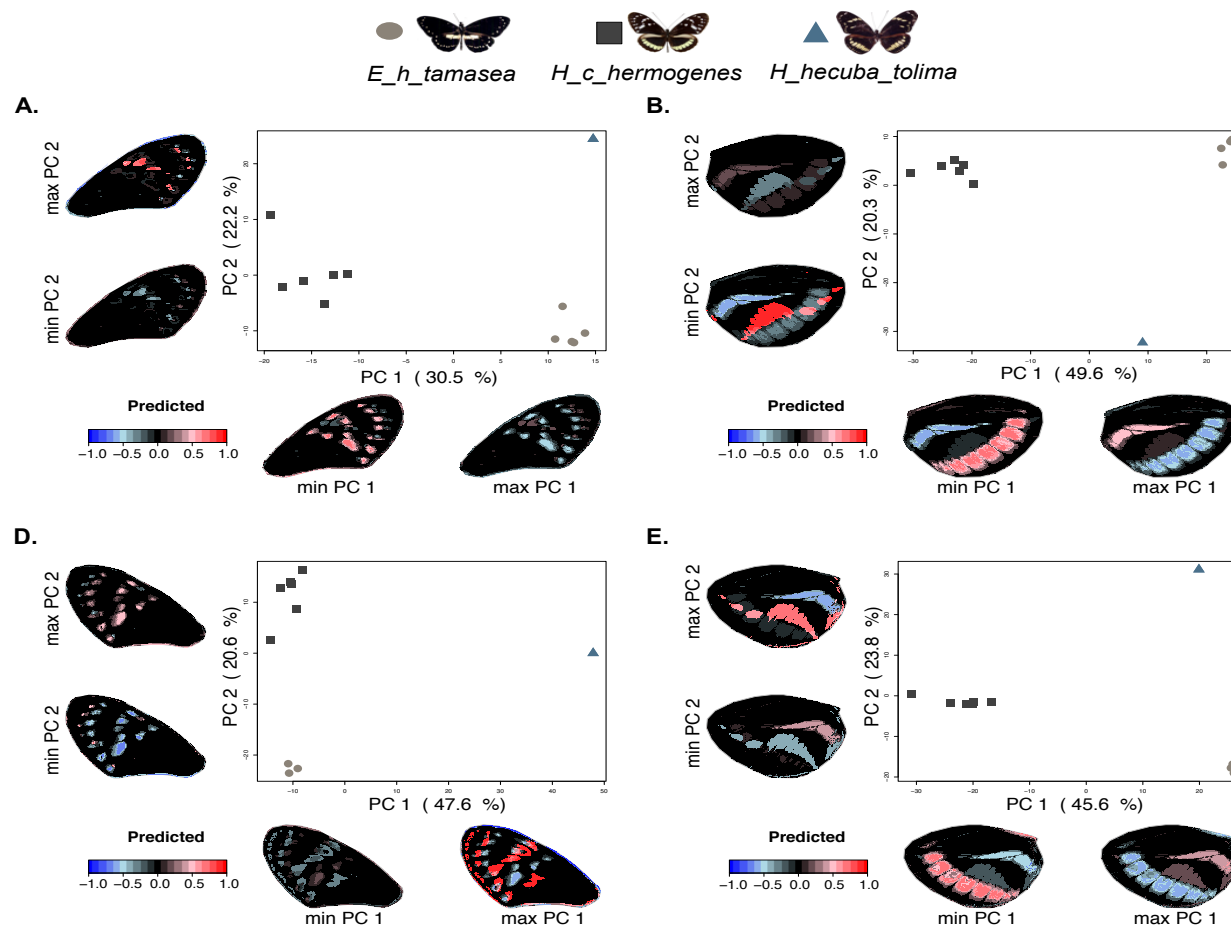


Figure S1.21. Comparison of colour pattern between *Elzunia humboldt tamasea*, *H. hecuba tolima* and *H. cydno hermogenes*, subspecies exhibiting the yellow/white phenotype. Scale of predicted values indicates the expression of colour pattern (positive/red: full presence, and negative/blue: full absence). Wing elements analysed: white/yellow submarginal dots on the dorsal FW (A) and ventral FW (C); yellow bar on the dorsal HW (B) and ventral HW (D). MANCOVA test values are in Table S1.2 – Comparison 16.

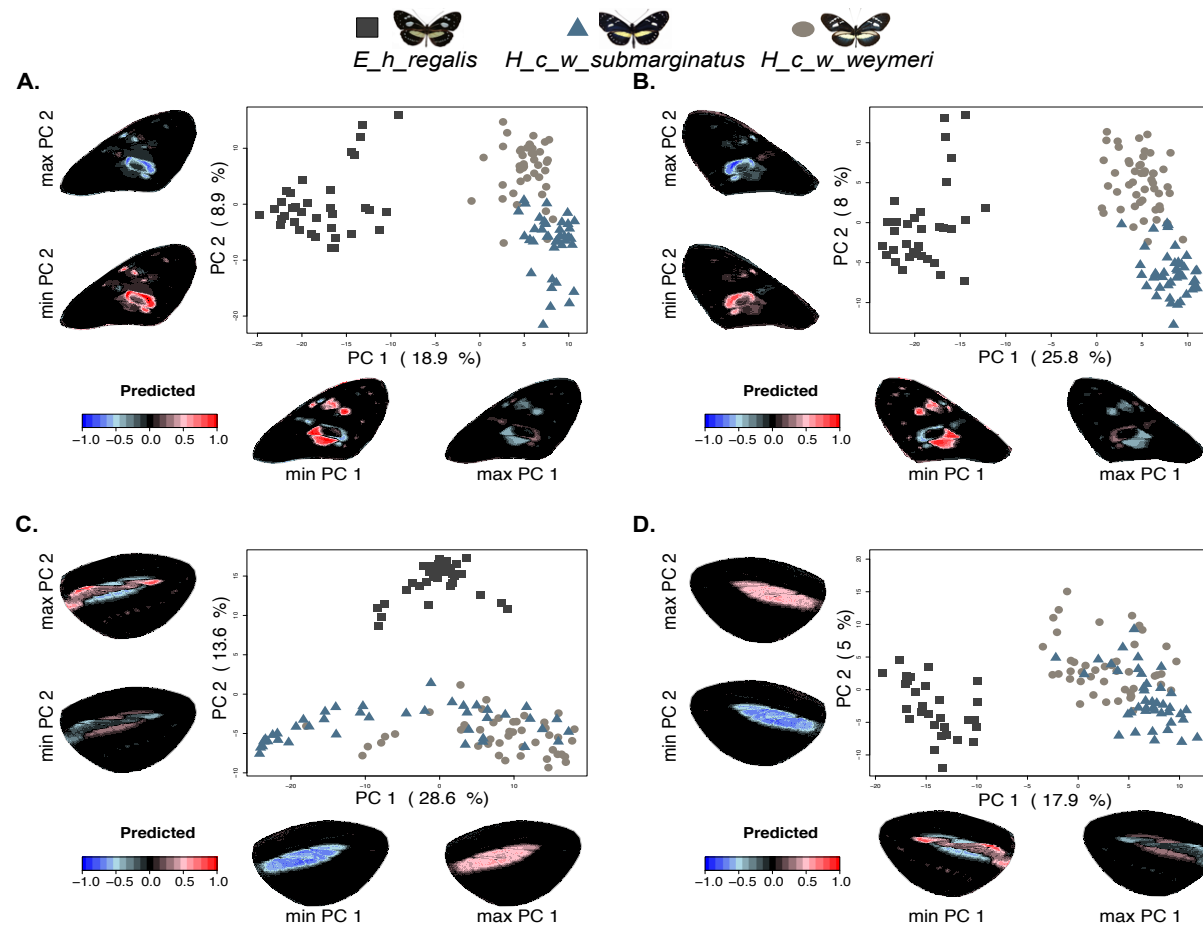


Figure S1.22. Comparison of colour pattern between *Elzunia humboldt regalis* and two races of *H. cydno weymeri*, exhibiting the yellow/white phenotype. Scale of predicted values indicates the expression of colour pattern (positive/red: full presence, and negative/blue: full absence). Wing elements analysed: white/yellow submarginal dots on the dorsal FW (**A**) and ventral FW (**B**); yellow bar on the dorsal HW (**C**) and ventral HW (**D**). MANCOVA test values are in Table S1.2 – Comparison 17.

CHAPTER 2. REPRODUCTIVE ISOLATION DRIVEN BY PHEROMONES IN MIMETIC AND CLOSELY RELATED BUTTERFLIES

Table S2.1. Samples included in the quantification of wing phenotype. A total of 89 individuals were used. The wings were obtained from “Colección de Artrópodos de la Universidad del Rosario (CAUR229)”. Last column specifies the analysis in which each specimen was used, D, dorsal; V, ventral; HW, hindwing; FW, forewing.

ID Collection	ID Wing Scan	Taxon	Locality	Analysis in which the sample was used
M54	LGE-WS-00351	<i>H. t. florencia</i>	Quebrada_Las_Doraditas	D-HW; D-FW
M63	LGE-WS-00349	<i>H. t. florencia</i>	Finca_Piñacue	D-HW; D-FW; V-HW; V-FW
M64	LGE-WS-00350	<i>H. t. florencia</i>	Finca_Piñacue	D-HW; D-FW; V-HW; V-FW
M244	LGE-WS-00373	<i>H. m. malleti</i>	Florencia	D-HW; D-FW; V-HW; V-FW
M253	LGE-WS-00375	<i>H. m. malleti</i>	Florencia_Sucre	D-HW; D-FW; V-HW; V-FW
M255	LGE-WS-00326	<i>H. t. florencia</i>	Florencia_Sucre	D-HW; D-FW
M257	LGE-WS-00346	<i>H. t. florencia</i>	Florencia_Sucre	D-HW; D-FW; V-HW; V-FW
M259	LGE-WS-00325	<i>H. t. florencia</i>	Florencia_Sucre	D-HW; D-FW
M415	LGE-WS-00397	<i>H. m. malleti</i>	Florencia_Sucre	D-HW; D-FW; V-HW; V-FW
M418	LGE-WS-00305	<i>H. t. florencia</i>	Florencia_Sucre	D-HW; D-FW; V-HW; V-FW
M426	LGE-WS-00361	<i>H. m. malleti</i>	Florencia_Sucre	D-HW; D-FW; V-HW; V-FW
M433	LGE-WS-00390	<i>H. m. malleti</i>	Florencia_Sucre	V-HW; V-FW
M434	LGE-WS-00363	<i>H. m. malleti</i>	Florencia_Sucre	V-HW; V-FW
M451	LGE-WS-00304	<i>H. t. florencia</i>	Florencia_Sucre	D-HW; D-FW; V-HW; V-FW
M462	LGE-WS-00337	<i>H. t. florencia</i>	Florencia_Sucre	D-HW; D-FW; V-HW; V-FW
M468	LGE-WS-00383	<i>H. m. malleti</i>	Florencia_Sucre	D-HW; D-FW; V-HW; V-FW
M471	LGE-WS-00307	<i>H. t. florencia</i>	Florencia_Sucre	D-HW; D-FW;
M472	LGE-WS-00311	<i>H. t. florencia</i>	Florencia_Sucre	D-HW; D-FW; V-HW; V-FW
M474	LGE-WS-00359	<i>H. m. malleti</i>	Florencia_Sucre	V-HW; V-FW
M583	LGE-WS-00367	<i>H. m. malleti</i>	Florencia	D-HW; D-FW; V-HW; V-FW
M584	LGE-WS-00357	<i>H. m. malleti</i>	Florencia_Sucre	D-HW; D-FW
M587	LGE-WS-00306	<i>H. t. florencia</i>	Florencia_Sucre	D-HW; D-FW; V-HW; V-FW
M588	LGE-WS-00310	<i>H. t. florencia</i>	Florencia_Sucre	D-HW; D-FW; V-HW; V-FW
M589	LGE-WS-00370	<i>H. m. malleti</i>	Florencia_Sucre	D-HW; D-FW; V-HW; V-FW
M590	LGE-WS-00395	<i>H. m. malleti</i>	Florencia_Sucre	D-HW; D-FW; V-HW; V-FW
M592	LGE-WS-00394	<i>H. m. malleti</i>	Florencia_Sucre	D-HW; D-FW; V-HW; V-FW
M593	LGE-WS-00309	<i>H. t. florencia</i>	Florencia_Sucre	D-HW; D-FW; V-HW; V-FW
M594	LGE-WS-00368	<i>H. m. malleti</i>	Quebrada_Las_Doraditas	D-HW; D-FW; V-HW; V-FW
M595	LGE-WS-00318	<i>H. t. florencia</i>	Florencia_Sucre	D-HW; D-FW; V-HW; V-FW
M596	LGE-WS-00308	<i>H. t. florencia</i>	Florencia_Sucre	D-HW; D-FW; V-HW; V-FW
M598	LGE-WS-00377	<i>H. m. malleti</i>	Florencia_Sucre	D-HW; D-FW; V-HW; V-FW
M602	LGE-WS-00303	<i>H. t. florencia</i>	Florencia_Sucre	D-HW; D-FW; V-HW; V-FW
M606	LGE-WS-00352	<i>H. m. malleti</i>	Florencia_Sucre	D-HW; D-FW; V-HW; V-FW
M607	LGE-WS-00317	<i>H. t. florencia</i>	Florencia_Sucre	D-HW; D-FW; V-HW; V-FW
M610	LGE-WS-00379	<i>H. m. malleti</i>	Florencia_Sucre	D-HW; D-FW; V-HW; V-FW
M611	LGE-WS-00316	<i>H. t. florencia</i>	Florencia_Sucre	D-HW; D-FW; V-HW; V-FW
M612	LGE-WS-00319	<i>H. t. florencia</i>	Florencia_Sucre	D-HW; D-FW; V-HW; V-FW

M614	LGE-WS-00355	<i>H. m. malleti</i>	Florencia_Sucre	D-HW; D-FW; V-HW; V-FW
M616	LGE-WS-00334	<i>H. t. florenci</i>	Florencia_Sucre	D-HW; D-FW; V-HW; V-FW
M618	LGE-WS-00324	<i>H. t. florenci</i>	Florencia_Sucre	D-HW; D-FW
M620	LGE-WS-00302	<i>H. t. florenci</i>	Florencia_Sucre	D-HW; D-FW; V-HW; V-FW
M622	LGE-WS-00332	<i>H. t. florenci</i>	Florencia_Sucre	D-HW; D-FW
M1009	LGE-WS-00333	<i>H. t. florenci</i>	Florencia_Sucre	D-HW; D-FW; V-HW; V-FW
M1010	LGE-WS-00313	<i>H. t. florenci</i>	Florencia_Sucre	D-HW; D-FW; V-HW; V-FW
M1016	LGE-WS-00378	<i>H. m. malleti</i>	Florencia_Sucre	D-HW; D-FW; V-HW; V-FW
M1074	LGE-WS-00315	<i>H. t. florenci</i>	Florencia_Sucre	D-HW; D-FW; V-HW; V-FW
M1075	LGE-WS-00314	<i>H. t. florenci</i>	Florencia_Sucre	D-HW; D-FW; V-HW; V-FW
M1079	LGE-WS-00348	<i>H. t. florenci</i>	Florencia_Sucre	D-HW; D-FW; V-HW; V-FW
M1084	LGE-WS-00328	<i>H. t. florenci</i>	Florencia_Sucre	D-HW; D-FW; V-HW; V-FW
M1085	LGE-WS-00329	<i>H. t. florenci</i>	Florencia_Sucre	D-HW; D-FW
M1094	LGE-WS-00330	<i>H. t. florenci</i>	Florencia_Sucre	D-HW; D-FW; V-HW; V-FW
M1098	LGE-WS-00396	<i>H. m. malleti</i>	Florencia_Sucre	D-HW; D-FW; V-HW; V-FW
M1196	LGE-WS-00354	<i>H. m. malleti</i>	Florencia_Paraiso	D-HW; D-FW; V-HW; V-FW
M1283	LGE-WS-00353	<i>H. m. malleti</i>	Florencia_Paraiso	D-HW; D-FW; V-HW; V-FW
M1288	LGE-WS-00364	<i>H. m. malleti</i>	Florencia_Paraiso	V-HW; V-FW
M1321	LGE-WS-00365	<i>H. m. malleti</i>	Florencia_Paraiso	D-HW; D-FW; V-HW; V-FW
M1441	LGE-WS-00381	<i>H. m. malleti</i>	Florencia_Sucre	D-HW; D-FW; V-HW; V-FW
M1507	LGE-WS-00389	<i>H. m. malleti</i>	Florencia_Paraiso	V-HW; V-FW
M1511	LGE-WS-00387	<i>H. m. malleti</i>	Florencia_Paraiso	D-HW; D-FW; V-HW; V-FW
M1512	LGE-WS-00386	<i>H. m. malleti</i>	Florencia_Paraiso	D-HW; D-FW; V-HW; V-FW
M1514	LGE-WS-00384	<i>H. m. malleti</i>	Florencia_Paraiso	D-HW; D-FW; V-HW; V-FW
M1522	LGE-WS-00385	<i>H. m. malleti</i>	Florencia_Paraiso	D-HW; D-FW; V-HW; V-FW
M1754	LGE-WS-00331	<i>H. t. florenci</i>	Florencia_Sucre	D-HW; D-FW; V-HW; V-FW
M1757	LGE-WS-00376	<i>H. m. malleti</i>	Florencia_Sucre	D-HW; D-FW; V-HW; V-FW
M1758	LGE-WS-00345	<i>H. t. florenci</i>	Florencia_Sucre	D-HW; D-FW; V-HW; V-FW
M1767	LGE-WS-00391	<i>H. m. malleti</i>	Florencia_Sucre	D-HW; D-FW; V-HW; V-FW
M1769	LGE-WS-00343	<i>H. t. florenci</i>	Florencia_Sucre	D-HW; D-FW; V-HW; V-FW
M1770	LGE-WS-00388	<i>H. m. malleti</i>	Florencia_Sucre	V-HW; V-FW
M1771	LGE-WS-00344	<i>H. t. florenci</i>	Florencia_Sucre	D-HW; D-FW; V-HW; V-FW
M1772	LGE-WS-00321	<i>H. t. florenci</i>	Florencia_Sucre	D-HW; D-FW; V-HW; V-FW
M1773	LGE-WS-00369	<i>H. m. malleti</i>	Florencia_Sucre	D-HW; D-FW; V-HW; V-FW
M1774	LGE-WS-00360	<i>H. m. malleti</i>	Florencia_Sucre	D-HW; D-FW; V-HW; V-FW
M1805	LGE-WS-00320	<i>H. t. florenci</i>	Florencia_Sucre	D-HW; D-FW; V-HW; V-FW
M1808	LGE-WS-00322	<i>H. t. florenci</i>	Florencia_Sucre	D-HW; D-FW
M1813	LGE-WS-00366	<i>H. m. malleti</i>	Quebrada_Las_Doraditas	D-HW; D-FW; V-HW; V-FW
M1814	LGE-WS-00399	<i>H. m. malleti</i>	Florencia_Sucre	D-HW; D-FW
M1817	LGE-WS-00323	<i>H. t. florenci</i>	Florencia_Sucre	V-HW; V-FW
M1823	LGE-WS-00356	<i>H. m. malleti</i>	Florencia_Paraiso	D-HW; D-FW; V-HW; V-FW
M1845	LGE-WS-00362	<i>H. m. malleti</i>	Florencia_Paraiso	D-HW; D-FW; V-HW; V-FW
M1846	LGE-WS-00336	<i>H. t. florenci</i>	Florencia_Sucre	D-HW; D-FW; V-HW; V-FW
M2347	LGE-WS-00393	<i>H. m. malleti</i>	Florencia_Paraiso	D-HW; D-FW; V-HW; V-FW
M2360	LGE-WS-00374	<i>H. m. malleti</i>	Florencia_Paraiso	D-HW; D-FW; V-HW; V-FW
M2408	LGE-WS-00382	<i>H. m. malleti</i>	Florencia_Paraiso	D-HW; D-FW; V-HW; V-FW
M3544	LGE-WS-00358	<i>H. m. malleti</i>	Florencia_Paraiso	D-HW; D-FW; V-HW; V-FW
M3765	LGE-WS-00347	<i>H. t. florenci</i>	Florencia_Sucre	D-HW; D-FW; V-HW; V-FW

M3767	LGE-WS-00339	<i>H. t. florenci</i>	Florencia_Sucre	D-HW; D-FW; V-HW; V-FW
M3874	LGE-WS-00341	<i>H. t. florenci</i>	Florencia_Sucre	D-HW; D-FW; V-HW; V-FW
M3875	LGE-WS-00327	<i>H. t. florenci</i>	Florencia_Sucre	D-HW; D-FW

Table S2.2. Amount (ng) of compounds that remained in the wings of perfumed males before evaporation. I quantified the presence of the perfumed applied at the beginning of the experiment, at 1 minute, at 30 minutes and at 60 minutes after spreading the perfume. RI, retention index.

Name	RI	<i>H. melpomene malleti</i>				<i>H. timareta florencia</i>			
		Beginning	1 minute	30 minutes	60 minutes	Beginning	1 minute	30 minutes	60 minutes
Unknown	958	0.14	0.26	0.00	0.00	-	-	-	-
Limonene	1023	-	-	-	-	0.29	0.20	0.00	0.00
Phenylacetaldehyde	1036	-	-	-	-	0.17	0.00	0.00	0.00
Alkane	1117	-	-	-	-	2.78	2.82	2.01	1.15
Unknown	1174	0.20	0.14	0.14	0.41	0.45	2.35	2.20	0.83
Methyl salicylate	1187	-	-	-	-	1.44	1.37	0.00	0.03
(Z)-3-Hexenyl isobutyrate	1233	19.22	17.46	0.00	0.00	-	-	-	-
Hexyl 3-methylbutyrate	1239	53.33	0.00	0.00	0.00	-	-	-	-
Unknown	1243	0.58	0.30	0.00	0.00	-	-	-	-
Alkane	1265	-	-	-	-	1.82	0.46	0.00	0.00
Tridecane	1300	15.16	18.51	15.01	5.62	7.67	7.24	4.64	1.72
Tetradecane	1302	-	-	-	-	0.67	0.70	0.64	0.62
5-Decanolide	1369	-	-	-	-	4.80	4.76	4.44	1.16
α -Copaene	1371	1.31	0.00	0.00	0.00	-	-	-	-
Dihydroactinidiolide	1391	17.67	17.35	14.13	8.36	14.40	13.25	7.91	6.63
Unknown	1394	0.90	0.73	0.41	0.00	-	-	-	-
Ethyl 4-ethoxybenzoate	1402	8.29	9.40	1.03	0.56	12.09	15.41	14.39	14.06
Homovanillyl alcohol	1412	1.56	1.68	1.16	0.45	0.25	0.00	0.00	0.00
Methyl 4-hydroxybenzoate	1449	2.51	2.10	0.00	0.00	-	-	-	-
Methyl 3,4-dimethoxybenzoate	1464	8.97	7.53	5.88	3.25	-	-	-	-
Unknown	1470	0.92	0.57	0.56	0.30	-	-	-	-

Unknown	1488	-	-	-	-	0.11	0.00	0.00	0.00
Unknown	1495	0.10	0.16	0.12	0.06	-	-	-	-
Syringaaldehyde	1519	291.80	293.20	280.37	251.10	277.15	263.46	207.00	174.30
3,5-Dimethoxy 4-hydroxybenzyl alcohol	1565	-	-	-	-	7.17	0.00	0.00	0.00
Propyl 4-hydroxybenzoate	1614	-	-	-	-	2.70	0.00	0.00	0.00
Methyl 1 <i>H</i> -indol-3-carboxylate	1663	-	-	-	-	0.24	0.28	0.26	0.07
Unknown	1715	1.22	2.10	0.00	0.64	-	-	-	-
Unknown	1922	16.56	22.88	21.86	0.80	-	-	-	-
Hexadecanoic acid	1960	-	-	-	-	1.75	1.46	0.61	0.31
Eicosane	2000	2.65	1.34	2.17	5.26	2.56	3.27	2.36	1.83
Octadecanal	2015	1094.90	826.74	202.60	130.10	-	-	-	-
Isopropyl palmitate	2025	-	-	-	-	1.93	2.62	2.04	1.60
1-Octadecanol	2076	27.83	34.65	34.44	21.10	26.23	15.28	9.59	0.00
Isopropyl oleate	2187	-	-	-	-	0.00	0.03	0.00	0.00
Heneicosene	2088	-	-	-	-	12.30	3.45	0.00	0.00
Heneicosane	2088	298.84	325.10	287.02	171.70	174.57	193.60	165.48	146.40
Unknown	2109	-	-	-	-	0.50	0.00	0.00	0.00
Unknown	2135	1.54	1.99	1.77	0.64	0.20	0.25	0.23	0.11
Ethyl stearate	2190	-	-	-	-	1.77	1.24	0.00	0.00
(<i>Z</i>)-11-Eicosenal	2192	231.99	63.82	59.68	32.72	3.86	2.48	0.00	0.00
Docosane	2200	0.28	4.70	4.41	0.00	-	-	-	-
Eicosanal	2218	26.43	35.88	31.85	0.00	-	-	-	-
Tricosene	2270	-	-	-	-	1.13	1.27	1.23	0.56
Tricosane	2300	27.27	0.00	0.00	0.00	3.36	0.00	0.00	0.00
(<i>Z</i>)-13-Docosenal	2396	23.67	0.00	0.00	0.00	-	-	-	-
Unknown	2686	-	-	-	-	0.31	0.32	0.30	0.00

Heptacosane	2700	60.12	78.75	79.10	219.00	31.49	30.28	21.81	11.74
Octacosane	2800	-	-	-	-	0.40	0.00	0.00	0.00
Hexacosanal	2829	-	-	-	-	0.66	0.00	0.00	0.00
Nonacosane	2900	25.34	26.21	24.79	0.00	14.03	11.58	2.88	1.34
13,17- Dimethylnonacosane	2960	-	-	-	-	1.83	0.89	0.00	0.00
Octacosanal	3033	12.51	15.64	13.83	0.00	28.55	24.31	11.60	1.18
Hentriacontane	3100	58.10	53.88	47.26	0.00	115.60	65.82	18.58	15.55
Cholesterol	3120	286.19	229.63	128.30	0.00	236.60	92.43	87.18	38.70
2-Eicosyl-5- nonyltetrahydrofuran	3121	-	-	-	-	3.89	0.00	0.00	0.00
13,17- Dimethylhentriacontane	3358	12.95	10.76	1.64	0.00	3.93	2.65	1.74	0.00

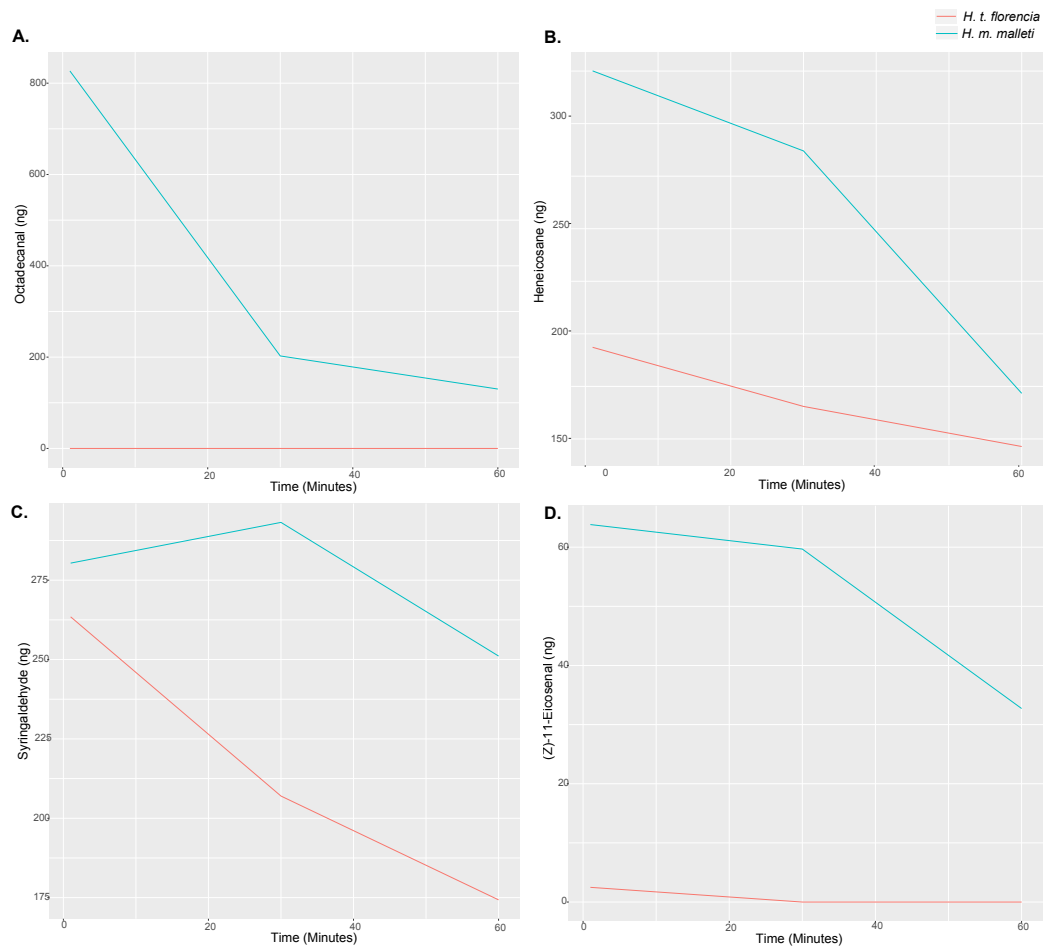


Figure S2.1. Amount (ng) of compounds that remained in the wings of perfumed males before evaporation. I quantified the presence of the perfume applied at the beginning of the experiment, at 1 minute, at 30 minutes and at 60 minutes after spreading perfume. **(A)** Octadecanal; **(B)** Heneicosane; **(C)** Syringaldehyde; **(D)** Z-11-Eicosanal. The blue line represents the pattern present in *H. m. malleti* and red line represents *H. t. florenxia*.

CHAPTER 3. MATE PREFERENCE AND PHEROMONE COMPOSITION IN A PAIR OF CLOSELY RELATED AND MIMETIC SPECIES OF THE GENUS *Heliconius*

Table S3.1. Compounds identified in wing androconia's extracts of *H. melpomene malleti*, *H. timareta florencía*, F₁ and backcross. RI, retention index. Mean ± SD amounts in ng.

Name	RI	<i>H. melpomene malleti</i>	<i>H. timareta florencía</i>	F1	Backcrosses
		Mean ± SD	Mean ± SD	Mean ± SD	Mean± SD
Unknown	902	-	-	3.80 ± 4.91	0.78 ± 1.60
Dimethyl sulfone	916	-	-	0.76 ± 1.33	0.50 ± 1.99
Unknown	958	0.13 ± 0.76	0.43 ± 1.69	7.15 ± 4.04	11.25 ± 5.68
Limonene	1023	-	0.28 ± 0.52	-	-
Phenylacetaldehyde	1036	-	0.16 ± 0.77	-	-
Unknown	1037	-	-	1.50 ± 2.40	1.16 ± 1.85
Nonanal	1100	0.58 ± 1.51	1.47 ± 2.94	3.67 ± 4.97	-
Alkane	1117	-	2.91 ± 5.72	-	-
Unknown	1174	-	0.06 ± 3.09	-	-
Methyl salicylate	1187	2.44 ± 2.51	1.39 ± 1.99	-	-
Decanal	1200	-	-	3.20 ± 8.32	-
(Z)-3-Hexenyl isobutyrate	1233	19.21 ± 14.04	-	-	-
Hexyl 3-methylbutyrate	1239	53.33 ± 144.25	-	-	-
Alkane	1265	-	1.76 ± 9.72	-	-
Tridecane	1300	15.16 ± 12.07	8.15 ± 9.15	-	-
Tetradecane	1302	-	0.92 ± 2.54	-	-
5-Decanolide	1369	-	4.65 ± 5.40	1.06 ± 1.88	0.12 ± 0.64
α-Copaene	1371	1.31 ± 1.88	-	-	-
Dihydroactinidiolide	1391	17.67 ± 11.54	13.96 ± 15.69	1.71 ± 1.84	0.93 ± 2.02
Ethyl 4-ethoxybenzoate	1403	8.28 ± 6.87	12.12 ± 16.23	8.28 ± 5.88	5.65 ± 6.65

Homovanillin alcohol	1413	1.55 ± 2.93	0.249 ± 0.78	0.27 ± 0.53	0.12 ± 0.47
6,10-Dimethyl 5,9-undecadien-2-one	1447	2.64 ± 3.10	-	-	-
Methyl 4-hydroxybenzoate	1449	2.51 ± 4.83	-	-	-
Methyl 3,4-dimethoxybenzoate	1465	8.97 ± 18.25	-	-	-
Unknown	1470	0.19 ± 0.50	-	-	0.33 ± 0.65
Unknown	1488	-	0.09 ± 0.46	-	-
Unknown	1495	-	-	0.06 ± 0.22	-
Syringaldehyde	1519	291.8 ± 234.84	268.75 ± 285.36	56.11 ± 62.01	34.18 ± 50.06
3,5-Dimethoxy-4-hydroxybenzyl alcohol	1565	-	6.95 ± 36.05	-	-
Propyl 4-hydroxybenzoate	1614	-	3.02 ± 5.43	-	-
Methyl 1 <i>H</i> -indol-3-acetate	1663	-	0.23 ± 0.75	-	-
Unknown	1715	0.89 ± 1.51	-	2.60 ± 3.14	1.57 ± 1.77
Unknown	1765	-	0.30 ± 0.89	0.19 ± 0.53	-
Macrolide	1769	-	-	-	0.92 ± 4.01
Unknown	1795	-	3.72 ± 20.66	0.16 ± 0.40	-
Hexadecanoic acid	1826	-	2.76 ± 8.24	-	-
Unknown	1873	-	-	0.14 ± 0.48	1.64 ± 4.85
Unknown	1923	16.56 ± 14.99	-	-	-
Unknown	1929	0.57 ± 2.42	-	1.02 ± 1.39	-
Octadecanal	2015	1094.91 ± 519.64	1.40 ± 5.84	19.25 ± 35.04	1.86 ± 5.38
Isopropyl palmitate	2025	-	1.86 ± 6.02	-	3.00 ± 8.28
1-Octadecanol	2076	27.83 ± 33.07	29.85 ± 138.42	2.82 ± 6.48	-
Heneicosene	2079	0.47 ± 1.90	26.80 ± 104.03	5.97 ± 18.76	4.22 ± 11.20
Heneicosane	2085	298.83 ± 335.05	174.57 ± 225.37	132.51 ± 102.24	125.07 ± 122.00
Unknown	2109	0.91 ± 4.15	-	0.28 ± 0.72	0.37 ± 0.86
Unknown	2135	1.53 ± 4.23	-	-	-
Ethyl stearate	2190	-	1.71 ± 3.18	-	0.05 ± 0.19
(<i>Z</i>)-11-Eicosenal	2198	231.98 ± 255.99	4.39 ± 11.48	22.25 ± 20.38	3.75 ± 9.35
Docosane	2200	-	0.19 ± 0.92	1.75 ± 3.75	0.36 ± 0.86
Eicosane	2200	2.63 ± 5.25	3.43 ± 7.06	0.10 ± 0.35	0.23 ± 0.56

Eicosanal	2219	43.43 ± 53.98	-	1.46 ± 3.12	-
Unknown	2088	-	1.93 ± 11.14	-	-
Tricosene	2280	-	2.84 ± 16.35	0.20 ± 0.68	-
Tricosane	2300	27.27 ± 151.83	8.46 ± 31.72	-	-
Unknown	2321	0.10 ± 0.57	-	-	0.98 ± 2.78
(Z)-13-Docosenal	2396	23.66 ± 68.98	-	0.62 ± 2.08	-
Unknown	2687	-	0.39 ± 2.25	0.43 ± 1.44	-
Heptacosane	2700	56.11 ± 73.64	12.16 ± 39.18	23.78 ± 17.25	36.12 ± 30.35
Methylheptacosane	2733	15.88 ± 26.13	12.42 ± 39.54	4.24 ± 6.31	6.34 ± 15.06
Unknown	2794	1.21 ± 3.23	-	0.15 ± 0.52	21.78 ± 69.18
Octacosane	2800	-	2.63 ± 15.11	-	-
Hexacosanal	2826	-	5.20 ± 26.32	-	-
Nonacosane	2900	25.34 ± 41.2	13.60 ± 25.45	31.43 ± 23.85	31.24 ± 38.05
13,17 Dimethylnonacosane	2957	-	1.77 ± 4.84	7.26 ± 7.19	1.17 ± 3.04
Octacosanal	3024	12.50 ± 21.93	28.82 ± 52.43	28.71 ± 28.59	23.6 ± 24.67
Hentriacontane	3100	58.09 ± 100.82	118.43 ± 206.82	88.60 ± 39.46	52.32 ± 32.19
Cholesterol	3119	286.19 ± 445.59	250.36 ± 219.16	218.74 ± 95.74	204.56 ± 135.52
13,17-Dimethylhentriacontane	3156	12.95 ± 28.21	3.81 ± 17.50	18.13 ± 17.65	4.16 ± 8.97
2-Eicosyl-5-heptyltetrahydrofuran	3179	97.19 ± 257.04	-	-	-
2-Eicosyl-5-nonyltetrahydrofuran	3380	10.11 ± 56.30	4.69 ± 13.95	-	1.44 ± 7.23

Table S3.2. Compounds identified in extracts of abdominal glands' extracts of males of *H. melpomene malleti*, *H. timareta florencia*, *F1* and backcross. RI, retention index. Mean \pm SD amounts in ng.

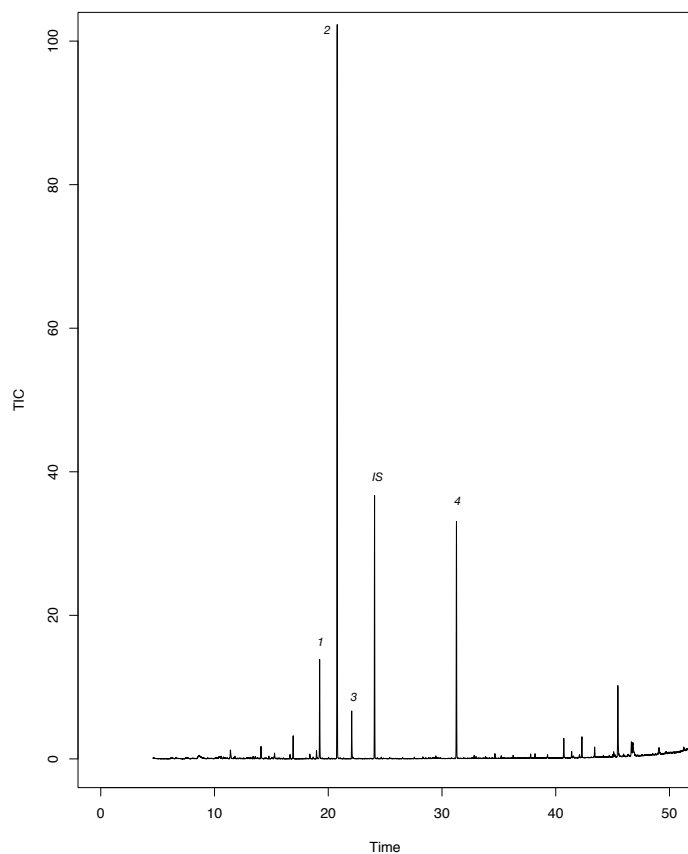
Name	RI	<i>H. melpomene malleti</i>	<i>H. timareta florencia</i>	F1	Backcrosses
		Mean \pm SD	Mean \pm SD	Mean \pm SD	Mean \pm SD
Unknown	902	-	1.58 \pm 3.99	7.08 \pm 5.85	13.70 \pm 12.24
Dimethyl sulfone	916	-	0.34 \pm 1.22	-	-
(Z)- β -Ocimene	1037	366.56 \pm 500.54	-	142.08 \pm 270.49	34.18 \pm 75.04
Phenylacetone nitrile	1039	-	62.59 \pm 95.31	-	-
(E)- β -Ocimene	1048	12831.60 \pm 8067.12	-	2247.58 \pm 3047.13	78.92 \pm 243.28
2-sec-Butyl-3-methoxypyrazine	1170	-	74.80 \pm 91.67	12.45 \pm 16.86	55.28 \pm 34.86
2-Isobutyl-3-methoxy pyrazine	1177	0.02 \pm 0.11	-	1.26 \pm 1.51	2.43 \pm 3.94
Methyl salicylate	1187	-	0.12 \pm 0.54	1.74 \pm 1.28	1.27 \pm 1.68
Dihydroedulan II	1284	43.92 \pm 40.09	5.52 \pm 14.98	1.82 \pm 2.26	-
Tridecane	1300	1.33 \pm 1.91	0.44 \pm 0.87	-	-
Nonadecane	1302	554.93 \pm 1403.34	721.14 \pm 3082.59	-	-
5-Decanolide	1369	0.42 \pm 2.24	0.18 \pm 1.03	-	-
α -Copaene	1371	0.02 \pm 0.14	2.53 \pm 6.81	-	-
Dihydroactinidiolide	1391	0.09 \pm 0.48	21.34 \pm 120.35	-	-
Unknown	1395	264.14 \pm 333.29	622.68 \pm 661.95	122.10 \pm 124.78	47.67 \pm 66.71
Ethyl 4-ethoxybenzoate	1403	8.81 \pm 7.73	18.26 \pm 40.40	9.51 \pm 6.44	6.02 \pm 7.69
Homovanillin alcohol	1413	1.43 \pm 2.86	1.40 \pm 4.25	0.18 \pm 0.48	1.38 \pm 2.72
Unknown	1542	0.18 \pm 1.00	0.49 \pm 2.54	3.83 \pm 5.72	0.55 \pm 1.05
Heptadecane	1700	155.78 \pm 602.03	0.13 \pm 0.76	0.24 \pm 0.82	-
Benzyl salicylate	1708	0.34 \pm 0.84	-	-	-
Unknown	1712	-	23.37 \pm 69.08	0.76 \pm 1.33	-
Tetradecanolide	1721	5.86 \pm 14.98	30.18 \pm 62.64	40.03 \pm 48.57	9.77 \pm 15.12
Macrolide	1726	-	3.14 \pm 6.25	-	-
Macrolide	1734	-	13.31 \pm 25.54	-	-
Unknown	1764	6.86 \pm 14.56	11.54 \pm 20.45	-	-

Unknown	1771	-	1.06 ± 3.42	32.52 ± 50.73	-
Macrolide	1773	0.5423 ± 2.86	0.81 ± 2.44	-	0.34 ± 1.78
Macrolide	1806	-	1.75 ± 6.20	-	-
Hexadecen-11-olide	1819	-	12.32 ± 16.05	-	-
Macrolide	1823	32.10 ± 32.03	26.36 ± 36.51	-	-
Hexadecenolide	1857	11.18 ± 24.31	126.3 ± 214.21	6.04 ± 11.35	13.09 ± 23.92
Macrolide	1923	6.98 ± 36.97	2.85 ± 10.88	-	0.45 ± 2.33
Heptadecanal	1923	-	-	8.64 ± 12.30	12.93 ± 22.66
16-Hexadecanolide	1924	-	124.38 ± 160.04	4.16 ± 11.61	-
Brassicalactone	1960	-	278.62 ± 496.97	11.79 ± 22.16	20.40 ± 50.00
Octadecenolide	2002	2.26 ± 9.61	242.74 ± 436.73	5.09 ± 7.11	11.28 ± 22.48
Isopropyl palmitate	2025	2.17 ± 9.03	75.63 ± 183.90	8.99 ± 13.25	11.63 ± 32.00
(Z)-9-Octadecen-11-olide	2032	4.33 ± 10.11	841.29 ± 1138.35	319.30 ± 450.38	985.96 ± 1393.24
(Z)-9-Octadecen-13-olide	2038	221.76 ± 278.84	1933.83 ± 2671.28	544.38 ± 452.76	1779.89 ± 1709.61
12-Octadecanolide	2051	-	3.13 ± 7.20	0.54 ± 1.29	0.61 ± 2.44
Macrolide	2056	0.8512 ± 2.40	0.19 ± 1.12	-	-
(E)-Octadec-9-en-12-olide	2057	-	64.11 ± 79.56	-	25.10 ± 123.85
Macrolide	2058	5.31 ± 10.70	11.75 ± 22.80	3.83 ± 5.72	0.55 ± 1.05
Isopropyl octadecanoate	2063	5.57 ± 16.87	277.67 ± 399.88	-	-
(Z9,E11)- Octadeca-9,11-dien-13-olide	2069	0.06 ± 0.35	1417.08 ± 3035.70	2.66 ± 7.33	165.54 ± 258.28
11-Octadecanolide	2070	-	29.81 ± 101.85	36.17 ± 31.27	47.18 ± 166.82
Isopropyl linoleate	2073	2.53 ± 7.92	929.63 ± 1218.84	-	-
1-Octadecanol	2076	116.92 ± 160.41	67.52 ± 138.34	16.10 ± 32.72	-
Henicosene	2079	28.17 ± 40.01	20.59 ± 25.93	16.14 ± 15.61	327.90 ± 762.56
Heneicosane	2085	2122.79 ± 1879.48	1176.11 ± 2609.26	531.93 ± 392.53	610.33 ± 960.01
Octadecen-18-olide	2123	0.27 ± 1.47	15.88 ± 45.96	18.74 ± 29.46	20.29 ± 30.55
Isopropyl octadecadienolate	2130	1.67 ± 6.25	99.43 ± 369.98	-	-
17-Octadecanolide	2136	-	25.34 ± 143.36	109.12 ± 263.67	149.48 ± 501.09
9-Octadecen-18-olide	2138	44.04 ± 122.04	159.13 ± 217.98	152.97 ± 190.59	190.42 ± 325.61
18-Octadecanolide	2158	-	-	6.56 ± 2.35	-

Ethyl oleate	2165	377.55 ± 474.37	606.93 ± 733.31	101.26 ± 172.42	0.34 ± 1.78
Octadecadienolide	2171	29.60 ± 71.78	700.86 ± 919.28	598.20 ± 448.49	1413.63 ± 1228.55
Butyl hexadecanoate	2186	9.05 ± 13.25	122.77 ± 197.54	28.75 ± 61.82	46.27 ± 79.45
Isopentyl octadecadienoate	2189	-	402.28 ± 1692.33	32.41 ± 48.63	25.33 ± 53.00
Isopropyl oleate	2196	969.26 ± 828.53	7715.08 ± 6651.53	2070.673 ± 1733.78	3285.38 ± 4207.11
Docosane	2200	3.00 ± 7.09	39.28 ± 124.92	6.32 ± 13.64	1.74 ± 4.54
Eicosane	2200	1.04 ± 3.16	1354.90 ± 1833.53	12.15 ± 27.11	10.83 ± 11.16
Ester	2209	17.85 ± 27.85	115.71 ± 162.59	-	-
Eicosanal	2219	0.42 ± 2.24	1.05 ± 5.98	0.48 ± 1.60	0.70 ± 3.36
Unknown	2248	8.56 ± 20.40	19.21 ± 26.10	0.39 ± 1.29	0.23 ± 1.18
13-Eicosanolide	2252	-	6.53 ± 18.44	33.26 ± 62.74	40.95 ± 71.75
Tricosene	2280	23.00 ± 33.65	45.26 ± 73.63	19.37 ± 23.37	30.76 ± 45.55
Isobutyl oleate	2297	243.89 ± 916.10	883.52 ± 1294.80	146.69 ± 205.08	51.79 ± 163.49
Tricosane	2300	168.89 ± 166.76	191.35 ± 273.22	61.88 ± 84.02	59.88 ± 67.54
2-Heneicosanol	2310	-	196.39 ± 488.74	7.84 ± 26.02	-
11-Icosenol	2317	11.18 ± 19.08	1260.80 ± 4099.99	2.66 ± 6.30	2.09 ± 5.97
Butyl oleate	2359	539.28 ± 615.35	2633.57 ± 3949.56	1805.67 ± 1680.41	3411.09 ± 4616.37
Hexenyl hexadecanoate	2379	-	12.53 ± 29.20	4.44 ± 10.55	10.27 ± 14.82
Tetracosane	2405	15.69 ± 68.45	104.19 ± 513.61	1.60 ± 5.31	-
1,3-Eicosanediol	2409	0.08 ± 0.32	17.25 ± 42.61	-	-
Macrolide	2417	2.324 ± 8.02	2.17 ± 11.45	0.76 ± 1.33	-
Macrolide	2418	2.318 ± 3.72	11.22 ± 16.59	19.73 ± 37.04	63.50 ± 97.01
Isoprenyl octadec-11-enoate	2433	-	92.19 ± 313.63	-	-
Unknown	2434	5.90 ± 17.08	17.35 ± 51.73	0.39 ± 1.29	0.23 ± 1.18
(Z)-13-Docosen-1-ol	2461	87.02 ± 176.14	297.51 ± 425.23	39.84 ± 63.69	26.27 ± 71.84
Macrolide	2475	-	-	26.80 ± 44.29	58.17 ± 102.54
1-Docosanol	2488	37.55 ± 57.04	140.36 ± 331.25	108.25 ± 126.81	137.70 ± 162.27
Pentacosane	2500	136.3 ± 141.58	206.84 ± 803.27	33.49 ± 39.19	30.39 ± 37.85
Tricosenol	2514	-	17.94 ± 38.29	-	-
11-Methylpentacosane	2532	48.70 ± 52.49	7.45 ± 22.8	-	-

Docosan-22-olide	2537	-	92.32 ± 117.00	38.40 ± 69.37	-
Hexyl octadecadienoate	2538	-	11.25 ± 35.99	7.01 ± 23.26	22.09 ± 37.33
Hexyl octadecenoate and Hexenyl octadecenoate	2553	114.56 ± 243.75	679.70 ± 974.09	586.15 ± 580.31	1173.90 ± 1111.75
Hexenyl octadecatrienoate and Hexenyl octadecatrienoate	2555	-	16.35 ± 41.97	41.83 ± 96.64	157.85 ± 196.27
Benzyl hexadecanoate	2571	-	12.51 ± 26.71	1.20 ± 4.00	1.10 ± 4.26
Hexenyl octadecanoate	2580	6.08 ± 16.75	4.99 ± 9.47	1.53 ± 2.67	2.33 ± 5.92
Hexyl octadecanoate	2594	0.743 ± 3.93	81.33 ± 95.56	25.69 ± 38.66	68.48 ± 95.79
Hexacosane	2601	5.54 ± 11.89	179.42 ± 1012.18	6.31 ± 15.96	-
Tetracosenol	2666	205.96 ± 239.41	220.54 ± 319.25	439.32 ± 530.86	405.506 ± 481.61
1-Tetracosanol	2691	9.04 ± 21.35	47.67 ± 116.63	138.60 ± 309.57	45.47 ± 73.74
Heptacosane	2700	19.83 ± 47.97	225.04 ± 1162.37	98.30 ± 85.46	129.81 ± 143.60
Tetracosenolide	2735	2.96 ± 7.36	42.87 ± 56.81	33.63 ± 55.08	59.24 ± 128.91
1,3-Tetracosanediol*	2811	-	-	58.20 ± 120.24	8.24 ± 19.93
Unknown	2869	8.19 ± 19.09	0.29 ± 1.51	3.56 ± 9.01	3.15 ± 16.12
Unknown	2871	8.43 ± 28.03	28.60 ± 49.18	-	-
Nonacosane	2900	1.57 ± 6.43	167.65 ± 924.25	15.15 ± 19.06	20.82 ± 35.97
13,17-Dimethylnonacosane	2957	-	32.82 ± 147.47	43.77 ± 115.55	6.94 ± 20.82
Cholesterol	3119	192.05 ± 273.18	153.25 ± 263.26	617.34 ± 599.42	700.25 ± 647.53
Unknown	3147	0.08 ± 0.33	0.68 ± 3.85	6.26 ± 16.19	-
13,17-Dimethylhentriacontane	3156	153.09 ± 173.73	395.95 ± 485.06	438.67 ± 328.29	349.94 ± 422.70
2-Nonyl-5-octadecyltetrahydrofuran	3177	0.08 ± 0.33	0.20 ± 0.82	22.65 ± 57.78	-
Campesterol or Ergosterol	3207	1.42 ± 5.61	7.37 ± 17.36	16.35 ± 21.95	56.38 ± 120.37
13,17-Dimethyltrtriacontane	3348	24.37 ± 39.54	42.23 ± 105.73	93.10 ± 75.05	64.86 ± 88.28
2-Eicosyl-5-nonyltetrahydrofuran	3380	14.77 ± 35.28	20.68 ± 48.38	63.61 ± 50.82	39.84 ± 72.41

A.
Heliconius timareta florencia



B.
Heliconius melpomene malleti

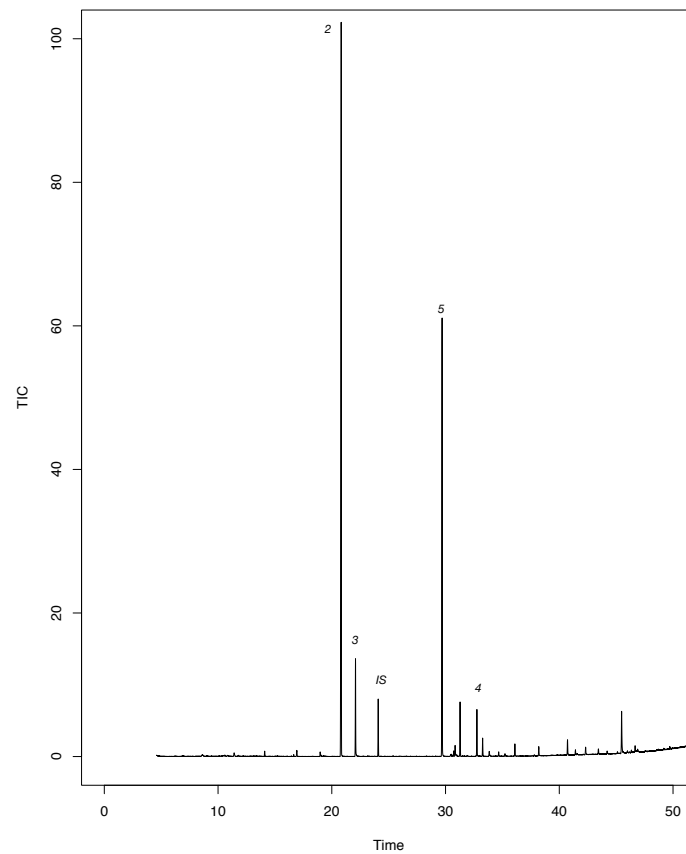


Figure S3.1. Species differences in male androconial extracts. Chromatogram of extract of androconial region from **(A)** *H. timareta florencia* and **(B)** *H. melpomene malleti*. IS, internal standard (2-tetradecyl acetate); 1, dihydroactinidiolide; 2, syringaldehyde; 3, unknown; 4, hencosane; 5, octadecanal

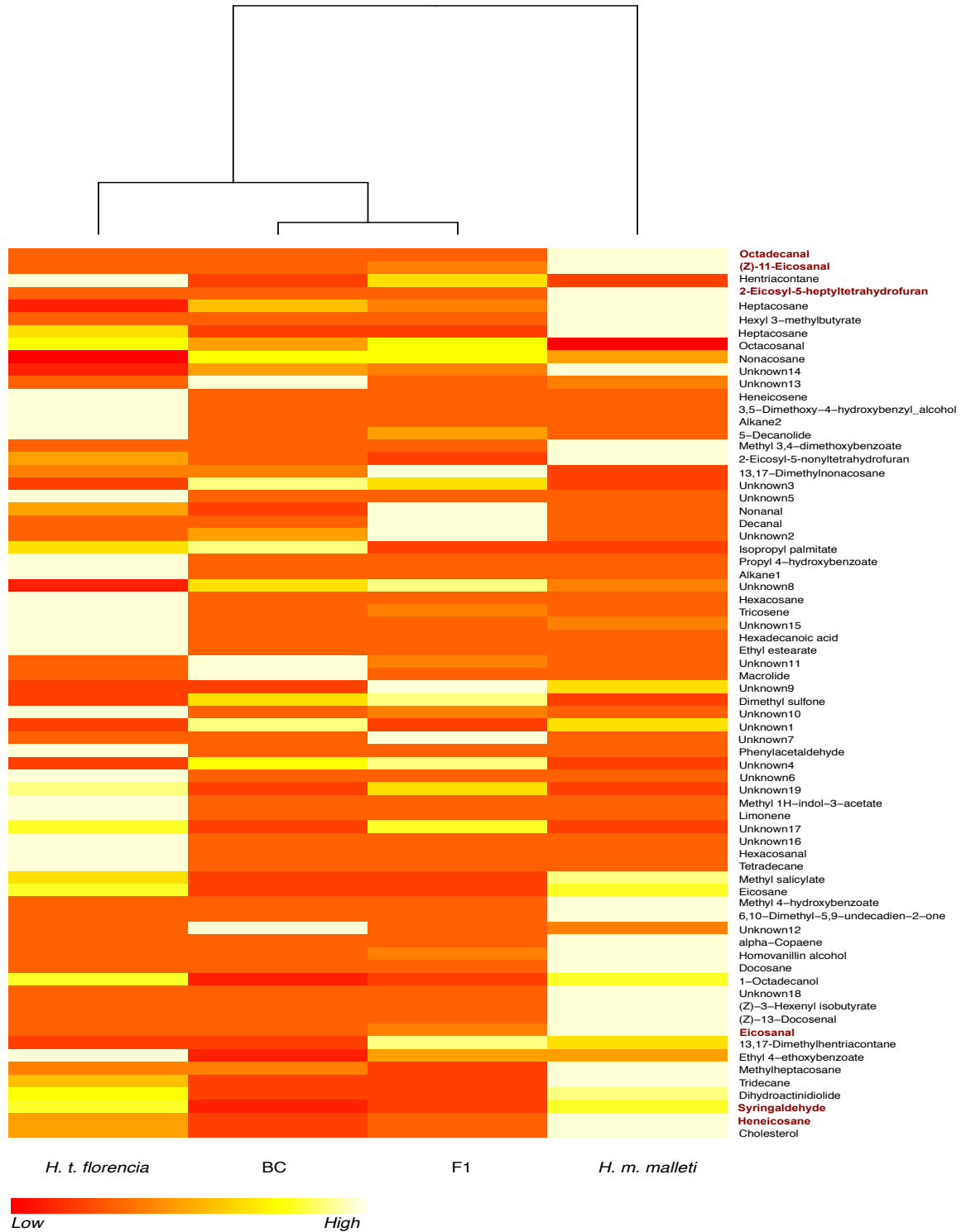


Figure S3.2. Cluster analysis based on Euclidian distance of compound composition in the wing androconia of males of *H. m. malleti*, *H. t. florencia*, F_1 and BC. Compounds highlighted in red are the most abundant.

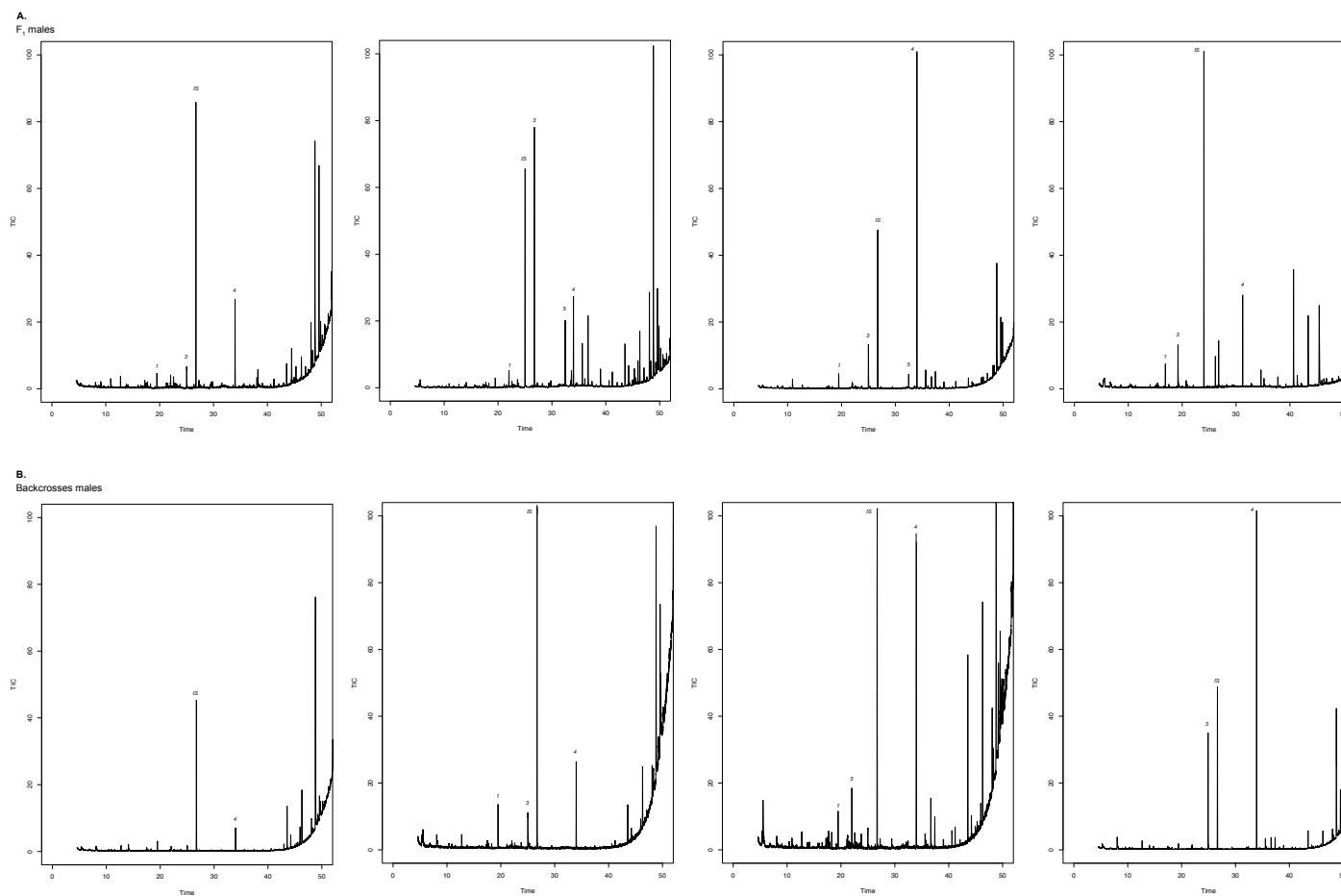
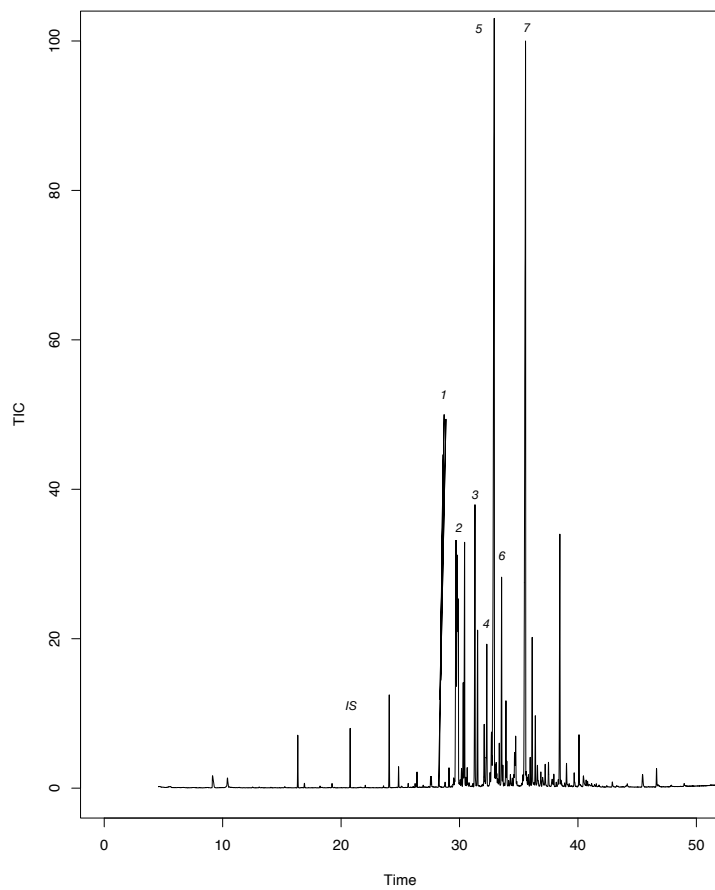


Figure S3.3. Chromatogram patterns obtained from androconial extracts of hybrid F₁ and backcross males. (A) F₁ individuals and (B) backcross individuals. IS, internal standard (2-tetradecyl acetate); 1, dihydroactinidiolide; 2, syringaldehyde; 3, unknown; 4, heneicosane; 5, octadecanal

A.

Heliconius timareta florencia



B.

Heliconius melpomene malleti

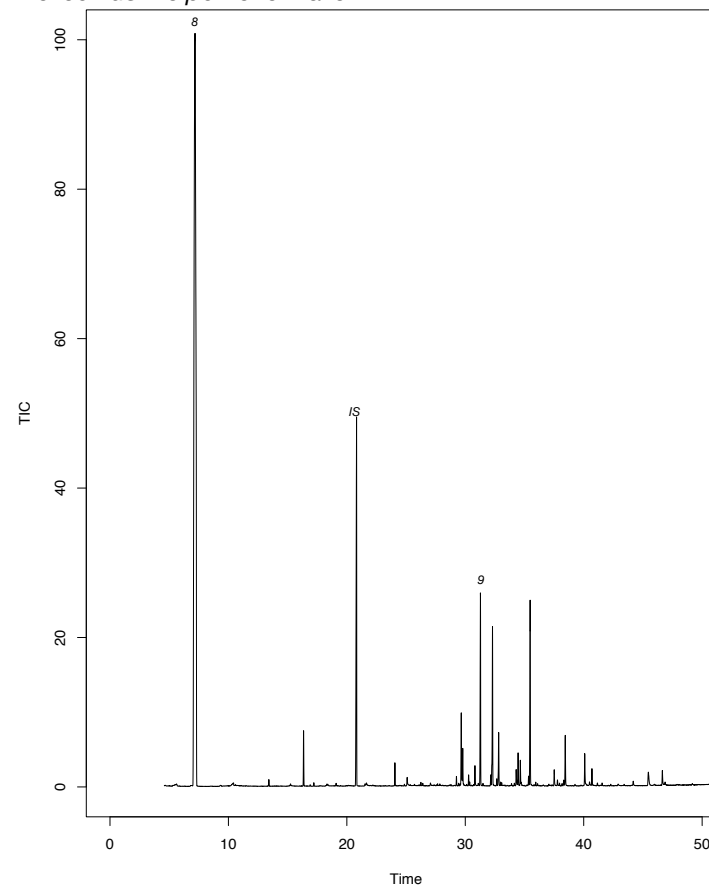


Figure S3.4. Chromatogram pattern of the abdominal gland bouquet of males. (A) *H. timareta florencia* and (B) *H. melpomene malleti*. IS, internal standard (2-tetradecyl acetate); 1, eicosane; 2, (Z)-9-octadecen-11-olide; 3, heneicosane; 4, ethyl oleate; 5, isopropyl oleate; 6, isopropyl octadecanoate; 7, butyl oleate; 8, β -ocimene; 9, henicosenes.

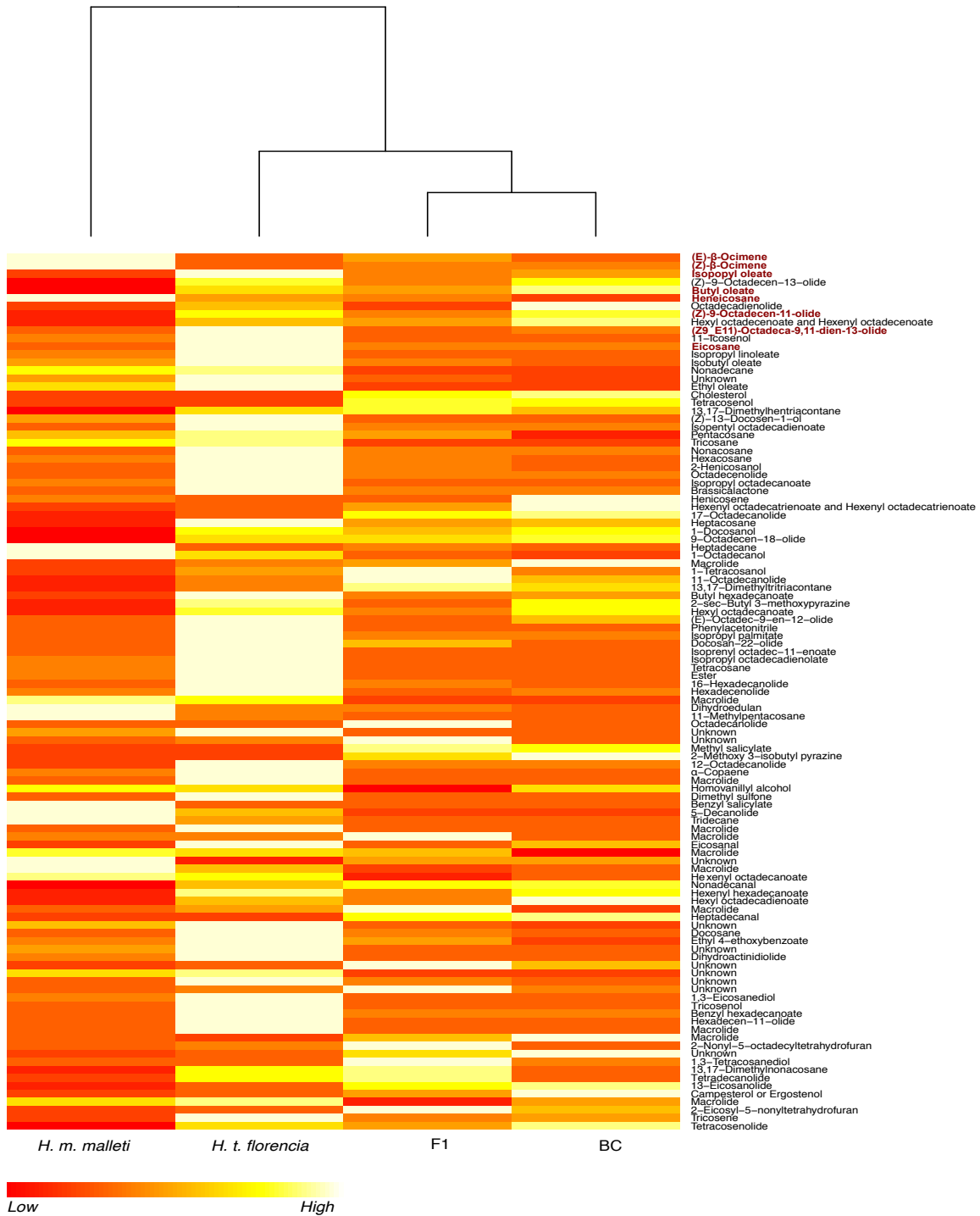


Figure S3.5. Cluster analysis based on Euclidian distance of the compound composition of the wing androconia of males of *H. m. malleti*, *H. t. florencia*, F₁ and BC. Compounds highlighted in red are the most abundant.

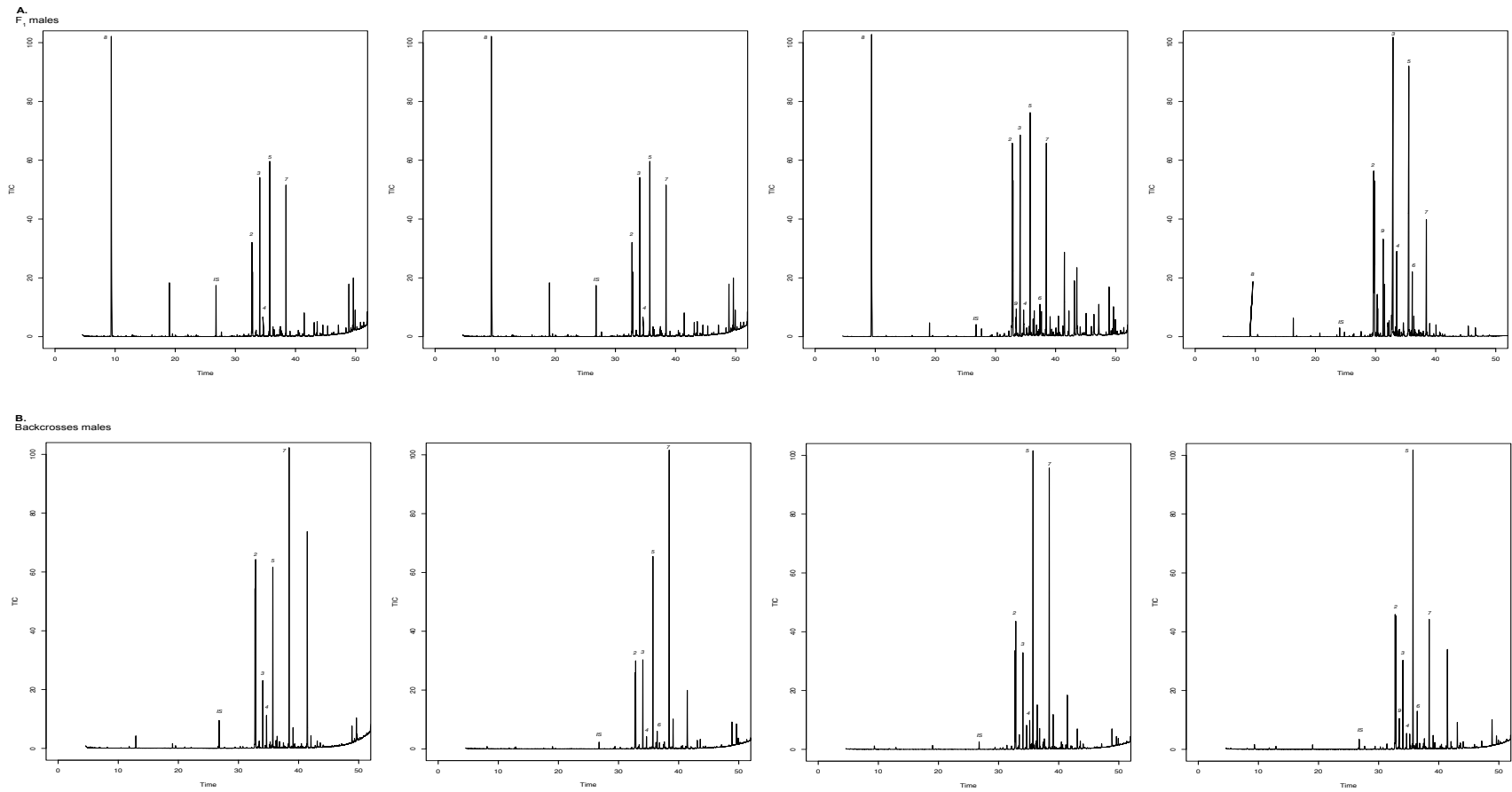


Figure S3.6. Chromatogram patterns obtained from abdominal gland bouquet of F₁ and backcross males. (A) F₁ individuals and (B) backcross individuals. IS, internal standard (2-tetradecyl acetate); 1, eicosane; 2, (Z)-9-octadecen-11-olide; 3, heneicosane; 4, ethyl oleate; 5, isopropyl oleate; 6, isopropyl octadecanoate; 7, butyl oleate; 8, β -ocimene; 9, heneicosene.